R&T 1994

Research & Technology

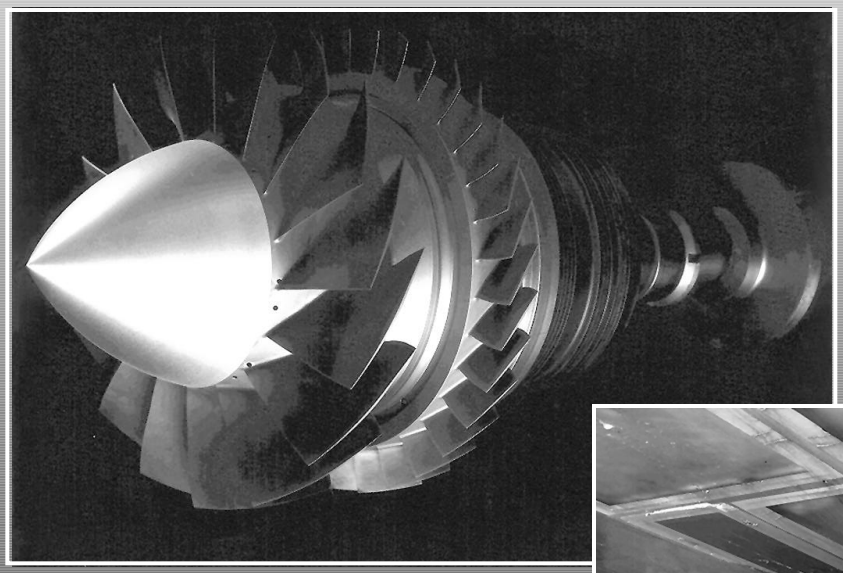

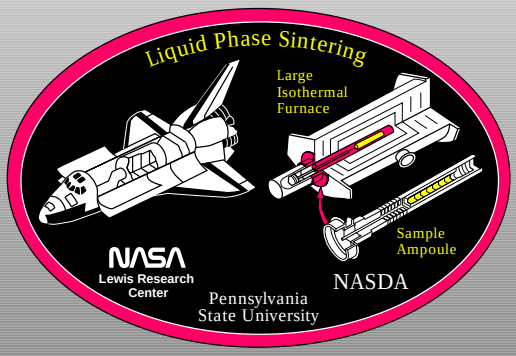

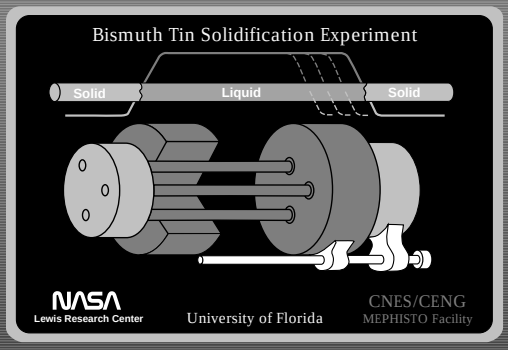

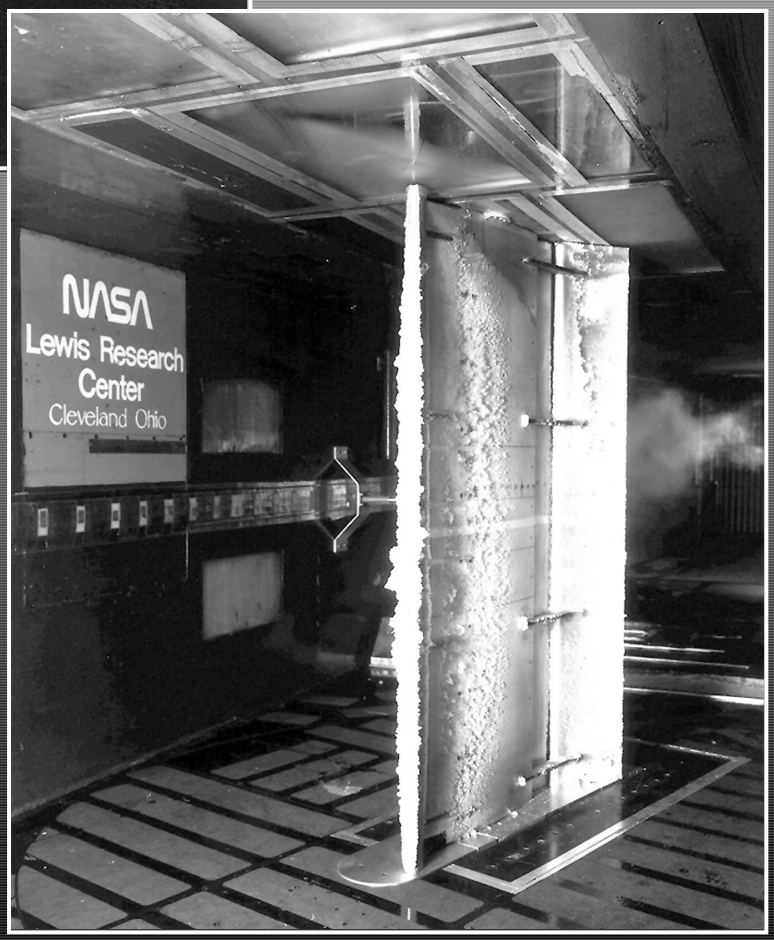

NASA

Lewis Research Center
Cleveland, Ohio

Research & Technology 1994

National Aeronautics and Space Administration

Lewis Research Center
Cleveland, Ohio 44135

TM–106764

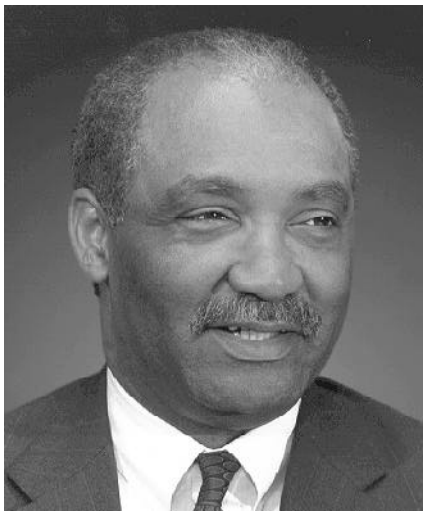

Introduction

NASA Lewis Research Center has undergone changes over the past year. An important thrust has been realignment of our activities in space and aeronautics. Technology transfer activities and opportunities continue to expand as NASA attempts to make its resources more easily available to the private sector.

The 1994 Research & Technology report is organized so that a broad cross section of the community can readily use it. A short introductory paragraph begins each article and will prove to be an invaluable reference tool for the layperson. The articles summarize the progress made during the year in various technical areas and portray the technical and administrative support associated with Lewis technology programs. If additional information is desired, the reader is encouraged to contact the authors identified in the articles.

The principal purpose of this report is to give a brief but comprehensive review of the technical accomplishments of the Center during the past year. It is a testimony to the dedication and competence of all the employees, civil servants and contractors, who make up the staff.

The Lewis Research Center is a unique facility, located in an important geographic sector, with a long and distinguished history of performing research and developing technology in support of NASA's mission and the Nation's needs.

D. J. Campbell

Donald J. Campbell
Director

Inquiries regarding this report can be addressed to the Office of Interagency and Industry Programs, Mail Stop 3–7. The telephone number is (216) 433–2912.

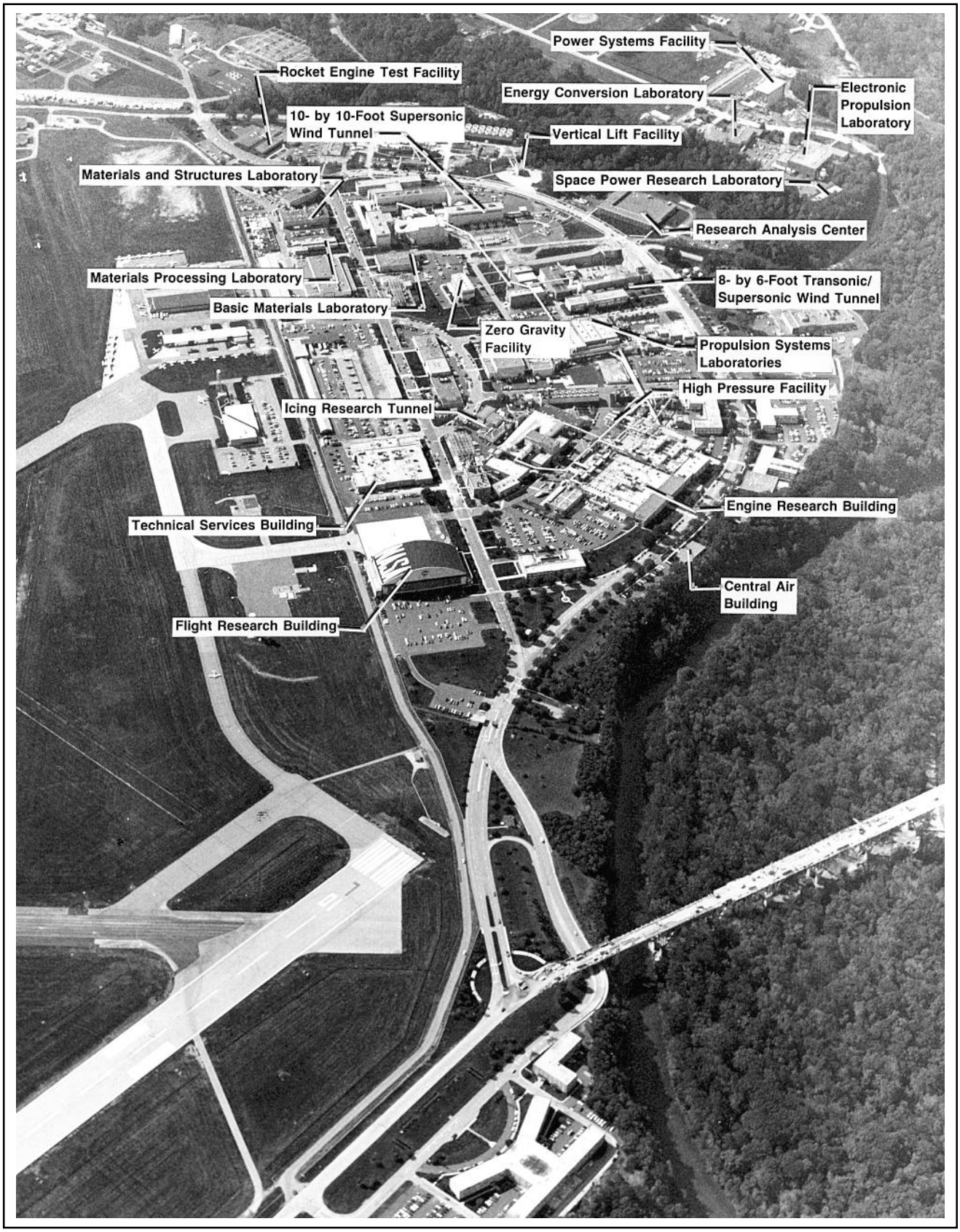

Lewis Research Center, Cleveland, Ohio

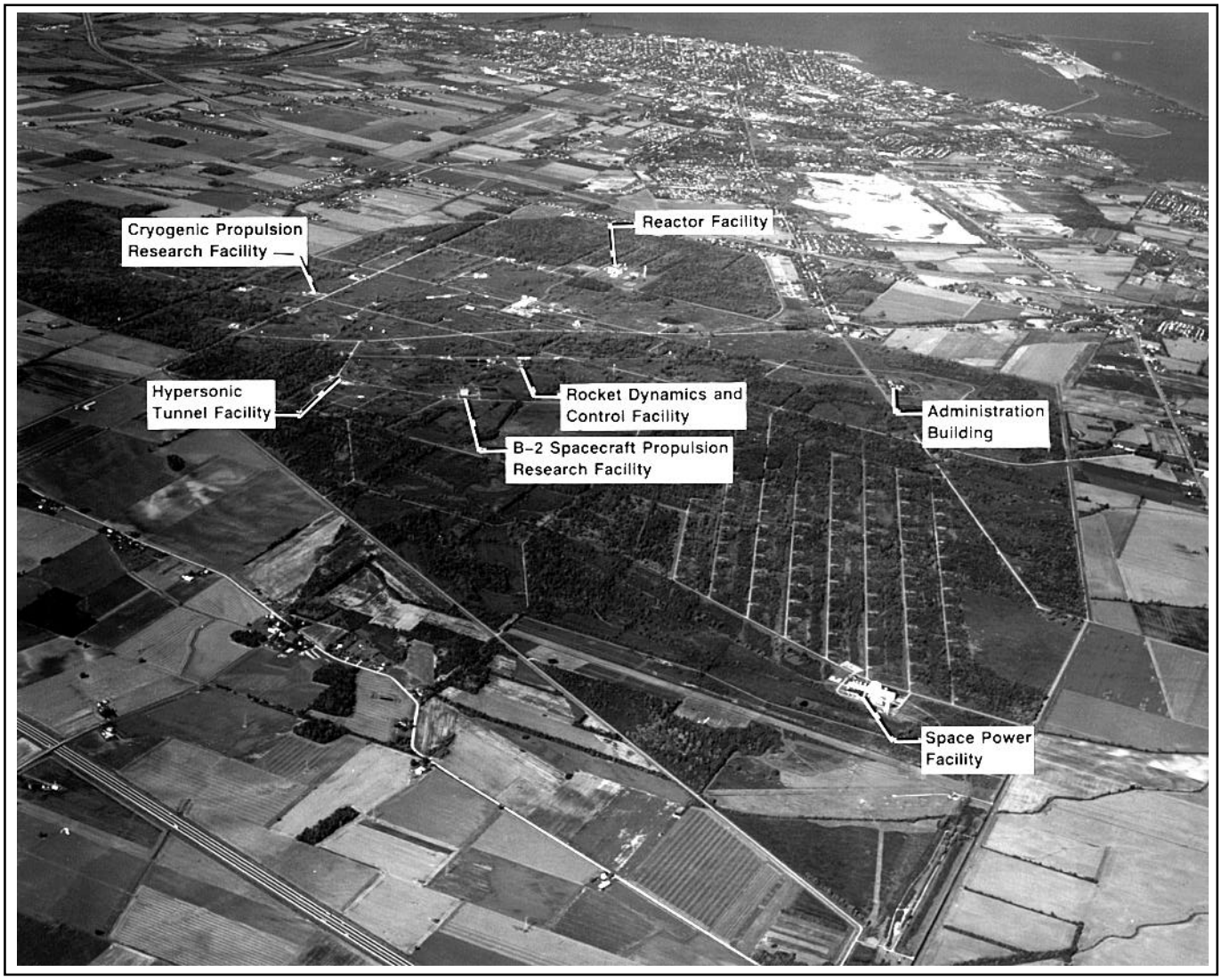

Plum Brook Station, Sandusky, Ohio

NASA Lewis Research Center Senior Management

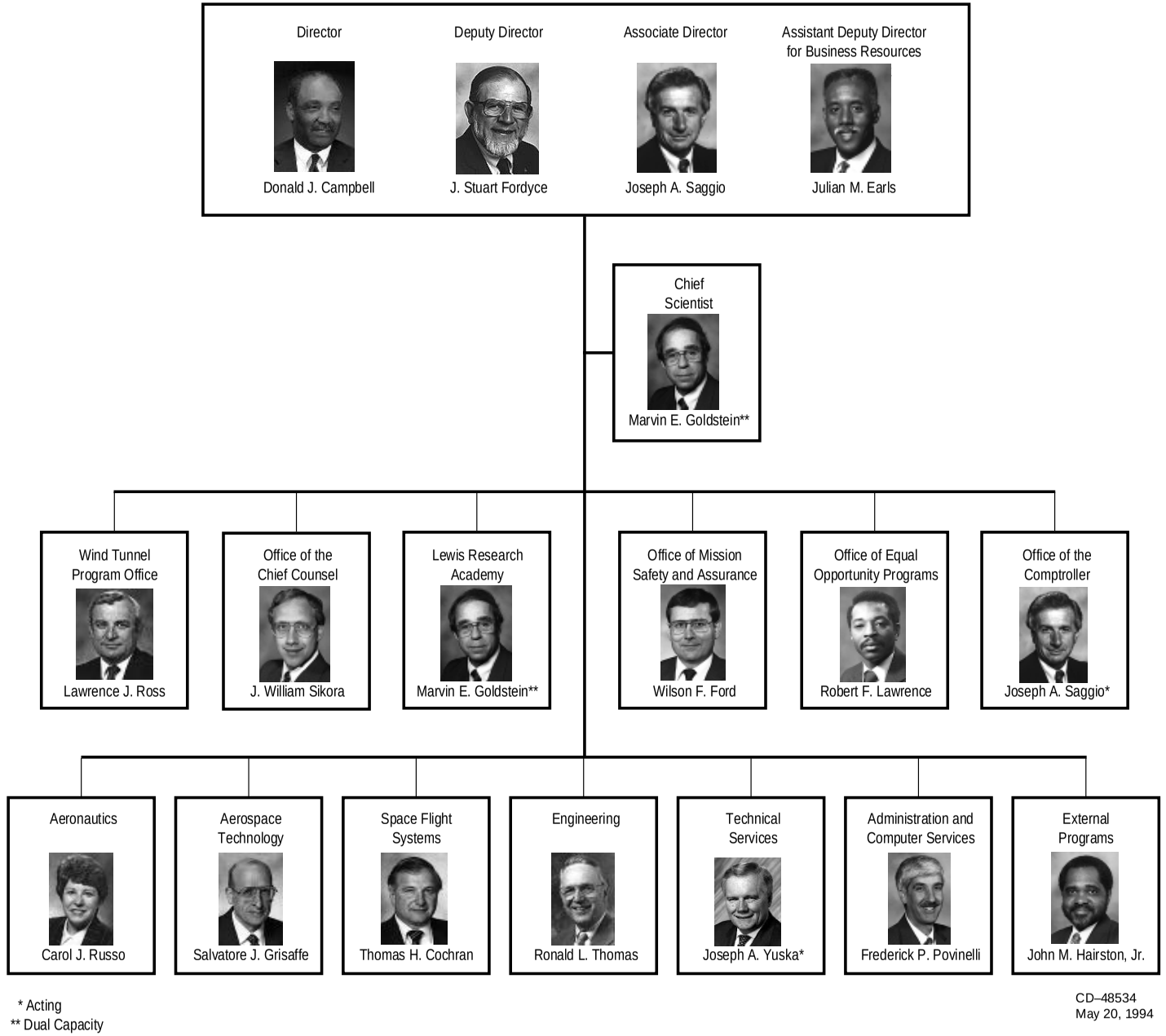

* Acting
** Dual Capacity

CD–48534
May 20, 1994

NASA Lewis Research Center

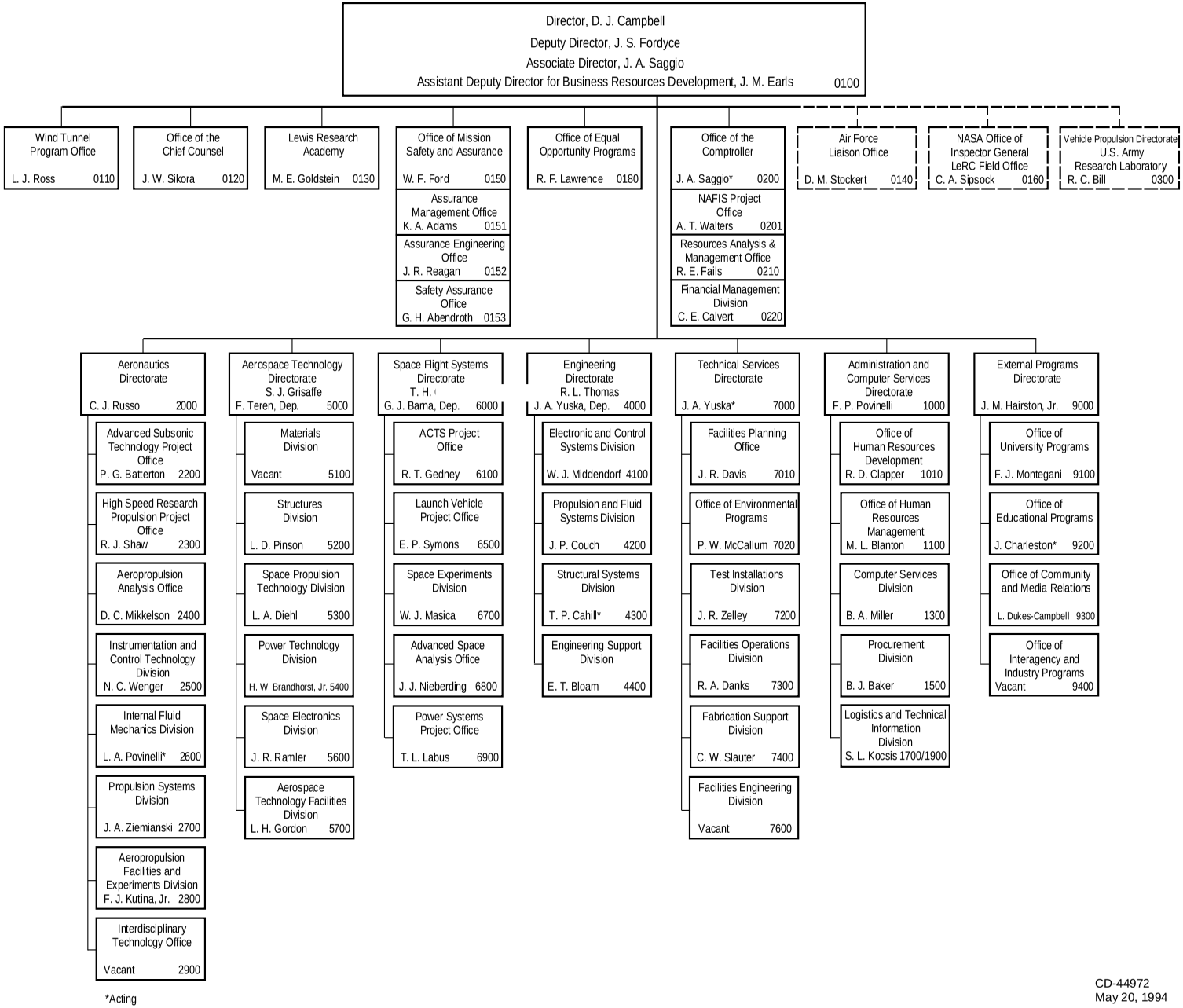

*Acting

CD-44972
May 20, 1994

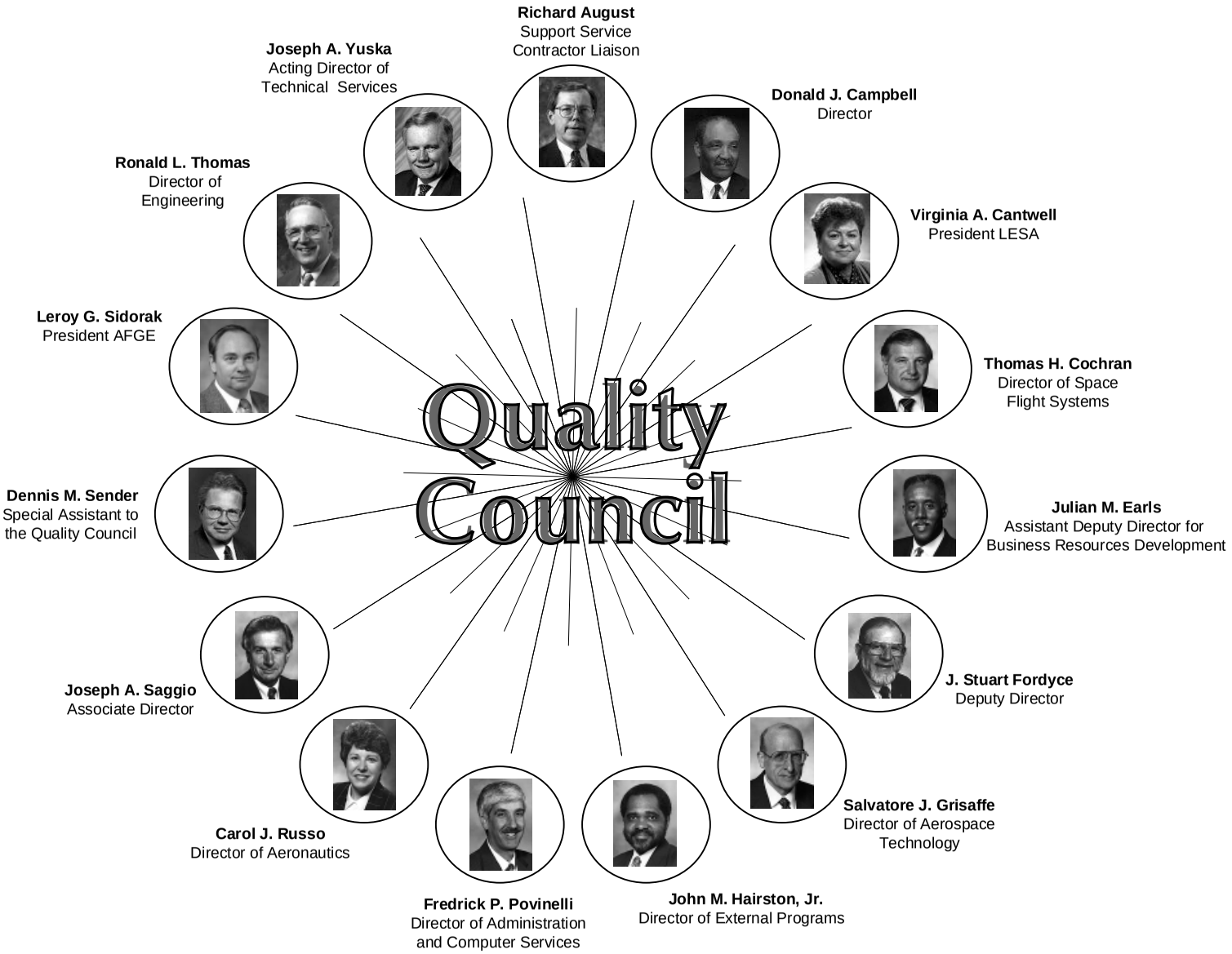

The Quality Council was established in October 1992 to adopt and implement a Total Quality (TQ) plan for Lewis. It is composed of Executive Council members as well as the president of the American Federation of Government Employees (AFGE), Local 2812, and the president of the Lewis Engineers and Scientists Association (LESA), IFPTE Local 28. A representative of major on-site support service contractors serves as liaison.

Contents

Aeronautics

Aerospace Technology

* Lewis Distinguished Paper and Lewis Materials Division Paper of the Year for 1993.

Space Flight Systems

Engineering and Computational Support

Lewis Research Academy

Technology Transfer

Author Index 156

Aeronautics

Aeropropulsion Analysis

Ability to Predict Engine Weight and Flow Path Enhanced

NASA is working to develop technology that can be used in designing economically viable and environmentally acceptable aircraft engines. Typically, many preliminary tradeoff studies are needed to identify these key technologies—and are important to key NASA programs, such as High-Speed Research and Advanced Subsonic Technology. Improved preliminary design tools will greatly enhance the ability to identify these new technologies and help guide the direction of these programs.

NASA Lewis has developed a series of codes to predict turbine engine performance, weight, geometry, and installation effects. By using a very flexible method of input, a set of standard components are connected at execution time to simulate almost any turbine engine configuration that the user could contemplate. A key element of this capability is the Weight Analysis of Turbine Engines (WATE) computer program, originally written in the mid-1970's to obtain engine weight and geometry. Unlike most other preliminary weight-estimating tools available at the time, WATE determined the weight of each major engine component by using its key relevant design parameters to obtain an overall accuracy of ±10%. Since the WATE code's original development, engine component technology, design, and materials have evolved and computer simulation capabilities have increased. Therefore, in 1991 McDonnell Douglas and NASA joined in an effort to upgrade and enhance the WATE code's capabilities. GE Aircraft Engines joined the effort in 1994.

A major portion of the modification effort involved replacing many of the correlation-based component weight prediction methodologies with a more accurate "first principles" approach. Several new weight components were also added, including a high-bypass-ratio fan, a mixer-ejector nozzle, and engine controls and accessories. The ability to weigh inlets and nacelles has also been incorporated into WATE to allow the engineer to obtain a complete propulsion system weight if desired. At the same time the graphical representation of the engine has been greatly improved to realistically represent the engine flow path and mechanical layout. An example of the graphical output now available from the upgraded version of the WATE code is shown. First-order aerodynamic prediction codes have also been

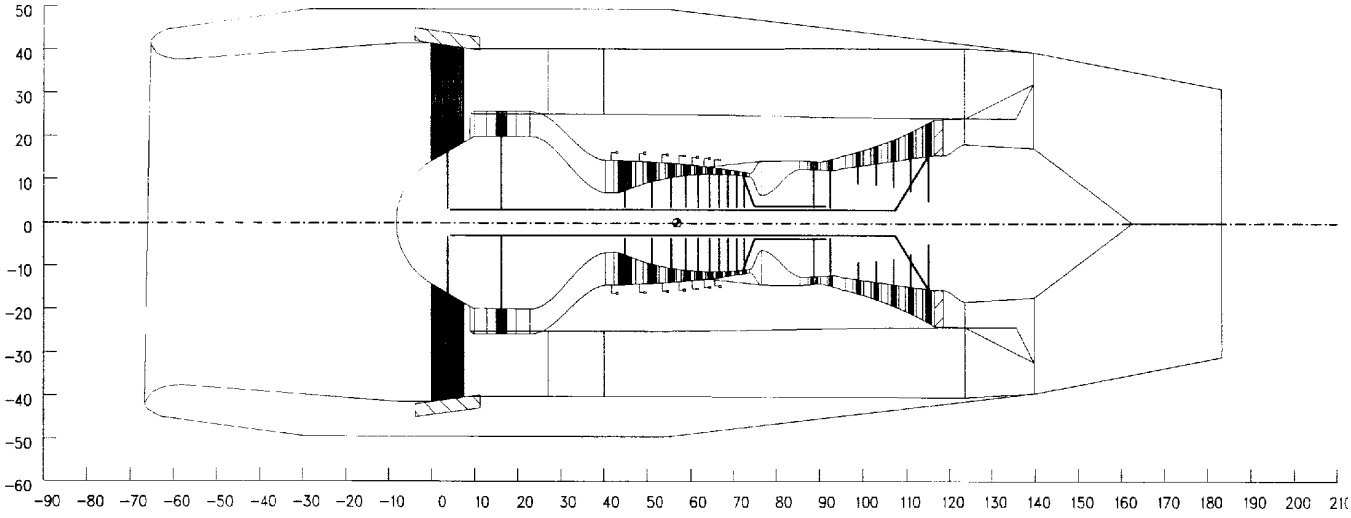

E^3 turbofan model.

coupled to the WATE code to ensure consistency between the mechanical design assumptions and the engine performance assumptions used in the analysis. These modifications and enhancements have increased the accuracy of the weight predictions to ±5% for most applications.

Moreover, they give the systems analyst more design details early in the conceptual design process.

Lewis contact: William J. Haller, (216) 977–7004
Headquarters program office: OA

Instrumentation and Control Technology

Thin-Film Thermocouples Hot Tested on Ceramic-Matrix Composite Hoop

Thin-film thermocouples are a minimally intrusive means of measuring surface temperature in hostile, high-temperature environments. Wire thermocouples mounted on engine surfaces disrupt the gas flow over the surface, thereby changing the environment at the surface. However, wire thermocouples set into machined grooves in engine surfaces compromise the structural integrity of the component—so that the surface thermal profiles they provide do not accurately reflect true operating conditions. Because thin-film thermocouples are sputter deposited directly onto the surface and are only a few micrometers thick, the surface is not structurally altered and there is minimal disturbance of the gas flow over the surface. Consequently, the sensors have minimal impact on the temperature distribution.

Thin-film thermocouples are used on the superalloy materials in jet aircraft engines. However, advanced propulsion systems presently being developed must withstand higher operating temperatures, spurring the development of thin-film thermocouples for the ceramic components of these engines.

NASA Lewis has used thin-film thermocouples to measure surface temperatures on a ceramic-matrix composite hoop developed by Allison Engine Co. under an Air Force contract to design material systems that meet propulsion capability goals set by the Integrated High-Performance Turbine Engine Technology (IHPTET) Program. The hoop material contains hydroply filiazane (HPZ) fibers in a silicon carbide matrix.

We fabricated three thin-film thermocouples on the hoop at NASA Lewis. The sensors had several layers: an electrically insulating layer, the thermocouple legs, and a protective overcoat. The electrical insulator between the substrate and the thermocouple was a thermally grown oxide layer enhanced with a 2- to 3-µm-thick layer of sputter-deposited aluminum oxide. The thermocouple was platinum–13% rhodium versus platinum sputtered deposited onto the aluminum oxide to an approximate thickness of 5 µm. An additional sputter-deposited layer of aluminum oxide protected the sensor elements against the harsh testing environment. Platinum–13% rhodium and platinum lead wires 75 µm in diameter were parallel gap welded to the films. The wires were spliced to larger diameter wires routed to the facility instrumentation panel.

The hoop was tested for 50 hr in the Lewis Ceramic Matrix Composite Test Facility, a burner rig that operates on jet fuel at 0.7 to 2 MPa (100 to 300 psig). For this test the facility was designed to run at heat flux levels simulating near-IHPTET conditions. The average gas stream temperature was approximately 1500 °C (2800 °F), and the average material temperature was 1200 °C (2200 °F). The thin-film sensors obtained suface temperature data for over 25 hr of testing—much longer than in previous attempts with wire thermocouples on this material in these conditions. As a result we have obtained a larger data base of surface temperature for this ceramic-matrix composite under harsh operating conditions. Thin-film thermocouples proved to be capable of operating on advanced materials under test conditions in which wire thermocouples were unable to survive.

Lewis contact: Lisa C. Martin, (216) 433–6468
Headquarters program office: OA

Dual, Active, Surface Heat Flux Gage Probe Passes Test

A unique miniature, dual, active, surface plug type of heat flux gage probe was successfully tested in NASA Ames Research Center's 5- by 23-Centimeter Turbulent Flow Air Duct Facility. Heat flux was provided by an arc jet that produces high free-stream temperatures in an extremely hostile environment. The probe was mounted in a fixture bolted to the duct wall and fabricated from 2.54-cm-thick thermal insulation material in an aluminum holder. The probe (designed and fabricated at NASA Lewis) was inserted through the metal and ceramic materials with the front of the gage flush with the ceramic surface. The back surface of the gage was actively and passively air cooled.

Heat fluxes measured by the miniature gage probe were compared with heat fluxes obtained by water-cooled reference calorimeters mounted in a water-cooled duct wall located opposite the miniature gage probe. Both transient and steady-state heat fluxes generally corresponded within a satisfactory ±20%, even though the front surface temperature of the gage was 850 K and the surrounding ceramic surface temperature was 1750 K. (The latter temperature exceeds the melting point of the gage but does not exceed the melting point of the ceramic.) Surprisingly, this large temperature disparity did not greatly affect the accuracy of the heat flux measurement.

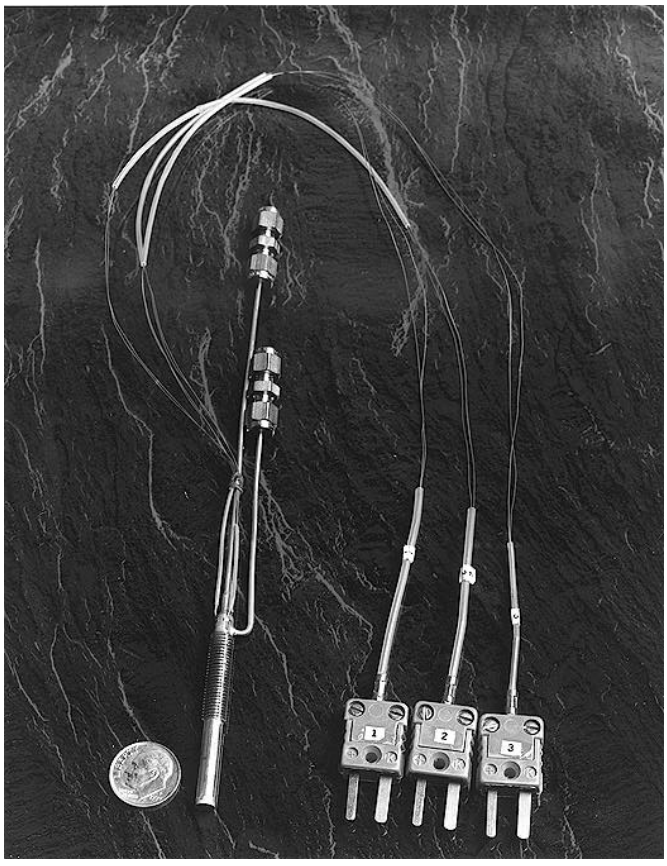

Dual, active, surface heat flux gage probe.

These tests suggest that this sensor can be used to measure heat flux under simultaneous conditions of high free-stream temperatures and large temperature gradients along a wall. A possible application is for transient and steady-state heat flux measurements on the walls of advanced gas turbine and rocket engine apparatus.

Lewis contact: Curt H. Liebert, (216) 433–6483
Headquarters program office: OA

Ratioing Multiwavelength Pyrometer Developed

Temperature is one of the most fundamental measurements in research and development. Often it is necessary to make the measurement from a remote location without physically contacting the measured object. Pyrometry is commonly employed to meet this "remote" requirement.

An object at absolute zero temperature does not emit thermal radiation, but at temperatures above absolute zero it will emit varying amounts, depending on the temperature, according to Planck's law of radiation. With suitable precalibrated detectors the emitted radiation is measured and used to determine temperature. This is pyrometry. It works most conveniently for blackbodies, but real objects are not black. They are called gray or nongray bodies because they radiate less efficiently than an ideal blackbody. Gray objects have constant emissivity at all wavelengths. Nongray objects have different emissivities at different wavelengths. (Wavelength is one of the characteristics of radiation.) Without knowing the emissivity of an object, pyrometry determines only an erroneous radiant temperature, not the actual temperature.

In application environments, in addition to radiation emitted from the measured surface,

radiation originating from other sources and reflected from the measured surface is also detected. The temperature determined from the total radiation would thus be in error. Traditional pyrometers operating at one or two wavelength regions (one-color or two-color pyrometers) cannot correct for errors due to emissivity uncertainty and reflected radiation.

At NASA Lewis an in-house program has developed a new ratioing multiwavelength pyrometer (RMP) that measures temperature by detecting the complete spectra at many wavelengths. The recording times of two spectra are separated by short intervals during which a temperature excursion has occurred such that the emissivity can be considered to remain unchanged. A ratio spectrum is formed by a wavelength-by-wavelength division of these two spectra, whose temperatures are not known. The ratio spectrum does not depend on emissivity because it has been divided out. The equation representing the ratio spectrum is a function of wavelength containing just the two temperatures as unknown parameters. Analysis of this ratio spectrum yields the two temperatures.

In the development of ceramics these nongray emissivity materials are often heated by exposing them to a constant quartz-lamp radiation source. The working principle of RMP allows the ceramic temperatures to be determined by recording the radiation spectra from the ceramics sequentially while the sample temperature is increasing. The ratio of sums and differences of the recorded spectra eliminates the unknown reflected radiation and the unknown emissivity to form a set of new data. Again, analysis of these data as a function of wavelength containing two unknown parameters yields the two temperatures. Other spectra are similarly analyzed to determine their temperatures. Because only the ratios are analyzed, the new pyrometer has the added advantage of not requiring precalibration.

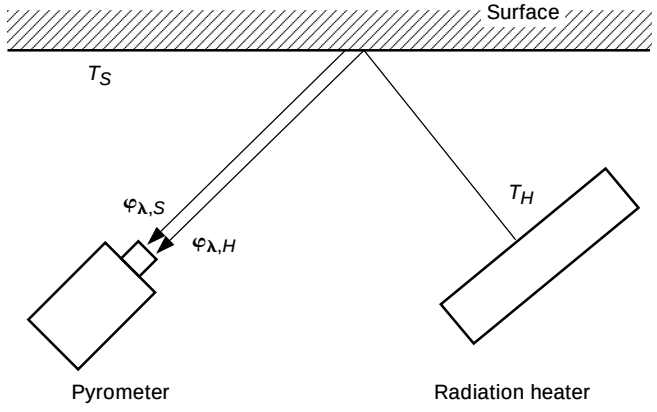

Pyrometer arrangement in a ceramic application.

NASA Lewis has demonstrated RMP under simulated conditions. Blackbody radiation transmitted through an optical medium simulated emitted radiation, while intense quartz radiation specularly reflected from the optical medium simulated the reflected radiation. The blackbody radiation source was heated in steps to allow the slow-working spectrometer enough time to completely record a spectrum. A fast spectrometer is being designed to make a portable version of this instrument for use in projects related to the Advanced High-Temperature Engine Materials Technology Program and the Enabling Materials Program.

Lewis contact: Daniel L.P. Ng, (216) 433–3638
Headquarters program office: OA

Resistance Strain Gage Comparison-Tested Against High-Temperature Extensometry

A palladium-chromiun (PdCr) resistance strain gage developed at NASA Lewis was evaluated and compared with high-temperature extensometry, not only to contrast the two strain measurement techniques but also to investigate the applicability of the PdCr strain gage where extensometry is not viable or practical. Various thermal and mechanical loading spectra were applied by using a high-temperature thermomechanical uniaxial testing system. Strain measurement capabilities to 800 °C were investigated with a nickel-based superalloy (IN100) substrate material, and application to titanium matrix composite (TMC) materials was examined with an SCS–6/Ti–15–3 $[0]_8$ system.

Each specimen was instrumented with two PdCr wire strain gages applied by flame spraying, one gage on each side. A commercially available air-cooled, resistance-based extensometer with a 12.7-mm gage section was mounted on the thick edge of the specimen; the strain gages were mounted on the face of the specimen. A radiant quartz lamp heater was used for specimen

Gaged IN100 test specimen in thermomechanical loading frame equipped with quartz-lamp heating system.

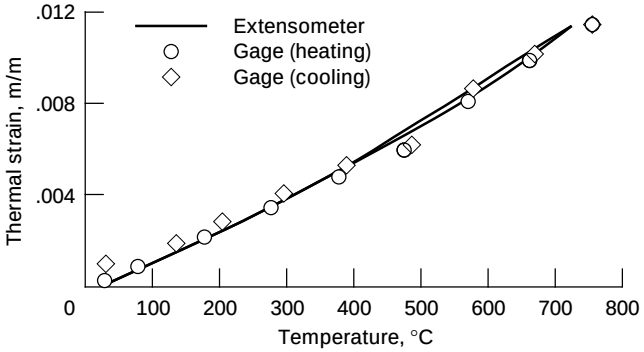

Excellent agreement in thermal expansion strain response of extensometer and PdCr wire gage on IN100.

heating, and type K thermocouples were used to monitor and control temperature.

In general, the PdCr wire strain gage was found to be a useful strain-monitoring device in a thermomechanical loading system equipped with quartz lamp heating. Its apparent strain response was repeatable on both the IN100 and SCS–6/Ti–15–3 specimens. The thermal expansion strain data obtained from the two measurement systems showed excellent agreement to 800 °C. Quasi-static mechanical strain responses of the two systems on both IN100 (to 800 °C) and TMC (to 600 °C) were also in good agreement (within 10%) to 2000 με. At room temperature strain measurements were accurate to approximately 4500 με.

Bibliography

Castelli, M.G; and Lei, J.–F.: A Comparison Between High Temperature Extensometry and PdCr Based Resistance Strain Gages With Multiple Application Techniques. HITEMP Review 1994: Advanced High-Temperature Engine Materials Technology Program, NASA CP–10146, Vol. II, 1994, p. 36–1.

Lewis contacts: Dr. Jih-Fen Lei, (216) 433–3922; Michael G. Castelli, (216) 433–8464; Dr. W. Dan Williams, (216) 433–3725; Rod Ellis, (216) 433–3340
Headquarters program office: OA

Nonintrusive System Measures ASTOVL Hot Gas Ingestion in Wind Tunnel

Nonintrusive techniques for measuring gas parameters in aerospace research facilities are needed to provide flow-field characteristics. The harsh environments encountered in these facilities place demands on measurement systems. Often the mere intrusion of a physical sensor can adversely affect the needed measurement. Optical techniques and promising innovative concepts are not lacking, but there is a large gap between laboratory techniques and accurate and reliable operation in a propulsion research facility. The spectral Rayleigh technique was demonstrated as viable for the first time in such a facility.

Designing high-performance, vertical-lift aircraft requires knowledge of the temperature and velocity of the lift-generated flow field in all operating modes, especially near the engine inlets. During hover or vertical landing, the lift jets impinge on the ground plane and recirculate near the aircraft. Under some conditions the hot exhaust gases can be ingested by the engine inlets, causing loss of efficiency or catastrophic compressor stall. NASA Lewis and McDonnell Douglas conducted an extensive program in Lewis' 9- by 15-Foot Low-Speed Wind Tunnel to study the problem of hot gas ingestion for new ASTOVL (advanced short-takeoff, vertical-landing) aircraft designs.

A nonintrusive optical system based on Rayleigh scattering from ambient air molecules was used to measure the gas temperature and the wingspan component of the velocity in the tunnel. A laser beam was focused in the region under the model in the lift-generated flow field. Light scattered from gas molecules was collected and analyzed by using a Fabry-Perot interferometer, which measured the frequency spectrum of the scattered light. It is this spectrum that contains the information about gas temperature and velocity.

In a significant breakthrough this technique was demonstrated in the harsh environment of a wind tunnel facility, with "dirty" gases, high vibration levels, and high temperatures. Because Rayleigh scattering is from molecules, no seed particles have to be added to the flow to obtain a scattering signal. In fact, noise caused by scattering from unwanted particles in the flow has been an obstacle to applying Rayleigh techniques outside the laboratory environment. This test demonstrated that the spectrally resolved technique used can extract sufficient Rayleigh signal (i.e., temperature and velocity) in the presence of particle noise to make valid measurements in the flow field. Also, laser beam delivery and signal capture was achieved by using fiber optic cables to isolate the laser and interferometer systems from the noisy wind tunnel environment.

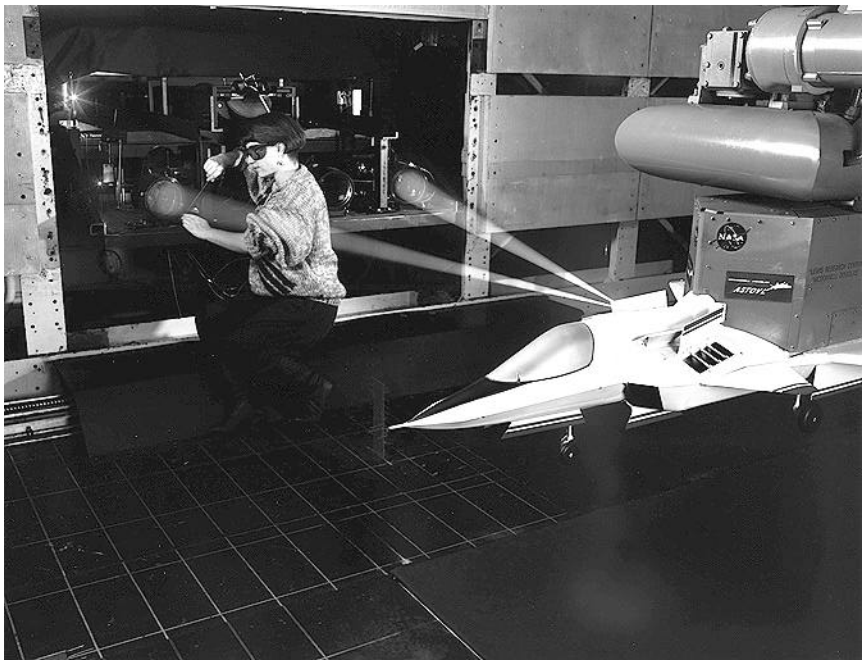

Spectral Rayleigh system in 9- by 15-Foot Low-Speed Wind Tunnel.

The system took data at over 900 measurement locations in a volume under the model while the tunnel and model simulated ground-effect flow (i.e., hover or landing). Temperature measurements were obtained with a 5% mean uncertainty, and single-component velocity measurements (along the wingspan direction) with 10-m/sec uncertainty.

Lewis contacts: Helen E. Kourous, (216) 433–6569; Dr. Richard G. Seasholtz, (216) 433–3754
Headquarters program office: OA

Liquid-Crystal, Point-Diffraction Interferometer Invented

A new instrument, the liquid-crystal, point-diffraction interferometer (LCPDI), was invented at NASA Lewis to measure optical wavefronts in transparent media, such as glasses, gases, and liquids. Typical applications are in verifying the optical performance of lenses and optical elements and in measuring temperature, density, or concentration distributions in air or water during wind tunnel or microgravity experiments. The LCPDI represents an improvement over other techniques because it has both a common-path design and the ability to make digital measurements, providing automated data reduction in a robust package.

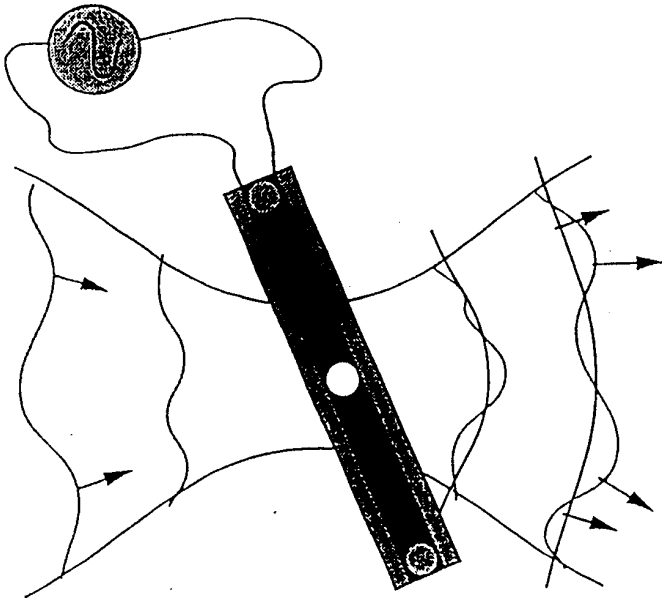

Liquid-crystal, point-diffraction interferometer.

The LCPDI consists of a thin liquid-crystal layer sandwiched between two glass plates. Transparent electrodes are deposited on the inner surface of each plate. The refractive index of the liquid-crystal layer can be modified by altering the strength of an electric field applied across the electrodes. A transparent microsphere is embedded in the liquid-crystal layer near the center of a clear aperture. The refractive index of the microsphere is unaffected by the electric field.

A collimated laser beam is passed through the medium under study and then focused onto the microsphere in the LCPDI. Because the focused spot is larger than the microsphere, some of the light passes through the liquid crystals. This portion of the transmitted beam is called the object beam because it contains information about the transparent medium through which it passed. The rest of the beam passes through the microsphere. This light is diffracted into a spherical reference beam. The object and reference beams travel together until they illuminate a viewing screen, where they combine to form an interferogram. A solid-state camera records the interferogram. Phase-stepping interferometry is used to extract the two-dimensional phase of the object beam from the interferogram. A relative phase shift is introduced between the object and reference beams by changing the strength of the electric field applied across the liquid crystals. A sequence of interferograms is recorded with the phase stepped by nominally 90° between frames. The recorded images are then digitally recombined to extract the phase front. This phase front is analyzed to determine the shape of the lens or the properties of the flow under study.

This work was performed in-house. Two papers have so far been generated from this work, a patent application has been filed, and a joint proposal with a microgravity group has been submitted. The program is ongoing.

Bibliography

Mercer, C.R.; and Creath, K.: Liquid Crystal Point Diffraction Interferometer. Optics Letters, vol. 19, no. 12, 1994, pp. 916–918.

Lewis contact: Carolyn R. Mercer, (216) 433–3411
Headquarters program office: OA

Performance-Limiting Micropipe Defects Identified in SiC Wafers

The in-house High-Temperature Integrated Electronics and Sensors (HTIES) Program at NASA Lewis is currently developing a family of silicon carbide (SiC) semiconductor devices for use in high-temperature, high-power, and/or high-radiation conditions. Conventional semiconductors, such as silicon and gallium arsenide (GaAs), cannot adequately perform under these conditions. Integrated electronics and sensors capable of operating in a hostile environment would have numerous important aerospace-related applications, such as propulsion control, power control, radar and communications, and radiation-hardened circuits. They also would find numerous spinoff applications in the Earth-bound commercial power and automobile industries.

Theoretical appraisals have indicated that SiC power devices would operate over higher voltage and temperature ranges, have superior switching characteristics, and yet have die sizes nearly 20 times smaller than correspondingly rated silicon-based devices. However, these tremendous theoretical advantages have yet to be realized in experimental SiC devices. Prototype SiC devices constructed to date have failed to operate at currents of more than 2 A. Investigations by the NASA Lewis HTIES research group recently identified the crystal defects restricting SiC power devices to these relatively small electrical current levels.

All useful SiC devices are fabricated starting from commercially available silicon carbide wafers. These wafers contain crystal defects called micropipes, small tubular voids that run through the wafers in a direction normal to the polished wafer surface. The NASA Lewis HTIES team showed that micropipe defects originating in SiC wafers are responsible for premature electrical failures in most SiC devices larger than 1 mm^2 in area. In particular, the micropipes were experimentally linked to localized reverse failures at reverse-bias voltages well below the known breakdown voltage inherent to homogeneous SiC. This was found to be the case even when the device is fabricated entirely within high-quality SiC epitaxial layers that have been grown on top of the original SiC wafer, due to the observed fact that the defects propagate from the wafer into the SiC epitaxial layers as they are grown. The accompanying figure shows the visible microplasma that is observed within a micropipe when an SiC diode junction fails prematurely.

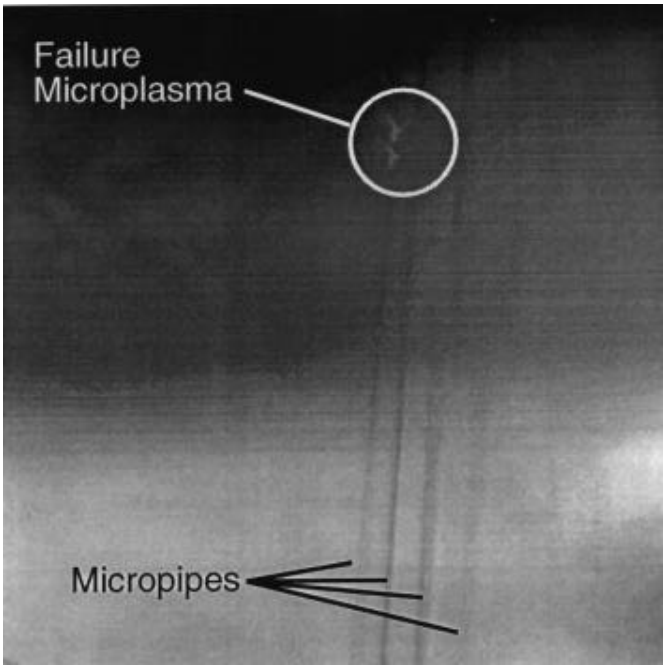

Failure microplasma and micropipes.

The establishment of micropipes in SiC wafers as a defect limiting the performance of high-voltage SiC devices has serious implications for the near-term realization of high-current SiC power devices. Until micropipe density is significantly reduced, SiC power device ratings will be restricted because the defects prevent scaleup to the large device areas (>1 mm^2) needed to carry high current (>10 A). Higher than existing voltage and current ratings will not be attained until improvements in SiC crystal growth enable larger defect-free areas.

The announcement of these findings by the NASA Lewis HTIES team has triggered intensified research worldwide toward eradicating micropipe defects from SiC wafers. A twofold reduction in micropipes was recently announced by Cree Research, Inc.

Lewis contacts: Dr. Philip G. Neudeck, (216) 433–8902; J. Anthony Powell, (216) 433–3652
Headquarters program office: OA

Fiber Optic Control System Integration Program Concluded

The Fiber Optic Control System Integration (FOCSI) Program was a NASA/NAVY program designed to demonstrate that passive optical sensor systems can operate in the severe environment of advanced aircraft. As part of the program an attempt was made to design a standard electro-optic interface that would accommodate analog and digital sensors using various optical modulation techniques.

This program is a foundation for future fly-by-light (FBL) programs. An FBL system utilizes passive optical sensors and fiber optic data links to monitor and control aircraft systems. This technology has many benefits for commercial and military aircraft. It improves reliability and reduces certification costs because FBL aircraft are more immune to electromagnetic effects than fly-by-wire (FBW) aircraft. It reduces waveguide harness and run-length weight and volume. It eliminates short circuits and sparking due to insulation degradation. Other anticipated benefits are lower maintenance costs, absence of signal ground loops, and wider flexibility in control architecture and data bus design.

In the FOCSI program a number of passive optical sensors for the primary flight and propulsion control system were designed to fit alongside electrical sensors in an F–18 aircraft and F404 engine. Flight tests conducted at NASA Dryden indicated that most of the optical sensors tracked the F–18's electrical sensors very well. The flight tests concluded a successful program. The sensors will continue to operate during other missions to obtain some long-term reliability information. In addition to the flight tests a number of useful lessons learned in installation, maintenance, and installed troubleshooting are reported in the final reports of the FOCSI program. The FOCSI program will provide useful information to the military and commercial FBL programs and will help to transition the technology into production aircraft and engine control systems.

Lewis contact: Robert J. Baumbick, (216) 433–3735
Headquarters program office: OA

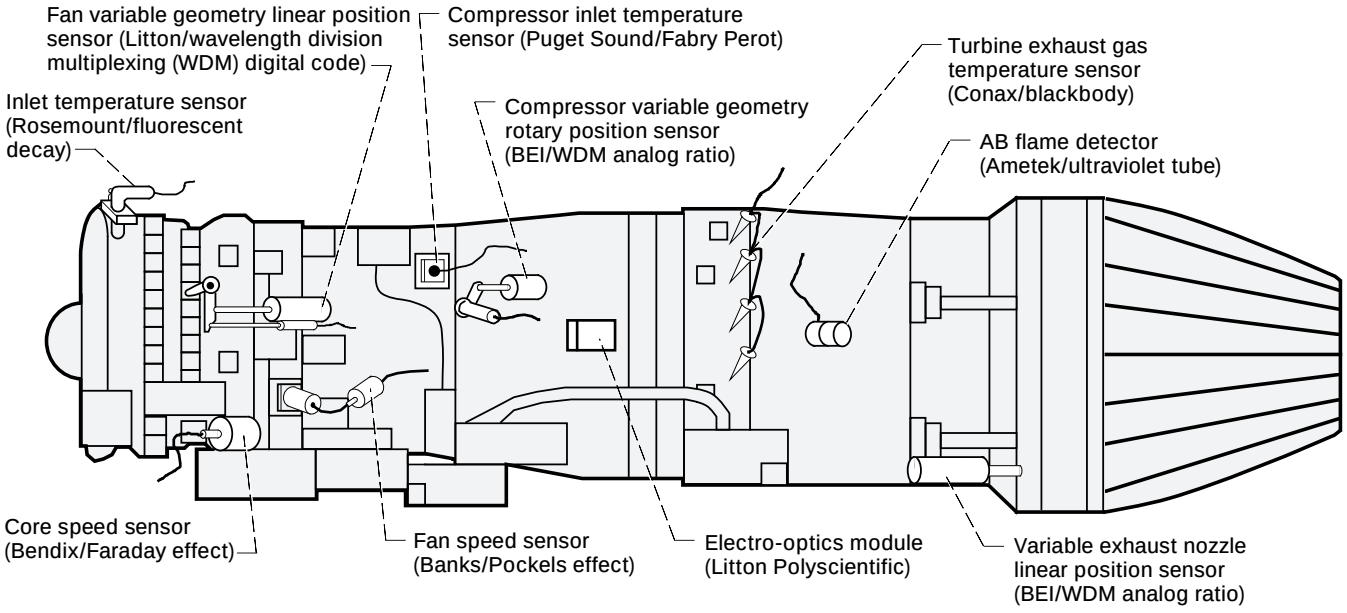

FOCSI propulsion sensors.

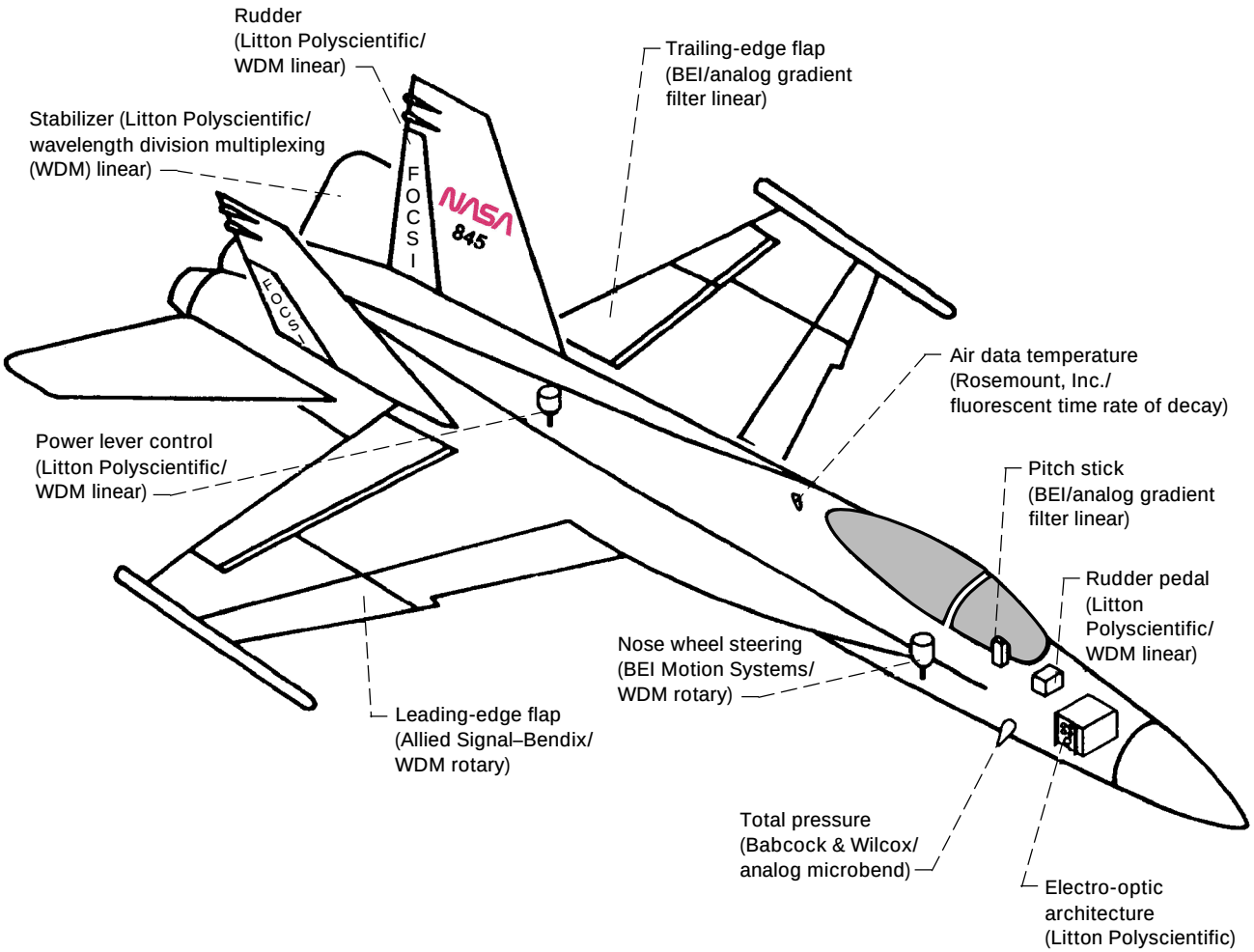

FOCSI flight system configuration.

Silicon Carbide Junction Field-Effect Transistors Developed

The in-house High-Temperature Integrated Electronics and Sensors (HTIES) Program at NASA Lewis is currently developing silicon carbide (SiC) for use in harsh conditions where silicon, the semiconductor used in nearly all of today's electronics, cannot function. Silicon carbide's demonstrated ability to function under extreme high-temperature, high-power, and/or high-radiation conditions will enable significant improvements to a wide variety of applications and systems. On Earth these range from improved high-voltage switching for energy savings in public electric power distribution and electric vehicles to more powerful microwave electronics for radar and cellular communications to sensors and controls for cleaner burning, more fuel-efficient jet aircraft and automobile engines. Silicon carbide electronics will also figure into a variety of NASA missions, from planetary probes needing to withstand high-radiation space environments and Venus' 450 °C atmosphere to advanced supersonic and hypersonic aerospace vehicles that will need advanced sensor and control electronics operating above 550 °C.

Along with small-scale detector and amplification circuits, discrete medium-power diodes and field-effect transistors (FET's) are expected to be among the first SiC electronic components incorporated into these systems. Using its recently developed site-competition epitaxy technique, the NASA Lewis HTIES group has fabricated and characterized several batches of buried-gate junction field-effect transistors (JFET's) that exhibit very promising characteristics. Despite the severe device area limitation (~1 mm^2) imposed by present-day SiC wafer defect densities, SiC JFET's

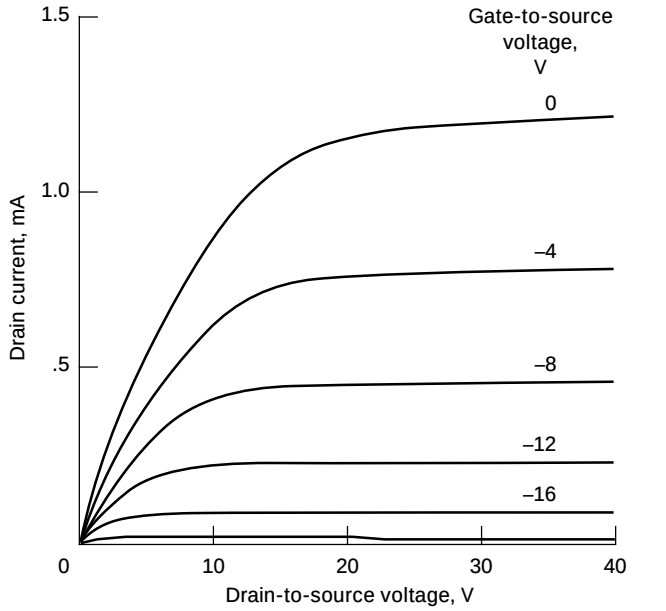

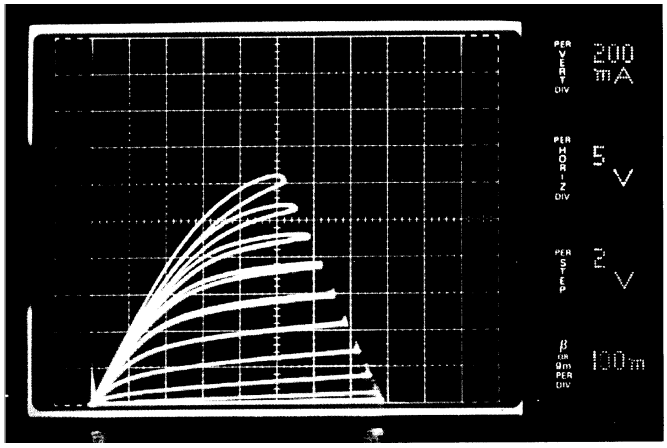

Top: Electrical characteristics of 1.2-A SiC JFET at 24 °C.
Bottom: Electrical characteristics of SiC JFET operating at 600 °C.

with peak drain currents above 1 A at room temperature (top graph) and standoff voltages of 100 V (only40 V of which ar e shown) have been realized. The 1.2-A peak drain current exhibited in the graph represents a record for any SiC FET rated at 100V or mor e with a less-than-20-V switching gate voltage spread. Further substantial increases in device performance can be expected as SiC wafer defect densities are decreased.

JFET's optimized for high-temperature operation were also fabricated as part of this work. These JFET's operated for a record 30 hr in the 600 °C air environment with only a small degradation in device characteristics due to oxidative reactions of the metals used to make electrical contact with the SiC. High-temperature device lifetime should increase when process refinements designed to prevent contact metal oxidation are implemented.

Lewis contacts: Dr. Philip G. Neudeck, (216) 433–8902; Dr.David J. Larkin, (216) 433–8718
Headquarters program office: OA

Site-Competition Epitaxy Controls Doping of Silicon Carbide

Silicon carbide (SiC) is emerging as the material of choice for high-power and/or microwave-frequency semiconductor devices suitable for high-temperature, high-radiation, and corrosive environments. Currently, the initial step in making SiC semiconductor devices is a process called chemical vapor deposition (CVD), which allows single-crystal layers (epilayers) of varying electrical character to be grown. The SiC epilayers are produced in the CVD process by thermally decomposing commercially available silicon and carbon source gases onto boule-derived SiC substrates. The electrical character is tailored by adding dopants, impurity elements that affect the epilayer electrical properties, during the CVD SiC epilayer growth by flowing either nitrogen (for n type) or trimethylaluminum (for p type). However, for the inherently superior high-temperature semiconductor properties of SiC to be realized in advanced electronic devices, control over the electronic properties of the CVD SiC epilayers must be improved.

Control over dopant incorporation for CVD SiC epilayers had been very limited. Reproducible doping was typically confined to a relatively narrow doping range, restricting SiC device performance to below theoretically predicted values. This narrow doping range was recently greatly expanded by the NASA Lewis discovery that the ratio of silicon source flow to carbon source flow during the CVD epilayer growth could be used to control dopant incorporation and therefore the electrical properties of the growing SiC epilayers. This process, named site-competition epitaxy, produces much lower doped SiC epilayers than was previously possible. In addition, site-competition epitaxy can produce more highly doped layers when more electrically conductive SiC epilayers are desired. Expanding the reproducible doping range to include lower concentrations has enabled the fabrication of

multikilovolt SiC power devices, whereas the availability of higher doping concentrations has resulted in devices with improved performance because of lower parasitic resistances.

The site-competition epitaxy working model is based on the competition between the SiC and dopant source gases for the available substitutional lattice sites on the growing SiC crystal surface. Dopant incorporation is controlled by appropriately adjusting the Si/C ratio within the growth reactor to affect the amount of dopant atoms incorporated into these sites, either carbon-lattice sites (C sites) or silicon-lattice sites (Si sites), located on the active growth surface of the SiC crystal. Specifically, our model for site-competition epitaxy is based on the principle of competition between nitrogen and carbon for the C sites and between aluminum and silicon for the Si sites of the growing SiC epilayer. The concentration of n-type (nitrogen) dopant atoms, which can occupy only C sites, incorporated into a growing SiC epilayer can be decreased by increasing the carbon source concentration so that C "out competes" N for the available C sites.

In summary, the nitrogen donor concentration in the grown epilayer is proportional to the Si/C ratio during epilayer growth, whereas the aluminum acceptor concentration is inversely proportional to the Si/C ratio. Site-competition epitaxy was used (as depicted) to produce the very low-doped epilayers required for the world's first 6H-SiC 2000-V and 3C-SiC 300-V diodes. More recently, this novel growth technique has enabled the fabrication of SiC junction field-effect transistors (JFET's) that can operate at 600 °C in air for 30 hr. The site-competition epitaxy technique not only greatly expands the doping range for SiC but also allows for more

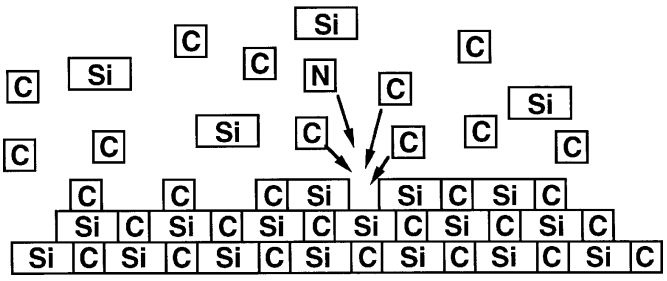

Schematic representation of site-competition epitaxy model illustrating carbon (C) out-competing nitrogen (N) for the vacant C-lattice site of the SiC crystal, resulting in lower N-doping in the epilayer.

reproducible dopant control within the previously attainable doping range. Additionally, site-competition epitaxy is the only known route for growing degenerately doped epilayers that result in ohmic as-deposited (i.e., unannealed) contacts for a variety of metals on both p-type and n-type SiC epilayers.

This work was performed in-house as part of the High-Temperature Integrated Electronics and Sensors (HTIES) Program at NASA Lewis.

Lewis contacts: Dr. David J. Larkin, (216) 433–8718; Dr. Philip G. Neudeck, (216) 433–8902; J. Anthony Powell, (216) 433–3652; Dr. Lawrence G. Matus, (216) 433–3650
Headquarters program office: OA

Parallel Implementation of Real-Time Expert Diagnostic System Achieved

Intelligent rocket engine control systems are desired that significantly reduce operating costs, increase flight rates, improve performance, and extend engine life. Achieving these goals requires engine controllers that have integrated capabilities to diagnose anomalous operation, that implement accommodating closed-loop control to extend engine life, and that maximize available system performance (ref. 1). A reusable rocket engine diagnostic system (ReREDS) has been developed for use in intelligent control systems of the space shuttle main engines (SSME's) and other reusable rocket engines (refs. 2 and 3). However, a practical implementation of this expert system was needed that would allow failure diagnosis to be carried out in real time. NASA Lewis has developed and demonstrated a methodology for the parallel, real-time implementation of expert systems using the ReREDS expert diagnostic system.

A sequential, or serial, implementation of ReREDS using the CLIPS expert system development tool on an off-the-shelf microcomputer was found to be too slow to be practical. However, as implemented serially, ReREDS already exhibited a certain degree of inherent parallelism. Ten sensor measurements are used to diagnose the presence of five different failures that may manifest themselves in the working SSME. Each module of code that diagnoses one failure is called a failure detector. Although some sensor measurements

are shared between failure detectors, the computations within these detectors are completely independent of one other. Thus, the failure detection problem was partitioned so that each failure detector was assigned to its own processor. Because the failure detectors can be processed simultaneously, a speedup in the execution is expected.

This partitioned architecture for the expert diagnostic system and the CLIPS expert system development tool were ported to the NASA Lewis iPSC/860 hypercube parallel computer. Each failure detector resides on a node of the hypercube. The correct operation of each individual failure detector was verified by using simulated SSME sensor data. An ANSI C program was written initializing the copy of CLIPS on each node, so that CLIPS was used as an embedded application on each failure detector node to evaluate the ReREDS failure detection rules. All other program requirements, including opening and closing of sensor measurement data files, preliminary data analysis, and program flow control, are handled in C language. In addition, a server node, programmed entirely in C language, transfers incoming sensor data into an indexed memory array, or blackboard, from which data are distributed on request to the failure detector nodes. A manager node coordinates timing between failure detector nodes and the server node. Using a C language executive on each node and embedded CLIPS language reasoning on each failure detector node provides an efficient structure for realizing context focusing, process interruption, and overall expert system communications and synchronization.

Profiling studies found that the parallel ReREDS implementation could process the sensor measurements and report confidence levels for all five failure modes in 18 msec, nearly three times faster than the serial implementation on the same computer, and much faster than the 100 msec normally required. Additional speedup could be achieved by parallelizing the data source because the failure nodes tended to spend considerable time waiting while contending for data from the server node. However, in general the method used provides a fast, predictable, continuously operating failure detection system. In addition, this method should be useful for implementing other expert systems requiring real-time operation.

This work was carried out through a cooperative agreement between NASA Lewis and Cleveland State University.

References

1. Merrill, W.; and Lorenzo, C.: A Reusable Rocket Engine Intelligent Control. 24th Joint Propulsion Conference, Cosponsored by AIAA, ASME, and ASEE, Boston MA, July 1988.

2. Guo T.–H.; and Merrill, W.: A Framework for Real-Time Engine Diagnostics. 1990 Conference for Advanced Earth-to-Orbit Propulsion Technology, Marshall Space Flight Center, Huntsville, AL, May 1990.

3. Anex, R.P.; Russel, J.R.; and Guo, T.–H.: Development of an Intelligent Diagnostic System for Reusable Rocket Engine Control. AIAA Paper 91–2533, 1991.

Lewis contact: John C. DeLaat, (216) 433–3744
Headquarters program office: OA

Closed-Loop Control Demonstrated for Rocket Engine Faults

The goal of the Intelligent Control System Program is to extend the useful life of a reusable rocket propulsion system while minimizing flight maintenance and maximizing performance through improved control and monitoring algorithms. During the past years the program has successfully demonstrated real-time fault accommodation of two classes of faults: sensors and actuators. The closed-loop simulation of the engine control during the fault and after the accommodation provides important information for the actual implementation of the algorithms. For sensor faults an autoassociative neural network is used to detect an abnormal sensor reading and also to estimate the actual value. For actuator faults a model-based fault detection system with a reconfigurable control is used in the closed-loop environment.

In sensor failure accommodation a group of analytically redundant measurements, including all the variables used in the closed-loop control for engine performance, is first identified. The data generated from the engine model as well as from the test-bed engine firing are used to train the autoassociative neural network, which operates on the principle of dimensionality

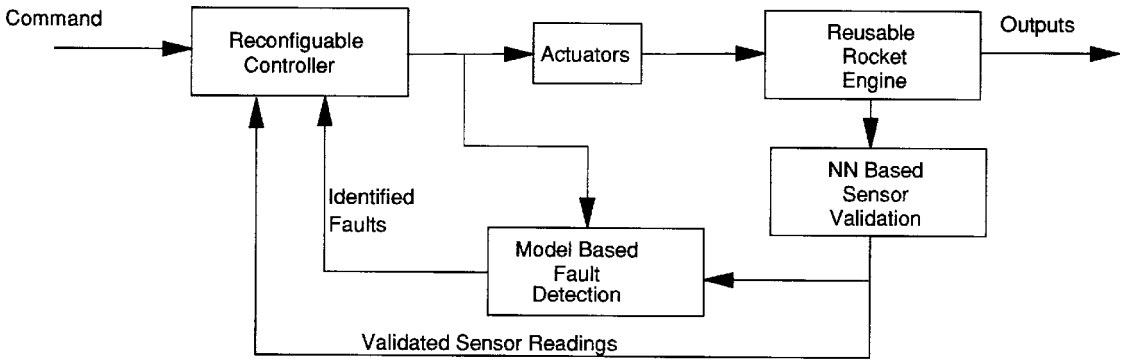

Fault accommodation in closed-loop control for reusable rocket engines.

reduction. The network is trained to produce an output vector equal to its original input vector. The redundant sensor information is compressed, mixed, and regenerated to provide an estimate of the true measurement. Sensor failure is accommodated by replacing the failed sensor with the estimate for the controller. Simulation results show that the proposed sensor validation scheme can adequately identify the failed sensors and provide reasonable estimates for control purposes.

Model-based fault detection is used to detect actuator failures. A nominal engine model detects any abnormal operating behavior that can be classified into a specified structure. A fault model with a vector of fault parameters associated with all actuator faults is first developed. Different fault parameters represent different types of faults of a specific actuator. A recursive, least-squares error algorithm performs the real-time estimation of the fault parameters from the most current input/output data and the system matrices, which have been determined a priori. An actuator fault is accommodated on two levels. On the vehicle level the information about the actuator fault is used to determine the thrust command to the engine in order to maintain the mission goal. On the engine level a reconfigurable control is used to execute the engine command with a reduced capability in actuation.

References

1. Merrill, W.C.; and Lorenzo, C.F.: A Reusable Rocket Engine Intelligent Control. 24th Joint Propulsion Conference, Boston, MA, July 11–13, 1988.

2. Guo, T.-H.; and Musgrave, J.: Closed Loop Evaluation of Neural Network Based Sensor Validation. Advanced Earth-to-Orbit Propulsion Technology Conference, NASA Marshall Space Flight Center, Huntsville, AL, May 16–18, 1994.

3. Musgrave, J.; Guo, T.–H.; Wong, E.; and Duyar, A.: Real-Time Accommodation of Actuator Faults on a Reusable Rocket Engine. Advanced Earth-to-Orbit Propulsion Technology Conference, NASA Marshall Space Flight Center, Huntsville, AL, May 16–18, 1994.

Lewis contacts: Dr. Walter C. Merrill, (216) 433–6328; Dr. Ten–Huei Guo, (216) 433–3734
Headquarters program office: OA

Piloted Evaluation Performed for Integrated Propulsion and Airframe Control Design Methodology

The trend is toward military fighter and tactical aircraft with new or enhanced maneuver capabilities, such as short takeoff and vertical landing (STOVL) and high-angle-of-attack performance. An integrated flight and propulsion control system is required to obtain these enhanced capabilities while maintaining reasonable pilot workload. At NASA Lewis an integrated control design methodology called IMPAC, Integrated Methodology for Propulsion and Airframe Control, has been developed and then applied to the development of a STOVL aircraft control design (ref. 1). A piloted evaluation of this control design has been performed in-house at NASA Lewis on a fixed-base flight simulator (ref. 2).

The NASA Lewis flight simulation facility consists of a cockpit equipped with five pilot effectors, a control computer where the integrated control algorithm resides, a simulation computer that houses the integrated propulsion and airframe model, a Unix workstation for graphics development, an image generation system, and three overhead projectors that display the out-the-

window scenery and heads-up display symbology on a wraparound forward projection screen. For this program the cockpit and displays were configured to simulate the operation of a STOVL aircraft.

A piecewise linear airframe model was created to simulate the dynamic operation of an ejector-configured conceptual STOVL aircraft. This airframe model was then coupled with a multinozzle turbofan engine model. For this evaluation the integrated engine and airframe model was limited to the flight envelope in the transition from cruise to hover. The integrated flight and propulsion control algorithm was developed using IMPAC. Initial pilot comments and suggestions were very helpful in arriving at the simulator configuration used for the final piloted evaluation.

In the final piloted evaluation two NASA test pilots were asked to fly several predefined evaluation tasks to assess controllability, performance, and workload during a series of four flight scenarios. The selected tasks required the control to undergo the longitudinal, lateral, acceleration, and deceleration commands necessary for a STOVL aircraft flying in the transition flight envelope. The pilots successfully completed the evaluation and commented favorably about the performance and workload for all the tasks.

This work has resulted in the development of a flexible, fixed-base flight simulation facility for integrated airframe and propulsion control systems research. It has also resulted in the successful demonstration of IMPAC as a highly useful control design methodology. Plans include using the simulation facility and IMPAC for other integrated flight and propulsion control programs.

References

1. Garg, S.; and Mattern, D.L.: Application of an Integrated Methodology for Propulsion and Airframe Control Design to a STOVL Aircraft. AIAA Paper 94–3611–CP, 1994.

2. Bright, M.M.; Simon, D.L.; Garg, S.; and Mattern, D.L.: Piloted Evaluation of an Integrated Methodology for Propulsion and Airframe Control Design. AIAA Paper 94–3612–CP, 1994.

Lewis contacts: Michelle M. Bright, (216) 433–2304;
Donald L. Simon, (216) 433–3740
Headquarters program office: OA

Dynamic Wave Rotor Performance Modeled

The wave rotor is being investigated for use as a core gas generator in future gas turbine engines in order to achieve high peak cycle temperatures and pressures. The device uses gas-dynamic waves to transfer energy directly to and from the working fluid through which the waves travel. It consists of a series of constant-area passages that rotate around an axis. Through rotation the ends

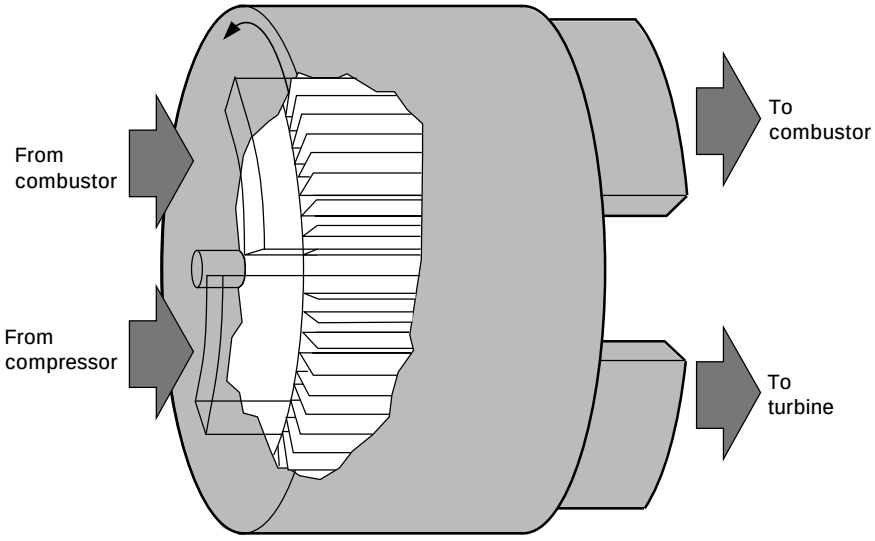

Wave rotor schematic.

of the passages are periodically exposed to various circumferentially arranged ports that initiate the traveling waves within the passages. Because each passage of the wave rotor is periodically exposed to both hot and cold flow, the mean temperature of the rotor material should remain considerably below the peak cycle temperature. Preliminary steady-state design calculations were made for a four-port wave rotor core using subsonic engine technology planned for entry into service in the year 2015. The results indicate that the wave rotor can readily meet aerothermodynamic requirements and maintain a mean passage wall temperature approximately 440 deg C below the peak cycle temperature.

Although the steady-state performance of the wave rotor appears promising, critical questions concerning dynamic performance when the port conditions are transient (i.e., fuel flow or inlet pressure perturbations) remain. To answer these questions, NASA Lewis developed a model that predicts the state of the fluid in all wave rotor passages as they are exposed to the various ports at the ends. The conditions in the ports may be either steady or transient. The passages are assumed to have uniform properties at any cross section (i.e., one-dimensional flow), and the gas is assumed to be calorically perfect. The model can assess losses induced by viscosity, by heat transfer to and from the passage walls, by the finite opening time of the passages as they enter and exit port regions, and by gas leakage between the passage ends and the stationary walls to and from the cavity in the rotor center. The combustor and cavity, having much larger time constants than the rotor passages, are modeled by using lumped-volume techniques. The wave rotor model has been tested in preliminary simulations using step changes from the design point in fuel flow and exhaust port backpressure.

Lewis contact: Daniel E. Paxson, (216) 433–8334
Headquarters program office: OA

Internal Fluid Mechanics

DRAGON Grid Developed

When numerically simulating flows in a typical real-world device for aerospace applications, grid generation has been a time-pacing portion of the overall calculation. In aeropropulsion calculations, such as for seals, combustors, turbine coolant passages, nozzles, and integrated engine/airframe, grid generation can be tedious and cumbersome. The ability to model geometry closely and quickly for each configuration change during the design and analysis cycle is the key to reducing cost and increasing productivity. Hence, development of an efficient, reliable, and accurate grid-generation technique was the subject of research at NASA Lewis.

During the last two decades both structured and unstructured grid techniques have been developed and employed for solving computational fluid dynamics (CFD) problems. These techniques are the two mainstream approaches for dealing with situations where complex geometry imposes great constraints and difficulties in generating grids. (The CHIMERA method, which oversets grids generated separately for resolving individual geometrical or flow features, belongs to the first category.) Both approaches have strengths and weaknesses but can complement each other. Thus, we propose a hybrid grid scheme that maximizes each approach's advantages and minimizes its weaknesses.

As in the CHIMERA method we first divide up the physical domain by a set of high-quality, body-fitted structured grids separately generated and overlaid about a complex configuration. To eliminate any pure data manipulation in interpolating the overlapped region, which does not necessarily follow governing equations, we directly replace only the region of arbitrary grid overlapping with nonstructured grids. Thus, the term "DRAGON grid" is coined. Because the nonstructured grid region sandwiched between the structured grids is limited in size, the increase in memory and computational effort is small. The DRAGON method has three important advantages:

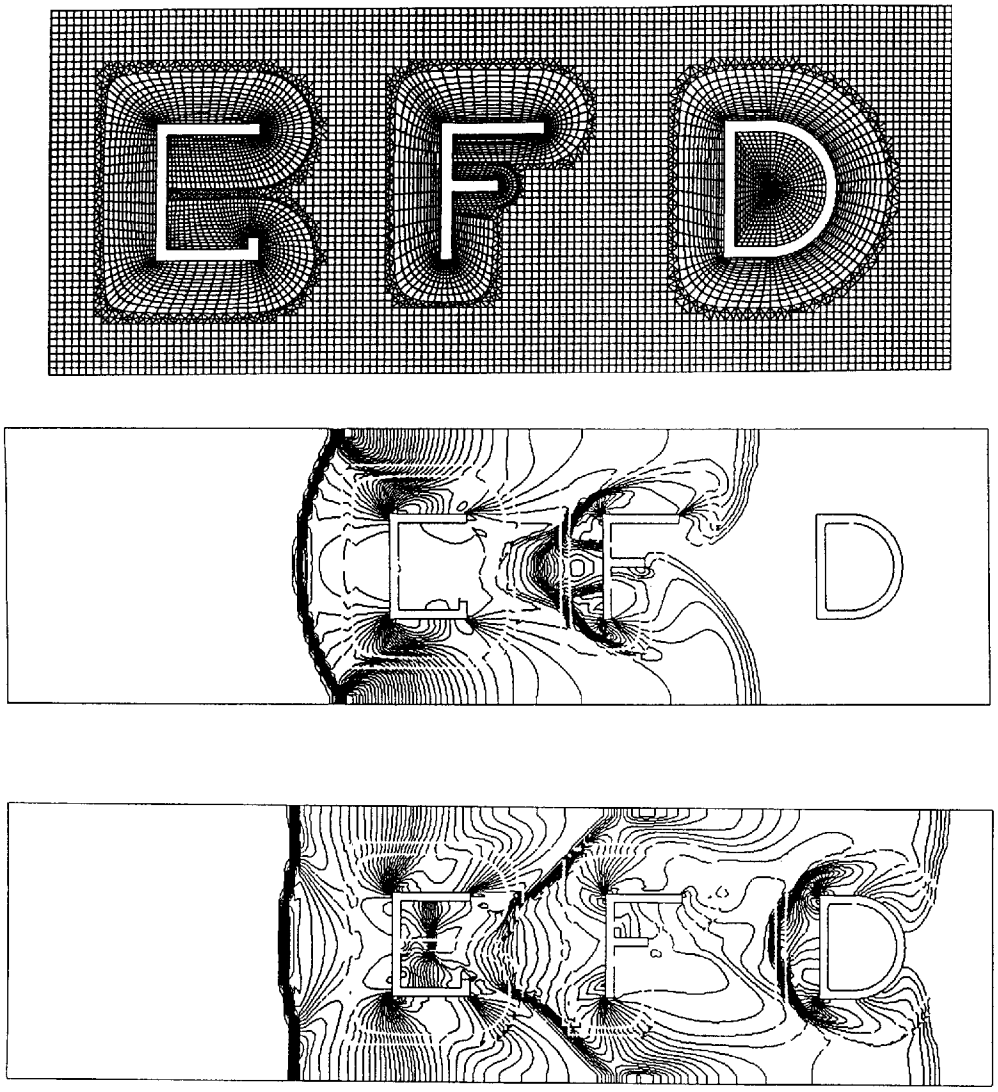

Top: DRAGON grid for letters "CFD." Bottom: Evolution of pressure contours at two representative times.

- It preserves the strengths of the CHIMERA method.
- It eliminates difficulties sometimes encountered in CHIMERA.
- It makes grid communication fully conservative and consistent.

To demonstrate DRAGON's capability, we show various types of grid topologies used for the letters "CFD," together with the resulting DRAGON grid and the evolution of flow over these letters at two different times. Extension to three dimensions is under way. This work has been conducted in collaboration with Dr. Kai-Hsiung Kao of the Institute for Computational Mechanics in Propulsion at NASA Lewis.

Bibliography

Kao, K.–H.; and Liou, M.–S.: An Advance in Overset Grid Schemes: From CHIMERA to DRAGON Grids. 2nd Overset Composite Grid and Solution Technology Symposium, Oct. 25–28, Fort Walton Beach, FL, 1994.

Liou, M.–S; and Kao, K.–H.: Progress in Grid Generation: From CHIMERA to DRAGON Grids. *Frontiers of Computational Fluid Dynamics*, John Wiley, 1994.

Lewis contact: Dr. Meng-Sing Liou, (216) 433–5855
Headquarters program office: OA

Predictive Capability Improved for Transition Region of Turbine Vanes and Blades

Predicting heat transfer and aerodynamic performance for a turbine blade or vane is a formidable task. High-temperature combustion gases flow with turbulence intensities ranging from 5 to 20% over curved surfaces that experience favorable and adverse pressure gradients. This task is further complicated if a significant portion of the turbine blade or vane flow is in transition between laminar and turbulent boundary layer states. To improve prediction of turbine blade performance, a NASA/university/industry team is evaluating the effects of free-stream turbulence, convex and concave curvature, favorable and adverse pressure gradients, and wakes on transition. The team consists of researchers from NASA Lewis, NASA Ames, NASA Langley, the University of Minnesota, the University of Texas at Austin, Texas A&M, Case Western Reserve University, the University of Toledo, and Dynaflow, Inc.

Experiments on flat surfaces, curved surfaces, and airfoil shapes with and without simulated rotor wakes are being carried out in a number of facilities. Measurements from the experiments are providing benchmark data for investigating fundamental mechanisms, developing models, and checking numerical predictions.

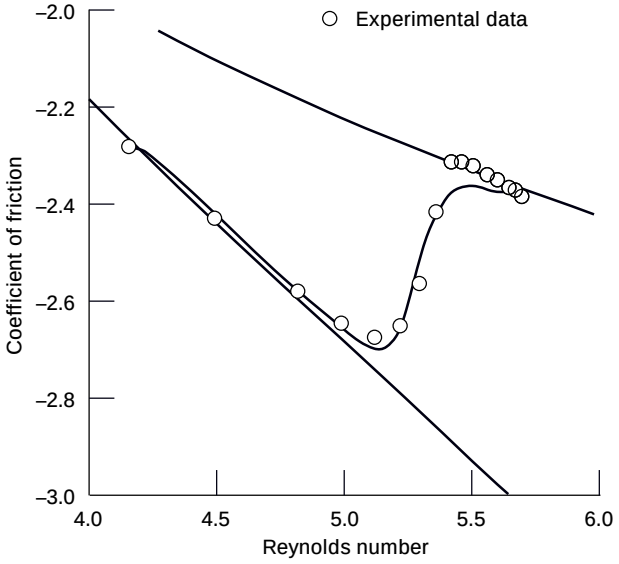

Numerical prediction of transition flow using University of Texas multi-time-scale model compared with experimental data of Savill.

Direct numerical simulation (DNS) analyses are being made to provide a numerical data base for modeling and investigating mechanisms. The experimental data generated in the program aid in validating the DNS results.

Turbulence models are being developed for the numerical prediction of transition heat transfer. The development and assessment of these models are being guided by the experimental and DNS results. Using two-equation turbulence models has in general successfully predicted bypass transition onset. DNS results have shown that a two-equation turbulence model can simulate the nonlinear disturbance growth that produces the first sign of laminar-to-turbulent transition. Single-wire measurements of the boundary layer also agree with the DNS results for disturbance growth.

Experimental measurements made in the transition region indicate the incomplete development of the cascade of energy from large to small scales, pointing to the need for a multi-time-scale k-ε equation. Such a model has been developed and shows much promise for the numerical prediction of the transition region.

Some program accomplishments are as follows:

- An extensive experimental data base of bypass transition on flat and curved surfaces has been generated.
- Two-equation turbulence models appear to capture the growth of nonlinear disturbances in bypass transition and can predict transition onset. These models, however, underpredict the transition length. Prediction of the transition length has been accomplished by modeling the intermittent and nonequilibrium nature of the transition region.
- DNS has proven to be a very powerful tool for understanding the physics, has supported and guided the experimental results, and has generated a data base for the development and testing of transition turbulence models.

Bibliography

Savill, A.M.: Turbulence Model Predictions for Transition Under Free-Stream Turbulence. Presented at the RAeS Transition and Boundary Layer Conference, Cambridge, England, 1991.

Simon, F.F.: A Research Program for Improving Heat Transfer Prediction for the Laminar to Turbulent Transition Region of Turbine Vanes/Blades. NASA TM–106278, 1993.

Lewis contact: Frederick F. Simon, (216) 433–5894
Headquarters program office: OA

Heat Transfer Data Obtained in Transition Ducts

A continuing objective in gas turbine technology is higher engine efficiency. The resulting higher turbine-inlet temperatures and pressures increase the importance of knowing the gas path surface temperatures and, thus, require accurate knowledge of the heat transfer for design and code validation.

At NASA Lewis we tested several transition ducts in a transient air tunnel (atmospheric inlet and vacuum exhaust) using thermochromic (temperature sensitive) liquid crystals painted on the ducts' complex curved surfaces to produce high-resolution, heat-transfer-coefficient maps. Maps were produced at various inlet Reynolds numbers to 2,400,000; Mach numbers to 0.55; and grid-generated, high free-stream turbulence intensities to over 15%. The geometries included one square-inlet, rectangular-exit duct and three round-inlet ducts (a long superelliptic; a short superelliptic; and a short conical cornered). The figure (for the round-inlet, long superelliptic duct test) shows isotherms (constant-temperature bands produced by the liquid-crystal coating on the surface of the preheated transition duct) at various times during duct cooling. Each isotherm corresponds to a different heat-transfer-coefficient value.

The transient, liquid-crystal heat transfer technique used is based on the classic one-dimensional, semi-infinite-wall heat transfer conduction problem. A transition duct was preheated (not over 66 °C (150 °F)) before allowing room-temperature air to be suddenly drawn through it. The resulting isotherms on the duct surfaces were revealed by using a surface coating of thermochromic liquid crystals, which display distinctive colors at particular temperatures (typically around 38 °C (100 °F)). A videotape was made of the temperature and time data for all points on the duct surfaces during each test. The

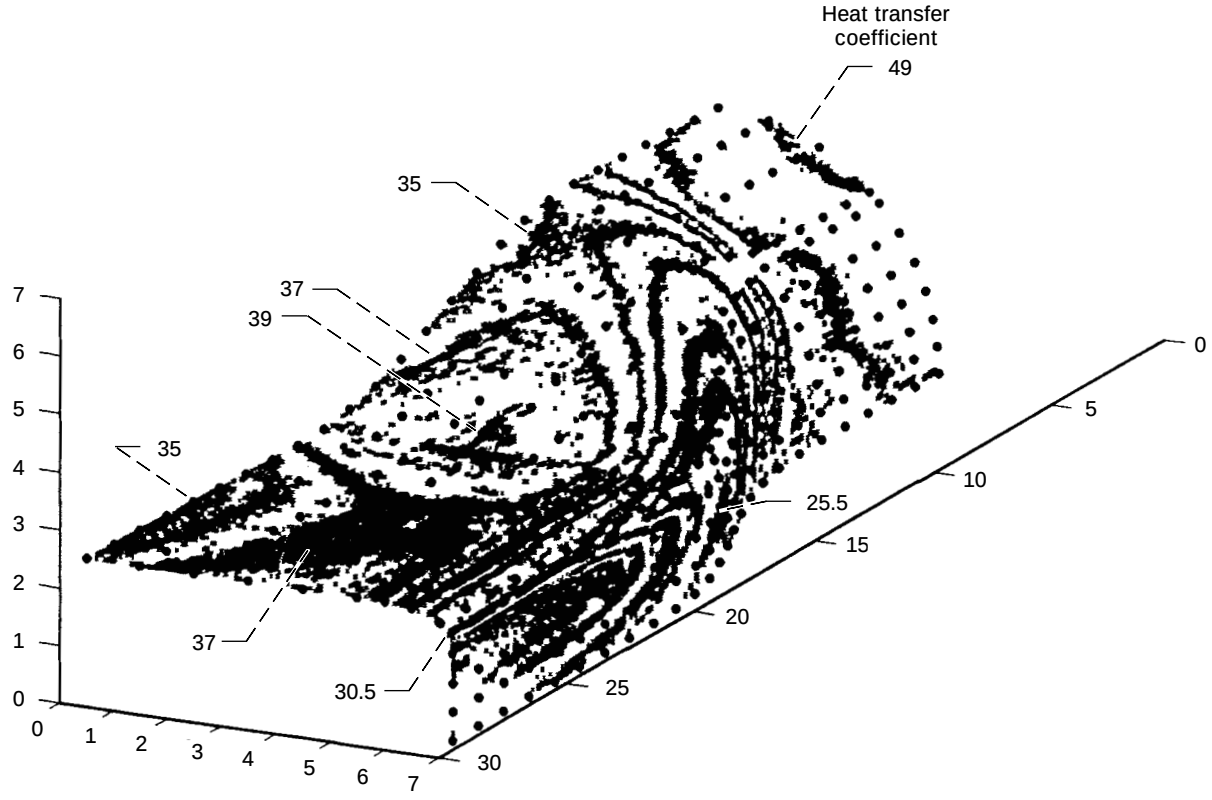

Heat-transfer-coefficient map for superelliptic transition duct.

duct surfaces were uniformly heated by using two heating systems: an automatic-temperature-controlled heater blanket completely surrounding the test duct like an oven, and an internal hot-air loop through the inside of the test duct. The hot-air loop path was confined inside the test duct by insulated heat dams at the duct inlet and exit. A recirculating fan moved hot air into the duct inlet, through the duct, out the duct exit, through the oven, and back to the duct inlet. The temperature nonuniformity of the test duct model wall was kept very small. The heat transfer coefficients could be calculated for the color isothermal patterns produced when the temperature of the air flowing through the duct, the initial temperature of the duct wall, and the surface cooling rate measured at any location with time were known. Although the tests were run transiently, the heat transfer coefficients are for the steady-state case.

This transient, liquid-crystal heat transfer technique is applicable to compound curved surfaces. Because the model rather than the tunnel air is heated, large mass flows of heated air are not required—saving heating costs. The short time for the transient test (2 min), in contrast to running a steady-state tunnel for long periods of time, also saves air-generating costs. This technique should now be considered as possibly a superior alternative to thermocouples for such low-temperature tests as described here because it is nonintrusive, cheaper, and continuous in coverage.

This technique (with unheated tunnel airflow) was first presented by Jones and Hippensteele in 1987 (ref. 1). A grant with Professor C. Camci, of Pennsylvania State University, had the objective of implementing a highly automated heat-transfer-coefficient mapping technique on a digital image-processing system (PC–AT compatible using data translation boards). The digital image-processing system captures color images in the hue-saturation-intensity mode. Data from the square-inlet transition duct were also used by Camci et al. (refs. 2 to 4) in developing the hue-capturing technique for the color video image processing used in the data reduction to calculate the heat transfer coefficients. The ASME awarded reference 5 the Heat Transfer Division Best Paper of the Year for 1994.

References

1. Jones, T.V.; and Hippensteele, S.A.: High-Resolution Heat-Transfer-Coefficient Maps Applicable to Compound-Curve Surfaces Using Liquid Crystals in a Transient Wind Tunnel. Developments in Experimental Techniques in Heat Transfer and Combustion, HTD, vol. 71, 1987, pp. 1–9.

2. Camci, C.; Kim, K.; Hippensteele, S.A.; and Poinsatte, P.E.: Convection Heat Transfer at the Curved Bottom Surface of a Square to Rectangular Transition Duct Using a New Hue Capturing Based Liquid Crystal Technique. ASME Fundamental Experimental Measurements in Heat Transfer, HTD, vol. 179, 1991, pp. 7–22.

3. Camci, C.; Kim, K.; and Hippensteele, S.A.: A New Hue Capturing Technique for the Quantitative Interpretation of Liquid Crystal Images Used in Convective Heat Transfer Studies (91–GT–122). J. Turbomach., vol. 114, no. 4, 1992, pp. 765–775.

4. Camci, C.; Kim, K.; Hippensteele, S.A.; and Poinsatte, P.E.: Evaluation of a Hue Capturing Based Transient Liquid Crystal Method for High-Resolution Mapping of Convective Heat Transfer on Curved Surfaces. J. Heat Trans., vol. 115, 1993, pp. 311–318.

5. Hippensteele, S.A.; and Poinsatte, P.E.: Transient Liquid-Crystal Technique Used to Produce High-Resolution Convective Heat-Transfer-Coefficient Maps. NASA TM–106083, 1993.

Lewis contact: Steven A. Hippensteele, (216) 433–5897

Headquarters program office: OA

Roughness Added to Transonic Axial Compressor Rotor

To study the performance deterioration of a high-speed axial compressor rotor caused by an increase in surface roughness, a coating was applied to the rotor blades that produced a surface roughness comparable to that obtained from in-service use. The coating decreased efficiency by 6 percentage points and reduced the pressure ratio across the rotor by 9% at an operating condition near the design point. To assess which portions of the airfoil were most sensitive to roughness variations, the coatings were applied to different portions of the blade surface, and aerodynamic performance measurements were acquired for each coating configuration.

The results at design speed for a constant rotor-inlet mass flow are shown in the graph. The blade

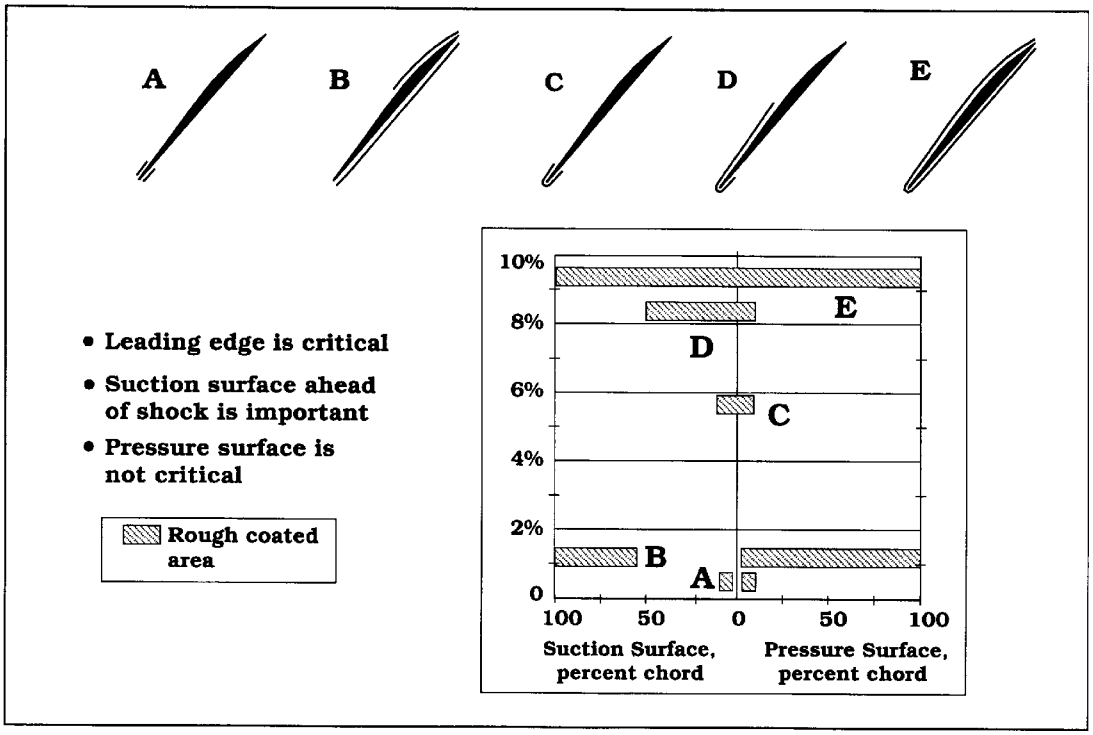

Loss in pressure rise as function of rough-coated surface area.

leading edge and the first 50% chord of the blade suction surface (configuration D) account for about 90% of the performance degradation observed for the fully coated configuration, E. In addition, comparing coating configurations A and C indicates that the leading-edge region is very sensitive to roughness effects. However, case B shows that the pressure surface is insensitive to roughness variations.

To determine the flow mechanisms responsible for the observed performance deterioration, detailed measurements using laser anemometry—as well as predictions generated by a quasi-three-dimensional, Navier-Stokes flow solver, which includes a surface roughness model—were performed on the baseline blade and the fully coated configuration. The results indicate that the rough coating increases the suction-surface boundary layer upstream of the shock, significantly thickening the suction-surface boundary layer downstream of the shock/boundary layer interaction. This increase in blockage reduces the overall diffusion across the blade passage, thereby reducing the aerodynamic performance of the rotor.

Bibliography

Suder, K.L.; Chima, R.V.; Strazisar, A.J.; and Roberts, W.B.: The Effect of Adding Roughness and Thickness to a Transonic Axial Compressor Rotor. ASME Paper 94–GT–339, 1994.

Lewis contact: Kenneth L. Suder, (216) 433–5899
Headquarters program office: OA

Mass Flow Removal Used to Control Supersonic Boundary Layer Separation

Renewed interest in high-speed civil transport has brought with it concerns about the performance of mixed-compression supersonic inlet systems. Such systems present several key challenges to an inlet aerodynamicist. One of these challenges is the control of their inherent shock wave/boundary layer interactions. These interactions can create boundary layer separations, which can cause unacceptable reductions in inlet performance.

When attacking the problem of boundary layer separation caused by a reflected oblique shock wave impinging on a turbulent boundary layer,

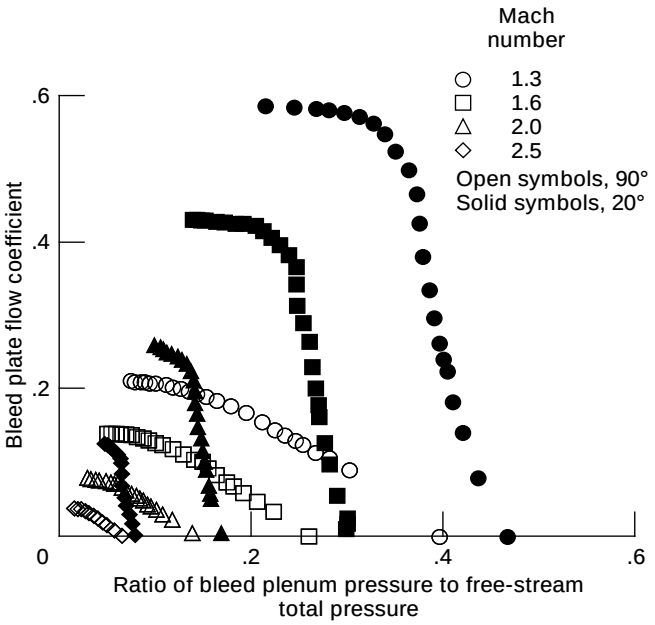

Bleed plate flow coefficient for 20° and 90° hole configurations.

inlet aerodynamicists have consistently turned to the technique of mass flow removal. Colloquially referred to as "bleed," the technique uses a suction pressure differential across a porous surface to draw off the low-momentum air associated with the boundary layer. Typically, the porous surface is an array of holes (scaled to the boundary layer displacement thickness) machined into the flow surface. When applied to the shock wave/boundary layer interaction region, bleed controls the separation by increasing the average kinetic energy of the boundary layer, thus helping it overcome the adverse pressure gradient associated with the shock wave. Most of the data on bleed effectiveness were gathered from systems tests of mixed-compression supersonic inlets. Relatively minimal effort has been spent on the basic "why and how it works" level. Because of this imbalance, bleed application tends to be heuristic.

In an effort to provide technology tools for the development of highly efficient supersonic boundary layer bleed systems, NASA Lewis began a program in the 1- by 1-Foot Supersonic Wind Tunnel to explore the fundamental dynamics of bleed mass flow removal. The initial task for this program was to develop a parametric data base describing bleed hole efficiencies for a range of supersonic conditions (Mach 1.3, 1.6, 2.0, and 2.5). Nine configurations were evaluated; the first graph shows the results of round holes inclined 20° and 90° to the flow surface.

The next task was to apply one of these configurations (90° holes) to a reflected oblique shock wave/boundary layer interaction typical of a mixed-compression inlet. For this effort the inviscid impingement point of the shock wave was placed at the center of the bleed configuration. The second graph shows streamwise surface static pressure plots for the interaction with maximum bleed and with no bleed—the first-order measure of goodness being the comparison to the inviscid surface static pressure profile. It is evident that bleeding the boundary layer moves the static pressure profile toward the inviscid (optimal) solution. Characterization of the bleed system dynamics included taking pitot pressure profiles throughout the interaction zone as well as applying a pressure-sensitive paint technique to the interaction region.

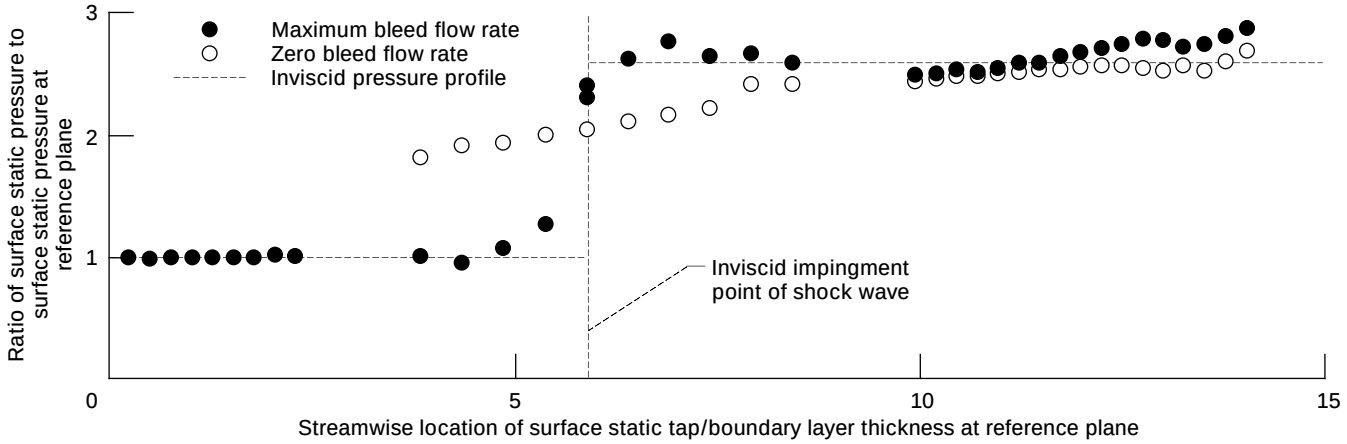

Streamwise surface static pressure profiles throughout interaction region of Mach 2.5, 8°-wedge-angle reflected oblique shock wave/turbulent boundary layer interaction.

This initial effort helped establish a baseline for the program. Future efforts are planned that will further characterize bleed system dynamics by subjecting the bleed region to various flow fields, such as distorted boundary layers. Additional bleed hole efficiency tests aimed at characterizing typical inlet nacelle materials will be performed.

Lewis contact: Brian P. Willis, (216) 433–2176
Headquarters program office: OA

Interactive Design Software Developed

To maintain a competitive edge in the marketplace, American aerospace companies must shorten the time spent on design. In the preliminary design phase the engineer must consider many possible geometric configurations and must accurately estimate or calculate the performance of each to determine trends that lead to an optimum configuration. To assist the design engineer, NASA Lewis has developed a software tool that couples the computing power of a desktop workstation with an interactive graphical user interface (GUI) to allow interactive preliminary design of high-speed inlets.

Output from the software package, called VU–INLET, is shown in the accompanying figure. The inlet shown at the top of the figure must slow the supersonic external flow to subsonic speeds to feed a gas turbine engine at the right with a minimum of drag and with maximum pressure. The flow is turned and slowed through shock waves generated by the inlet geometry. Using VU–INLET, the designer can interactively manipulate the geometry with the GUI sliders and buttons. The software package instantly solves the appropriate flow equations (ref. 1) and displays the computed shock locations and total inlet performance. After a configuration has been developed at the design conditions, the designer can use the GUI to interactively change the free-stream Mach number, altitude, and angle of attack in order to assess off-design operation. This leads to a better, faster, and therefore less expensive design cycle. The user can save the design configuration and performance to a data file by simply pushing a button on the screen.

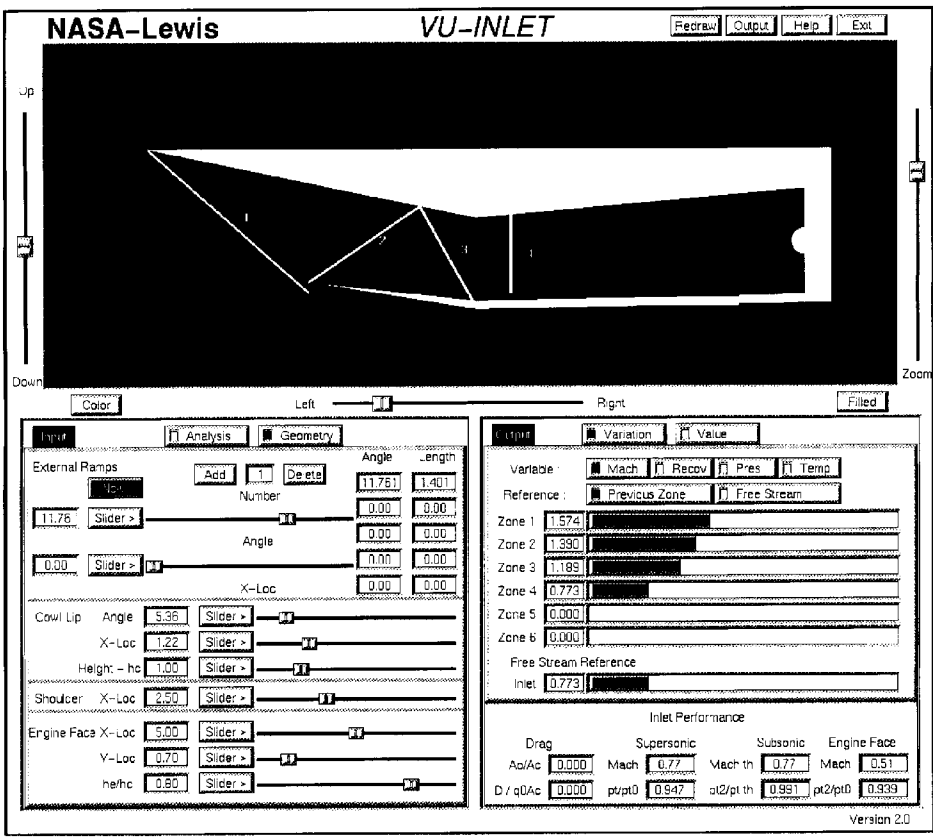

Interactive supersonic inlet design tool.

The latest version of VU–INLET can solve rectangular external or mixed-compression inlets. Because the new package models and displays most phenomena present in supersonic inlets, it can also be used as an educational tool to learn basic inlet operation and design. VU–INLET contains on-line help screens to assist the designer in both operating the tool and interpreting the results.

This tool is a preliminary attempt at using new computational technologies for interactive fluid dynamics. The software was developed in conjunction with an interactive undergraduate educational package (ref. 2) to study shock waves. Other interactive fluid dynamics packages have also been developed to study and design subsonic wind tunnels and coupled turbojet/ramjet propulsion modules and for basic turbojet analysis. All the packages are available to the public and run on either Silicon Graphics or IBM RISC 6000 machines employing the FORMS library of GUI's (ref. 3). Work is under way to port the packages to 486 PC's and Apple computers, using a different GUI package. Technical papers detailing the analysis techniques are available from the author (refs. 2 and 4).

References

1. Equations, Tables and Charts for Compressible Flow. NACA Report 1135, 1953.

2. Benson, T.J.: An Interactive Educational Tool for Compressible Aerodynamics. AIAA Paper 94–3117, June 1994.

3. Overmars, M.H.: FORMS Library, A Graphical User Interface Toolkit for Silicon Graphics Workstations, Version 2.1. Department of Computer Science, Utrecht University, The Netherlands, 1992.

4. Benson, T.J.: An Interactive, Design and Educational Tool for Supersonic External Compression Inlets. AIAA Paper 94–2707, June 1994.

Lewis contact: Thomas J. Benson, (216) 433–5920; e-mail, benson@ptah.lerc.nasa.gov

Headquarters program office: OA

Propulsion Systems

Single-Stage-to-Orbit Flow Path Studied

Flying into low Earth orbit in a single-stage vehicle that takes off from a conventional runway represents a new frontier for aeronautics. Operational flexibility and cost savings motivate development of an aircraft that fulfills this vision. This aircraft would have a low structural mass fraction and greater propulsion performance than current chemical or solid rockets. An air-breathing propulsion system has the potential to enable single-stage-to-orbit capability.

Because of the wide speed range over which they must operate and the multitude of takeoff and low-speed cycles available, propulsion system concepts for a single-stage-to-orbit (SSTO) vehicle have taken many forms in past studies. However, a single-flow-path arrangement would minimize both variable geometry and the number of auxiliary systems used over a limited speed range but necessarily carried to orbit. In this system a common propulsive duct accommodates the subsonic combustion "ramjet" cycle from about Mach 2 to Mach 6 and the supersonic combustion "scramjet" cycle from Mach 6 to its practical limit. (A rocket-based system is required for propulsion outside this envelope.) Design of the single duct satisfying these requirements must be biased toward efficient scramjet operation because the vehicle's gross takeoff weight is most sensitive to propulsion performance at higher speed. The design must, however, also be compatible with the ramjet and low-speed cycles that accelerate the vehicle through the transonic and supersonic flight regimes.

An SSTO flow-path test program recently completed in the 1- by 1-Foot Supersonic Wind Tunnel investigated the compatibility of a flow

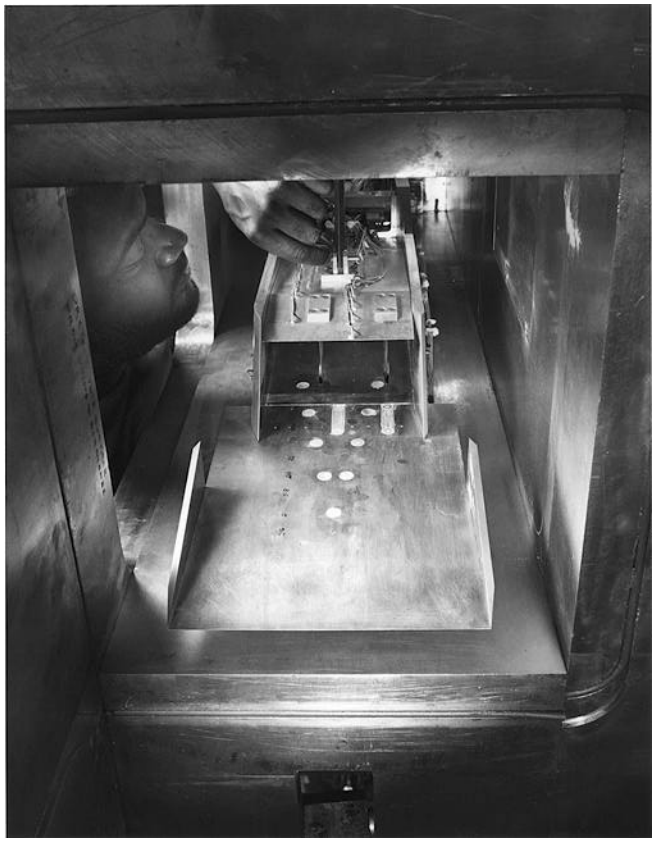

Single-stage-to-orbit flow-path model in wind tunnel.

path biased toward optimum scramjet performance with the ramjet mode of operation. The baseline geometry chosen for the study was that of the National AeroSpace Plane (NASP) concept demonstrator engine (CDE). The CDE configuration embodies the latest design philosophies of the NASP contractor team, and its use maximizes the benefit of the test results to the NASP program. The model was a 30%-scale, nonburning replica of the CDE. Although the model was not fueled, the entire ramjet compression process was properly modeled. The test was conducted at simulated flight Mach numbers of 3.5, 4.8, 6.3, and 7.1. Following completion of a baseline performance and operability matrix, the effects of other parameters, including forebody boundary layer height and isolator length, were determined. Performance with and without scramjet fuel injectors and inlet flap actuation struts was compared. The effect of inlet bleed was also studied.

The flow-path model was integrated into the sidewall of the tunnel test section. The inlet started and operated in a stable manner without bleed over the range of Mach numbers tested. The maximum stable contraction ratios exceeded those predicted for the CDE. Even though performance was less than that usually obtained with cruise, point-design configurations, these results are encouraging for the SSTO application.

Lewis contact: Charles J. Trefny, (216) 433–2162
Headquarters program office: OA

Successful Combustor Sector Tests Performed

In support of the High-Speed Research Program, combustor sector tests were performed that achieved ultralow oxides of nitrogen (NO_x) emissions. A combustor sector is a slice of an annular combustor that includes several fuel injectors. This sector simulates more closely the performance of a combustor in an actual engine, moving the combustion concepts tested in flame tubes last year into more realistic hardware configurations. These sector tests were encouraging in that the low-NO_x results found in the flame tubes have been repeated in this more realistic hardware.

NASA Lewis applies laser diagnostics and advanced probe diagnostic techniques to analyze details of combustion chemistry and uses flow visualization to optimize combustor fuel injector design and aerodynamics. Planar laser-induced fluorescence was successfully applied for the first time to a combustion flame tube at temperatures and pressures characteristic of actual combustor operating conditions. The images obtained suggest the degree of uniformity of the fuel injection process, allowing fuel injector designers to optimize their injectors for more uniform fuel distribution in the combustor.

In other experiments fuel droplet sizes and velocities were obtained in the combustion flame tube at actual engine operating pressures using water to simulate fuel. This difficult measurement in a extremely dense spray was obtained using a phase Doppler anemometer, which simultaneously measures droplet sizes and velocities nonintrusively. The combustion and spray diagnostics were obtained through unique high-pressure and high-temperature windows that provide optical access on all four sides of the square flame-tube test section.

In another breakthrough in diagnostic techniques a gas chromatograph/mass spectrometry system was applied to gas samples extracted through ultraclean probes inserted into the combustion test section. The breakthrough was in obtaining parts-per-billion resolution of hydrocarbon concentrations using industry-standard equipment but performing special dilution techniques to increase the resolution capability.

Lewis contact: Richard W. Niedzwiecki, (216) 433–3407
Headquarters program office: OA

Improved Ice-Scaling Method Demonstrated

In both wind tunnel and flight testing there are frequently limits on the available ranges of test conditions. In wind tunnels the test model is also often smaller than the device of interest, be it a complete aircraft or a component, such as a wing. Reliable techniques are needed to permit scaling of both size and test conditions so that wind tunnel results are a good simulation of what would be achieved for full-size tests at desired flight conditions.

For tests in an icing tunnel, scaling methods must produce ice shapes with the same features and relative size for the scaled test as for the full-size test. A number of scaling "laws" have been derived over the past 40 years or so, but all have limitations. As part of an ongoing in-house program, recent work at NASA Lewis has demonstrated an improved scaling method for testing when the cloud water content is different from that desired. The new method reproduces both shape and quantity of ice accurately. This result permits greater use of relatively low-cost tunnel tests in place of flight tests and permits more reliable extrapolation of flight data to different cloud conditions.

Lewis contact: Dr. David N. Anderson, (216) 433–3585
Headquarters program office: OA

Ice Measured on Multielement Wings

Modern transport aircraft use multielement wing designs to achieve high lift. However, little experimental ice-accretion data exists for these wing geometries for present and future aircraft. The aeronautics industry needs such data to assess the effects of icing on performance and to verify analytical ice-accretion computer code predictions.

In a cooperative venture between NASA Lewis and McDonnell Douglas, ice shapes have been measured on a multielement airfoil in the Lewis Icing Research Tunnel. This venture is part of an ongoing NASA Lewis program to study advanced-design airfoils in icing conditions. Ice-shape measurements on a two-dimensional airfoil were completed in July 1994. These shapes are being

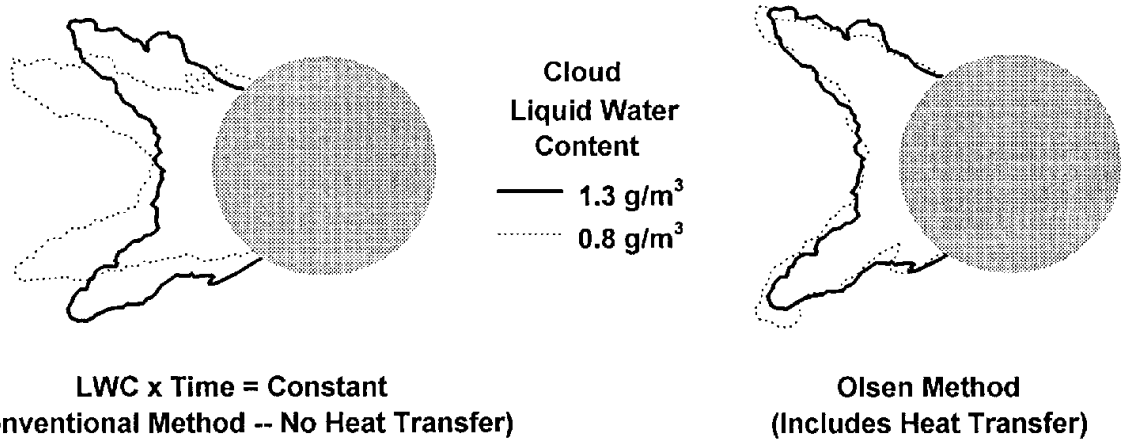

Determination of improved ice-scaling method.

Ice on multielement wing in Lewis Icing Research Tunnel.

machined in aluminum and applied to wing sections for performance testing in the NASA Langley Low Turbulence Pressure Tunnel in September 1994. These performance tests will be the first of their kind with ice shapes. NASA Langley and McDonnell Douglas have been testing multielement airfoils without ice for several years. The results from the clean-airfoil tests will be compared with the September test results using simulated ice to determine the performance penalty due to ice.

Lewis contact: Dr. Jaiwon Shin, (216) 433–8714
Headquarters program office: OA

LEWICE Ice-Accretion Code Modified

The LEWICE ice-accretion code is a two-dimensional computer code used to predict the amount of ice that will form on a surface, such as a wing, and the shape of the ice for different flight and cloud conditions. The information from the code is used to assist in designing aircraft components and to reduce the number of expensive flight tests needed to certify aircraft and ice-protection systems. The code, developed in-house at NASA Lewis, presently has about 80 users in various elements of the U.S. aeronautics industry.

LEWICE had been found in the past to predict ice shapes very accurately for many operating conditions. However, for some cases involving long icing times, the ice shapes were not considered to be reliable. As part of an on-going effort the numerical methods used in LEWICE have been improved during the past year to enhance the accuracy of the ice-shape predictions. A new version of LEWICE that overcomes many of the previous problems has been made available to the aeronautics industry. We are working to improve the accuracy of LEWICE by developing better physical models of the processes involved in ice accretion.

The three-dimensional version of the ice-accretion code, called LEWICE3D, was originally structured to calculate ice accretion on swept wings, such as those on high-speed aircraft. This code has been modified to permit calculations for engine inlets as well. In addition, the ability to interact with various types of user-supplied codes has been incorporated to enhance the code's usefulness. LEWICE3D with these modifications is being used to develop data for the icing certification of the Gulfstream G4 aircraft.

Lewis contacts: William B. Wright, (216) 977–1246;
Colin S. Bidwell, (216) 433–3947
Headquarters program office: OA

Advanced Analytical Methods Developed for Spiral Bevel Gears

Spiral bevel gears are a necessary drive system component for many aerospace applications. In helicopters these gears must transmit power from the horizontal engines to the vertical rotor shafts. Using this type of gear permits the most efficient use of space in the aircraft, as shaft angle between the meshing gears can be chosen over a wide range. However, the extremely complex geometry of spiral bevel gears has stagnated the development of analytical techniques. Recent

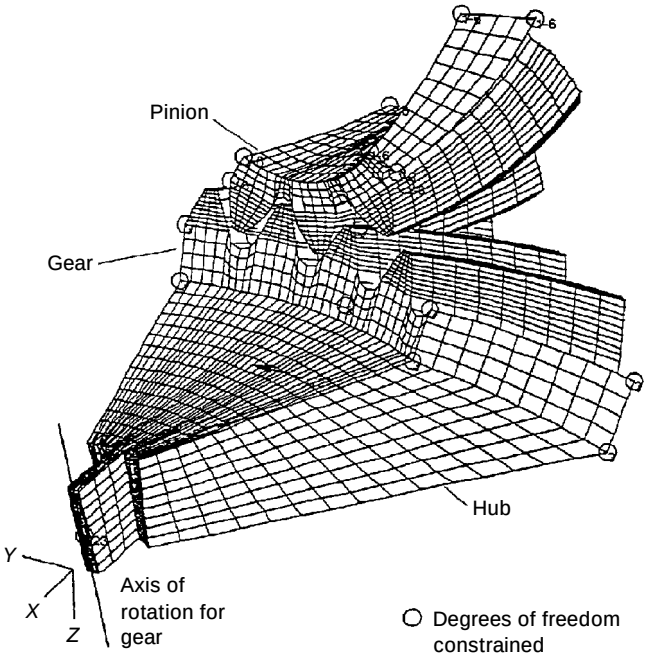

Model used for three-dimensional contact of spiral bevel gears.

advances in modeling this gear geometry gave the opportunity to analyze certain unexplored aspects and resulted in two recent analytical modeling developments.

A thermal analysis procedure was developed that uses a finite element technique to conduct a full steady-state and transient three-dimensional heat transfer analysis of meshing spiral bevel gears. Industry now uses a method developed in the 1960's that gives a single value of the "flash temperature," or the maximum temperature attained during the meshing process. Designers typically compare this value with their successful applications where thermal problems were avoided or use it to compare design options. The new procedure can predict the full three-dimensional temperature field and the "flash temperature" behavior of the entire meshing gear.

Another new analytical technique was developed for full three-dimensional contact modeling during the meshing process. This nonlinear finite element analysis code has successfully modeled multiple teeth in contact. The advantage of this technique is that the load distribution and contact are found and not assumed for the multiple contacts that can occur in this gear system. This analytical technique can predict load sharing, transmission error, bending stress, and contact stresses.

Bibliography

Handschuh, R.; and Kicher, T.: A Method for Thermal Analysis of Spiral Bevel Gears. NASA TM–106612, ARL–TR–457, 1994.

Bibel, G.; Kumar, A.; and Tiku, K.: Contact Analysis of Spiral Bevel Gears. NASA CR–195305, ARL–CR–146, 1994.

Lewis contact: Robert F. Handschuh, (216) 433–3969
Headquarters program office: OA

New Method Detects Gear Tooth Damage

Drive train diagnostics is becoming one of the most significant areas of research in rotorcraft propulsion. Accident statistics show the need for a reliable health and usage monitoring (HUM) system for rotorcraft propulsion systems. An investigation of serious rotorcraft accidents resulting from fatigue failures traced 32% to engine and transmission components. In addition, governmental aviation authorities are demanding that the safety record of civil helicopters must soon match that of conventional fixed-wing turbojet aircraft. Practically, this can only be accomplished with the aid of a highly reliable, on-line HUM system. Because such a system must be able to determine if a fault exists as early and reliably as possible, research was performed, under a joint NASA/U.S. Army project, to develop and prove various fault detection concepts and methodologies. A newly developed method, in particular, was found to reliably detect a variety of gear tooth damage modes.

The new method, NA4*, was developed to detect the onset of gear tooth damage and to continue to react to the damage as it increases. It was designed to overcome the deficiencies of other gear fault detection methods, which either fail to react for certain damage modes or tend to lose their effectiveness as the damage increases. NA4*, a time-based, nondimensional statistical parameter, uses the vibration signal from an accelerometer mounted on the housing of a gear system. The vibration signal is first time averaged, using a time pulse synchronous to the rotation of the gear being monitored, before method NA4* is applied. The time-synchronous averaging eliminates all vibration not coincident with the rotation of the gear being evaluated. NA4* produces a value of 3 under normal conditions for

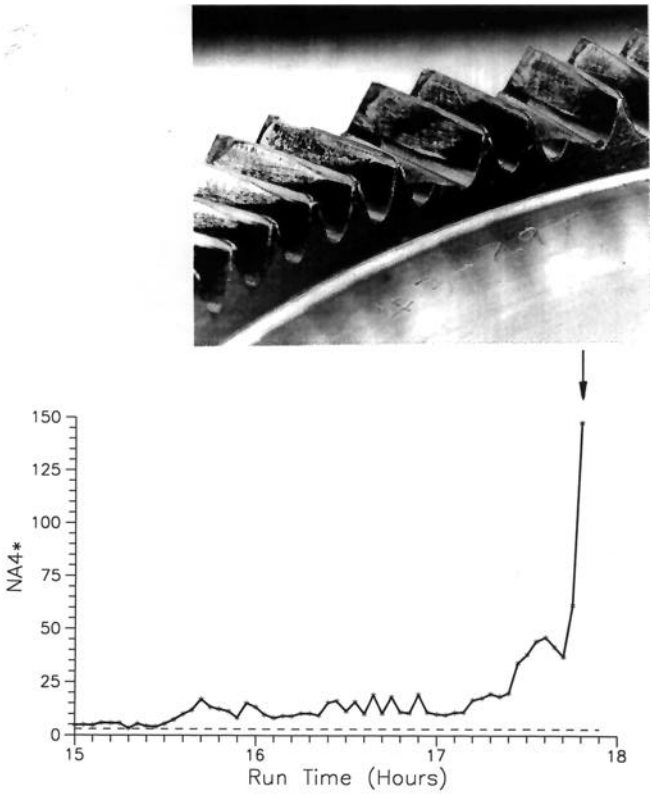

Face gear run 5 results.

all gear types regardless of the transmission system configuration. NA4* has the ability to compare the current condition of the gear being monitored to a weighted baseline of the gear in "good" condition, which allows it to both detect faults and grow with the increasing damage.

Method NA4* was applied to experimental vibration data from a number of spur gear, face gear, and spiral bevel gear fatigue tests conducted on various fatigue test rigs at NASA Lewis and involving a variety of damage modes. The primary purpose of these test rigs is to study the effects of gear tooth design, gear materials, and lubrication types on the fatigue strength of aircraft-quality gears. Gear damage modes ranged from moderate pitting to complete fracture of several teeth on one gear. NA4* robustly detected a wide range of gear tooth damage modes and magnitudes on a variety of gear types. In a face gear fatigue test NA4* increased from the nominal value of 3 to a value of 150, which reflected the major damage of two fractured teeth on the gear. In a spur gear test, NA4* increased to a value of 9 as pitting started and finally to a value of 45 as pitting covered the complete face width of the damaged gear tooth.

Method NA4* can be a significant part of an onboard health and usage monitoring system for current and future rotorcraft. The early and reliable detection of gear tooth damage is a crucial part of an in-flight fault warning system.

Bibliography

Decker, H.J.; et al.: An Enhancement to the NA4 Gear Vibration Diagnostic Parameter. NASA TM–106553, 1994.

Zakrajsek, J.J.; et al.: An Analysis of Gear Fault Detection Methods as Applied to Pitting Fatigue Failure Data. NASA TM–105950, 1993.

Zakrajsek, J.J.; et al.: Application of Fault Detection Techniques to Spiral Bevel Gear Fatigue Data. NASA TM–106467, 1994.

Zakrajsek, J.J.: A Review of Transmission Diagnostics Research at NASA Lewis Research Center. NASA TM–106746, 1994.

Lewis contacts: James J. Zakrajsek, (216) 433–3968; Harry J. Decker, (216) 433–3964
Headquarters program office: OA

High-Speed Exhaust Nozzle Test Proves Noise Goal Realistic

Under the High-Speed Research (HSR) Program, NASA Lewis and Langley and the aerospace industry (General Electric, Pratt & Whitney, and Boeing) have been testing exhaust nozzle concepts for future high-speed civil transport (HSCT) applications. The HSCT is a 300-passenger aircraft envisioned for the year 2005 that would cruise supersonically at speeds of about Mach2.4. For such an aircraft to be both economically viable and environmentally acceptable, the exhaust nozzles must combine highly efficient operation at cruise speeds with low noise levels at takeoff. The initial phase of the HSR program has focused on environmental challenges, with nozzle-related research emphasizing the takeoff noise issue. This effort has produced nozzle designs that not only meet but surpass HSR noise reduction goals. The government-industry team developing HSR nozzle

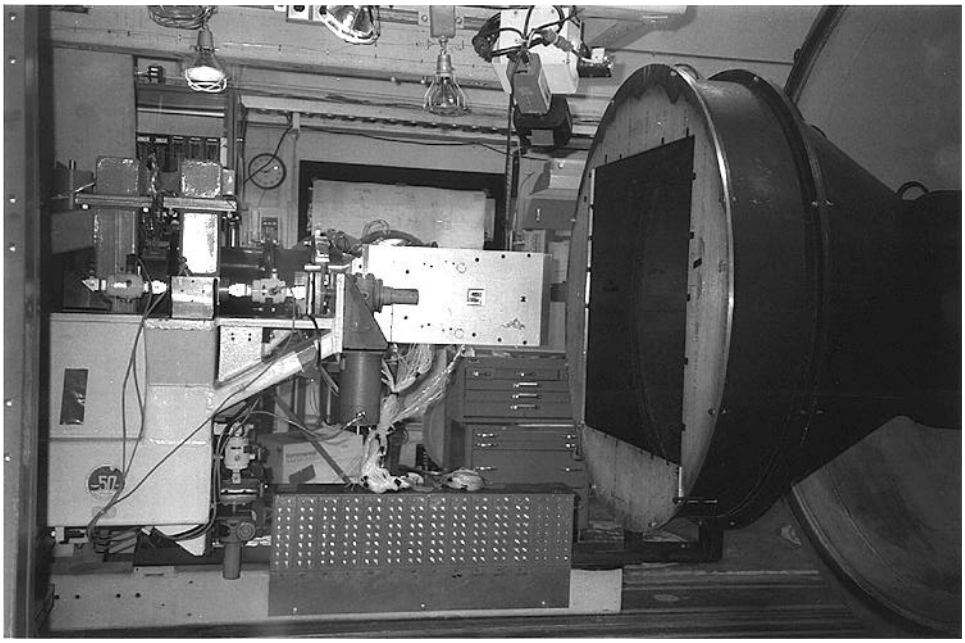

HSR exhaust nozzle in CE–22 test facility.

technology desired experimental verification that the internal aerodynamic performance of these new designs had not been unduly compromised by low-noise considerations, particularly at high-speed cruise conditions.

NASA Lewis has recently completed a joint experimental program with Pratt & Whitney and General Electric to measure the internal performance of several candidate HSR exhaust nozzle concepts. The models were tested at simulated altitude conditions in the NASA Lewis CE–22 facility to determine their performance over a wide range of geometric variations and nozzle pressure ratios representing conditions from takeoff to supersonic cruise.

The tests were successfully completed and results agreed well with contractors' predictions, indicating that the high-speed nozzle performance goal was realistic. In addition, improvements to the CE–22 facility resulted in 99.75% accuracy and repeatability in both thrust and flow measurements, enabling the results of these tests to establish a broad comprehensive data base. The data base will be used to validate current performance prediction methodology and to help select an optimal exhaust nozzle design for the HSCT propulsion system.

Lewis contact: David W. Lam, (216) 433–8875
Headquarters program office: OA

ASTOVL Lift Fan Nozzle Evaluated in Powered-Lift Facility

As part of a cooperative program, in 1995 NASA and the Advanced Research Projects Agency (ARPA) will test a near-full-scale model of an advanced short-takeof, vertical-landing (ASTOVL) aircraft concept in the NASA Ames 80- by 120-Foot Wind Tunnel. The Allison Engine Co. of Indianapolis, Indiana, is providing a shaft-driven, forward-fuselage-mounted lift fan with a vectoring exhaust nozzle as part of the installed propulsion system for this model. The lift fan nozzle, which vectors to provide yaw and pitch control as well as augmented lift for takeoff, is critical to the low-speed performance of the aircraft. Allison had used computational fluid dynamic (CFD) analysis to estimate the performance of their lift fan nozzle concept but wanted experimental verification before manufacturing the nozzle for near-full-scale testing at NASA Ames.

Allison identified the Powered-Lift Facility (PLF) at NASA Lewis as an ideal facility for such a test, and Lewis subsequently entered into a cooperative test program with them. The PLF is a large static thrust stand with a six-component, multiaxis thrust-measuring system. It is located inside a 130-ft-diameter geodesic dome, which shields against noise during testing. Allison provided a one-third-scale model of the lift fan nozzle for testing in PLF. Nozzle flow rates, thrust forces,

Nozzle vectored at 60° to augment thrust during takeoff.

and vector angles were measured for various nozzle orientations and pressure ratios. The nozzle is designed to vector up to 10° for yaw and to pitch forward up to 20° or rearward up to 60° to augment forward thrust during takeoff.

Results from the test demonstrated that the nozzle met design requirements and also agreed well with the thrust and flow performance predicted by Allison's CFD analyses. The test was performed in a timely manner, enabling Allison to proceed as scheduled with fabrication of the large-scale lift fan hardware for the NASA Ames test.

Lewis contact: David W. Lam, (216) 433–8875
Headquarters program office: OA

UTRC Tests Baseline SSTF Core Inlet/Bypass Nozzle

The supersonic through-flow fan (SSTF) engine is an advanced propulsion system being considered for potential supersonic cruise aircraft applications after the year 2015. A unique feature of this engine concept is the maintaining of supersonic flow through the fan stage, which eliminates the need for both variable geometry in the primary inlet and a subsonic diffuser. As a result the inlet can be smaller and the potential exists for increased inlet efficiency. Downstream of the fan the airflow is always supersonic and is split between an inlet supplying the core turbomachinery and an exhaust nozzle for the bypass flow. The core inlet and bypass nozzle must operate in a highly integrated fashion across the flight Mach number range. Under a NASA Lewis contract, United Technologies Research Center (UTRC) has been exploring design requirements and options for these integrated components and has recently completed initial tests of a baseline core inlet/bypass nozzle scale model.

UTRC began work on the SSTF core inlet/bypass nozzle by screening several potential concepts. The concepts had to provide the weight flow required by the engine compressor, high inlet pressure recovery, and high nozzle thrust performance. They selected one concept, with a variable core inlet and a variable bypass nozzle, for further study with the GASP Navier-Stokes code. The GASP results indicated that high inlet pressure recovery was possible with significant bleed of the boundary layer entering the core inlet. UTRC then began testing a two-dimensional scale model of the selected concept in their new dual-flow test facility.

Core inlet/bypass nozzle installed in UTRC dual-flow test facility.

The dual-flow facility was constructed to permit testing of the variable core inlet/variable bypass nozzle at flight conditions ranging from Mach 0.9 (loiter) to Mach 2.8 (design point). The core inlet was designed with variable geometry cowls to control the inlet captured airflow and contraction ratio. In addition, the inlet has a bleed scoop to remove the low-energy boundary layer along the hub. The bypass nozzle was designed with a variable-geometry flap to optimize nozzle performance at various operating conditions.

Initial tests of the core inlet/bypass nozzle model installed in the dual-flow test facility have been successfully completed. Fully supersonic flow in the core inlet and bypass nozzle was achieved and maintained as the cowls of the core inlet were translated. Additional tests will be conducted to characterize the performance of the core inlet and bypass nozzle and to determine any necessary design modifications. Finally, experimental results will be compared with the flow predictions obtained previously with the GASP code.

Lewis contact: Nicholas J. Georgiadis, (216) 433–3958
Headquarters program office: OA

Small Two-Stage Axial Compressor Designed and Tested

The need to improve fuel efficiency, reduce weight, and lower the life cycle of small turboshaft engines has produced aggressive compression system design, performance, and operability goals. Future engines will be required to have extremely high stage loading to reduce the number of parts, engine length, cost, and weight. Obtaining such loading is made difficult by increased shock, diffusion, and secondary flow losses. The resulting very complex three-dimensional airfoil shapes in highly three-dimensional flows have not been modeled accurately enough by present design technologies. To meet future small compressor performance goals, a three-dimensional, Navier-Stokes, multistage flow model must be incorporated into the design process.

NASA Lewis, Allison, and the U.S. Army established a joint program to design a small, highly loaded, two-stage axial compressor using an advanced three-dimensional, viscous, multistage flow analysis code. We would try to demonstrate the performance improvements

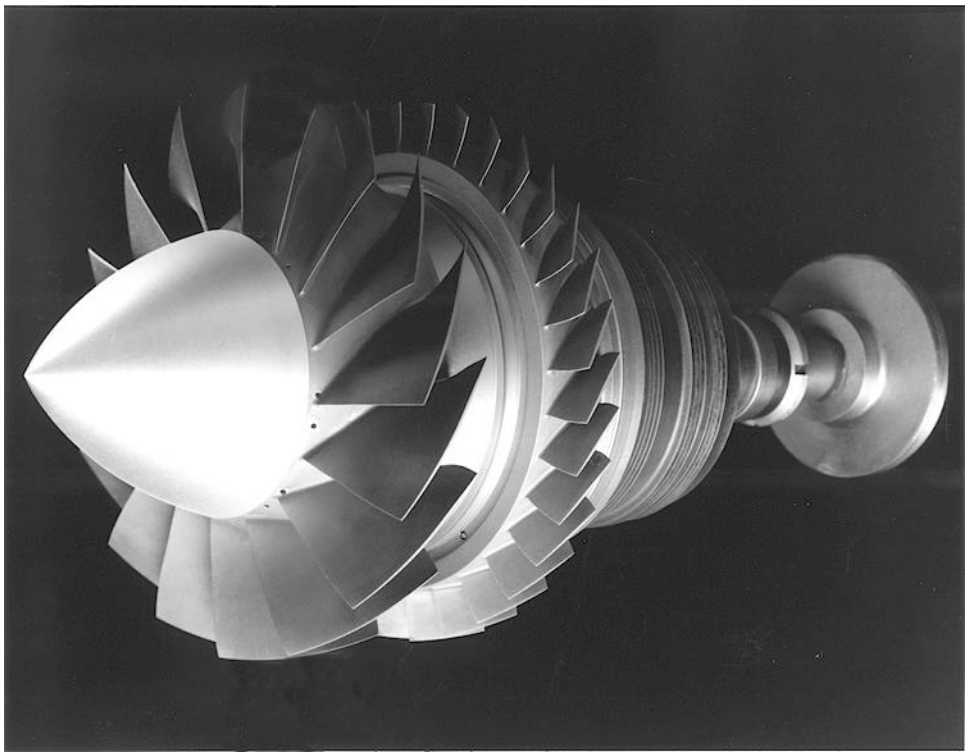

Two-stage rotor assembly for advanced small turboshaft compressor.

achievable through the use of such modeling (ref. 1). We would also use the test data to validate and calibrate the multistage code used in the design phase.

The performance testing has been completed. The compressor achieved a 5:1 pressure ratio in two stages, and the performance data indicated good efficiency and stall margin. The test provides a unique data base for small multistage axial compressors. Even though the stall margin was acceptable, we have established a follow-on program to enhance the original compressor design.

Reference

1. Adamczyk, J.J.: Model Equations for Simulating Flows in Multistage Turbomachinery. ASME Paper 85–GT–226, 1985.

Lewis contact: Dr. David P. Miller, (216) 433–8352
Headquarters program office: OA

Blade Row Interaction Effects on Flutter and Forced Response Modeled

In the flutter analysis of a turbomachine blade row, the blade row is commonly assumed to be isolated—disturbances created by the vibrating blades are free to propagate away from the blade row without being disturbed. Any reflections of these outgoing waves by other structural members or nonuniformities in the mean flow field are neglected. Although the forced-response problem is typically concerned with blade row interaction, forced-response analyses also generally neglect any reflections of outgoing waves. However, in an engine environment, structural elements (such as neighboring blade rows or struts) and nonuniformities in the mean flow field will reflect some wave energy back toward the vibrating blades, causing additional unsteady forces on them. Whether these reflected waves can significantly affect the aeroelastic stability or forced response of a blade row is a question of fundamental importance.

NASA Lewis has developed a procedure for calculating intra-blade-row, unsteady aerodynamic interactions that relies on results from isolated-blade-row unsteady aerodynamic analyses. Using influence coefficients that express the unsteady forces on one blade row due to the motion of another, we obtained an aeroelastic model that accounts for coupling of the vibratory responses of multiple blade rows. The model was applied to two configurations, each consisting of three blade rows. The flutter analysis showed that interaction effects can be destabilizing, and the forced-response analysis showed that interaction effects can significantly increase the resonant response of a blade row.

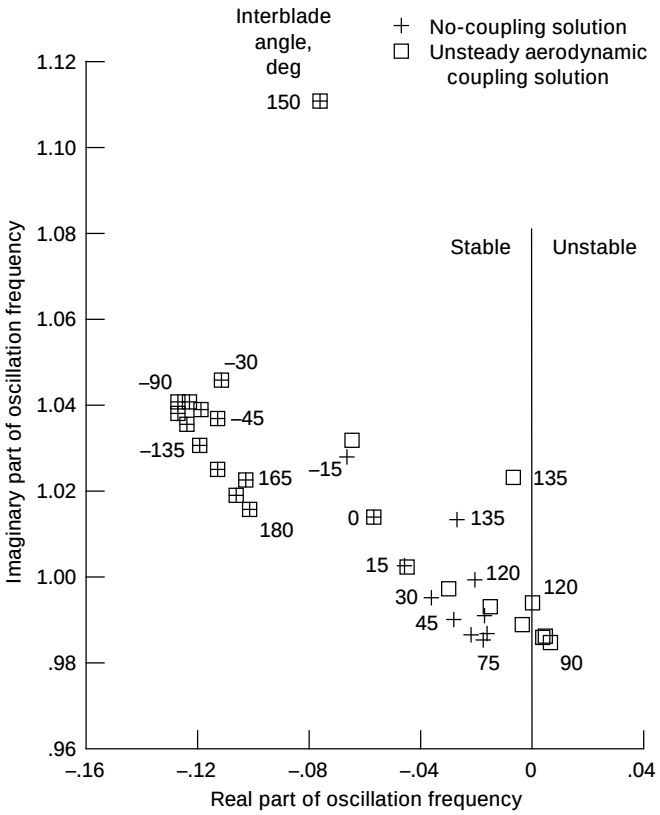

Rotor stability with and without aerodynamic coupling.

Bibliography

Buffum, D.H.: Blade Row Interaction Effects on Flutter and Forced Response. NASA TM–106438, 1993.

Lewis contact: Dr. Daniel H. Buffum, (216) 433–3759
Headquarters program office: OA

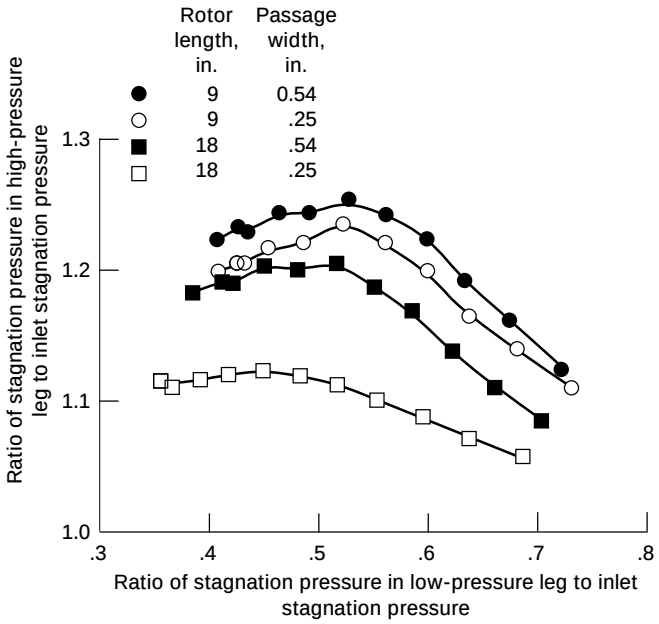

Wave rotor performance.

First Phase of Wave Rotor Testing Completed

NASA has a theoretical and experimental program to investigate wave rotors as a potential topping cycle for jet engines. Wave rotors could increase specific power and reduce specific fuel consumption while still using conventional components (i.e., materials). The first phase of the experimental program, measurement of three-port cycle performance levels, was completed in July 1993. The three-port cycle experiment was aimed at characterizing the principal wave rotor loss mechanisms—viscous losses, losses due to passage gradual opening time, and leakage losses. The resulting data are used for code validation.

Wave rotor sensitivity to leakage losses was determined by installing false end-walls, whose position relative to the rotor could be altered to vary the leakage gap. Passage gradual opening time and viscous losses were characterized by parametrically varying rotor length, passage width, and rotor speed. As the passages were made shorter and wider, the efficiency improved, indicating that friction plays a major role.

The design effort is under way for the second phase of the research, which involves a four-port rotor. The four-port cycle, along with a conventional external combustor, is appropriate for use as a topping cycle. The experiment, however, is designed to use a heater rather than a combustor, to keep temperatures lower.

Extensive validation of the one-dimensional (ref.1) and two-dimensional (ref. 2) codes used for modeling the wave rotor dynamics has also been accomplished this year. The one-dimensional design/analysis code was used to design the four-port wave rotor cycle and to generate wave rotor component maps. The maps were used by the Advanced Aeronautics Office in a cycle study to evaluate wave rotor performance enhancement in a GE–90 class, an Allison 250, and a Lycoming T–55 class engine. The studies show that small turboshaft engines are significantly enhanced, both in increased specific power and in reduced specific fuel consumption, by a wave rotor topping cycle. Finally, in collaboration with NASA Lewis, the Allison Engine Co. is investigating the application of a wave rotor to an existing engine, using available hardware.

References

1. Paxson, D.E.: A Comparison Between Numerically Modelled and Experimentally Measured Loss Mechanisms in Wave Rotors. AIAA Paper 93–2522, 1993.

2. Welch, G.: Two-Dimensional Numerical Study of Wave Rotor Flow Dynamics. AIAA Paper 93–2525, 1993.

Lewis contacts: Jack Wilson, (216) 891–1204;
Dr. Gerard E. Welch, (216) 433–8003
Headquarters program office: OA

Test Bed for Active Control of Fan Noise Installed

With the advent of ultra-high-bypass engines the space available in the nacelle for passive acoustic treatment is becoming more limited while noise regulations are becoming more stringent. Active noise control (ANC) holds promise as a solution to this problem. ANC is the use of secondary (added) noise sources to reduce or eliminate the offending noise radiation.

A large low-speed fan has been designed, fabricated, and installed in the NASA Lewis Aeroacoustic Propulsion Laboratory for the purpose of developing and demonstrating various ANC concepts aimed at reducing fan tone noise. This work is part of the Advanced Subsonic Technology Noise Reduction Program. Several concepts identified by Pratt & Whitney, General Electric, Hersh Acoustical Engineering, and NASA

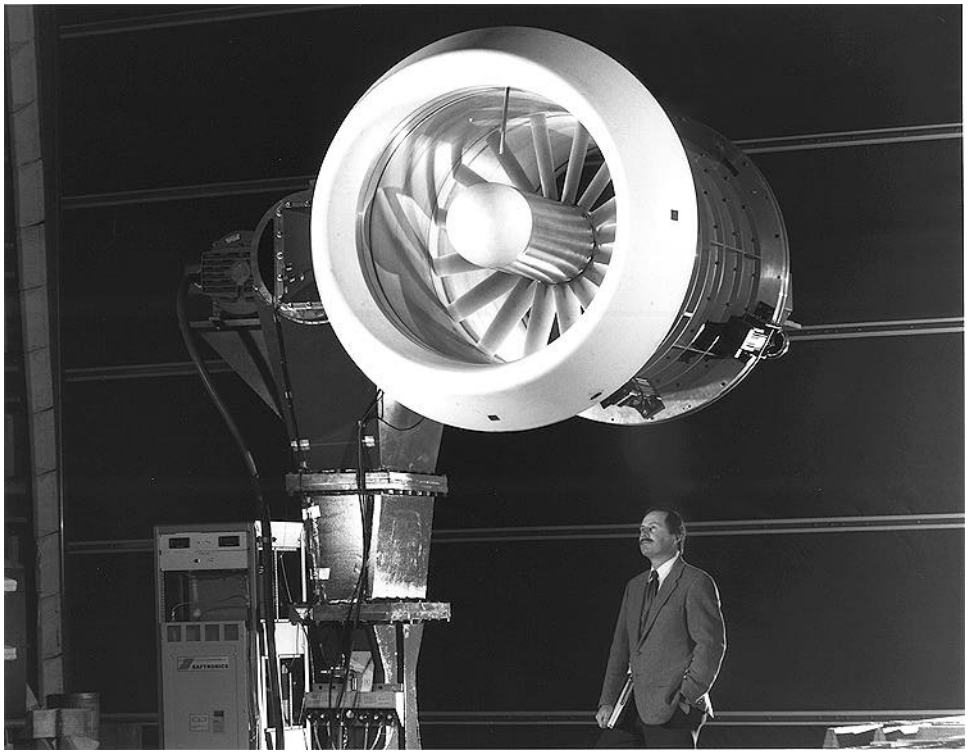

Active noise control fan installed in Aeroacoustic Propulsion Laboratory.

will be tested on this 48-in.-diameter fan as a proof of concept before a full-scale engine demonstration. The first test of an ANC system is scheduled for the first half of 1995.

The combination of the large fan diameter and low (400 ft/sec) tip speed produces fan tones of the same frequencies produced by full-size advanced engines. A unique feature of this fan is the direct attachment of the rotor centerbody to the rig support column, eliminating the need for struts or pylons, which could contaminate acoustic measurements. Another important feature is the built-in rotating microphones, which separate the fan tone into individual modes, allowing better determination of the noise generation mechanisms.

Lewis contact: Laurence J. Heidelberg, (216) 433–3859
Headquarters program office: OA

Acoustic Data Acquisition Capability Improved in Low-Speed Wind Tunnel

Acoustic background noise calibration tests have been completed in the NASA Lewis 9- by 15-Foot Low-Speed Wind Tunnel. Recent tunnel improvements reduced test section turbulence and the tunnel drive noise reaching the test section. Additionally, the in-flow microphone installation was improved with NASA Ames-designed microphone holders and a streamlined fairing over the traversing microphone mechanism. The tunnel can now measure noise levels from quieter, future-generation turbofan models.

These changes have reduced the measured in-flow background noise in the test section at Mach 0.20 by about 7 to 8 dB at frequencies from 200 Hz to 40 kHz. Far-field acoustic instrumentation in the tunnel consists of fixed, wall-mounted microphones and a remote-controlled translating microphone probe. The translating probe covers most of the axial length of the tunnel test section. The computer data acquisition system also moves the microphone to (typically) 48 data positions, pausing for data acquisition at each position.

Tunnel background noise calibration tests with the fixed, wall-mounted microphones have shown that upstream microphone holder wakes may interact with downstream microphones. In particular, the microphone holders generate a viscous wake with less than a 7° half-angle and

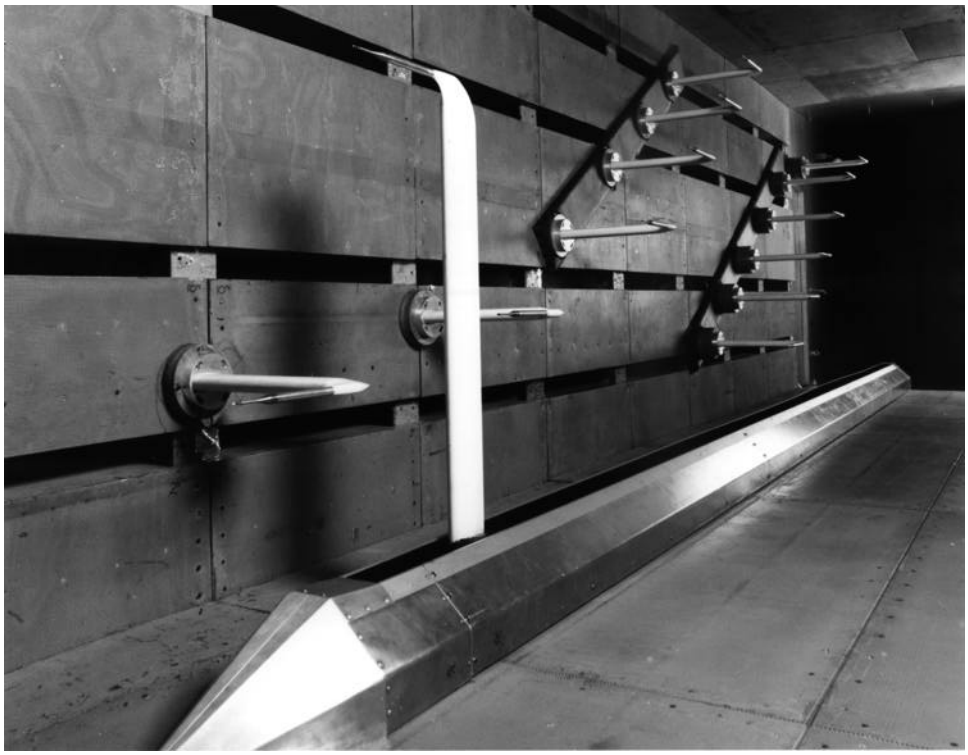

9- by 15-Foot Low-Speed Wind Tunnel test section showing fixed and translating microphones.

also an apparent tip vortex that persists directly downstream from the probe. Thus, the wall microphones must be displaced vertically and into the flow to minimize wake interaction. The translating microphone probe avoids the issue of upstream wake interaction while providing significantly more data measurement locations.

Comparisons of fixed and translating microphone data for a model turbofan show good agreement at comparable tunnel locations. These results suggest that fixed, wall-mounted microphones are not required for model fan noise tests. The translating microphone probe was shown to take accurate noise samples with good spatial resolution and eliminates possible wake disturbances from upstream microphones.

Lewis contact: Richard P. Woodward, (216) 433–3923
Headquarters program office: OA

Scale-Model, High-Bypass-Ratio Turbofans Tested at Simulated Takeoff/Approach

Tests were recently completed using the General Electric universal propulsion simulator (UPS) in the NASA Lewis 9- by 15-Foot Low-Speed Wind Tunnel. The test objectives were to determine the acoustic, aerodynamic, and aeromechanic performance of several new wide-chord, high-bypass-ratio fan stage concepts and several new engine nacelle acoustic treatment concepts for the next generation of turbofan aircraft engines, at speeds simulating aircraft takeoff and approach. The effect of fan blade sweep was also investigated.

The GE UPS is designed to simulate full-scale engine components in scale-model size. The complete engine fan module (comprising engine nacelle, bypass fan stage, and nozzle), the first one-and-a-half stages of the engine core booster stage, the wing mounting pylon, and engine acoustic treatment within the nacelle are all simulated. The 22-in.-diameter test model fan is powered by a four-stage air turbine drive module using high-pressure, high-temperature (450 psi, 550 °F) air at flow rates to 25 lb/sec. During the test approximately 1900 performance and operating parameters were obtained, both for measuring the fan module performance and for monitoring the safety and health of the entire model. Unique with this model is the ability to measure fan module performance by using force balances mounted internally in the model. Fan thrust and torque forces can be measured by using a two-component rotating balance; bypass

GE universal propulsion simulator installed in wind tunnel.

stator and nacelle drag and torque forces can be measured by using a six-component static balance. Acoustic measurements of the model were made by using an array of 13 wall microphones at fixed azimuthal locations, in addition to a unique track-mounted, axially translating microphone with the capability to stop at any selected angular location along the entire length of the test section.

The data obtained during this test will be used by NASA and GE research engineers to validate the many computer design and analysis codes used to design both high-bypass-ratio fan stage components and fan module acoustic treatment. The data will be compared with the predictions generated by engineers using computer codes to determine how well scale-model engine components can be designed to simulate full-scale engine performance and where these codes can be improved for better engine component performance predictions in the future.

Lewis contacts: Christopher E. Hughes, (216) 433–3924; Richard P. Woodward, (216) 433–3923
Headquarters program office: OA

Aeropropulsion Facilities and Experiments

Airspeed of Icing Research Tunnel Increased 40% by Fan Blade Change

The NASA Lewis Icing Research Tunnel (IRT) is the world's largest refrigerated icing tunnel and one of only three such facilities in the United States. In this unique facility the icing conditions encountered by today's aircraft are duplicated to test ice effects on actual aircraft components and models of complete airplanes and helicopters as well as the effectiveness of ice detection and protection methods. Although very difficult to simulate in a wind tunnel, natural icing conditions have been successfully achieved in the

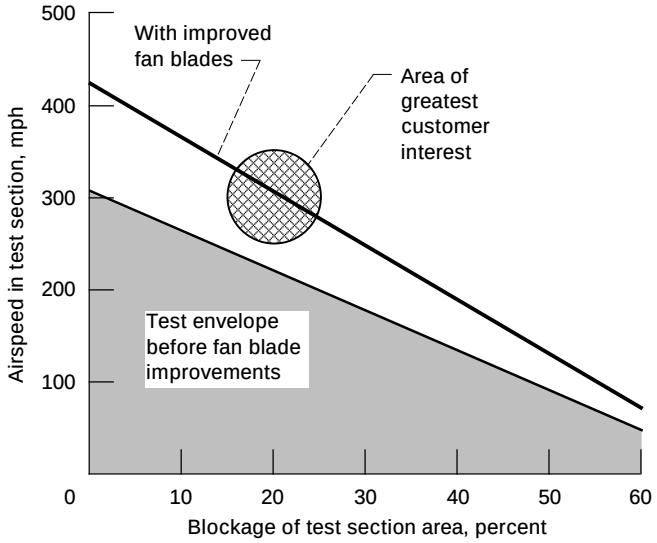

Test airspeed capability of IRT.

IRT by carefully controlling the tunnel air temperature (down to −20 °F) and spraying an air-water mixture into the airstream upwind of the test article. An artificial "cloud" is created in which the liquid water content and droplet size are carefully controlled. The resulting icing conditions so closely simulate actual flight conditions that the Federal Aviation Administration (FAA) recognizes IRT testing as an alternative to flight testing for the certification of new icing instrumentation and ice protection systems.

The test section of the IRT is 6 ft high, 9 ft wide, and 20 ft long, a size that makes it unique among refrigerated wind tunnels. Often, however, a significant amount of this large flow area is blocked when the test model is a full-scale component. Blockages of 20% and more are common in IRT tests, relative to typical blockages of less than 5% in conventional wind tunnels. High blockage significantly reduces the maximum airspeed that the tunnel fan can produce, as illustrated in the graph. Here the downward-sloping lines show how rapidly the maximum airspeed capability declines with increasing blockage by the test model.

The area of the graph of greatest interest to the U.S. aeronautics industry and the Department of Defense (the principal IRT customers) is the crosshatched area centered on an airspeed of 300mph and a model blockage of 20%. As shown by the lower shaded area, before improved fan blades were installed, the airspeeds in the IRT test envelope fell below the area of greatest customer interest by approximately 30 to 130 mph.

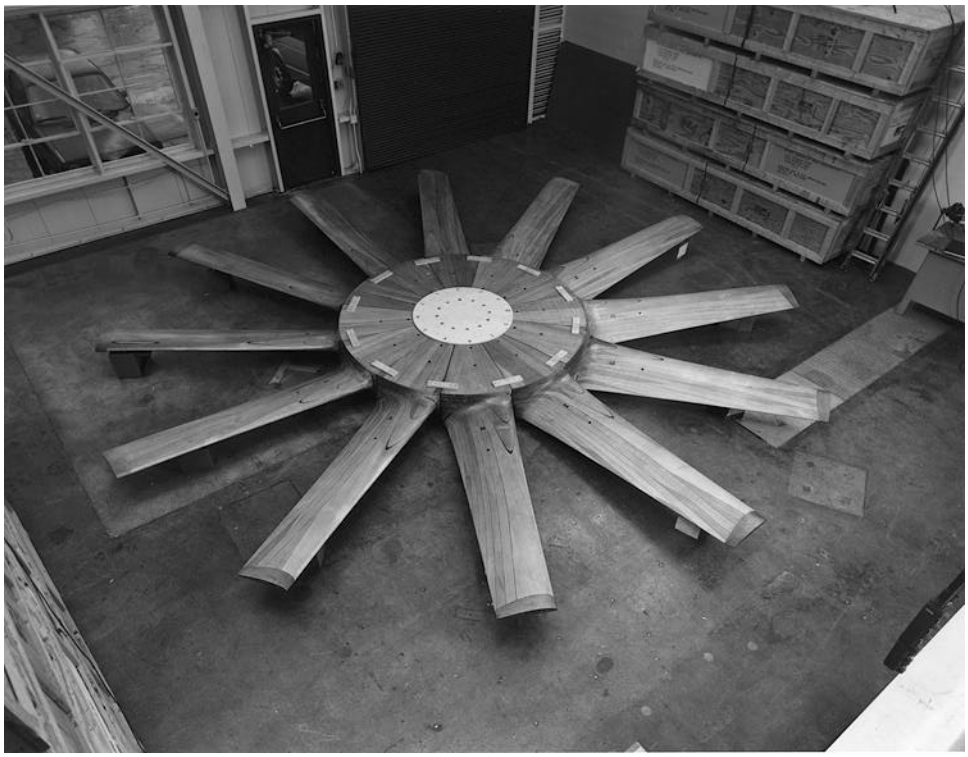

New IRT fan blade assembly before installation.

The photograph shows the set of improved fan blades before they were installed in the IRT drive in November 1993. Blade pitch angle was increased by 5° and tip clearances were reduced. The resulting benefits are shown by the bold line in the graph, which defines the current IRT test envelope. At zero blockage maximum airspeed has been raised 40%, from 300 mph to over 420 mph. More importantly, the test envelope now passes through the customers' area of interest. The potential benefits of these fan blade improvements to certification testing are closer correlation between test and expected service, fewer test points required for the same level of result reliability, clearer evidence of meeting/not meeting certification requirements, and greater flight safety. A special-purpose computer program developed at NASA Lewis (ref. 1) was used to model the aerodynamic behavior of the IRT fan drive and guide the redesign of the blades. This software is now available through NASA's Computer Software Management and Information Center (COSMIC).

Use of the IRT is open to commercial and academic organizations as well as government agencies, both civilian and military. Commercial organizations compensate NASA for testing expenses in accordance with an established fee schedule. Testing falls into three general categories:

- Basic research on ice accretion and ice protection systems, with users including Lewis research organizations, university and college grantees, and industry contractors
- Hardware research and development on advanced ice protection systems, performed by airframe and ice protection system manufacturers
- Certification of ice protection systems, by organizations such as the Federal Aviation Administration, its European equivalent, and the Department of Defense.

Reference

1. Viterna, L.A.: Calculated Performance of the NASA Lewis Icing Research Tunnel. NASA TM–105173, 1991.

Lewis contacts: David W. Vincent, (216) 433–5719; David W. Sheldon, (216) 433–5662
Headquarters program office: OA

Microphone Holder for Low-Speed Wind Tunnel Improved

NASA Lewis has been engaged in ongoing efforts to reduce the level of background noise recorded in the 9- by 15-Foot Low-Speed Wind Tunnel in order to promote it as a premier acoustic facility for future fan testing. Soon all aircraft engines will need to satisfy stringent noise regulations set forth by the Federal Aviation Administration (FAA). The acoustic band in which engine manufacturers will be required to test (due to scaling effects) was discovered to be within the existing background noise levels of the tunnel. The background noise was effectively masking an acoustic band of interest.

Early test results (March 1993) indicated that a major contributor to the background noise levels was generated by the microphone holders (stands). A parametric study of several types of stands followed. Among those tested was a 1-ft-tall machined aluminum aerodynamic foil on loan from the NASA Ames Research Center. (Ames demonstrated that improving the design of in-flow microphone holders could significantly reduce their contribution to the overall background noise levels. This work was accomplished under the direction of Paul Soderman and Christopher Allen.) The test results showed that the NASA Ames microphone stand generated less self-noise than any previously tested microphone stand.

A team was then formed to determine the optimum stand design appropriate for the 9- by 15-Foot Low-Speed Wind Tunnel. The Ames 1-ft-tall contoured airfoil design was used as a baseline. A mold was made of the Ames stand before it was returned to Ames. Considering weight, stiffness, and acoustic interaction requirements, we decided to fabricate the new microphone stands out of a composite material. The new stands were designed and primarily fabricated in-house. The composite shells were made by NASA Lewis' Wood Model Shop.

The microphone stand hardware consists of a fiberglass shell (≃22 in. long for the wall-mounted stands) filled with foam. (See photograph on page 36.) The design was optimized by creating an internal duct within the shell and baseplate for routing the microphone cabling, thus eliminating tones produced by extraneous wires. The mounting baseplate was made of aluminum and sealed to the bottom of the fiberglass shell. A

boom extension holds the actual microphone probe away from the stand body. The boom is approximately 18 in. long. A 4-ft-tall stand was also designed and fabricated to operate on the tunnel's traversing hardware.

Acoustic calibration testing has proven that the new stands have significantly reduced the measurable background noise levels in the tunnel test section. The stands are durable and easy to use and maneuver within the test section. The fiberglass construction minimized the cost and has shown no evidence of inducing noise due to lack of stiffness. Richard P. Woodward will present a paper at the 33rd AIAA Aerospace Sciences Meeting and Exhibit, January 1995, detailing the background noise level reduction in the 9- by 15-Foot Low-Speed Wind Tunnel. The general conclusion of the acoustic calibration is that the improved tunnel is capable of measuring in-flight noise levels of future low-noise test articles and provides a background aeroacoustic environment comparable to state-of-the-art test facilities.

Lewis contacts: Richard P. Woodward, (216) 433–3923; Bonnie A. Kee-Bowling, (216) 433–5681
Headquarters program office: OA

Surface Pressures on Wind Tunnel Models Visualized With Pressure-Sensitive Paint

Surface pressures on wind tunnel models are one of the most frequently made measurements in aeronautical testing. Until recently, pressure measurements were limited to at most several thousand predetermined locations. The relatively new technique of photoluminescent paint fills in the data gaps that result from using only discrete pressure measurement systems. By using a combination of these two types of systems, accurate pressure mappings can be obtained over entire wind tunnel model surfaces.

Pressure-sensitive paint (PSP) measurement is a nonintrusive, noncontact technique that creates a continuous pressure map of the surface of a wind tunnel model. To obtain the desired readings, a fluorescent coating of PSP is sprayed on the model. During testing the coating is illuminated with blue light and emits light at a longer wavelength, in this case yellow-orange. The amount of luminescence (or brightness) change depends on the partial pressure of oxygen molecules in air at the model surface. The lower the pressure, the brighter the area or the less quenching done by the oxygen molecules. Areas of higher pressure appear dimmer owing to more quenching. This emitted luminescence is detected by a precision, digital, charge-coupled-device camera, and the acquired images are stored on a personal computer. The measured luminescence images can then be calibrated to give absolute pressure readings. The luminescent/oxygen quenching process is self-refreshing, eliminating

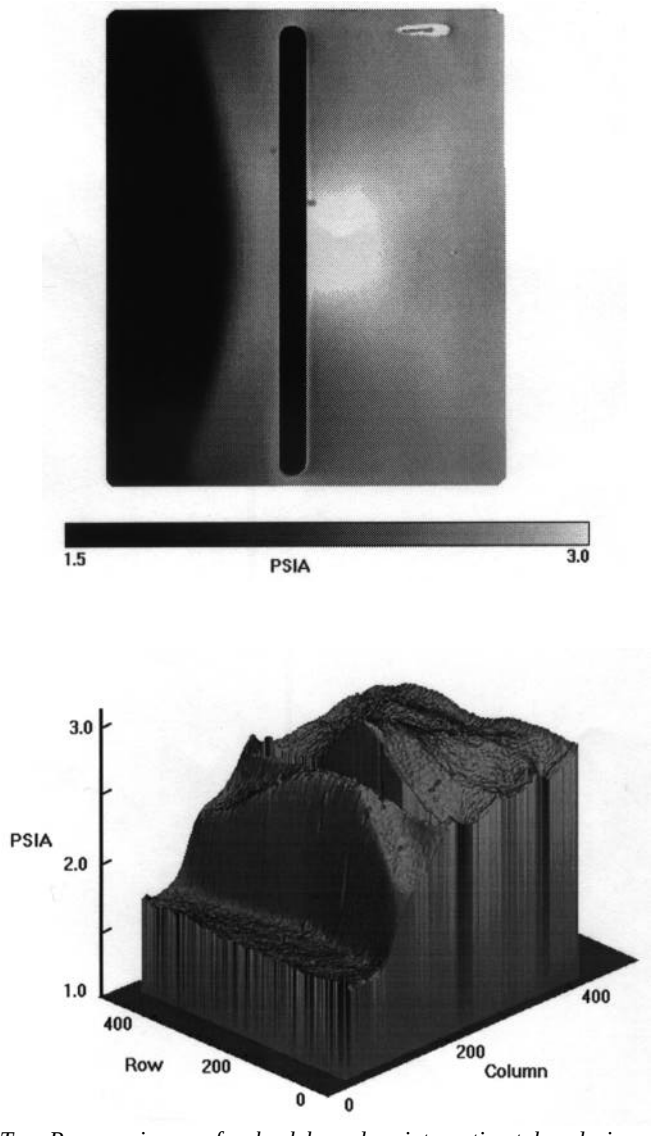

Top: Pressure image of a shock boundary interaction taken during inlet bleed study test at Mach 2.5 in the 1- by 1-Foot Supersonic Wind Tunnel. Bottom: Three-dimensional plot of same image.

the need for cleaning or repainting the surface after each test condition.

The calibration procedure requires the acquisition of two images, a reference and the run or test image. The reference image is taken with a constant pressure on the surface of the test article, typically at atmospheric pressure with no wind hitting the surface. This image is used to normalize or ratio out nonuniformities in the illumination system as well as inconsistencies in the application of the paint. The run image is acquired with the wind tunnel flowing air at the desired test condition. Before a ratio of the two images can be performed, any model movement or deformation needs to be corrected so that the two images overlap each other pixel for pixel. The images are then ratioed, the reference image is divided by the run image, and the PSP calibration is applied to the ratioed image—resulting in the pressure image.

The PSP technique has been used in Lewis wind tunnels with air speeds ranging from 30 knots to Mach 4.0. These tests have shown that pressure changes as low as 0.02 psi can be seen using PSP. The pressure-sensitive paint used at Lewis was developed by McDonnell Douglas Aerospace (MDA) chemists, originally for their internal use. MDA has since provided the PSP to the research community for use in other wind tunnel environments. The PSP system was developed at Lewis from commercially available components, including the digital camera, the personal computer, and the software required for acquisition and data reduction. This technique can now be used by our research customers to complement existing discrete pressure measurement systems.

PSP gives a visual understanding of the pressure phenomena occurring on the surface of aeronautical wind tunnel models, changing the procedures used in wind tunnel test programs. Depending on the results of PSP data taken early in a test program, test matrices and methods can be varied to investigate any anomalies not consistent with pretest predictions.

Lewis contacts: Timothy J. Bencic, (216) 433–5690; Brian P. Willis, (216) 433–2176
Headquarters program office: OA

Hypersonic Tunnel Facility Reactivated

NASA Lewis' Hypersonic Tunnel Facility, located at Plum Brook Station, in Sandusky, Ohio, has undergone a 4-year reactivation that was completed in May 1994 with an integrated systems test. This reactivation has made available to the nation a powerful hypersonic research tool that provides clean airflow to the test article. Its capability can be expanded to Mach 10 by adding an in-line heater.

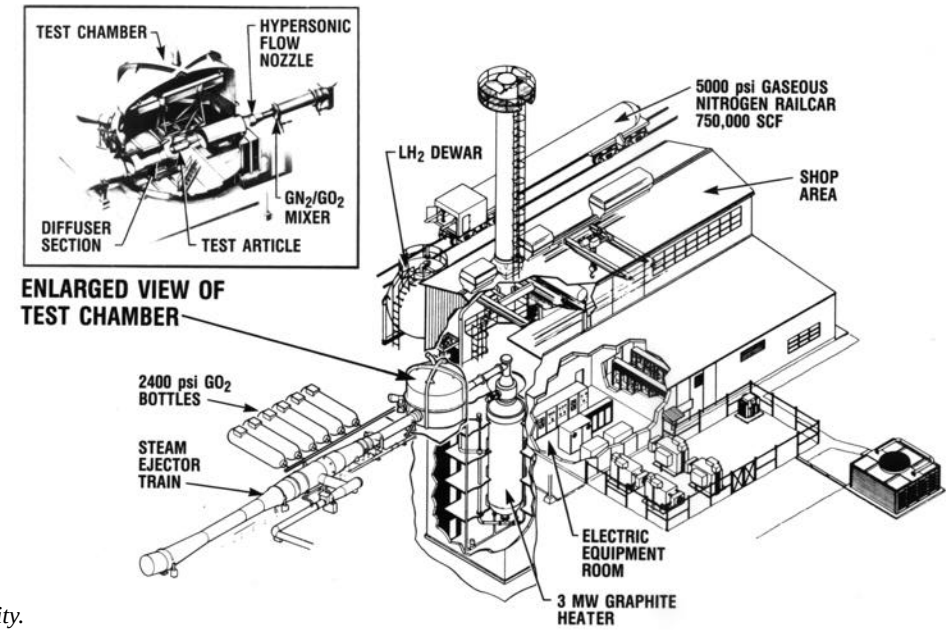

Cutaway view of Hypersonic Tunnel Facility.

From 1971 to 1974 the facility was used to test a model of the hypersonic research engine, an axisymmetric, dual-mode combustion, hydrogen-fueled scramjet engine. Fifty-two tests were successfully completed, for a total test time of 112min.

The facility develops its clean air capability by using a 3-MW inductively heated storage heater. Graphite blocks 6 ft in diameter and 2 ft high with 1100 drilled-through holes are heated to 4500 °R by 4600-psig gaseous nitrogen passed through them. Gaseous oxygen is added to create the synthetic air that is expanded through one of the presently available nozzles at Mach 5, 6, or 7. The free-jet, blowdown tunnel has a 42-in.-diameter, 10-ft-long test section. After the air is passed over the test article, it is exhausted to a diffuser section that is pumped by a large steam ejector. The facility controls and instrumentation system were completely updated.

The facility's support systems have not been reactivated. The facility has extensive hydrogen handling capability and can supply hydrogen as a liquid, at ambient temperature, or heated to 1200 °F. It also has a single-pass schlieren system and a model injection system with a single-axis thrust table for thrusts to 8500 lb. Water for cooling the models is available.

The Hypersonic Tunnel Facility stands ready to provide knowledge in many advanced fields, including (but not limited to) hypersonic ramjets and scramjets, combined-cycle engines, advanced rocket engines (with or without air augmentation), direct-coupled combustor tests, and structures thermodynamic testing.

Lewis contact: William D. Pack, (419) 621–3347
Headquarters program office: OA

Aerospace Technology

Materials

Advanced High-Temperature Engine Materials Technology Makes More Progress

The objective of the Advanced High-Temperature Engine Materials Technology (HITEMP) Program is to generate technology for advanced materials and structural analysis that will lead to increased fuel economy, improved reliability, extended life, and reduced operating costs for 21st century civil aviation propulsion systems. The primary focus is on fan and compressor materials (polymer-matrix composites, PMC's), compressor and turbine materials (superalloys; metal- and intermetallic-matrix composites, MMC's and IMC's), and turbine materials (ceramic-matrix composites, CMC's). These advanced materials are being developed by in-house researchers and on grants and contracts.

NASA considers this program to be a focused materials and structures research effort that builds upon our base research programs and supports component development projects, such as NASA's new initiative to develop the technology for advanced subsonic transport engines. HITEMP is closely coordinated with the Advanced Subsonic Technology (AST) Program and the Department of Defense/NASA Integrated High-Performance Turbine Engine Technology Program. Advanced materials from HITEMP may be used in these future applications.

A Lewis-developed polymer resin with greatly improved processability has been transferred to the AST program to be further developed and scaled up for engine components. An oxidative life prediction model has been developed and verified

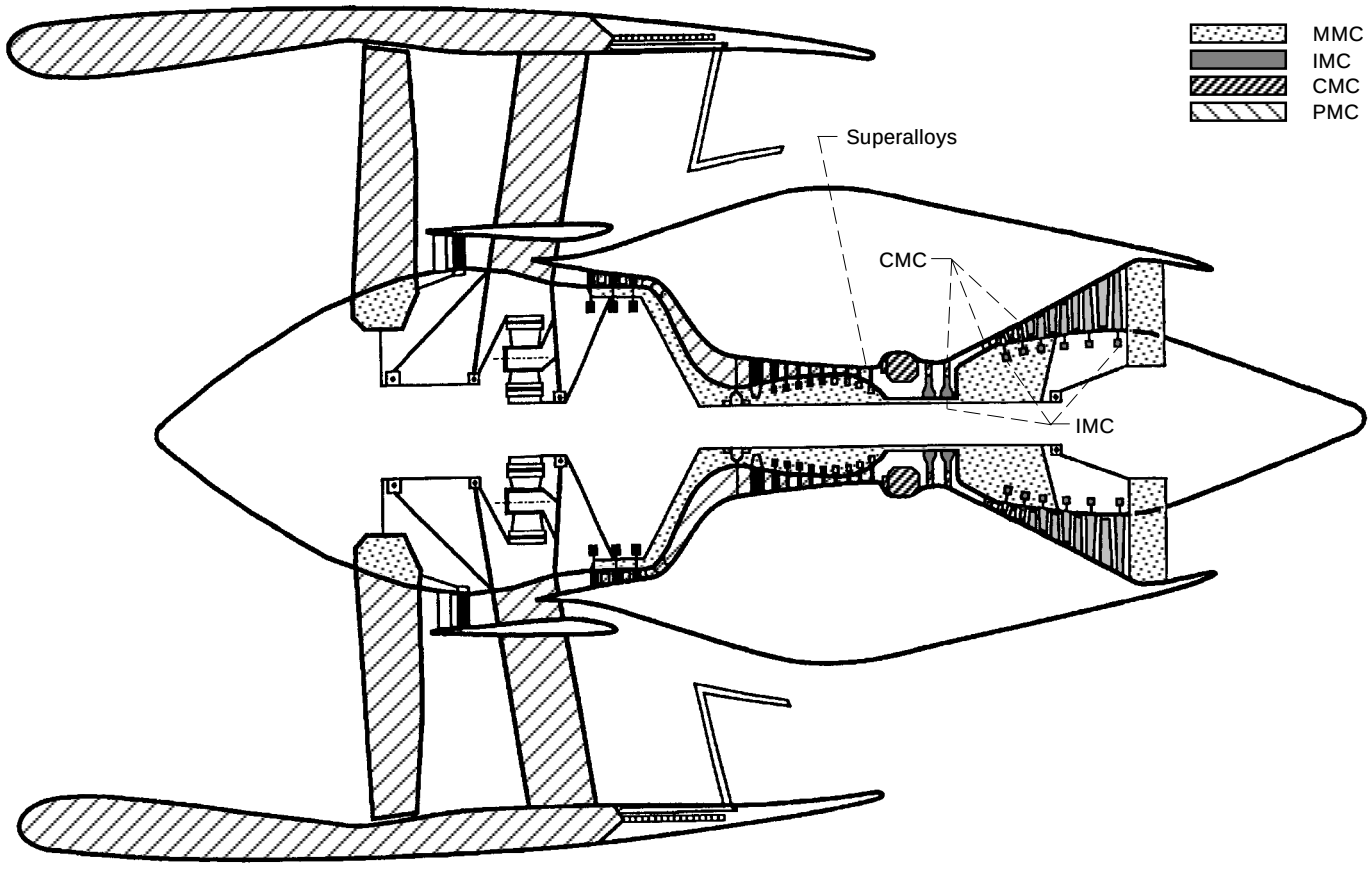

Use of advanced materials in engines.

for nickel aluminum (NiAl) and delivered to General Electric Co. and Pratt & Whitney. An x-ray tomographic system has been developed and is being applied for the nondestructive evaluation of composite materials. Protective coatings on silicon carbide ceramic composites have demonstrated a threefold improvement in thermal mechanical fatigue life. Thin-film palladium-chromium strain gages have been developed and demonstrated at temperatures as high as 1900 °F. A new single-fiber microcomposite test technique has been developed to determine the interface properties of ceramic-matrix composites. Coated silicon carbide ceramic composite vanes have been successfully engine tested to 2000 °F in a cooperative project with the Army and Williams International.

The seventh annual review of the HITEMP program was held October 25 and 26, 1994. Details of research accomplishments are published in a conference report, NASA CP–10146.

Lewis contacts: Dr. Hugh R. Gray, (216) 433–3230; Carol A. Ginty, (216) 433–3335
Headquarters program office: OA

Enabling Propulsion Materials Program Restructured

The NASA High-Speed Research (HSR) Program is developing the technologies for a next-generation supersonic transport, the high-speed civil transport (HSCT). In order for the HSCT to be economically viable and environmentally acceptable, the propulsion system must be efficient, must not generate significant polluting emissions, and must not raise airport or community noise levels beyond acceptable standards. The Enabling Propulsion Materials (EPM) Program, a part of NASA's HSR program, is developing the materials technologies necessary to support the HSR propulsion effort while maintaining U.S. leadership in commercial aircraft propulsion systems. The necessary material technologies include materials and fabrication process development, analytical tools for design and life prediction, and component fabrication and validation through engine testing.

The EPM program focuses on developing advanced materials technologies for HSCT propulsion system components that have the greatest impact on environmental and economic barriers. A high-temperature, long-life combustor liner is required to allow the use of advanced low-emissions combustion concepts. High-temperature, lightweight, durable materials are required for subcomponents in noise-suppressing exhaust nozzles. The economics of an HSCT can be severely impacted if advanced materials technologies are not developed for fan containment, turbine airfoil alloys, and compressor/turbine disks. Novel design concepts and possibly new materials are required for a lightweight, compact fan containment system that must be effective at elevated temperatures. Advances in turbine airfoil alloys, processes, and coatings are required to achieve acceptable lifetimes. New alloys as well as validation technologies are required for compressor and turbine disks that will be large and must operate at elevated temperatures for extended times during supersonic cruise.

One key feature of the EPM program is that the two major U.S. aircraft engine manufacturers, GE Aircraft Engines and Pratt & Whitney, have teamed up to conduct the contractual effort. Other U.S. engine companies, material suppliers, and component manufacturers are subcontractors to the GEAE/P&W HSCT team. NASA Lewis is an integral partner of this team, contributing to the overall critical-path effort. EPM is dedicated to maintaining U.S. leadership in the aircraft industry and is accomplishing this by restricting key data to the U.S. HSCT community. Conversely, strategic technology transfer is required to ensure sufficient markets for continuation of advanced technologies developed under EPM.

Another key aspect of EPM is the use of integrated technology development (ITD) teams. The ITD process implies that all disciplines required to achieve the end product, in this case materials technologies, are united into teams that work concurrently. This process is ideally suited for the EPM program because of the complex teaming arrangements among GEAE, P&W, NASA, and other U.S. industrial companies and because of the challenging technical and schedule milestones. An ITD team has been established for

each critical component, as well as for business management (finance, contracts, procurement, etc.) and product assurance (change control, quality of product, process, etc.).

A ceramic-matrix composite combustor liner is deemed necessary for low-emissions combustors, such as a rich-burn, quick-quench, lean-burn or a lean, premixed, prevaporized concept. Silicon carbide (SiC) fiber-reinforced SiC composites have been selected for this application. Significant accomplishments in fiber strength, matrix processing, test methods, and design approaches have been achieved during the past year. As a backup, efforts using high-temperature superalloy liners for low-emissions combustor concepts have begun.

A restructuring of exhaust nozzle program goals due to HSR engine-cycle selections has resulted in lower temperature requirements for nozzle structural materials. State-of-the-art material systems can likely be utilized for an HSCT exhaust nozzle, but advances in scaleup capability, designs, and life prediction methodologies are still required. The effort in developing these materials technologies for HSCT exhaust nozzles is well under way, with some relatively large-scale hardware already being fabricated.

The fan containment effort has focused on establishing system requirements and developing novel design concepts. Preliminary advanced superalloy compositions have been identified, fabricated, and tested for HSCT turbine airfoil alloy and compressor/turbine disk applications. Additional iterations of alloy development and testing will be required before downselecting candidates for each application.

Likewise, thermal barrier coating systems for turbine airfoils have been identified and initial testing has been completed.

EPM and the entire HSR program has undergone a major rebaselining effort completed at the end of government fiscal year 1994. The timing of this extensive programmatic restructuring is consistent with many of the technical changes occurring in the EPM program: revised exhaust nozzle requirements; initiation of technical efforts for fan containment, turbine airfoil systems, and compressor/turbine disks; and establishment of a feasible approach toward combustor backup materials. The outlook for fiscal 1995 is very positive as our efforts are now streamlined and focused toward achieving our goals.

Lewis contact: Joseph Doychak, (216) 433–8560
Headquarters program office: OA

Titanium-Matrix Composite Fatigue Studied in Realistic Engine Cycle

In a cooperative program, NASA Lewis and Textron Lycoming tested a titanium-matrix composite using stress/temperature cycles expected in a ring-reinforced impeller of a developmental turboshaft engine. Performance and thrust-to-weight goals of such advanced gas turbine engines require significant advances in material capabilities. Titanium-matrix composites (TMC's) offer great opportunities to reduce compressor weight and increase rotational speed. Encouraging lifetimes have been demonstrated for current TMC's in isothermal fatigue cycles, but lifetimes exhibited in thermomechanical fatigue tests with their idealized stress/temperature cycles have been a concern. Moreover, none of these fatigue tests fully represent realistic service conditions. The objectives of this program were to understand TMC material behavior under actual engine operating conditions and establish a correlation between isothermal fatigue data and more realistic mission testing.

A current-generation TMC, SCS–6/Ti–6–4 (carbon-coated silicon carbide fibers in a titanium alloy matrix containing 6% aluminum and 4% vanadium), was employed in this program. It was fabricated as eight-ply, unidirectional panels with a modest fiber content of 35%. Dogbone specimens cut from these panels were tested using a load-controlled, uniaxial test system to simulate the fiber-direction loads in a ring-reinforced impeller of an advanced turboshaft engine under development at Textron Lycoming. The mission test, a complex nonisothermal fatigue test, produces a peak temperature and stress of 800 °F and 160 ksi and has a 14-min period. Each cycle simulates the stress and temperature waveforms expected under actual operating conditions of a turboshaft engine in which engine speed changes in a prescribed fashion.

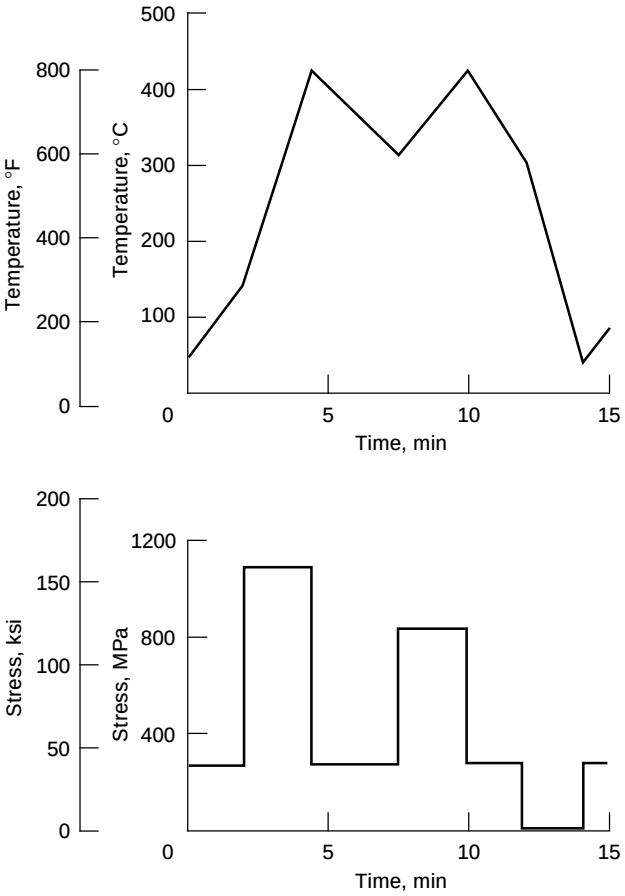

Temperature and stress waveforms used in mission testing of titanium-matrix composites.

Initial mission testing lasted 9528 cycles. In comparison, the isothermal fatigue life at comparable stress levels was about 22,000 cycles. As the time at elevated temperatures and stresses is much longer for the mission test, the shorter cyclic life was not unexpected. However, the fracture mode in the mission test was similar to that in isothermal fatigue tests. Initiation sites at cut edge fibers and other surface anomalies were followed by large regions of flat fatigue crack propagation, transitioning to a more ductile, tensile-overload region.

Although initial mission testing did not achieve the desired 15,000-cycle life, a common compressor life goal for human-rated turbine engines, the measured life of 9528 cycles suggests that the design goal is achievable by increasing fiber content and/or slightly decreasing peak stress or temperature. Alternatively, more advanced TMC's with stronger fibers and more creep-resistant Ti-alloy matrices are under development. These show considerable promise to exceed the 15,000-cycle life goal without cutting back on peak temperature or stress. Future work will attempt to answer these questions.

Bibliography

Gayda, J.; Aksoy, S.Z.; and Gabb, T.P.: Fatigue Behavior of $[0]_8$ SCS–6/Ti–6Al–4V Composite Subjected to High Temperature Turboshaft Design Cycles. Thermo-Mechanical Fatigue Behavior of Materials: 2nd Volume, ASTM STP 1263, M.J. Verrilli and M.G. Castelli, eds., American Society for Testing and Materials, 1995.

Lewis contacts: Dr. John Gayda, (216) 433–3273;
Dr. Timothy P. Gabb, (216) 433–3272
Headquarters program office: OA

Creep-Rupture Goals Set for Ceramic Fiber Reinforcement

The key to successfully applying composite materials at high temperatures is the judicious selection and incorporation of continuous-length ceramic fibers. These fibers must display high as-produced modulus and strength and must reliably maintain these properties throughout the intended thermostructural life of the composite. To ascertain which of the many available fiber types can best provide these performance needs for advanced aeropropulsion components, ongoing in-house research efforts under the NASA HITEMP and EPM programs are measuring and evaluating the creep and rupture strengths of single individual fibers. Typically, we subject a fiber to a constant stress at a constant temperature under environmental conditions of technical interest and then observe the times to reach a critical creep strain limit (creep failure) and to finally fracture (rupture failure). From these data, we can then determine upper-limit stresses (or strengths) for a given service life and use temperature.

To select fibers for a particular composite application, the creep and rupture strengths measured for individual fibers can then be compared against quantitative strength goals. These goals are derived from composite theory and the thermostructral requirements of the composite material (ref. 1). As an illustration, one might assume that to have any technical or commercial viability, advanced composite materials at a minimum should outperform the

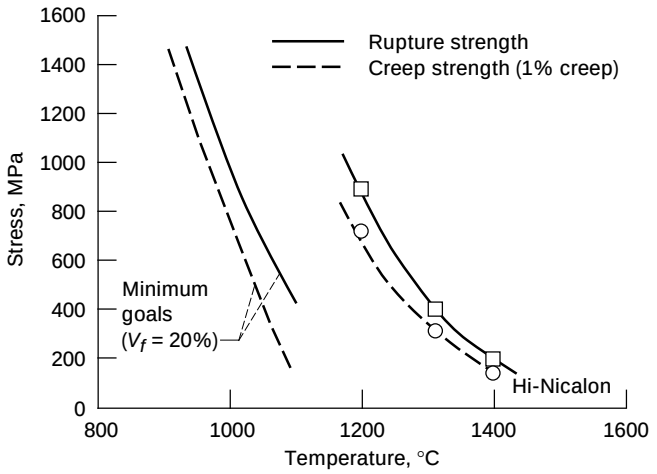

Fiber minimum creep and rupture strength goals based on composite performance equivalent to superalloys.

best conventional structural materials (nickel-based superalloys). Then, using creep and rupture strength data for the best superalloys (ref. 2), one can arrive at the temperature-dependent minimum fiber strength goals shown by the two curves near 1000 °C in the graph. Here it has been assumed that the material application requires a 100-hr service life in air with a creep strain limit of 1% and that the composite has a two-dimensional fiber architecture with an effective fiber volume fraction of 20% in the principal stress direction. Strength results for the silicon carbide-based Hi-Nicalon fiber (ref. 3) indicate that it should provide composites thermostructurally superior to superalloys at use temperatures above 1000 °C (see graph). However, similar data for commercial polycrystalline alumina fibers generally do not meet the minimum goals (ref. 4). This inadequacy has effectively eliminated these fibers from some NASA applications and has focused oxide-fiber developmental efforts toward more stable single-crystal and polycrystalline compositions (refs. 4 and 5).

Rererences

1. DiCarlo, J.A.: Property Goals and Test Methods for High Temperature Ceramic Fiber Reinforcement. Eighth CIMTEC Proceedings, 1994.

2. International Nickel Inc.: High Temperature, High Strength, Nickel Base Alloys. Company brochure, 1984.

3. Yun, H.M.; Goldsby, J.C.; and DiCarlo, J.A.: Tensile Creep and Stress Rupture Behavior of Polymer Derived SiC Fibers. NASA TM–106692, 1994.

4. Goldsby, J.C.; DiCarlo, J.A.; Yun, H.M.; and Morscher, G.N.: Thermomechanical Properties of Advanced Polycrystalline Oxide Fibers. HITEMP Review 1993: Advanced High-Temperature Materials Technology Program, NASA CP–19117, 1993, p. 85.

5. Sayir, A.; Farmer, S.C.; and Dickerson, P.O.: Status of Single Crystal and Directionally Solidified Oxide Fibers. ibid, p. 83.

Lewis contact: Dr. James A. DiCarlo, (216) 433–5514
Headquarters program office: OA

New Tensile Test Determines CMC Interfacial Properties

Fiber-reinforced, ceramic-matrix composites (CMC's) must have weak interfaces between fiber and matrix to be damage tolerant. Maintaining a weak interface at high temperatures in corrosive environments is the greatest hurdle to be overcome before CMC's can be used in high-temperature engine components. Only carbon and boron nitride interfaces now consistently provide the interfacial properties desired. But these materials degrade when subjected to oxidizing environments at high temperatures. Therefore, NASA Lewis is trying to develop alternative materials or approaches to provide weak fiber/matrix interfaces.

Large quantities of coated fiber are required to make CMC test specimens. But developmental fiber coating processes can only reliably coat small quantities of fiber—often insufficient for making even a single CMC test specimen. To address this need, NASA Lewis developed a single-fiber microcomposite test that requires only a small amount of fiber (~15 cm per test specimen), so that critical tests can be performed to evaluate the interface.

The single-fiber microcomposites tested in this work were made of a chemically vapor-deposited silicon carbide fiber (~0.143 mm in diameter) produced by Textron Specialty Materials (Lowell, Mass.), an interfacial coating, and a chemically vapor-deposited silicon carbide sheath (~0.15 mm thick) produced by B.F. Goodrich (Cleveland, Ohio). Conventional carbon and boron nitride interfaces were chosen because their known interfacial properties enable the accuracy of this test to be determined. The actual microcomposite

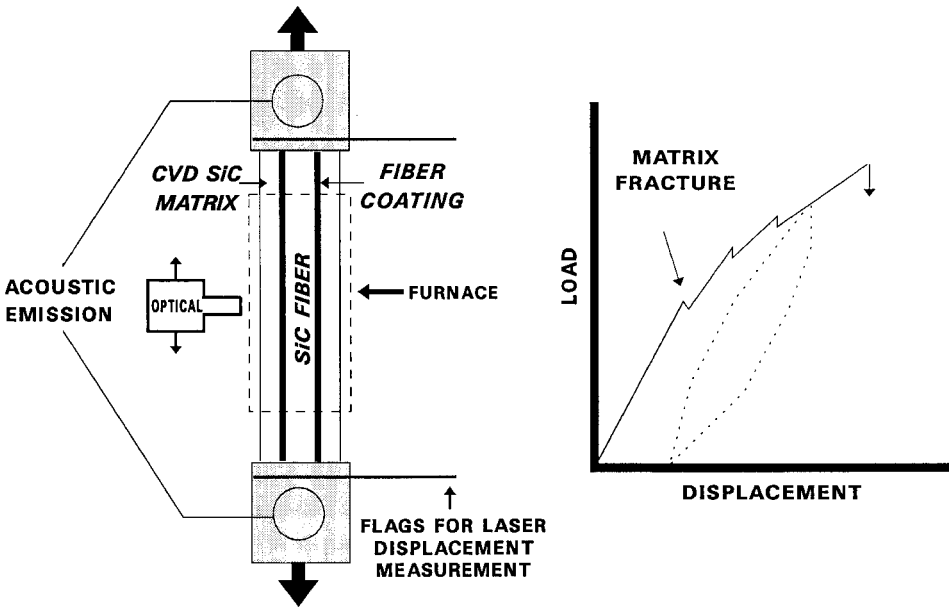

Microcomposite test setup and load displacement behavior.

tensile test is performed with a universal testing machine. Acoustic emission is monitored to "listen" for crack events, the microcomposites are monitored in situ with a traveling optical microscope, displacement is measured with a laser device, and a furnace can be inserted to perform tensile tests at high temperatures in oxidizing environments.

We used a variety of techniques to determine the interfacial properties from the tensile tests at room temperature. Three techniques worked considerably well: a matrix crack saturation approach, a load/displacement cyclic technique (hysteresis loop), and a crack opening displacement technique. The techniques were used to determine the interfacial shear strength indirectly. The interfacial shear strength was then measured directly with conventional push-out and pull-out techniques. Very good agreement was found between the indirect and direct methods. However, the microcomposite test better represents actual composite behavior and can be performed at the test conditions of interest. Therefore, we are now working to determine the interfacial properties at high temperatures in corrosive environments on developmental interfaces.

Bibliography

Morscher, G.N.; Martinez-Fernandez, J.; and Purdy, M.J.: Determination of Interfacial Properties Using a Single Fiber Microcomposite Test. HITEMP Review 1994: Advanced High-Temperature Engine Materials Technology Program, NASA CP–10146, 1994.

Lewis contact: Gregory N. Morscher, (216) 433–8675
Headquarters program office: OA

Oxidation-Resistant Coating Stable to 1400 °C Identified for SiC/RBSN Composites

To meet the goal of advanced engines with improved efficiency and performance, research efforts are directed at technologies for fabricating structurally reliable, fiber-reinforced, ceramic-matrix composites (FRCMC's) that are strong, tough, oxidation resistant, and able to withstand high temperature and heat fluxes. A variety of FRCMC's have been developed for these applications. NASA Lewis is developing silicon-carbide-fiber-reinforced, reaction-bonded silicon nitride (RBSN) composites fabricated primarily by reaction bonding. Presently, large-diameter (144 μm) chemically vapor-deposited (CVD) SiC fibers (Textron SCS–6) are being used. However, processing approaches are being developed for fabricating an RBSN matrix with small-diameter (14 μm) fibers.

Under fast-fracture conditions the SCS–6/RBSN composites display a metal-like, stress-strain behavior and graceful failure beyond matrix fracture at temperatures to 1500 °C in air. Even after a 100-hr exposure test in an oxidizing environment from 1200 to 1400 °C, these composites show excellent strength retention (>60%) at room temperature. However, prolonged exposure between 600 and 1000 °C causes significant strength loss (~50%). This loss was attributed to oxygen diffusion through the porous RBSN matrix and oxidation of the carbon interface coating on SCS–6 fibers, as indicated by large oxidative weight loss between 600 and 1000 °C. To avoid the intermediate-temperature oxidation problems in SiC/RBSN composites, NASA Lewis is investigating a variety of techniques. Surface coating applied by a CVD method is one of them.

A commercially available CVD external coating called RT–42 (an SiC-based coating from Chromalloy) was applied to SCS–6/RBSN composite test coupons. Oxidation and burner rig tests were performed from 600 to 1400 °C for up to 100 hr to determine oxidation behavior and cyclic stability of the coated composites. The oxidation tests were performed at NASA Lewis and the burner rig tests at Williams International under a cooperative agreement. Coated composites showed less oxidation attack than the uncoated composites. Also coated composites showed no evidence of internal or coating damage after five thermal cycles from 25 to 1400 °C in burner rig tests.

We concluded that CVD surface coating can significantly improve the oxidative stability of SiC/RBSN composites and that the coated composites

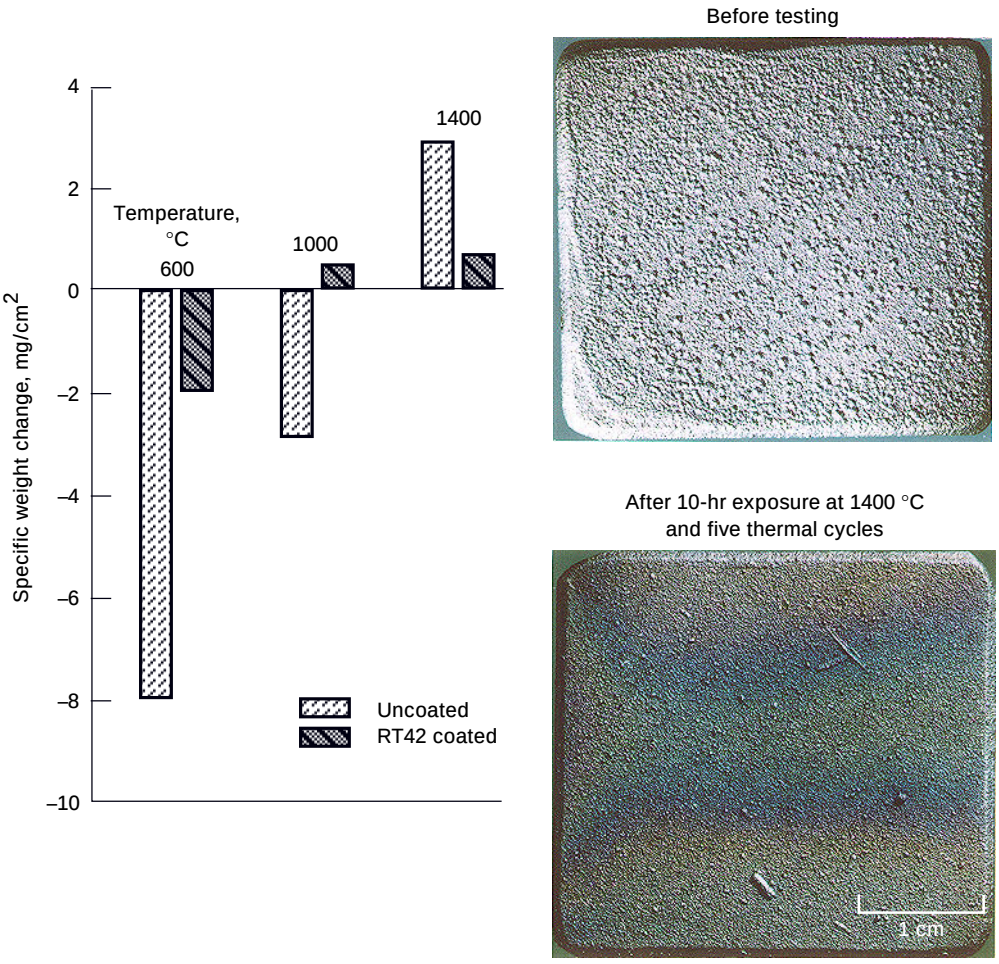

Oxidation data and photomicrographs of SiC/RBSN composites before (top) and after (bottom) 10-hr exposure at 1400 °C for five thermal cycles.

can be used for thermally loaded components in high-temperature applications.

Bibliography

Bhatt, R.T.: Oxidation Effects on the Mechanical Properties of an SiC-Fiber-Reinforced Reaction-Bonded Si_3N_4 Matrix Composite. J. Am. Cer. Soc., vol. 75, no. 2, 1992, pp. 406–412.

Fohey, W.; Bhatt. R.T.; and Baaklini, G.Y.: Burner Rig and Engine Test Results of SiC/RBSN Composites. Vol. III, NASA CP–19117, 1993, pp. 68–1 to 68–11.

Fox, D.S.: Oxidation Kinetics of Coated SiC/RBSN Composites. Vol. III, NASA CP–19117, 1993, pp. 69–1 to 69–10.

Lewis contact: Dr. Ramakhrishna T. Bhatt, (216) 433–5513
Headquarters program office: OA

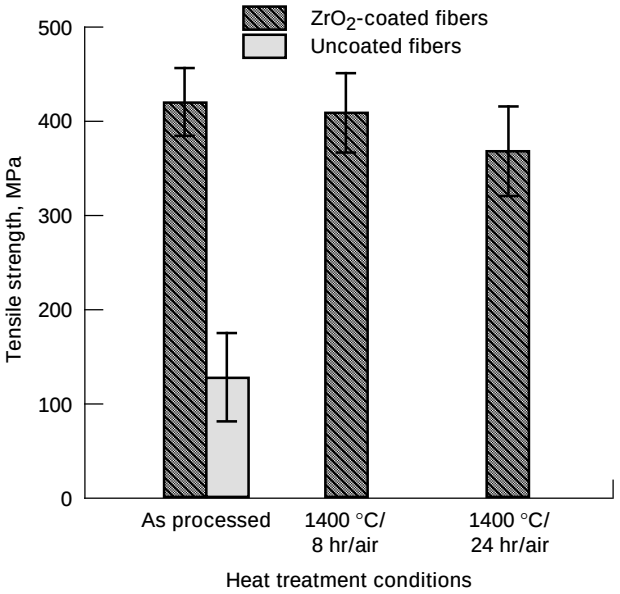

Alumina-matrix composite tensile strength before and after heat treating.

Strong, Tough Sapphire-Fiber-Reinforced Alumina Developed

To develop advanced engines, the aerospace industry requires materials that can withstand increasingly higher temperatures while under oxidizing conditions. Because of their inherent oxidation resistance, oxide-matrix composites reinforced with oxide fibers are being investigated for these applications. To enhance the strength and toughness of these composites, single-crystal sapphire (alumina) fibers coated with unstabilized zirconia are used as the oxide reinforcement. The single-crystal sapphire fibers provide better microstructural and thermomechanical stability than polycrystalline alumina fiber candidates. The unstabilized zirconia coatings enhance the toughness of the system by providing the weak fiber/matrix interface necessary for nonbrittle failure of the composite. Choosing a highly refractory alumina matrix avoids any problems due to mismatch of thermal expansion coefficients between fiber and matrix.

To optimize composite mechanical behavior, various composite processing conditions have been studied in-house at NASA Lewis. The effectiveness of the interfacial coatings was evaluated by fabricating and testing composites with 30 vol% of either coated or uncoated fibers. The uniform fiber coatings were porous, fine-grained, unstabilized zirconia, approximately 1 to 2 μm thick. Additional composites were fabricated for further heat treatment at 1400 °C for 8 or 24hr in an oxidizing envir onment. Then the as-fabricated and heat-treated composites were tensile tested at room temperature.

For the processing conditions studied, average tensile strengths to 421 MPa were measured for composites containing zirconia-coated fibers. In comparison, similar processing of composites containing uncoated fibers yielded samples with much lower tensile strengths of 130 MPa. The coated-fiber composites also displayed considerable strength retention after heat treatment. After treatment at 1400 °C for 8 or 24hr in air the composites r etained as much as 95 or 87%, respectively, of their as-fabricated tensile strength.

These results indicate the potential usefulness of oxide composites in oxidizing atmospheres at high temperatures. To fully explore the possibilities of these composites and the effectiveness of the zirconia interfacial coating, a series of high-temperature tests comparing the performance of these composites and nonoxide composites in oxidizing environments will be necessary.

Lewis contact: Martha H. Jaskowiak, (216) 433–5515
Headquarters program office: OA

Lewis Distinguished Paper and Lewis Materials Division Paper of the Year for 1993

Interfacial Chemistry of Perfluoroalkylether Lubricant Studied

Perfluoropolyethers (PFPE's) are being investigated for potential applications as high-temperature lubricants in advanced gas turbine engines. These fluids have also been used extensively as lubricants for space mechanisms, generally operating near room temperature. However, their performance in the presence of ionizing radiation, under tribological conditions, and in the presence of various catalytic materials has exposed serious deficiencies. In many cases, the PFPE fluids were extensively degraded and caused severe corrosion problems on metal surfaces.

Recent progress in electronics has resulted in longer life, lower weight satellites. Lubrication, and hence mechanism, failure is now becoming the life-limiting factor on spacecraft. New or improved (e.g., with soluble additives) lubricants are needed for long-term operation in space, requiring a deep understanding of the chemistry and interactions that take place at the metal/lubricant interface.

The interfacial chemistry of Fomblin Z25, a commercial perfluoropolyether used as a lubricant for space applications, with different metallic surfaces—440C steel, gold, and aluminum—was studied. Thin layers of Fomblin Z25 were evaporated onto the vacuum-cleaned, oxide-free substrates, and the interfacial chemistry was studied by x-ray photoelectron spectroscopy (XPS) and temperature desorption spectroscopy (TDS). The reactions were induced by heating the substrate and rubbing it with a steel ball. These experiments were done in ultrahigh vacuum to preserve the cleanliness of the surfaces.

Gold was found to be completely unreactive toward Fomblin at any temperature. Reaction at room temperature was observed only for the aluminum substrate, the most reactive toward Fomblin Z25 of the substrates studied. It was necessary to heat the 440C steel substrate to 190 °C to induce fluid decomposition. The degradation of the fluid was indicated by a debris layer at the interface. This debris layer, composed of inorganic and organic reaction products, when completely formed, passivated the surface from further attacking the Fomblin on top. The tribologically induced reactions on 440C steel formed a debris layer chemically like the thermally induced layer. In all cases the degradation reaction resulted in preferential consumption of the difluoroformyl carbon ($-OCF_2O-$).

Presently, the interfacial chemistry of Krytox, another PFPE widely used as a lubricant for space applications, with the same surfaces is being studied. These results will provide insight into the interfacial chemistry of the PFPE, knowledge necessary for developing inhibitors or additives that will improve the performance and extend the life of these fluids.

Bibliography

Herrera-Fierro, P.; Jones, W.R., Jr.; and Pepper, S.V.: Interfacial Chemistry of a Perfluoropolyether Lubricant Studied by X-Ray Photoelectron Spectroscopy and Temperature Desorption Spectroscopy. J. Vac. Sci. Technol. A, vol.11, no. 2, 1993, pp. 354–367.

Herrera-Fierro, P.; Pepper, S.V.; and Jones, W.R., Jr.: X-Ray Photoelectron Spectroscopy Study on the Stability of Fomblin

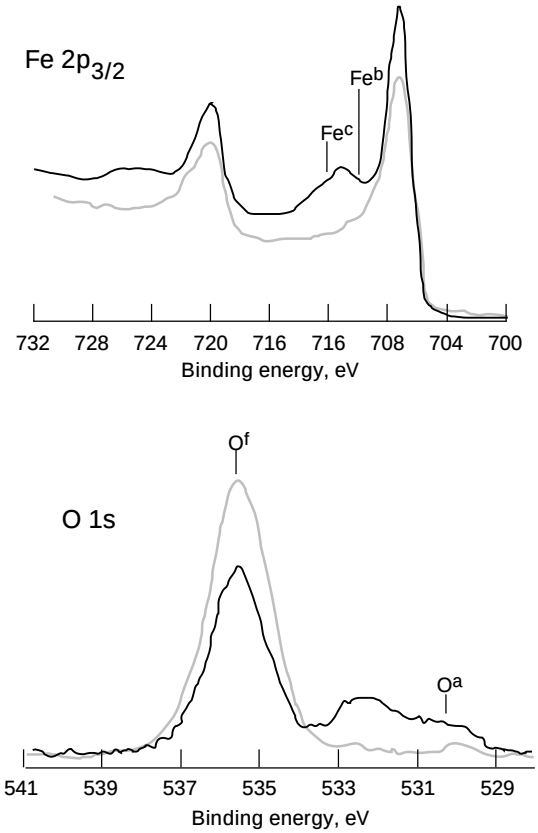

High-resolution XPS of worn area after sliding a 440C ball against Fomblin Z25 film 50 Å thick on 440C steel disk.

Z25 on the Native Oxide of Aluminum. J. Vac. Sci. Technol. A, vol. 10, no. 4, 1992, pp. 2746–2751.

Lewis contact: Dr. Pilar Herrera-Fierro, (216) 433–6053
Headquarters program offices: OA and OSAT

NASA Solid Lubricant Composite Technology Receives Technical Award

Over the past 5 years a family of high-temperature composites, designated PM212, has been developed. PM212 is a ternary composite made from a hard, wear-resistant, metal-bonded chromium carbide matrix with barium fluoride/calcium fluoride eutectic and silver added as high- and low-temperature lubricants, respectively. PM212 formed by powder metallurgy processing can be made into many free-standing components, such as bushings, bearings, valve guides, and seal faces. In plasma-sprayed coating form the composite has been successfully used to lubricate exhaust waste-gate valve shafts on large, heavy-duty diesel engines. In small engine applications the composite has lubricated rotary valves and thermal barrier coatings on Wankel engine sidewall seals. Further efforts are aimed at transferring this technology into industry.

A recent paper by NASA Lewis scientists has received the Society of Tribologists and Lubrication Engineers Captain Alfred E. Hunt Best Paper Award for 1993–1994. The paper (see bibliography) describes the results of an innovative in-house research program to develop self-lubricating composite materials for a wide variety of applications. The award-winning paper reviews the composites' formulation and functions and emphasizes the information (strength, thermal properties, friction and wear properties, etc.) needed by designers and engineers to assess the feasibility of using PM212 in their designs.

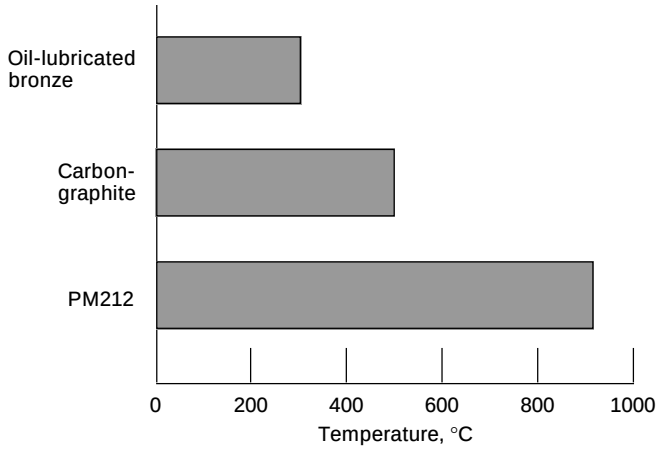

Maximum use temperatures of PM212 and conventional bearing materials.

Bibliography

DellaCorte, C.; Sliney, H.E.; and Bogdanski, M.S.: Tribological and Mechanical Comparison of Sintered and HIPped PM212: High Temperature Self-Lubricating Composites. Lubr. Eng., vol. 48, Nov. 1993, pp. 877–885. (Also NASA TM–105379.)

Lewis contact: Dr. Christopher DellaCorte, (216) 433–6056
Headquarters program office: OA

Screen-Cage Ion Plating Developed

It is well known that unlubricated ceramics are unacceptable for commercial sliding and rolling applications. Therefore, lubrication is required before they become useful. One way to reduce the friction of ceramics is to coat them with soft, metallic films. The screen-cage ion plating (SCIP) process, developed in-house at NASA Lewis, can apply adherent metallic films to complex shapes of electrically nonconductive materials, such as polycrystalline alumina and other ceramics. The primary objective of this development was to apply silver lubricating films to high-temperature ceramic components of advanced combustion engines so as to reduce friction and wear. Other potential uses for SCIP include coating substrates with metal for protection against corrosion, depositing electrical conductors on dielectric substrates, making optically reflective surface layers, and applying decorative metal coats to ceramic trophies or sculptures.

The SCIP system basically consists of a dc-diode configuration. The ceramic (Al_2O_3) substrate is mounted and surrounded with a screen cage to which a negative potential (–3000 V, 80 mA) is applied in an argon pressure of 20 mtorr. The effectiveness of SCIP is attributed to its ability to provide a high-energy flux of ions and energetic neutral atoms that contribute to the excellent adherence and desirable microstructure of the deposited film. An important additional advantage of this technique is known in the industry as "throwing power"—the ability to coat even non-

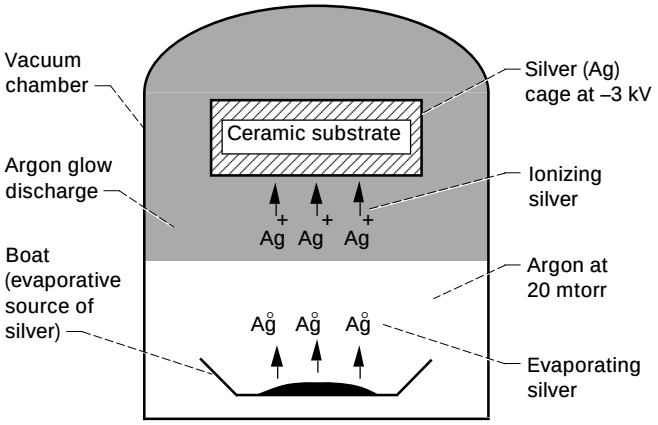

Screen-cage ion plating (SCIP) for ceramics.

line-of-sight surfaces to produce three-dimensional coverage of the substrate.

The deposited silver lubricating films reduce the coefficient of friction by 50% during sliding contact and thereby also reduce the surface tensile stresses that contribute to undesirable subsurface cracking and subsequently to severe wear. In this research the effect of friction on the critical stress for crack initiation was accurately predicted by a mathematical model.

The process is further extended to utilize reactive (oxygen-argon) glow discharge to deposit silver and gold films on ceramic (Al_2O_3) surfaces with high adherence. The oxygen presence in the glow discharge dramatically increases metallic film adherence. SCIP offers a simple, economic coating process to ion plate silver, gold, and other metals on ceramic surfaces with excellent adherence and three-dimensional coverage.

Bibliography

Sliney, H.E.; and Spalvins, T.: The Effect of Ion-Plated Silver and Sliding Friction on Tensile Stress-Induced Cracking in Aluminum Oxide. STLE J., vol. 49, no. 2, pp. 153–159. (This paper received STLE Al Sonntag Award (best solid lubricant paper written) at the 1994 STLE Annual Meeting in Pittsburgh.)

Spalvins, T.; and Sliney H.E.: Frictional Behavior and Adhesion of Ag and Au Films Applied to Aluminum Oxide by Oxygen-Ion-Assisted Screen Cage Ion Plating (SCIP). NASA TM–106522, 1994.

Tech Brief: LEW–15858, June 1994.

Lewis contact: Talivaldis Spalvins, (216) 433–6060
Headquarters program office: OA

Rigid-Rod Polyimide Fibers Studied

Rigid-rod polymers are well known for their interesting liquid crystalline behavior, in which the polymers exhibit order either in the melt or in solution at certain critical concentrations. Most importantly, rodlike polymers, such as Xydar, Kevlar, and polybenzobisoxazole (PBO), exhibit outstanding performance as high-strength, high-modulus fibers suitable for industrial applications. However, rigid-rod polymers are often insoluble in common organic solvents and difficult to process. For instance, the Kevlar fibers are spun from concentrated sulfuric acid. Efforts to increase the solubility have included the use of bulky groups, kinks, and crankshaft and noncoplanar structure units along the polymer backbones. Recently, researchers at the University of Akron have prepared high-strength, high-modulus polyimide fibers containing noncoplanar structure units on the polymer backbone. These polyimide fibers (namely, PIF and PIM) exhibit better thermo-oxidative stability than Kevlar, while retaining comparable mechanical properties.

NASA Lewis began a research program to synthesize additional rigid-rod polyimides and to evaluate them along with PIF and PIM against Kevlar as fabric wraps for soft-wall fan containment designs in engine applications. A novel polyimide, tetramethyl benzene (TMBZ), was prepared at NASA Lewis by substituting four bulky methyl groups for the hydrogens on the

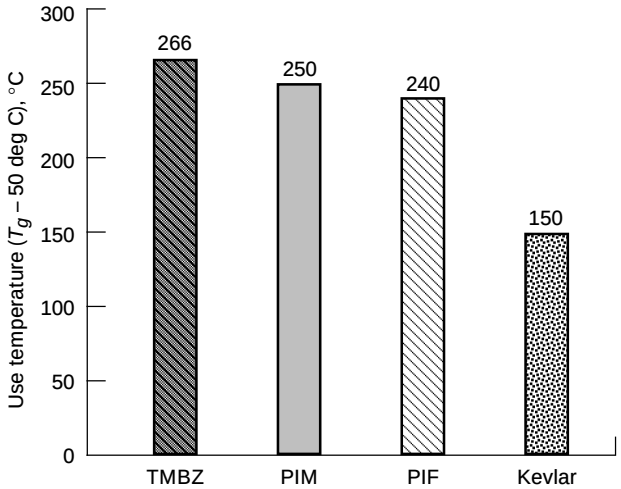

Use temperature of polyimide fibers.

noncoplanar structure units along the polyimide backbone. The objective was to raise the glass transition temperature T_g and thus increase the use temperature. In collaboration with researchers at the University of Akron, an investigation is currently in progress under the Enabling Propulsion Materials (EPM) Program to spin the TMBZ fiber and to evaluate the effect of isothermal aging at 200 to 250 °C on the properties of TMBZ, PIF, and PIM polyimide fibers along with Kevlar and PBO.

Lewis contact: Dr. Chun-Hua Chuang, (216) 433–3227
Headquarters program office: OA

Long-Term Aging Effects Measured for PMR–15 Composites

Polymer-matrix composites are attractive materials for aerospace applications because of their low densities and high specific strengths. Using these materials in aircraft (airframe and engine) can save considerable weight and improve system performance and fuel efficiency. Recent interest in these materials for such programs as High-Speed Civil Transport (airframe) and Advanced Subsonics Technology (airframe and engine) requires that they perform reliably for fairly long times (in some cases over 60,000 hr) at elevated temperatures (400 to 600 °F). However, the effects of long-term aging at these temperatures on composite properties and performance are not fully understood, even for some of the most mature systems, such as NASA Lewis' PMR–15. Most long-term data on these materials have been obtained on small, thin composite specimens, which are not representative of actual component geometries (ref. 1).

In a cooperative research program NASA Lewis and General Electric Aircraft Engines are examining the long-term durability of T650–35-graphite-reinforced PMR–15 composites at 400 to 650 °F. Specifically, this study measures how long-term, elevated-temperature exposure of composite specimens of varying geometries affects their weight retention and compressive strength. Of particular interest is the effect that machined surfaces have on material degradation. Data from this study will be used to develop models to predict the service life of engine components manufactured from this material.

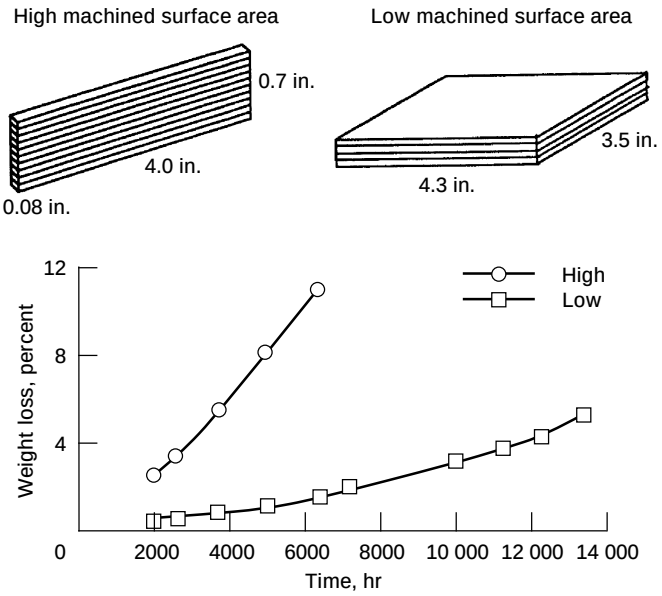

Results of aging PMR–15 composites at 500 °F in air.

Although the study is still ongoing, aging times of nearly 15,000 hr have been logged on composite specimens at 400 and 500 °F, revealing a pronounced effect of machined surface area on composite weight loss. Specimens with high machined surface areas had significantly higher weight losses at 500 °F than samples with low machined surface areas. Photomicrographs of aged specimens show that oxidative attack is more aggressive at machined surfaces because of the exposed fibers (ref. 2). Similar trends were observed for compressive strength loss.

References

1. Nelson, J.B.: Thermal Aging of Graphite/Polyimide Composites. *Long-Term Behavior of Composites*, ASTM STP813, T.K. O'Brien, ed., 1982, pp. 206–221.

2. Bowles, K.J.; and Kamvouris, J.E.: Penetration of Carbon-Fabric Reinforced Composites by Edge Cracks During Thermal Aging. NASA TM–106530, 1994. (Also to appear in the Journal of Advanced Materials.)

Lewis contact: Dr. Kenneth J. Bowles, (216) 433–3197
Headquarters program office: OA

Nontoxic Low-Cost Resin Replaces PMR–15

NASA Lewis-developed PMR–15 is the most widely used high-temperature matrix resin for advanced composite applications above 230 °C for four principal reasons: performance, price, availability, and processability. The applications of PMR–15 to aircraft engines, both military and commercial, are numerous. However, the expanding application of PMR–15 materials, particularly for commercial use, received a major setback when the Occupational Safety and Health Administration (OSHA) established rigid safe-handling regulations on resins containing methylenedianiline (MDA), a suspected carcinogen and a major component of PMR–15 resin. Establishing OSHA safe-handling procedures has significantly raised costs for both suppliers and users of PMR–15 materials. Efforts by industry to find a suitable low-cost nontoxic replacement for PMR–15 have been, to date, unsuccessful.

A recent NASA Lewis study resulted in the development of a nontoxic version of PMR called AMB–21. This MDA-free PMR resin formulation should eliminate most of the rigid handling regulations and reduce costs to suppliers and users of PMR materials. AMB–21 compares favorably with PMR–15 in terms of material cost, ease of processing, mechanical properties, and thermo-oxidative stability (see graph).

AMB–21 composite laminates can be fabricated by using either low-pressure autoclave or high-pressure compression molding process parameters identical to those used for PMR–15 composite materials. Because of the excellent flow characteristics of AMB–21 resin, resin transfer molding and braided "towpreg" fabrication processes are being investigated by Fiber Innovations Inc. under a NASA/General Electric contractual program.

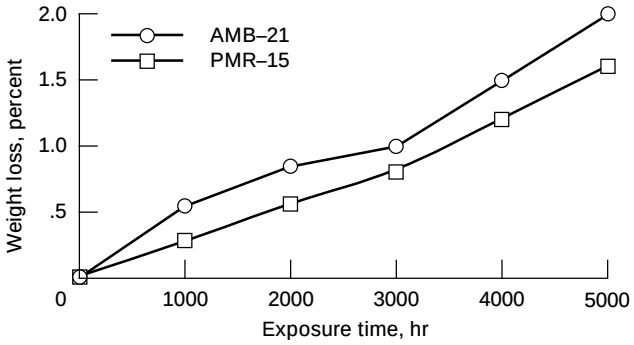

Weight loss of graphite-reinforced AMB–21 and PMR–15 composites after exposure to air at 260 °C.

MDA-free AMB–21 is available from several commercial suppliers in prepreg, powder, and solution forms and is being evaluated as a PMR–15 replacement by a number of major engine and aerospace companies.

Lewis contact: Raymond D. Vannucci, (216) 433–3202
Headquarters program office: OA

Optimization Study of Electrically Conductive Polymers

For aerospace applications, such as electromagnetic interference shielding, spacecraft grounding, and charge dissipation, using polymers would result in tremendous weight savings over metals (ref. 1). Suitable polymeric materials for such applications must combine high electrical conductivity with long-term environmental stability, good processability, and good mechanical properties. Recently, other investigators have reported on hybrid films made from an electrically conductive polymer combined with insulating polymers (refs. 2 to 9). In all instances the films were prepared by infiltrating an insulating polymer with a precursor for a conductive polymer (either polypyrrole or polythiophene) and oxidatively polymerizing the precursor in situ. The resulting composite films have good electrical conductivity while overcoming the brittleness inherent in most conductive polymers.

The highest conductivities reported ($\simeq$4-$\Omega^{-1}cm^{-1}$) were achieved with polythiophene in a polystyrene host polymer (ref. 9). The best films using a polyimide as base polymer (refs. 6 and 7) were four orders of magnitude less conductive than the polystyrene films. The authors suggested that this was because polyimides were unable to swell sufficiently for infiltration of monomer as in the polystyrene. It was not clear, however, if the different conductivities obtained were merely the result of differing oxidation conditions. Oxidation time, temperature, and oxidant concentration varied widely among the studies.

Many aerospace applications require a combination of properties. Thus, hybrid films made from polyimides or other engineering resins are of primary interest, but only if conductivities like those with a polystyrene base can be obtained. Hence, a series of experiments was performed to optimize the conductivity of polyimide-based composite films. The polyimide base chosen for this study was Kapton. 3-Methylthiophene (3MT) was used for the conductive phase.

Three processing variables were identified for producing these composite films, time, temperature, and oxidant concentration for the in-situ oxidation. Statistically designed experiments were used to examine the effects of these variables and synergistic/interactive effects among variables on the electrical conductivity and mechanical strength of the films. Temperatures were varied from –10 to 30 °C, times from 2 to 8hr, and oxidant concentrations from 0.4 to 1.2M. The experiments were carried out in a randomized order. Kapton films were soaked for 24 hr at room temperature with stirring in 3 MT. The monomer-treated films were then oxidized under the selected design conditions. Conductivity was measured with a standard four-point test using direct current. Maximum mechanical stress at maximum load was also measured with a tensile test. The measured values obtained under different oxidation conditions were analyzed by multiple linear regression. The conductivities were log transformed before analysis.

Multiple linear regression analysis of the tensile data revealed that temperature and time have the greatest effect on maximum stress. The response surface of maximum stress versus temperature and time (for oxidant concentration at 1.2 M) is shown. At the oxidation conditions predicted to give maximum conductivity for p-3MT/Kapton, the maximum stress is predicted to be 27,000 psi. If better mechanical properties are needed, compromise conditions can be chosen from the response surface models that give slightly lower conductivities. For example, to obtain predicted maximum stress values closer to untreated Kapton (~34,000 psi) for p-3MT/Kapton, oxidation time can be limited to 2 hr or temperature can be lowered to 10 °C.

Conductivity of the composite films, measured for over 150 days in air at ambient temperature, dropped only fivefold in that time. Films aged under vacuum at ambient temperature diminished slightly in conductivity in the first day but did not change thereafter. This suggests that if the films are protected from air and perhaps moisture, the conductivity will persist indefinitely.

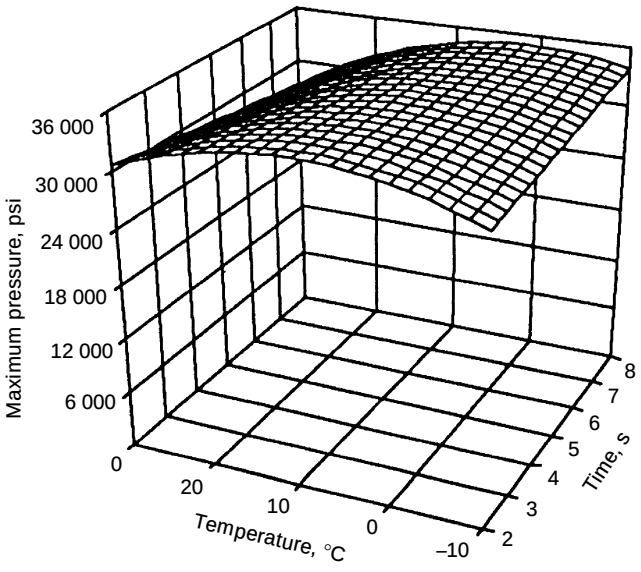

Predicted response surface for maximum mechanical stress in terms of oxidation conditions of conductive polymer films.

References

1. Meador, M.A.B.; Gaier, J.R.; Good, B.S.; Sharp, G.R.; and Meador, M.A.: A Review of Properties and Potential Aerospace Applications of Electrically Conducting Polymers. SAMPE Q., vol. 22, Oct. 1990, pp. 23–31.

2. Li, C.; and Song, Z.: Diffusion-Oxidative Polymerization of Transparent and Conducting Polypyrrole-Poly(Ethylene-Terephthalate) Composites. Synth. Met., vol. 40, 1991, pp. 40, 23.

3. Stanke, D.; Hallensleben, M.L.; and Toppare, L.: Electrically Conductive Poly(Methyl Methacrylate-G-Pyrrole) via Chemical Oxidation. Synth. Met., vols. 55–57, 1993, pp. 1108–1113.

4. Morita, M.; Hashida, I.; and Nishimura, M.: Conducting Polypyrrole Composite Thin Films Chemically Prepared by Spreading on Surface of Aqueous Solution Containing Oxidizing Agent. J. Appl. Polym. Sci., vol. 36, 1988, pp. 1639–1650.

5. Van Duk, H.; Aagaard, O.; and Schellekens, R.: Precursor Monomer Route: A Novel Concept for Producing Highly Conductive Polypyrrole Films. Synth. Met., vols. 55–57, 1993, pp. 1085–1090.

6. Tieke, B.; and Gabriel, W.: Conducting Polypyrrole-Polyimide Composite Films. Polymer, vol. 31, 1990, pp. 20–23.

7. Dao, L.H.; Zhong, X.F.; Menikh, A.; Paynter, R.; and Martim, F.: Proceedings of Annual Technical Conference of Society of Plastic Engineers, vol. 49, 1991, p. 783.

8. Ruckenstein, E.; and Park, J.S.: The Electromagnetic Interference Shielding of Polypyrrole Impregnated Conducting Polymer Composites. Polym. Compos., vol. 12, no. 4, Aug. 1991, pp. 289–292.

9. Ruckenstein, E.; and Park, J.S.: Polythiophene and Polythiophene-Based Conducting Composites. Synth. Met., vol. 44, 1991, pp. 293–306.

Lewis contact: Dr. Mary Ann B. Meador, (216) 433–3221
Headquarters program office: OA

New Refractory Oxide Coating Protects Silicon-Based Ceramics

Silicon-based ceramics are leading candidate materials for high-temperature structural applications, such as heat exchangers, advanced gas turbine engines, and advanced internal combustion engines. However, durability in high-temperature environments containing molten salts, water vapor, or a reducing atmosphere can limit their application. These environments react with silica, preventing the formation of stable protective silica scale. Therefore, protection schemes are needed for silicon-based ceramics. One promising approach is to apply a barrier coating that is chemically stable in these severe environments. Refractory oxides, such as mullite ($3Al_2O_3 \cdot 2SiO_2$), glass ceramics, yttria-stabilized zirconia ($ZrO_2 \cdot Al_2O_3$), and alumina, are promising candidate coating materials. In addition, refractory oxide coatings can serve as a thermal barrier.

A new fully crystalline plasma-sprayed mullite coating was developed at NASA Lewis. It exhibits dramatically better resistance to thermal shock and molten salt corrosion than conventionally plasma-sprayed mullite coatings (ref. 1). Although mostly free of microcracks and debonding, the new coating still tends to develop through-thickness cracks that can propagate into the substrate under repeated thermal cycling (ref. 2). In environments containing water vapor and/or a reducing atmosphere, the mullite coating offers only limited protection against silica vaporization because of the fairly high (~0.4) silica activity (ref.2).

In an effort to overcome these limitations various overlay coatings were studied. A cordierite overlay coating on mullite-coated silicon carbide (SiC) and SiC/SiC effectively inhibited the propagation of cracks in the mullite base coating under thermal cycling between room temperature and 1200 °C. This system also demonstrated excellent thermal shock resistance. Yttria-stabilized zirconia overlay coating reduced silica vaporization in water vapor and/or a reducing atmosphere.

The large mismatch in coefficient of thermal expansion between mullite (5.4×10^{-6} °C^{-1}) and yttria-stabilized zirconia (10×10^{-6} °C^{-1}) is of concern. However, SiC and SiC/SiC composites coated with mullite/yttria-stabilized zirconia dual-layer coating exhibited excellent thermal shock resistance under thermal cycling between room temperature and 1300 °C. This system also exhibited excellent chemical compatibility at the mullite/zirconia interface and appears to be effective even in inhibiting the propagation of through-thickness cracks in the mullite base coating by deflecting the cracks at the mullite/zirconia interface. Study of this dual-layer system will continue, to optimize its effectiveness as a high-temperature protective coating for silicon-based ceramic materials.

Bibliography

Lee, K.N.; Miller, R.A.; and Jacobson, N.S.: A New Generation of Plasma-Sprayed Mullite Coatings on Silicon-Based Ceramics. Accepted in J. Am. Ceram. Soc., 1994.

Lee, K.N.; Jacobson, N.S.; and Miller, R.A.: Refractory Oxide Coatings on SiC Ceramics. MRS Bulletin, Oct. 1994. (Also NASA TM–106677.)

Lewis contacts: Dr. Kang N. Lee, (216) 433–5634;
Dr. Robert A. Miller, (216) 433–3298
Headquarters program office: OA

Oxidation-Resistant TiAlCr Alloys Developed

NASA Lewis is developing two-phase γ(TiAl) + α_2(Ti_3Al)-based titanium aluminides for intermediate-temperature (600 to 1000 °C) aircraft engine applications. Interest in this use is due to their low density and to the identification of compositions and microstructures that have both reasonable mechanical properties and fair oxidation resistance. However, despite recent advances, oxidation-resistant coatings are still needed. Titanium-aluminum-chromium (TiAlCr) alloys in the composition range (at.%) Ti-(45–55)Al-(10–30)Cr have been identified as potential oxidation-resistant coatings for γ + α_2 titanium aluminides (ref. 1). Although such alloys are extremely oxidation resistant—forming slow-growing, protective aluminum oxide scales in air (ref. 1)—they are also extremely brittle. Therefore, the goal of this in-house study is to co-optimize oxidation resistance and ductility in the TiAlCr system.

We adopted an experimental approach to elucidating the relationships between microstructure, oxidation, and ductility in the Ti-Al-Cr system. The strategy involved

- Studying phase equilibria of alumina formers in the TiAlCr system
- Identifying key constituent phases
- Characterizing alloy oxidation resistance and Vickers microhardness

Property correlations between multiphase and single-phase alloys were then examined to provide a basis for property optimization through microstructural design.

The relevant phases were identified as τ($Al_{67}Ti_{25}Cr_8$), γ(TiAl), r-$TiAl_2$, TiCrAl (laves), and Cr_2Al. Alumina formation was associated with τ, Al-rich TiCrAl, and fine γ + TiCrAl mixtures. Brittleness was associated with TiCrAl, Cr_2Al + TiCrAl mixtures, and τ decomposition to r-$TiAl_2$ and Cr_2Al. Two-phase γ + TiCrAl alloys were identified that offered the potential for protective alumina formation up to 1000 °C in air and limited room-temperature ductility (≈0.5 to 1% based on literature data for single-phase γ alloys). A γ + TiCrAl alloy (Ti-51.25Al-12.25Cr at.%) was produced in which the γ phase was continuous, in order to increase ductility by interrupting the continuity of the brittle TiCrAl phase, and where protective alumina formation was observed.

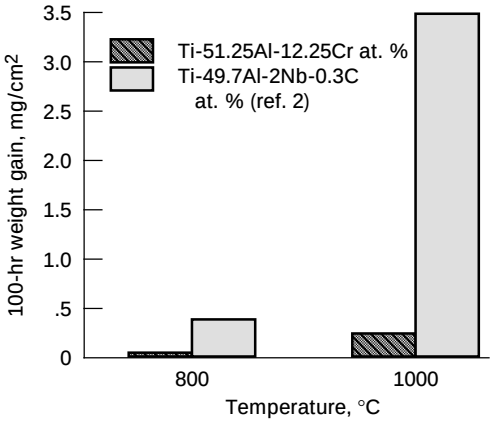

Isothermal 100-hr weight gain at 800 and 1000 °C in air for Ti-51.25Al-12.25Cr.

Future work will concentrate on optimizing ductility through reduced Al content and by additions of refractory elements.

References

1. Meier, G.H.; Perkins, R.A.; Schaeffer, J.C.; and McCarron, R.L.: GE Aircraft Engines Interim Report No.1. Naval Air Development Center Contract N62269–90–C–0287, Mar. 1991.

2. Becker, S.; Rahmel, A.; Schorr, M.; and Schutze, M.: Mechanism of Isothermal Oxidation of the Intermetallic TiAl and of TiAl Alloys. Oxidation of Metals, vol. 38, nos. 5/6, 1992, pp. 425–464.

Lewis contacts: Dr. Michael P. Brady, (216) 433–5504; Dr. James L. Smialek, (216) 433–5500

Headquarters program office: OA

Twin-Knudsen-Cell Mass Spectrometer Studies Alloy Thermodynamics

In developing high-temperature alloys it is important to know the thermodynamic activities for the various alloy components. These activities are used to predict the oxidation properties of the alloy and also the stabilities of second-phase reinforcement materials.

One of the most versatile and direct ways to measure thermodynamic activity is by vapor pressure. The vapor pressure of an alloy component is measured and divided by the vapor pressure of the pure component at a particular temperature. This gives the activity from a first-principles definition. One way to measure a

particular component's vapor pressure is with a Knudsen-cell mass spectrometer. A Knudsen cell is a small enclosure that allows equilibrium between a solid and vapor phase to be attained. A well-defined orifice allows this vapor to be sampled mass spectrometrically by measuring an ion intensity. This ion intensity is directly related to vapor pressure with an appropriate calibration constant. However, on most instruments the calibration constant changes from one analysis to another.

These changes in calibration constant can be avoided by using an internal standard. Instead of using of single Knudsen cell, two cells are used in such a way that a measurement may be taken on the pure component and then on the alloy without breaking the vacuum. There are several experimental problems with this approach. The cells are in a vacuum system and typically heated to 1000 °C or greater. They must be kept at exactly the same temperature and translated to and from the sampling region from outside the vacuum system. The most formidable problem is that the molecular beams emerging from each cell must not be allowed to mix.

Only a few research groups have built systems that completely address these problems. Some groups have separated the cells by a large distance to avoid beam mixing; others have used a system of apertures so that the ionizer effectively sees only inside the cell being sampled. Our approach involves a system of shutters.

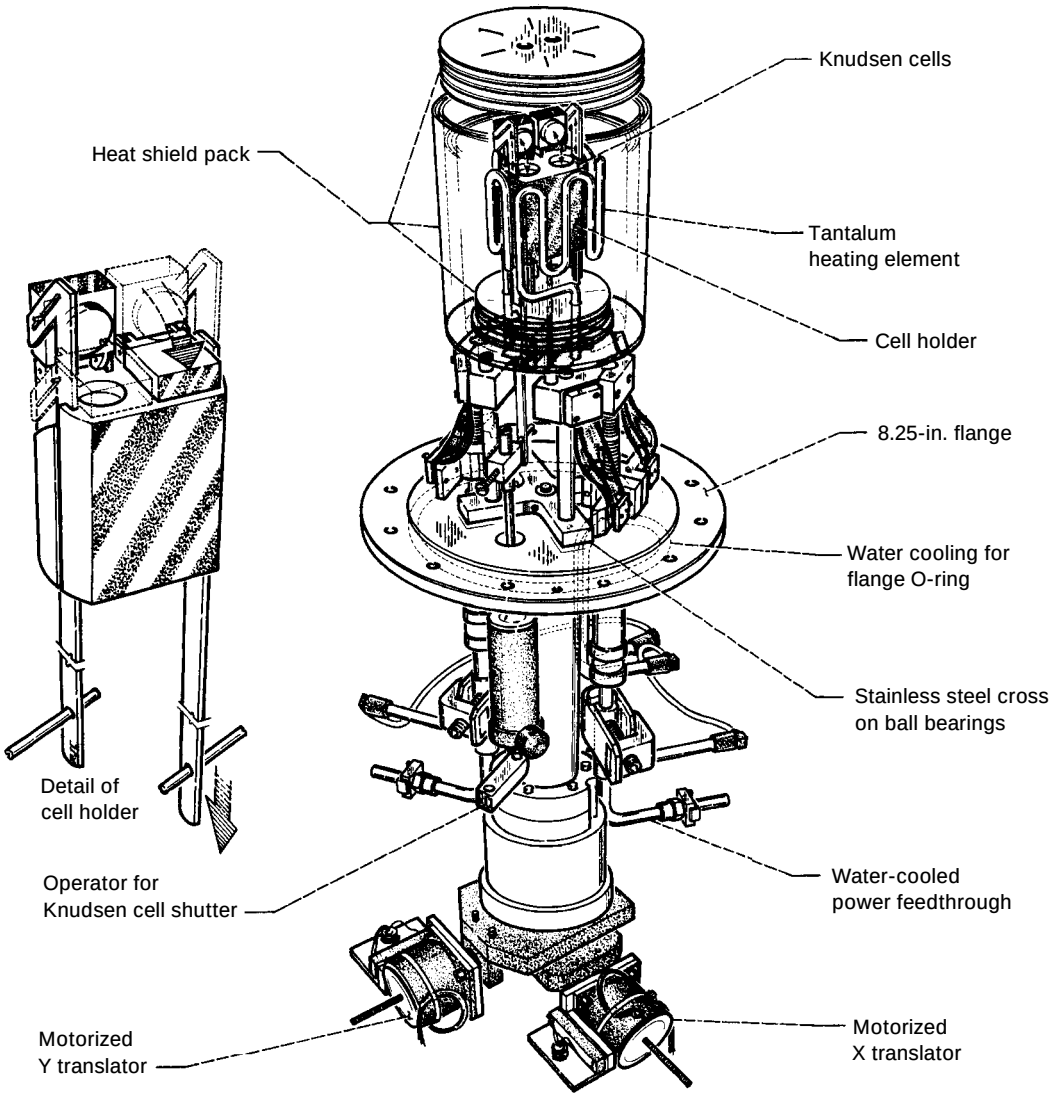

Schematic of twin-Knudsen-cell flange.

The entire furnace and cell assembly is translated from outside the vacuum system by stepper motors controlled by a "joystick." Linear potentiometers are mounted on the translator to provide a digital position indication. The entire cell assembly is mounted on an 8.25-in. flange attached to a commercial mass spectrometer. When the desired cell is in place, the shutter is opened and the signal intensity measured. The net signal is the difference between the shutter opened and the shutter closed.

Even with the shutters a limited amount of beam mixing was unavoidable owing to the mobility of molecules at these temperatures. For measuring higher activities (>0.05) this was not a problem, and the alloy component was compared with the pure component, as described. For measuring very low activities a second calibration material, such as gold, was used and the necessary corrections were made for different mass spectrometric detection characteristics.

The system has been tested on silver-copper and iron-aluminum alloys, for which extensive literature data exists. Our results show very good agreement with these literature values. Studies continue on the technically important nickel-aluminum and titanium-aluminum systems, for which few data are available.

Lewis contact: Dr. Nathan Jacobson, (216) 433–5498
Headquarters program office: OA

Structural Composite Made Strong, Tough, and "Pest" Resistant

The intermetallic compound molybdenum disilicide ($MoSi_2$) is an attractive high-temperature structural material for advanced engine applications. It has excellent oxidation resistance, high melting point, relatively low density, and high thermal conductivity and is easily machined. However, its use has been hindered by brittleness at low temperatures, accelerated oxidation (also known as "pest" oxidation) between approximately 800 and 950 °F, and relatively high coefficient of thermal expansion (CTE) compared to potential reinforcing fibers such as silicon carbide (SiC). The CTE mismatch between the fiber and the matrix results in severe matrix cracking during thermal cycling.

The pesting phenomenon in $MoSi_2$ is most pronounced at approximately 930 °F and has been attributed to the accelerated formation of voluminous molybdenum trioxide (MoO_3). Both monolithic $MoSi_2$ and its composites suffer total disintegration within 100 hr at this temperature. NASA Lewis has attempted to identify a new $MoSi_2$-based composition with excellent "pest" resistance, lower CTE, and good mechanical properties as a matrix suitable for SiC fiber reinforcement.

We investigated the addition of thermodynamically stable silicon nitride (Si_3N_4) as a low-CTE phase. A mixture containing commercial-purity $MoSi_2$ powder and 30 to 50 vol% of fine Si_3N_4 powder was mechanically blended in an attritor. The $MoSi_2$-Si_3N_4 powder and the SCS–6-fiber-reinforced $MoSi_2$-Si_3N_4 composite (fabricated by the powder cloth technique) were consolidated by vacuum hot pressing followed by hot isostatic pressing to produce fully dense panels. Mechanical and oxidation tests were conducted on both monolithic and composite materials.

Adding Si_3N_4 particulates to $MoSi_2$ lowered the low-temperature accelerated oxidation rate (by more than an order of magnitude) by forming an Si_2ON_2 protective scale and thereby eliminated the catastrophic "pest" failure. Adding Si_3N_4 also improved the high-temperature oxidation resistance and strength, doubled the room-temperature toughness, and more importantly, significantly lowered the CTE of the $MoSi_2$ (from 9×10^{-6} to 6×10^{-6} K^{-1}) and eliminated matrix

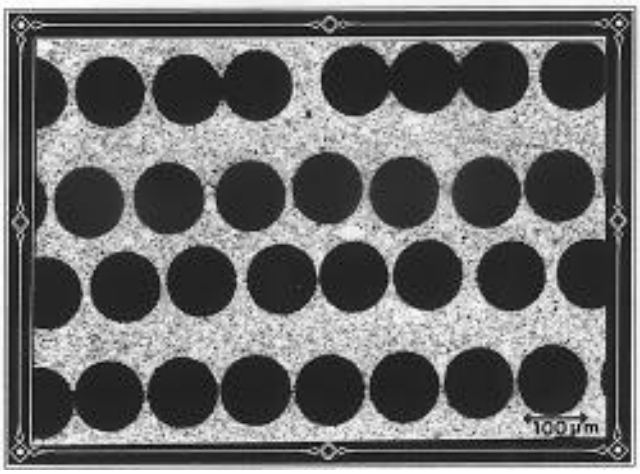

Scanning electron micrograph of fully dense, crack-free SCS–6/ $MoSi_2$-30Si_3N_4 composite fabricated by powder cloth technique.

cracking in SCS–6-reinforced composites even after thermal cycling. The composite exhibited excellent "pest" oxidation resistance to 930 °F. The SCS–6 fiber reinforcement provided attractive tensile strength and improved toughness by nearly an order of magnitude.

It is envisioned that small-diameter SiC tow reinforcement of the $MoSi_2$-Si_3N_4 matrix will most economically produce complex-shaped composite structures with a better combination of strength, environmental resistance, and reliability than any other $MoSi_2$-base material. This hybrid composite will compete with metal-, intermetallic-, and ceramic-matrix composites. Advanced processing techniques and mechanical tests to validate this vision are in progress.

Bibliography

Hebsur, M.G.: In Intermetallic Matrix Composites III. J.A. Groves, R.R. Bowman, and J.J. Lewandowski, eds., Materials Research Society, Pittsburgh, PA, 1994, pp. 177–182.

Lewis contact: Dr. Mohan G. Hebsur, (216) 433–3266
Headquarters program office: OA

Structures

Technology Benefit Estimator Designed for Aerospace Propulsion Systems

The technology benefit estimator (T/BEST) is a formal method for assessing advanced technologies and quantifying their benefit contributions for ranking. T/BEST provides guidelines for identifying and ranking high-payoff research areas, for managing research and limited resources, for showing the link between advanced concepts and the bottom line (i.e., accrued benefit and value), and for credibly communicating the benefits of research.

The T/BEST software is specifically designed for estimating the benefits and benefit sensitivities of introducing new technologies into existing propulsion systems. Key engine cycle, structural, fluid, cost, noise, and emissions analyses modules are used as a framework for interfacing with advanced technologies. The open-ended modular approach allows for modifying and adding both

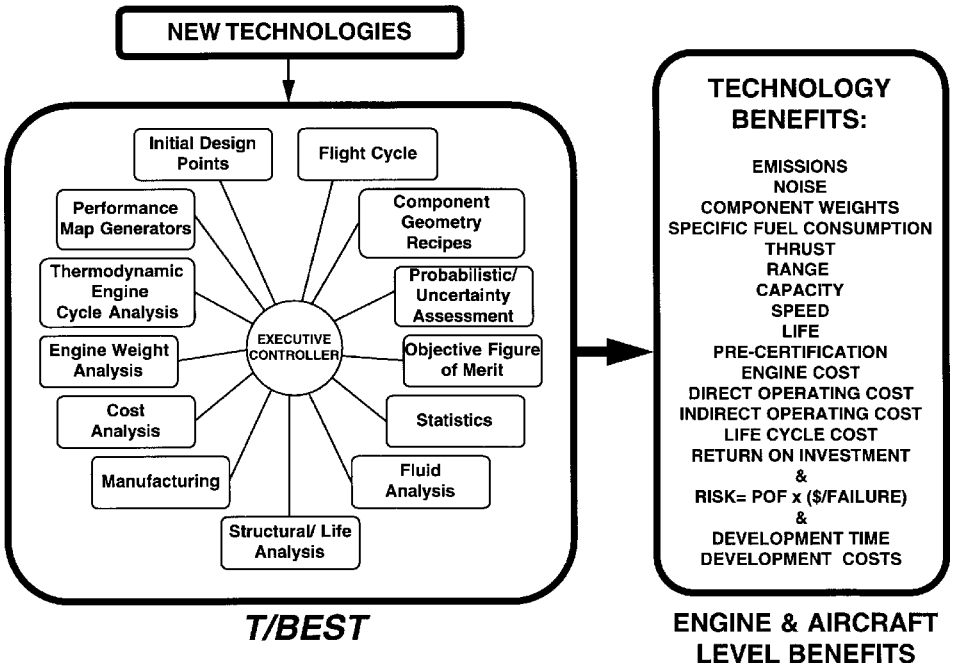

Technology benefit estimator.

key and advanced-technology modules. T/BEST's hierarchical framework yields varying levels of benefit estimation accuracy, depending on the degree of input detail available. This hierarchical feature permits rapid estimation of technology benefits even when the technology is at the conceptual stage. As knowledge of the technological details increases, so does the accuracy of the benefit analysis obtained.

Included in T/BEST's framework are correlations developed from a statistical data base, which are relied on if insufficient information is given in a particular area (e.g., fuel capacity or aircraft landing weight). Statistical predictions are not required if these data have been specified in the mission requirements. The engine cycle, structural, fluid, cost, noise, and emissions analyses modules interact with data libraries to yield estimates of specific global benefits: range, speed, thrust, capacity, component life, noise, emissions, specific fuel consumption, component and engine weights, precertification test, engine cost, direct operating cost, life-cycle cost, manufacturing cost, development cost, risk, and development time.

At present T/BEST operates on stand-alone or networked workstations and uses a Unix shell or script to control the operation of interfaced Fortran-based analyses. T/BEST's interface structure works equally well with non-Fortran or mixed software analyses. It is designed to maintain the integrity of the analyses modules by interfacing with experts' existing input and output files. Parameter input and output data (e.g., number of blades and hub diameters) are passed through T/BEST's neutral file while copious data (e.g., finite element models and profiles) are passed through file pointers that point to the experts' output files. To make the communications between T/BEST's neutral file and the attached analyses modules simple, only two software commands, PUT and GET, are required. This simplicity permits easy access to all input and output variables contained in the neutral file. Both public domain and proprietary analyses modules may be attached with minimal effort while maintaining full data and analysis integrity and security.

Lewis contact: Dr. Edward R. Generazio, (216) 433–6018
Headquarters program office: OA

Tailoring Code Enhanced To Predict Isothermal Fatigue Life of MMC's

Fatigue endurance is a primary consideration for high-temperature metal- and intermetallic-matrix composites (MMC's and IMC's), as these materials are expected to sustain aggressive mechanical and thermal cyclic loads. Fatigue life is typically reduced by microcracks in the matrix that are due to residual stresses or their interactions, the inelastic behavior of the metallic matrix, postfabrication loads, or environmental effects. To address this problem, analytical capabilities were incorporated into the MMLT (Metal-Matrix Laminate Tailoring) code, enabling

- Reliable and robust predictions of the isothermal fatigue life of MMC's and IMC's
- Optimal synthesis of process and material for explicitly improving the composite's fatigue life

This direct introduction of life prediction capabilities into the synthesis cycle allows for the concurrent synthesis of both process and material and ensures explicit improvements in fatigue performance. This technique automatically

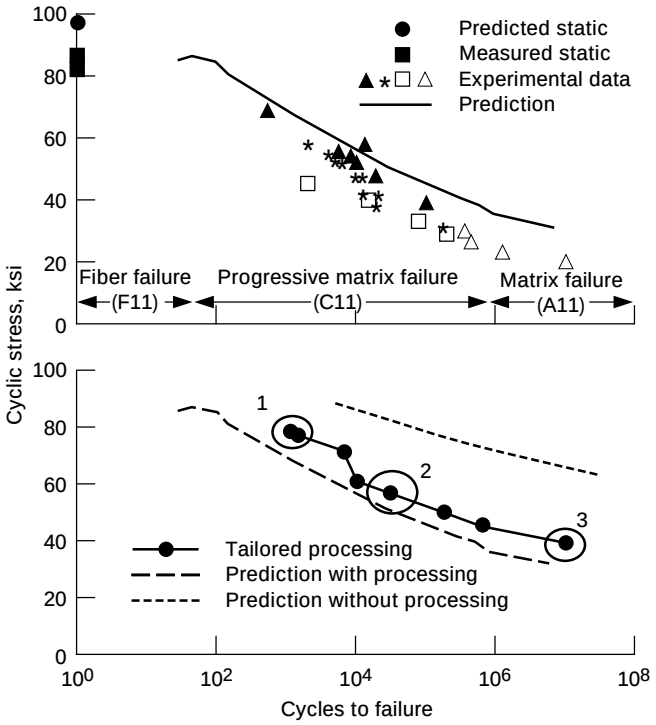

Isothermal fatigue prediction (top) and effect of processing optimization on fatigue life (bottom) for SiC/Ti-24Al-11Nb at 650 °C.

identifies which residual stresses are important for the composite's critical failure modes. It also optimally controls their evolution irrespective of the applied loads and thermomechanical fatigue cycle.

The method was evaluated on a ceramic silicon carbide fiber (SCS–6)/titanium aluminide (Ti-24Al-11Nb) matrix composite. This intermetallic matrix composite system was selected for its significance as a candidate high-temperature material and the availability of experimental data on its fatigue performance. Excellent isothermal life predictions were obtained at both room and elevated temperatures (top graph). The robustness of the method under low-, intermediate- and high-cycle fatigue conditions was validated. In addition, optimal processing temperatures and consolidation pressures were predicted that maximize the isothermal life at room and elevated temperatures (bottom graph).

Bibliography

Rabzak, C.; Saravanos, D.A.; and Chamis, C.C.: Optimal Synthesis of SiC/Ti-24Al-11Nb Composites for Improved Fatigue Behavior. HITEMP Review 1993: Advanced High-Temperature Engine Materials Technology Program, NASA CP–19117, Vol. 2, 1993, p. 41–1.

Lewis contacts: Dimitris A. Saravanos, (216) 433–8466; Dr. Christos C. Chamis, (2l6) 433–3252
Headquarters program office: OA

Mechanical Loads Significantly Change Structural Damping and Natural Frequencies of CMC's

Vibration damping and natural frequency were measured in ceramic-matrix composite (CMC) specimens before, and at various stages during, cyclic loading. The objective was to evaluate and refine this technique as a nondestructive evaluation method for detecting damage in CMC structures. Two-dimensional woven silicon carbide (SiC)/SiC specimens were subjected to tensile sinusoidal loading at a rate of 1 Hz from zero to 160 MPa. Damping and natural frequency were computed from impulse-response tests. These tests consisted of hanging the specimens at a vibration nodal point, impacting the specimens at the bottom end with an instrumented hammer, and measuring the acceleration at the top of the specimen. The vibration tests were conducted before loading and after 1, 10, and 100 cycles. Tests were also conducted to evaluate the effects of atmospheric pressure, specimen support conditions, and different damping evaluation techniques on the measured damping.

The stress-strain curves showed nonlinearities in the loading portion, significant hysteresis, and a residual strain after loading, indicating that damage had occurred in the specimens within the first load cycle (top graph). There was a significant increase in damping after the first load cycle and further increases after 10 and 100 cycles (bottom graph)—with a corresponding decrease in the

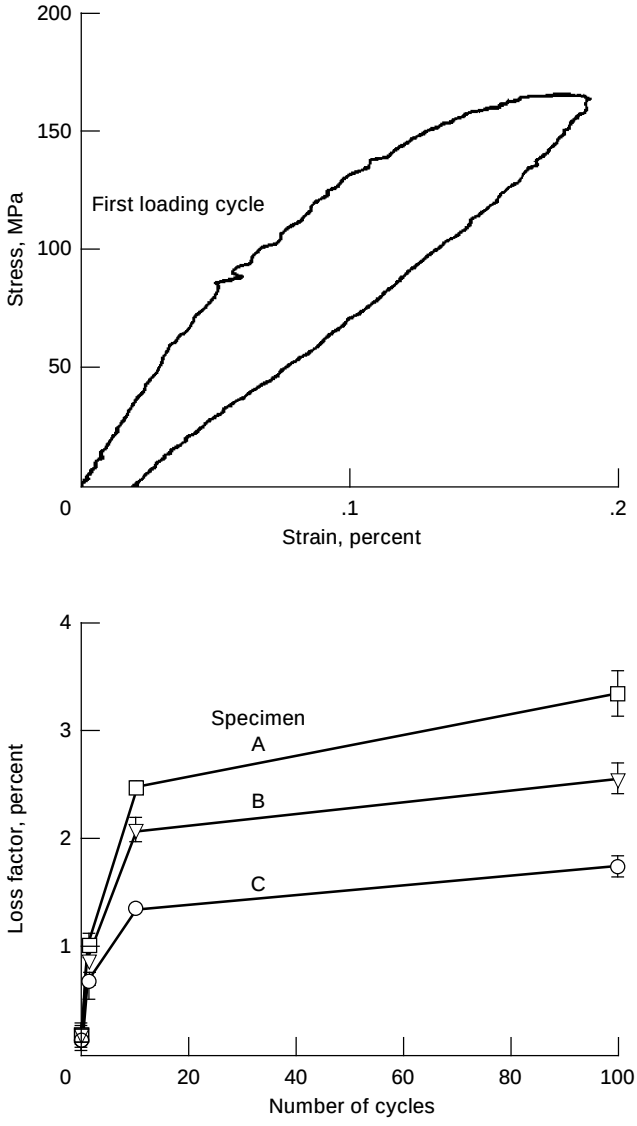

For SiC/SiC specimen (top) stress-strain curve and (bottom) loss factor as a function of number of load cycles.

natural frequency. Interspecimen variation in damping and natural frequency was consistent; the sample that had the largest increase in damping showed the largest decrease in natural frequency. Results were very sensitive to support conditions but insensitive to atmospheric pressure. The results indicate that both damping and natural frequency are sensitive to damage and may be useful techniques for monitoring damage progression in CMC structures.

Lewis contact: Dr. J. Michael Pereira, (216) 433–6738
Headquarters program office: OA

Optimality Criteria Method Provides Optimum Design for Select Structural Problems

The performance of the optimality criteria method for the minimum-weight design of structures subjected to multiple load conditions under stress, displacement, and frequency constraints has been investigated by examining several numerical examples. The examples were solved by using the optimality criteria design code developed for the purpose at NASA Lewis. The design code incorporates optimality criteria methods available in the literature with generalization for stress, displacement, and frequency constraints; fully stressed design concepts; and hybrid methods that combine both techniques. The design code also includes multiple choices for calculating Lagrangian multipliers and several design variable update rules, strategies for different constraint combinations, variable linking, displacement and integrated force method analyzers, and analytical and numerical sensitivities.

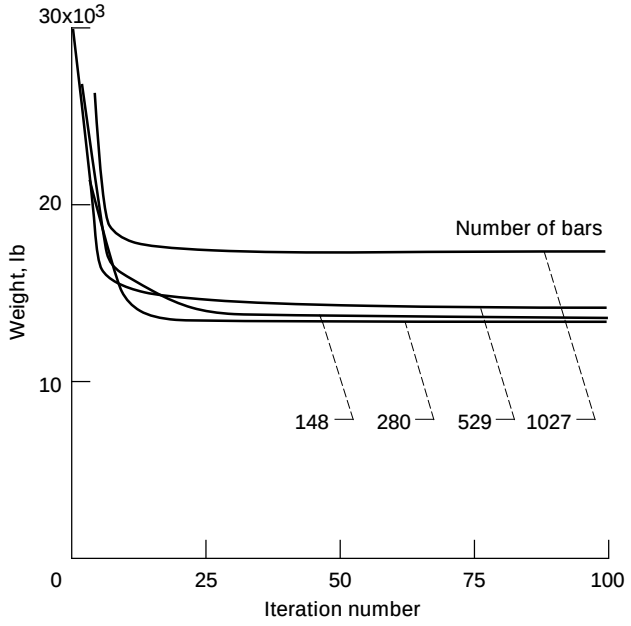

Convergence curves for three-dimensional truss problems.

We observed that when only displacement or only frequency constraints are used, the optimality criteria method is satisfactory even for large structural systems with many design variables. The monotonic convergence characteristics of an optimality criteria method for a large structure with 1027 design variables under only displacement constraints is shown in the graph. When extended for general application (with stress, displacement, and frequency constraints) the optimality criteria method satisfactorily provided optimal design for small problems. For problems with many behavior constraints and design variables, the method appears to follow a subset of active constraints that can result in a heavier, nonoptimal design. The fully utilized design methodology was adequate when stress constraints dominated the design. Hybrid methods, as formulated, were unsatisfactory, but further research could be fruitful. The computational efficiency of the optimality criteria method is similar to that of some nonlinear mathematical programming techniques.

Optimality criteria can be a useful tool to design, or modify an existing design of, a structure for displacement or frequency constraints.

Lewis contacts: Dale A. Hopkins, (216) 433–3332; Dr.Surya N. Patnaik, (216) 433–8468; Dr. Laszlo Berke, (216) 433–5648
Headquarters program office: OA

Active and Sensory Responses Simulated for Smart Composite Structures

Unified mechanics were developed that can model both sensory and active laminated composite structures with embedded piezoelectric layers. A discrete-layer formulation, applied on both displacements and electric potential, has provided the capability to accurately analyze not only the global but also the local electromechanical response of a smart composite structure. Including electric potential in the state variables

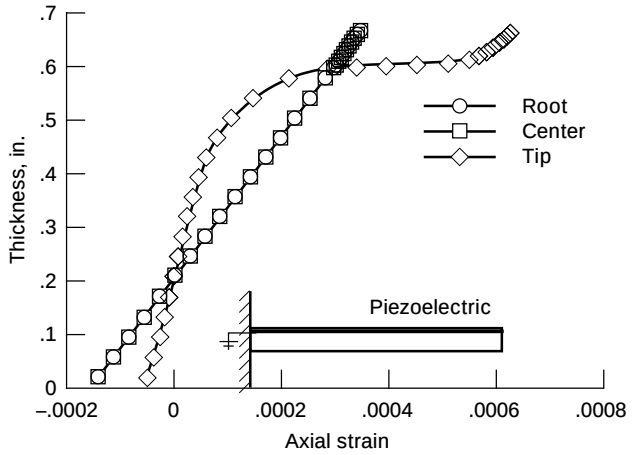

Typical mode shape and associated electric potential in top surface of sensory beam (second bending mode).

allows representation of general electromechanical boundary conditions and facilitates integration with controller models or other electronic components. Moreover, the formulation contains all energy contributions from elastic, piezoelectric, and dielectric components.

The static and dynamic responses of smart composite structures with embedded sensors and actuators were also obtained, and specialty finite elements were developed for this purpose. Evaluations on composite beams and plates have demonstrated that the mechanics can represent either sensory or active structures and can model the complicated stress-strain fields, including the interactions between passive and active layers (see graph), interfacial phenomena between sensors and composite plies, and critical damage modes in the material. The capability to predict dynamic characteristics under various electric circuit configurations was also demonstrated.

Lewis contacts: Dimitris A. Saravanos, (2l6) 433–8466;
Dale A. Hopkins, (216) 433–3332
Headquarters program office: OA

Efficiency of Elastoplastic Analysis Improved

Computing techniques are being developed that can exploit multiprocessor technology for more efficient computer simulations. In particular, a multilevel substructuring (MLS) approach is being taken to parallelize the overall finite element (FE) solution process. As shown, MLS decomposes an FE model into separate constituents or substructures. Each individual substructure can then be treated independently by employing a technique called static condensation. As a result each substructure can be assigned to a different processor so that they can be manipulated concurrently. Because we must account for the interaction of the individual substructures at their common boundaries, the statically condensed substructures are assembled so as to satisfy equilibrium requirements. If done properly, this process can be repeated many times, over several levels. The restructured data sets generated will literally reduce the number of computations needed to obtain the final solution. The new data sets also significantly reduce the memory required to store the coefficient matrix of the model, particularly for very large models.

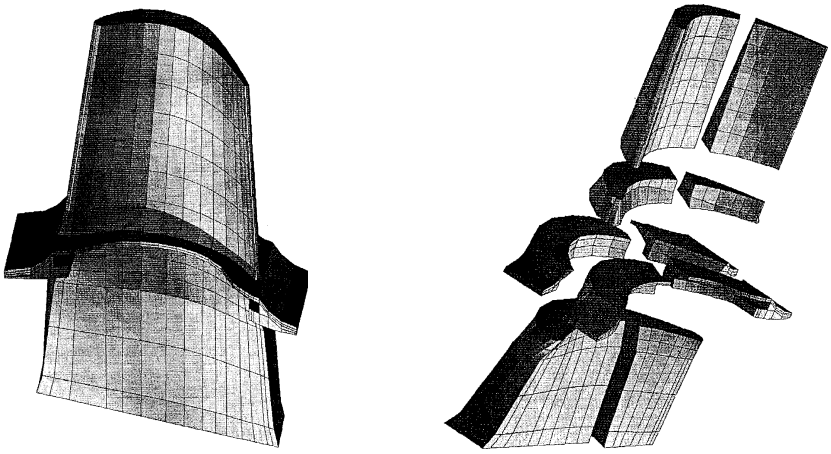

Left: Finite element model. Right: Nonlinear substructures.

In addition to its many beneficial computational characteristics, MLS also provides a logical and efficient means by which to isolate and localize the numerical treatment of nonlinear behavior. Those areas where the nonlinearity is occurring can be confined within the appropriate substructures. Consequently, only those substructures affected by the nonlinearity need be recalculated after the first iteration of the solution process. Computational effort for each iteration is substantially reduced because the linear portions of the model remain unchanged and do not have to be "re-solved." For example, a three-level MLS model required only 110 wallclock seconds to perform each iteration of the Newton-Raphson solver, as opposed to 435 wallclock seconds for the model without substructuring on a single processor. Moreover, because only two substructures behaved nonlinearly, only two processors were needed to perform the nonlinear iterations in parallel—reducing the wallclock time to only 60 sec per iteration. The remaining processors on the network could be used for other tasks. Or, as with a clustered workstation network, a nested hierarchy of parallelism could be used to perform the calculation. That is, each nonlinear substructure would be solved concurrently with a parallel equation solver of its own.

It is anticipated that the MLS solution strategy will ultimately be used to solve nonlinear FE models comprising thousands of degrees of freedom. Furthermore, by using MLS's inherent ability to separate, isolate, and localize the various constituents or components of an analysis, fluid and solid formulations could be combined to achieve more realistic and relevant simulations. These types of parallel computer simulations will be able to provide an extremely high level of accuracy in a relatively short turnaround time.

Lewis contact: Dr. Shantaram S. Pai, (216) 433–3255
Headquarters program office: OA

New Higher-Order Theory Analyzes Functionally Graded Materials

A new concept involving tailoring the internal microstructure of composite materials has recently evolved. A material's properties are spatially graded by using variable spacings between individual inclusions and using inclusions with different properties, sizes, and shapes. The term "functionally graded materials" has been coined to describe this emerging class of composites. By grading or tailoring the internal microstructure of a composite material or a structural component, the designer can truly integrate material and structural considerations into the final design and the final product. The entire structural design process is brought to the material level in the purest sense, thereby increasing the number of possible material configurations for a specific design application. For instance, a temperature gradient across the thickness of a structural component (such as a combustor liner or airfoil) causes a tendency to bend in the out-of-plane direction. Judiciously grading the microstructure of a heterogeneous material can reduce, if not eliminate, the thermal bending moment—decreasing the severity of warping.

The potential benefits of composites with tailored microstructures have led to increased activities in processing and materials sciences. Handicapping these activities, however, is the lack of appropriate computational strategies for the response of functionally graded materials that explicitly couple the material's heterogeneous microstructure with global analysis. Such coupling may be required in composites containing a relatively small number of large-diameter inclusions (e.g., fibers) along the dimension subjected to a thermal gradient (e.g., silicon carbide/titanium composites).

A new analytical approach has been developed at NASA Lewis to analyze the behavior of composites with tailored microstructures characterized by large-diameter reinforcement and thermal gradients. In this approach the microstructural and macrostructural details are explicitly coupled when solving the thermomechanical boundary-value problem. In contrast, standard micromechanical schemes based on classical homogenization procedures treat the local (micromechanics) and global (macromechanics) problems separately. Coupling the local and global analyses allows analysis of the response of functionally graded composites with continuously changing properties due to nonuniform fiber spacing or the presence of several phases. We have used this new "higher-order theory for functionally graded materials" (HOTFGM) to investigate how internal temperature and stress

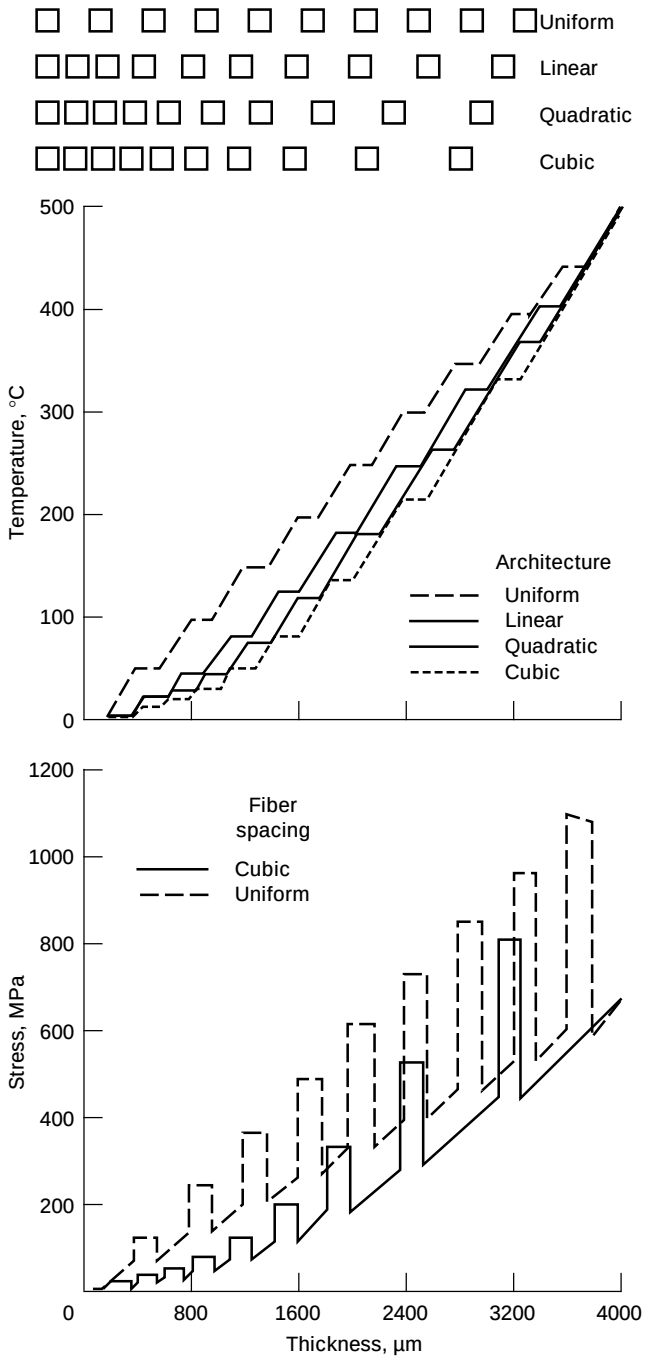

Thermal and mechanical analysis of functionally graded (FG) composite. Top: Through-the-thickness temperature distribution given various FG architectures. Bottom: Through-the-thickness normal stress in FG composites with cubic and uniform fiber spacing.

distributions affect an applied temperature differential across the thickness of a composite plate with different fiber spacings in the thickness direction and to investigate the force and moment resultants. Grading the composite microstructure appears to reduce the temperature distribution and thus yield more favorable stress distributions. This, in turn, reduces the in-plane force and moment resultants, maintaining the composite flat during a thermal gradient.

The manner in which the composite microstructure is graded must consider the sign of the thermal gradient. Future work will incorporate inelastic effects as well as temperature-dependent response of the constituent phases exhibited by advanced metal-matrix composites at elevated temperatures. The full potential of HOTFGM as a design tool will be realized when it is combined with an optimization approach.

Lewis contact: Dr. Steven M. Arnold, (216) 433–3334
Headquarters program office: OA

TMF Damage Progression Characterized in Titanium-Matrix Composite

Silicon-carbide-fiber-reinforced, titanium-matrix composites (TMC's) are receiving considerable attention for advanced high-temperature airframe and propulsion system applications. Their obvious attractions are their high ratios of stiffness and strength to weight at elevated temperatures relative to monolithic materials. Studies to experimentally characterize the elevated-temperature fatigue behavior of TMC's have revealed the complexities introduced by incorporating constituents with vastly differing mechanical properties. Many of these complexities, such as matrix load shedding and internal stresses created by mismatch in the fiber/matrix coefficient of thermal expansion (CTE), are highlighted under thermomechanical fatigue (TMF) conditions. There damage mechanisms are clearly functions of cycle type, as well as of the environmental and mechanical test parameters.

If TMC damage modeling is to be entirely successful under general TMF loading conditions, the fundamental mechanisms discerned from the various experimental studies must be accurately represented. Such studies often detail the damage mechanisms in qualitative fashion through fractographic and metallographic observations on specimens cycled to failure. Although this information is generally useful, it lack details about the actual progression of damage. To

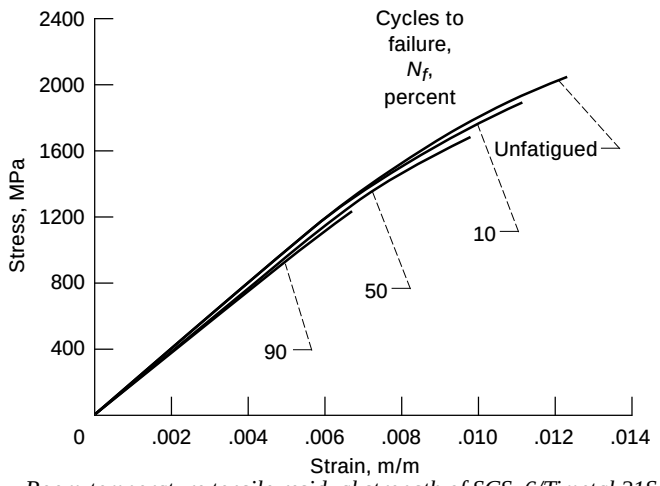

Room-temperature tensile residual strength of SCS–6/Timetal 21S $(0)_4$ subjected to various percentages of out-of-phase TMF cycling with maximum stress of 1000 MPa and strain rate of 0.0001 sec^{-1}.

supplement this information, recent advances in TMF testing were introduced to quantify damage progression at the macroscopic level. Now, explicit measurements tracked isothermal stiffness (E) and CTE degradations as functions of accumulated TMF cycles. These quantitative data, combined with microstructural observations, assisted in further characterizing the damage progression. However, details of the progression of physical damage within the microstructure and its relative impact on the macroscopic mechanical properties remained unknown. The experimental investigation highlighted here was undertaken to provide insight to this matter.

The TMF damage progression in SCS–6/Timetal 21S $[0]_4$ was thoroughly characterized at the macroscopic level by monitoring the E and CTE degradations to failure. A second set of specimens was cycled under identical conditions to 10, 50, and 90% of the cyclic life N_f and then subjected to destructive metallography to relate the extent of physical damage in the microstructure to the mechanical property degradation. Finally, a third set of specimens was cycled in identical fashion and tensile tested at room temperature to quantify residual strength at various stages of TMF damage progression, as shown in the graph. Damage began very early in cyclic life ($N < 0.1N_f$) for both in-phase and out-of-phase TMF loadings. In-phase TMF damage was dominated by fiber breakage in the absence of matrix damage. The progression of microstructural damage was difficult to quantify because fiber failure is based on probability. Out-of-phase TMF loadings produced matrix cracks that began exclusively at the surface. Here, damage progression was clear, both the number of cracks and their inward spread toward the outer fiber rows with increased cycling. The specimen interrupted at 50% N_f revealed that major cracks were near, but had not yet reached, the outer fiber rows. The stage at which this event occurred (when localized fiber/matrix debonding and matrix crack bridging occurred) appeared to be reflected in the macroscopic property degradation curves and is estimated at approximately 60% N_f.

Lewis contact: Michael G. Castelli, (216) 433–3334
Headquarters program office: OA

Isothermal Axial-Torsional Fatigue Data Bases Generated for Cobalt-Based Superalloy

Gas turbine and rocket engine components are routinely subjected to cyclic, multiaxial states of stress at different temperatures. Designing and reliably operating these aerospace propulsion system components require development of accurate multiaxial fatigue life prediction models. Multiaxial fatigue crack initiation data bases at different temperatures are necessary to develop and verify such life prediction models.

The cobalt-based superalloy Haynes188 is used for the combustion liner in the T800 turboshaft engine for the RAH–66 Comanche helicopter and for the liquid oxygen posts in the main injector of the space shuttle main engine. Both components are subjected to multiaxial stresses resulting from thermal gradients and mechanical loading. NASA Lewis has generated isothermal, axial-torsional, fatigue crack initiation data bases on Haynes188 at 316 and 760 °C. The elevated temperature 760 °C (minimum ductility temperature for Haynes188) was selected because low-cycle fatigue life is governed by ductility and because a lower bound on fatigue life is usually required for design. The intermediate temperature 316 °C was selected because it is the subcreep regime for Haynes 188. Four types of computer-controlled fatigue tests (axial, torsional, and in- and out-of-phase axial-torsional) were conducted on uniform-gage-section, tubular specimens of Haynes188 at each temperature. For comparing fatigue data from all the tests, the von Mises equivalent strain range, which reduces a given set of multiaxial

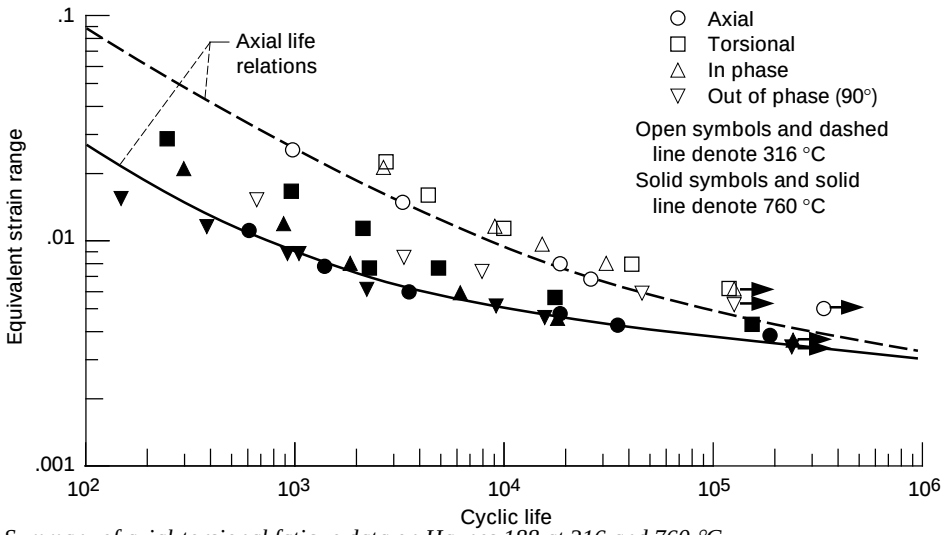

Summary of axial-torsional fatigue data on Haynes 188 at 316 and 760 °C.

strain ranges to an equivalent uniaxial strain range, was computed for each torsional and axial-torsional fatigue test. Fatigue data are summarized in the graph for the tests conducted on Haynes 188 at 316 and 760 °C. Fatigue life relations, computed from the axial fatigue data at the two isothermal temperatures, are also shown to clearly indicate the differences and similarities in the axial, torsional, and axial-torsional fatigue data of Haynes 188.

The isothermal, axial-torsional fatigue data bases were used to verify the applicability of room-temperature multiaxial fatigue life prediction models to intermediate- and elevated-temperature axial-torsional fatigue data on Haynes 188. These isothermal data bases were also employed to devise a thermomechanical, axial-torsional fatigue testing program on Haynes 188 with 316 and 760 °C as the minimum and maximum temperatures.

Lewis contact: Dr. Sreeramesh Kalluri, (216) 433–6727
Headquarters program office: OA

APPLE Incorporates All Aeroelastic Analyses for Turbomachines and Propfans

Developing analytical methods for avoiding flutter and minimizing forced response enables safer, more reliable, lower cost, and more quickly developed propulsion systems. It is estimated that vibration problems from flutter and forced response account for 14% of the total development costs of a typical turbofan engine—and often cause fatigue failure. In addition, flutter often results in sudden and catastrophic failure.

Flutter and forced response are aeroelastic phenomena involving the interaction of unsteady fluid forces and a flexible structure. In turbomachinery aeroelastic analysis the equations representing the structural dynamic and unsteady aerodynamic behavior of a fluid and blade system are combined to obtain an aeroelastic model. The resulting equations can be solved by either a frequency-domain or a time-domain solution for the system stability and forced vibration. Using a frequency-domain aeroelastic analysis, one assumes sinusoidal motion for the structure and calculates the unsteady aerodynamic forces at a fixed interblade phase angle and operating condition. The governing equations in this case lead to an eigenvalue problem; the eigenvalues determine the stability of the system. In a time-domain aeroelastic analysis the equations of motion for both the fluid and the structure are integrated simultaneously in time to obtain the response to a perturbation from a steady operating condition. An unstable response indicates a flutter condition. The time-domain method does not involve the assumption of linearity required by the frequency-domain method. Thus, it allows the modeling of systems that contain structural and/or aerodynamic nonlinearities.

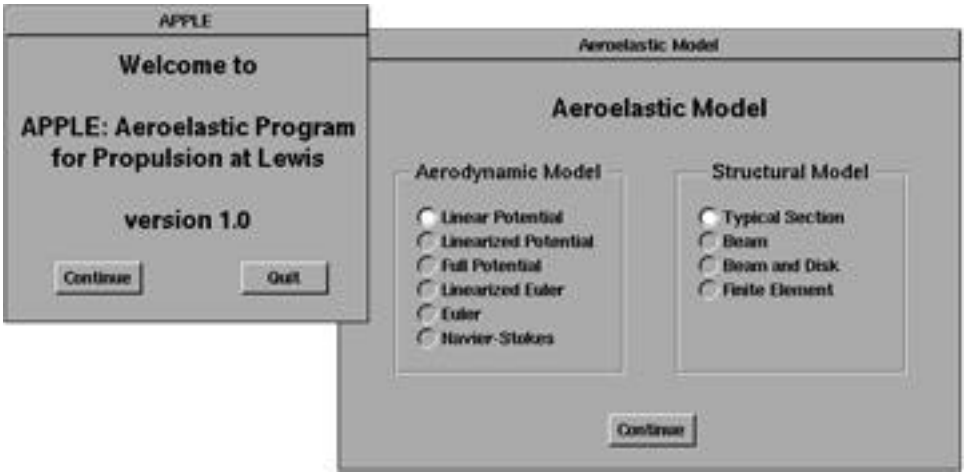

Some user options of APPLE system.

For several years NASA Lewis has been developing aeroelastic analyses for turbomachines and propfans. This work has resulted in individual codes with different aerodynamic and structural models. However, a single aeroelastic analysis system consolidating all computer codes did not exist. The availability of numerous computers—from desktop workstations to supercomputers, the development of graphical user interfaces, and the development of networking and concurrent engineering methods have paved the way to change this. All the existing aeroelastic analyses at Lewis are being incorporated on a single platform with a common input and output data base. Some user options of the system, named APPLE (Aeroelasticity Program for Propulsion at Lewis), are shown in the figure. Preliminary implementation and testing has begun on NeXT workstations.

Lewis contact: Oral Mehmed, (216) 433–6036
Headquarters program office: OA

Leakage Model Developed for Hypersonic Engine Seals

Combined-cycle ramjet/scramjet engines being designed for advanced hypersonic vehicles, including the National Aerospace Plane (NASP), require innovative high-temperature dynamic seals to seal the sliding interfaces of the articulating engine panels. New seals are required that will operate hot (1200 to 2000 °F), will seal pressures ranging from 0 to 100 psi, will remain flexible to accommodate significant sidewall distortions, and will resist abrasion over the engine's operational life. NASA Lewis is developing advanced seal concepts and sealing technology to meet these demanding seal challenges. One seal design that shows promise of meeting the demanding operating conditions of the NASP engine environment and sealing the gaps between the movable horizontal panels and the vertical splitter walls is the braided ceramic rope seal.

Key elements of a leakage flow model for the braided rope seal have been determined. Flow models help designers to predict performance-robbing parasitic losses past the seals and to estimate purge coolant flow rates. The leakage model is based on Kozeny-Carmen relations for flow through porous media. The model treats leakage flow through and around the braided seal structure as a system of flow resistances analogous to a series of resistors in an electrical network. These elemental resistances are combined in accordance with their electrical analogs to form an overall effective seal resistance that characterizes the seal. The current work extends previous flow models to predict seal leakage flow as a function of preload and engine pressures. A specially developed seal rig was used to collect the required leakage flow rates for validating the seal leakage flow models as a function of simulated engine pressures and preloads. The seals tested were braided of commercially available alumina-silica fibers. Seals were constructed by overbraiding a dense uniaxial core with several two-dimensional braided sheath layers having a high braid angle.

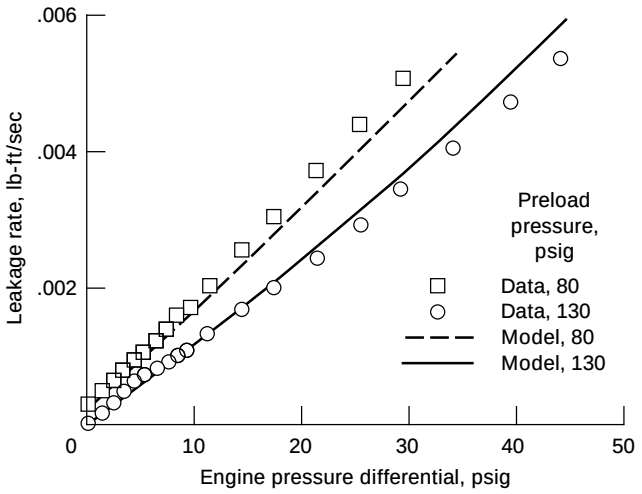

Flow model correlation for braided ceramic rope seal.

The logarithmic form of the semiempiric resistance preload model characterizes the observed variation of seal leakage resistance with increasing preload and engine pressures by using a two-term correlation. As shown in the graph the correlation between the measured and predicted leakage rates was quite good. The predicted leakage correlated well for both preloads over the engine pressure range tested.

This rope seal technology was developed by NASA Lewis and Drexel University. NASA/military program changes have curtailed further development.

Lewis contact: Dr. Bruce M. Steinetz, (216) 433–3302
Headquarters program office: OA

Active Control of Rotordynamic Vibrations Achieved

The research in rotordynamic vibration control concentrates on reducing vibrations in rotating machinery. There are two major strategies: passive control and active control. Passive control is achieved by changing system parameters through passive damping components or devices. Active control uses sensor-actuator systems to produce control forces that act directly on the rotor in response to measured vibrations. The advantage of active control over passive is its versatility in adjusting to a myriad of load conditions and machinery configurations. This advantage is clearly illustrated when one considers the very narrow bandwidth over which a tuned spring-mass absorber is effective. Other possible advantages of active vibration control include compact size, light weight, no lubrication systems needed in the control components, and operation in high or low-temperature environments. This technology is useful in gas turbines, helicopter transmissions, and automobiles. Lower vibrations will reduce fatigue, resulting in lighter, longer life systems with more flexible designs.

A vibration control package containing sensors, actuators, controllers, and power amplifiers is adapted to the machine. Research continues to be conducted on each component of the vibration control package, as well as on applying the package to the machine. The following four research projects were successfully completed within the past year.

Computer simulation of the completed research package has been developed and will be used as a design tool. Within the computer simulation the actuators must be modeled. In the past actuators have been treated as ideal devices. This assumption neglects phase and amplitude changes at high frequencies and may lead to coupled control system/structural system instability that limits the amount of active stiffness or active damping which can be achieved. Research has been completed for simulating the coupled "electrical/mechanical" system to predict rotordynamic stability and unbalance response along with control system stability.

A hybrid controller has been successfully tested that uses piezoelectric actuators to control vibrations of a flexible rotor. The controller includes active analog components and a hybrid interface with a digital computer. The computer uses a grid search algorithm to select feedback gains that minimize a vibration norm at a specific operating speed. These gains are then downloaded as active stiffnesses and dampings with a linear fit through the operating speed range to obtain very effective vibration control.

A robust controller has also been designed for active vibration control. This controller is based on a novel frequency-domain technique rooted in quantitative feedback theory. The advantages are a plant-based design according to performance specifications and the ability to include structured uncertainties in the critical plant parameters,

such as passive bearing stiffness or damping. Simulation studies have shown the effectiveness of this technique in attenuating vibration.

Research has also been completed in incorporating flexible casings into the computer simulation of active rotor vibration control. The trend toward lighter and more flexible designs in rotating machinery brings with it increasing demands for ways to dissipate the excess energy transferred to such structures by the action of dynamic forces. This work incorporates active feedback control mechanisms to suppress this unwanted vibration.

Lewis contact: Albert F. Kascak, (216) 433–6024
Headquarters program office: OA

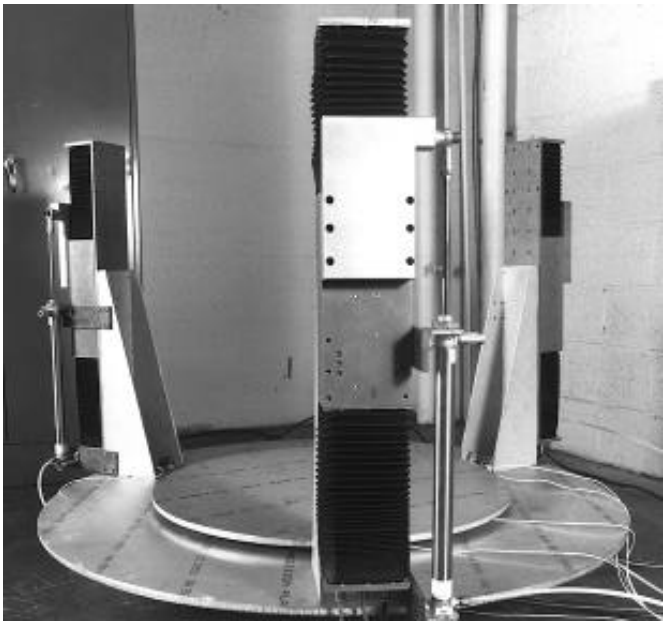

Reaction-compensating platform.

Reaction-Compensating Platform Preserves Microgravity Environment

Increasing research is being done into industrial uses for the microgravity environment on orbiting space vehicles. However, there is some concern over the effects of reaction forces produced by moving objects, especially motors, robotic actuators, and astronauts. These reaction forces may manifest themselves as undesirable accelerations in the space vehicle, making the vehicle unusable for microgravity applications. It is desirable to actively compensate for such forces.

At NASA Lewis we designed a three-degree-of-freedom reaction-compensating platform as a test bed for active attenuation of reaction forces caused by moving objects in a microgravity environment. Unique "linear motors" convert electrical current directly into rectilinear force. These reaction forces are used to counteract disturbance forces introduced to the platform.

The platform system consists of a passive spring-mass damper with added active components and sensors. The passive system attenuates forces at frequencies greater than the resonance and passes forces at frequencies below the resonance. Because the passive system provides at least –20-dB disturbance attenuation for frequencies above 88 rad/sec, the active system design should be most concerned with disturbance rejection below that frequency. The resonant frequency could be lowered by decreasing the spring constant, at the expense of larger platform excursion, or by increasing the system mass, which may not be desirable in spacecraft applications.

The displacers of the linear motors are constrained to vertical motions with respect to the platform and can thus react to vertical disturbance forces (along the z axis) and moments (about the x and y axes). The motors are each capable of 712-N maximum force. Below 4.8 Hz the force available is limited by the position constraint; above that frequency the position amplitude is limited by the maximum force constraint. Therefore, it is safe to attempt control at high frequencies, but commanding a large-amplitude control signal at low frequencies may be unsafe or ineffective.

Without accurate modeling of motor and composite system behavior, high-performance control is not possible. In particular, information on the force constant, mass, friction, maximum force and velocity, and bandwidth of each motor is needed before any active compensation using the motors can be attempted. Although the motors' electrical and mechanical characteristics are very like those of three-phase rotary motors, the mechanical stops prevent the use of rotary motor characterization techniques. Instead, techniques like those used in robotics were used to prevent motor damage.

The control consists of three discrete parts: the force feedforward controller, which directly responds to incoming forces read from the force sensors; the acceleration feedback controller, which responds to accelerations of the platform mass; and the motor position controller, which attracts the motors to equilibrium position, provides software damping for the motors, and also acts as a primary safety system.

The anticipated force disturbance rejection for the combined system is at least –20-dB attenuation for frequencies greater than 55 rad/sec, extending the lower bandwidth by 33 rad/sec below that of the passive system alone without increasing platform mass or decreasing spring stiffness.

Lewis contacts: Dr. Charles Lawrence, (216) 433–6048; Dr.Benjamin B. Choi, (216) 433–6040
Headquarters program office: OA

Unstalled Flutter of Counterrotating Propfan Experimentally Investigated

During wind tunnel testing of single-row (SR) propfans some models were found to flutter. The flutter was investigated experimentally and flutter analyses were developed. When interest shifted to counterrotating (CR) propfans, because of their higher propulsive efficiency, the flutter analyses developed for SR propfans were used to design CR propfans. However, the accuracy of such flutter predictions would change if the stability characteristics of one of the rows was significantly changed by the second row. The predictions would be less accurate if the second row caused a decrease in stability. Therefore, a study was conducted in-house to help guide the development of flutter analysis for CR propfans.

A fluttering blade row (called F21) was tested alone and with a stable aft row (called A21). The blades were research models for the General Electric Unducted Fan engine. The main objectives were to determine how the second blade row affected the stability of the fluttering row and to investigate the flutter. Flutter boundaries over the full operating range of the rotor, including transonic tip Mach numbers, were mapped. A nonintrusive optical system, used to measure blade vibrations at flutter, provided complete blade-to-blade phase information and an indication of the blade mode shapes at flutter. Conventional blade-mounted strain gages were used to measure blade frequency.

We found that at most conditions the second (aft)

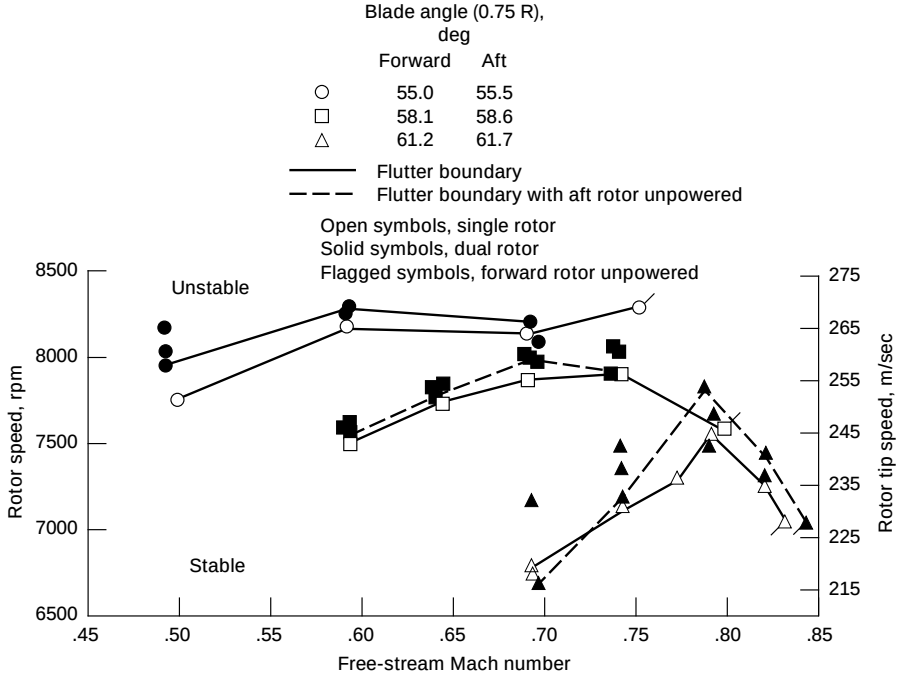

F21 flutter boundaries with rotor speed.

row had a small stabilizing effect that increased when the power of the aft row was increased. This result can be seen in the graph, which shows the measured stability boundaries in terms of the basic operating parameters. The solid symbols above the dashed boundaries are conditions where the aft row was powered, with increasing power moving toward the top of the graph. It can be concluded from the experiment that flutter analyses developed for single-row propfans should give conservative results when used for counterrotating rows similar to the ones tested.

We also found two distinct flutter modes within the rotor's operating regime, both apparently single-degree-of-freedom instabilities associated respectively with the first and second natural blade modes. Another finding was that the flutter physics changed with relative tip Mach number. At lower relative tip Mach numbers the flutter depended on both angle of attack into the blades and relative tip Mach number, and the dependence differed with the amount of twist-bending coupling in the flutter mode. However, when a relative tip Mach number of 1.10 was reached, it became the limiting parameter.

Lewis contact: Oral Mehmed, (2l6) 433–6036
Headquarters program office: OA

Integrated Design Software Predicts Durability of Monolithic Ceramic Components

Significant improvements in aerospace and terrestrial propulsion and power generation for the next century will require revolutionary advances in high-temperature materials and structural design. Advanced ceramics are relatively abundant materials that offer lighter weight and greater capacity to sustain loads at higher use temperatures than metals. However, ceramics are inherently brittle and have very low strain tolerance, low fracture toughness, and large variations in fracture strength caused by variable size and random distribution of flaws. Ceramics also exhibit time-dependent degradation of load-carrying capability due to stress corrosion cracking, effects of elevated temperatures, cyclic fatigue, and creep. Successful application of advanced ceramics depends on properly characterizing material behavior and using a probabilistic brittle material design methodology. This has been accomplished with the CARES/LIFE (Ceramics Analysis and Reliability Evaluation of Structures/Life) integrated design computer program developed to determine the reliability of monolithic ceramic components as a function of time in service.

Designing ceramic components requires specialized knowledge of statistics and fracture mechanics. Design accommodations for any given component shape and service environment require extensive numerical computational capabilities. Multidisciplinary research in fracture analysis, probabilistic modeling, model validation, and brittle structure design has been combined in CARES/LIFE and its accompanying documentation. Compiling the diverse elements of this technology into one package has made a comprehensive design tool readily available. CARES/LIFE enables the design engineer to assess the risk of fracture from various competing failure mechanisms and to determine or estimate overall failure probability for a component over its lifetime. Consequently, appropriate design changes can be made until an acceptable failure probability is predicted.

Through its use in an extraordinarily wide array of product designs, ranging from aerospace components to medical implants, the CARES/LIFE computer program has demonstrated a tangible public benefit. CARES/LIFE is the only public domain computer program of its kind available in the United States today. This technology applies to advanced ceramic materials,

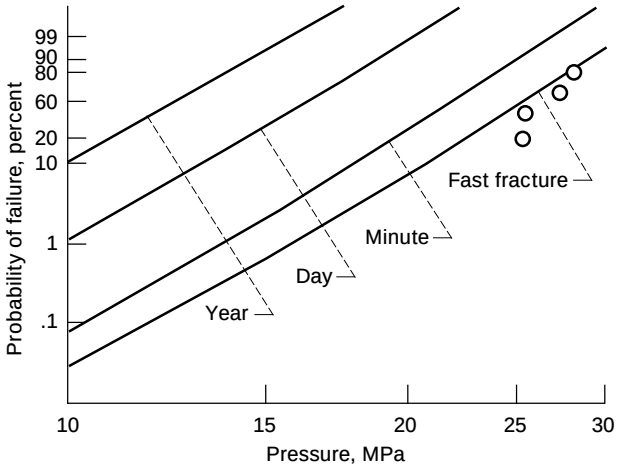

Probability of tube fracture with pressure over time.

including silicon nitride and silicon carbide, and other brittle materials, such as glass and graphite. Many commercial products—turbocharger rotors, rocker arm pads and cam followers, poppet valves, radiant heater tubes, heat exchangers, and prototype ceramic turbines—are designed using this software. In addition, CARES/LIFE is used to design large infrared transmission windows, glass panels for skyscrapers, ceramic packaging for microprocessors, cathode ray tubes, and even ceramic tooth crowns and kneecaps.

Lewis contact: Noel N. Nemeth, (216) 433–3215
Headquarters program office: OA

Postscan Interactive Data Display System Developed for Ultrasonic Scans

The postscan interactive data display (PSIDD) system, for which a patent is pending, has been developed for viewing, on video, raw (digitized) data and resulting properties at any scan location on any image formed from ultrasonic contact scans. It will be used to confirm the accuracy of images from both software signal processing and hardware performance standpoints and to interactively compare ultrasonic properties at different locations within samples.

In ultrasonic contact scanning two front-surface and two back-surface ultrasonic pulses obtained with the pulse-echo configuration are digitized and stored at every scan location. These pulses are later Fourier transformed to the frequency domain and used in calculating ultrasonic reflection coefficient, attenuation coefficient, cross-correlation (pulse) velocity, and phase velocity. Images of these ultrasonic properties are then formed at preselected frequencies by using spectral analysis software.

This ultrasonic method is especially sensitive for quantifying global variations (such as pore fraction variations) in microstructure as well as for detecting isolated material defects in monolithic and composite materials. Microstructural variations are indicated by gray or color-scale variations in an ultrasonic image; at such locations there can be questions as to the validity of the indication.

PSIDD allows the operator to examine the digitized ultrasonic waveforms at scan locations and to verify whether the waveforms and the resulting ultrasonic properties are valid, and if valid, how the waveforms and properties differ from those at other scan locations. Additionally, by waveform analysis, PSIDD allows automatic detection and visualization of scan locations considered “good” that may in fact show distorted waveforms. Thus, it is a sensitive quality control device.

Digitized and calculated property data obtained from an ultrasonic contact scan and stored in files are retrieved through a direct-access data retrieval algorithm that allows display of data at any point. Waveforms are autoscaled in both the horizontal and vertical directions and can be individually enlarged to take up the entire video display for more detailed viewing. The user can choose to view the two back-surface waveforms with or without the ultrasonic system noise subtracted. The user has the choice of linear or natural cubic spline interpolation of spectra or property data. This form of analysis is likely to yield more accurate predictions of material behavior, and it can be the basis for artificial intelligence techniques that allow defect identification based on waveform shapes and property versus frequency behavior. This type of comprehensive analysis in such a convenient format is not commonly done in conventional ultrasonic testing.

Lewis contact: Dr. Don J. Roth, (216) 433–6017
Headquarters program office: OA

RP–1 Effects on Bearing Performance Investigated

NASA Lewis has experimentally investigated the lubricating and cooling capabilities of RP–1 on ball bearings. Although RP–1 has been used to lubricate bearings in rocket engine turbopumps, a detailed investigation to document the performance of ball bearings operating in RP–1 over a wide range of speeds and loads had not been undertaken.

RP–1 has been and continues to be used by a number of rocket engine propulsion systems. Among them are the F–1 engine used in the Apollo program, which is no longer in production, as well as the RS–27A engine used in the Delta II program and the MA–5A engine used in the Atlas program, both of which are still in production. As various concepts are considered for future launch systems, RP–1 continues to be a viable fuel option. Because more emphasis is being placed on reliability, durability, maintainability, and cost effectiveness in the new design concepts, more information is needed about the effects the various fuels have on rocket engine systems.

Liquid-fueled rocket engines typically utilize turbopumps to transfer the fuel and oxidizer from the storage tanks to the combustion chamber. To reduce the weight and complexity of these turbopumps, their bearings are often lubricated and cooled by the liquid being pumped rather than having a separate lubrication system. Although a few limited investigations of the lubricating capabilities of RP–1 had been performed (refs. 1 to 3), this test program was carried out to more thoroughly assess the impact of RP–1 on rocket engine turbopump bearing performance and reliability.

Early tests (ref. 4) indicated that bearing operating temperature was highly dependent on both shaft speed and RP–1 flow rate but only slightly dependent on applied load over the ranges of interest. Moreover, there was a lower threshold limit of RP–1 flow below which the bearing temperature increased rapidly, indicating that bearing failure was imminent. Conversely, high RP–1 flow rates greatly increased the amount of shaft power lost to the bearing due to churning of the liquid RP–1.

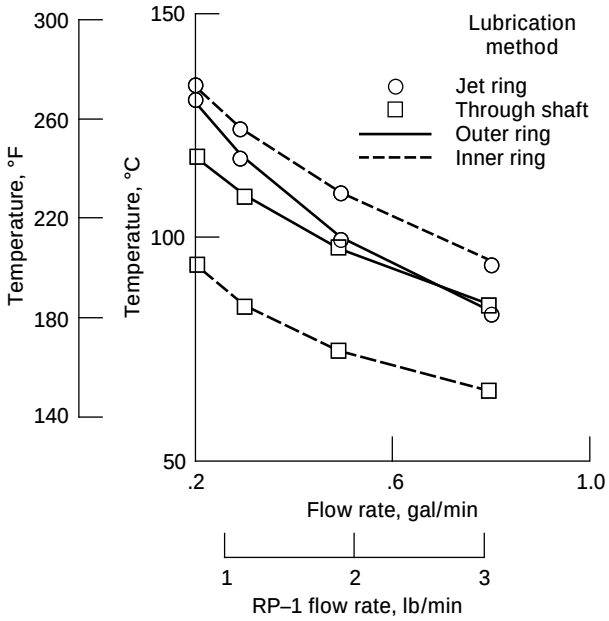

Effect of lubrication method on bearing inner and outer ring temperature.

Further tests (ref. 5) subjected the bearings to combinations of speeds and loads resulting in Hertzian contact stresses as high as 2802 N/mm^2 (406,400 psi)—much higher than the generally accepted Hertzian contact stress of 2068 N/mm^2 (300,000 psi). The bearings ran well under these extreme conditions as long as the RP–1 flow remained adequate. If the temperature of the bearing outer ring rose above 150 °C (300 °F), the RP–1 would begin to boil, causing a loss of lubricant between the balls and races of the bearing and leading to an unstable situation where temperature runaway is likely.

The final tests of the program (ref. 6) investigated an alternative method of introducing the RP–1 to the bearing as well as several different cage materials to determine whether the lower limit of RP–1 flow for safe bearing operation could be reduced. Conventionally, lubricant is introduced to bearings in turbopumps through a stationary jet ring located adjacent to the bearing. This method was used as the baseline for these tests. The alternative method was to direct the RP–1 through a channel in the center of the shaft and then radially outward and through small holes machined in the bearing inner ring. This alternative method reduced bearing operating temperatures as much as 30 deg C (54 deg F).

Three alternative cage materials (660 bronze, Vespel, and Bearium (bronze) were tested in addition to the baseline silver-coated 4340 steel cage. The bronze cages reduced bearing operating temperature as much as 10 deg C (18 deg F) more than the other two cage materials.

References

1. Butner, M.F.; and Rosenberg, J.C.: Lubrication of Bearings With Rocket Propellants. Lubr. Eng., Jan. 1962, pp.12–44.

2. Liquid Rocket Engine Turbopump Bearings. NASA SP–8048, 1971, p. 6.

3. Butner, M.F.,: Propellant Lubrication Properties Investigation. DTIC Technical Report WADD TR 61–77–PT–1, Dec. 1961, pp. 50–66.

4. Addy, H.E., Jr.; and Schuller, F.T.: Operating Characteristics of an 85-mm Ball Bearing in RP–1 to 1.7 Million DN. NASA CP–3174, Vol. II, 1992, pp. 471–483.

5. Addy, H.E., Jr.; and Schuller, F.T.: Lubrication of an 85-mm Ball Bearing With RP–1. AIAA Paper 93–2538, June 1993.

6. Addy, H.E., Jr.; and Schuller, F.T.: Effects of RP–1 on Ball Bearing Performance. ETO Conference, Huntsville, AL, May 1994.

Lewis contact: H. Eugene Addy, (216) 977–7467
Headquarters program office: OSAT

Space Shuttle Main Engine Health-Monitoring System Algorithms Validated

Making space shuttle main engine (SSME) ground test and flight operations safer has been a major focus throughout SSME development and operation. Therefore, a program was conceived to formulate an architecture for an SSME health-monitoring system (HMS) capable of flight and/or ground operations and then to demonstrate key enabling technologies. This program followed a systems analysis methodology to develop a conceptual hardware and software architecture for an HMS that would meet this broad objective. A key result was the demonstration of three different fault-detection algorithms as candidates for inclusion in the HMS architecture. This architecture and the three fault-detection algorithms, RESID, ARMA, and CLUSTER, were developed by United Technologies Research Center (UTRC) under contract to NASA.

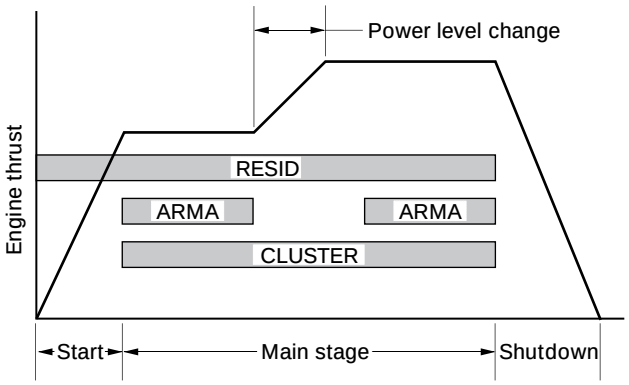

UTRC algorithms covering different portions of SSME operational profile.

The recursive structural identification (RESID) algorithm is a nonlinear regression algorithm similar to conventional regression analysis. It results in a single equation that relates the input parameters selected by the RESID algorithm to the predicted output parameter. Once the equation is established, new data can be applied to it to estimate the output parameter. The error, which is the difference between the estimated and measured parameter values, is then thresholded to make the fault detection.

Whereas the RESID algorithm uses instantaneous relationships between sensor measurements to detect an off-nominal engine condition, the mixed autoregressive moving average (ARMA) approach focuses on the behavior of individual sensor values over blocks of time. Signal structural changes, rather than cross-sensor relationships, are the indicators of an off-nominal engine condition. The basic approach uses a set of training data to develop an equation for predicting the present value of a sensor by using previous sensor values and white noise inputs.

The CLUSTER algorithm is a sensor fusion technique based on a classical pattern-recognition approach to data classification. In the classical clustering approach a training set consisting of data from n different sensors is selected and processed by a cluster-defining algorithm. This training algorithm uses the interrelationships between the sensors to group them into n-dimensional clusters that indicate the operating states of the system described by the training data. Once the clusters have been defined in the training stage, new data are processed and evaluated either as belonging to one of the predefined operating states (clusters) or as being

outside the experience base constructed during training.

The three algorithms were validated over a wide range of SSME configurations and over 150 SSME test firings. During this validation the algorithms demonstrated both robust fault detection and false-alarm rejection; 24 of 30 off-nominal conditions were detected and 21 of these 24 were detected significantly earlier than by the SSME redline system. Also, the algorithms demonstrated operational feasibility during real-time SSME hot-fire tests on the technology test-bed engine.

The algorithms are undergoing continual in-house improvement to expand the fault-detection capability and to add fault-diagnosis capability. When completed, these algorithms can be used to improve SSME safety both on the test stand and in flight; they can also be used as baseline algorithms for future NASA missions.

Bibliography

Hawman, M.W.; et al.: Framework for a Space Shuttle Main Engine Health Monitoring System. Final Report on Contract NAS3–25626, NASA CR–185224, 1990.

Hawman, M.W.; et al.: Space Shuttle Main Engine Health Monitoring System. Final Report on Contract NAS3–25804, NASA CR–195328, 1994.

Lewis contact: James W. Gauntner, (216) 977–7435
Headquarters program office: OSF

Performance and Heat Load Prediction Improved for Multistage Turbines

Flows in low-aspect-ratio turbines, such as the space shuttle main engine fuel turbine, are three-dimensional. They are also highly unsteady due to the relative motion of adjacent airfoil rows and the circumferential and spanwise gradients in total pressure and temperature. The systems used to design these machines, however, are based on the assumption that the flow is steady. The codes utilized in these design systems are calibrated against turbine rig and engine data by using empirical correlations and experience factors. For high-aspect-ratio turbines, these codes yield reasonably accurate estimates of flow and temperature distributions. However, future design trends will see lower aspect ratios (fewer parts) and higher inlet temperatures, which increase three-dimensionality and flow unsteadiness in the turbine. Analyses of recently acquired data indicate that temperature streaks and secondary flows generated in combustors and upstream airfoils can have a large impact on the time-averaged temperature and angle distributions in downstream airfoil rows.

NASA Lewis and Pratt & Whitney (under Contract NAS3–25804) developed “closure models” to predict time-averaged effects of unsteadiness in multistage turbines. The predictive capabilities of these closure models were verified through design and by testing hardware in a large-scale rotating rig at United Technologies Research Center (UTRC). Generalized formulations of these closure models will enhance the state of the art of turbine design procedures, allowing designers to cost-effectively optimize the performance, life, and structural integrity of turbines used in air-breathing and rocket propulsion systems.

Closure models were formulated by using both new and existing unique experimental and numerical data. These closure models provided numerical values needed for “average passage” solvers developed by scientists at NASA to predict effects of periodic unsteadiness on time-averaged flows in multistage machines. Computational fluid dynamics codes with these closure models were used to redesign airfoil flow for the UTRC large-scale rotating rig so as to reduce heat loads and improve the performance of the second stator. An experimental program was conducted to define the distribution of the second stator’s heat load and aerodynamic performance and to allow verification of the predictive capabilities of the closure models. The closure models were then assessed for their predictive capabilities and contribution to the enhancement of the current design system.

With the aid of this contract, NASA Lewis has developed a new understanding of turbine flow physics in low-aspect-ratio multistage turbines and is sharing the results of this contract with the U.S. turbomachinery community.

Bibliography

Adamczyk, J.J.: Model Equation for Simulating Flows in Multistage Turbomachinery. ASME Paper 85–GT–226, 1985. (Also NASA TM–86869.)

Adamczyk, J.J.; Mulac, R.A.; and Celestina, M.L.: A Model for Closing the Inviscid Form of the Average-Passage Equation System. J. Tribomach., vol. 108, no. 2, 1986, pp. 180–186.

Lewis contact: Dr. John J. Adamczyk, (216) 433–5829
Headquarters program office: OSAT

Self-Diagnosing Accelerometer Fabricated

Large, complex systems, such as the engines used on the space shuttle, are instrumented with great numbers and diverse types of sensors to monitor engine health and performance. It is increasingly difficult to check the accuracy and integrity of these sensors through traditional test and calibration techniques, particularly during flight. Typically, sensor failures occur in the sensing element, the electronics, or the sensor mounting. These failures may be "hard" failures, such as broken wires, or "soft" failures, such as drift due to temperature changes. An in-situ sensor failure detection and calibration technique would allow evaluation and (re)calibration of a sensor without removing it from the structure on which it is performing measurements.

Sensor failure can be detected by providing a known input and observing the response. For piezoelectric devices an input could be generated by supplying an electrical excitation signal to the piezoelement itself. When triggered, the excitation signal would produce a measurable vibrational response in the sensor, with its frequency content dependent on the health of the sensor element, the electronics, the mounting impedance, and the dynamic activity from other sources. Comparing the response with a known "good" response will provide information on sensor health.

NASA Lewis is supporting research to develop self-diagnostic and self-calibration technology. A self-diagnosing piezoelectric accelerometer has been fabricated and is scheduled for testing on the technology test-bed engine at NASA Marshall Space Flight Center. This technology, whether incorporated into a rocket engine health management and control system or other applications requiring highly reliable measurements, could improve system safety and cost effectiveness.

Lewis contact: George C. Madzsar, (216) 977–7434
Headquarters program office: OSAT

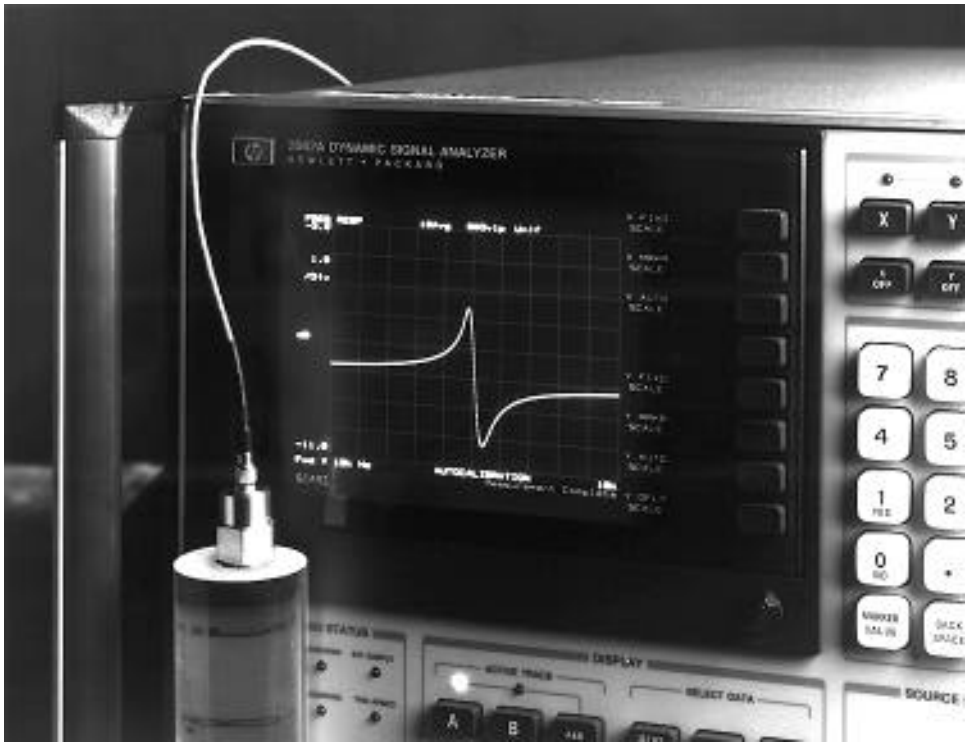

Accelerometer with self-calibration function displayed.

Prototype Real-Time Sensor Data Validation System Demonstrated

Rocket engines would be safer and more reliable if engine controllers and advanced safety systems could determine if sensors were supplying faulty data. This ability, called sensor data validation, would prevent the controller or safety system from making critical decisions, such as the decision to shut down an engine, on the basis of anomalous or failed sensors. NASA Lewis and Aerojet Propulsion Division are involved in an ongoing effort to develop software capable of detecting sensor failures on liquid-fueled rocket engines in real time and with a high degree of confidence.

We combined analytical redundancy with Bayesian belief networks to provide a solution that has well-defined, real-time characteristics and well-defined error rates and can be scaled to validate any number of engine sensors. Analytical redundancy is a technique in which a sensor's value is predicted by using values from other, usually nonredundant, sensors and known or empirically derived mathematical relations. For the example engine plant diagram, fuel flow can be related to either the low-pressure-pump speed or the high-pressure-pump speed by a pump affinity equation (assuming constant fuel density). As shown, a set of sensors and a set of relationships among them form a network of cross-checks that can be used to periodically validate all sensors in the network. In addition to simple binary empirical correlations and engine characteristic equations, we are developing neural network models to model parameters during the highly nonlinear start transient and those parameters difficult to approximate during main-stage engine operation.

Bayesian belief networks are a mathematically sound approach to information fusion—the combination of evidence from several sources into a single consistent solution regarding the status of all sensors in a network. In information fusion, uncertainties in the sources of evidence (i.e., inaccuracies in the sensors or uncertainties in the models themselves) are explicitly modeled and accounted for.

This approach has been used to validate a six-sensor network on Aerojet's advanced rocket engine controller. Data were received in real time from the technology test-bed engine at NASA

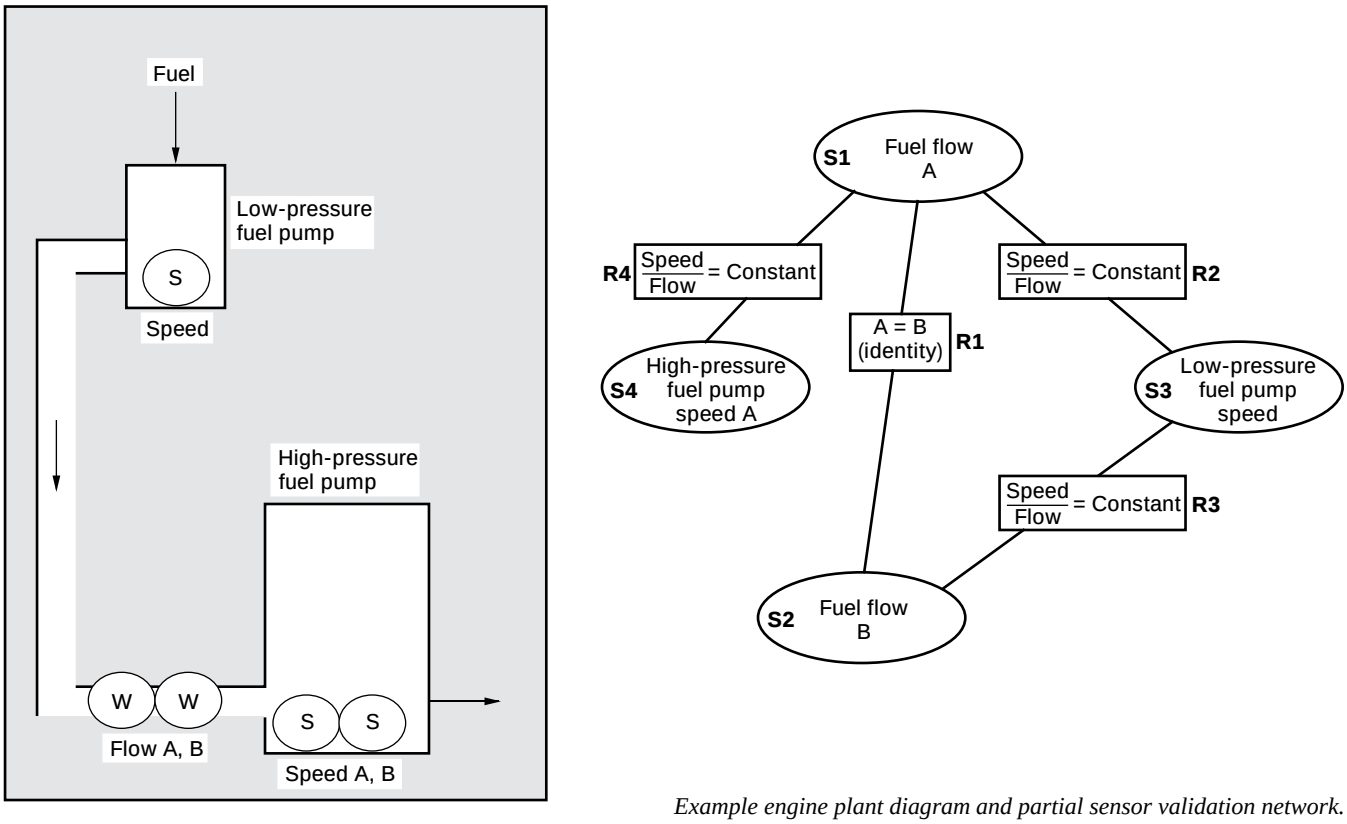

Example engine plant diagram and partial sensor validation network.

Marshall Space Flight Center. Current efforts are focused on extending the demonstration system to provide real-time validation capability for additional critical sensors on the space shuttle main engines.

Bibliography

Bickmore, T.W.: Real-Time Sensor Data Validation. NASA CR–195295, 1994.

Meyer, C.M.; Maul, W.A.; and Dhawan, A.P.: SSME Parameter Estimation and Model Validity Using Radial Basis Function Neural Networks. Proceedings of the 1994 Conference on Advanced Earth-to-Orbit Propulsion Technology, Huntsville, AL, May 1994.

Meyer, C.M.; Maul, W.A.; and Dhawan, A.P.: SSME Mainstage Sensor Signal Approximation Using Feedforward Neural Networks. Proceedings of the Fourth Annual Space System Health Management Conference, Cincinnati, OH, Nov. 1992.

Lewis contact: Claudia M. Meyer, (216) 977–7511
Headquarters program office: OSAT

Metallized Propellant Combustion Tested

Rocket engine combustion experiments using metallized gelled liquid fuels were completed in the rocket laboratories at NASA Lewis. These experiments used a small 30- to 40-lbf-thrust engine composed of modular injector, ignitor, chamber, and nozzle. The fuels used were traditional liquid RP–1 and gelled RP–1 with 0, 5, and 55 wt% loadings of fine microscopic aluminum particles. Gaseous oxygen was the oxidizer. Both fuel and oxidizer were mixed under precisely controlled conditions to create a high-temperature combustion flow. These experiments will help find the best operating conditions for burning metal particles and creating a higher efficiency rocket engine.

Metallized gelled propellants have been studied analytically and experimentally for over 60 years. The historical work has focused on the benefits of high specific impulse, high density, and safety (refs. 1 and 2). Several mission studies have indicated that O_2/RP–1/Al can have significant benefits by increasing propellant density (refs. 2 to 5). Testing was therefore conducted with O_2/RP–1/Al propellants using gelled RP–1 with various loadings of aluminum particles and with liquid propellants as a baseline.

Rocket performance and heat transfer measurements were desired in this test program. During the combustion of metal particles the different densities of the gas, liquid, and metal flows create a mismatch in their speeds. The heat transfer measurements were made to estimate the differences in ignition time for the parts of the combustion flow. The combustion temperatures and heat flow profiles of the different flows will be compared.

Both heat-sink and calorimeter experiments were conducted. The heat-sink combustion chamber has a 2.6-in. inside diameter and is 6 in. long, and the nozzle has a 0.6-in.-diameter throat. A 22-channel cooling passage calorimeter chamber was used. The associated calorimeter nozzle has nine cooling channels. Numerous thermocouples are located in the cooling passages of the calorimeter combustion chamber. The injectors use an oxidizer manifold within the injector body and have a fuel dome set atop it. The injector elements are an O–F–O design and both four- and eight-element patterns were tested. A wide range of oxidizer-to-fuel ratios (O/F) were investigated. The injectors were designed for O/F ranges of 1.2 to 4.2 for O_2/RP–1 and 1.4 to 3.7 for O_2/RP–1/Al.

All these preliminary results are for the heat-sink engine. With O_2/RP–1 the maximum combustion efficiency occurred near O/F = 3.0. With the gelled RP–1 (0 wt% RP–1/Al) the O/F for the maximum combustion efficiency was nearly the same. Both gelled and ungelled RP–1 demonstrated high combustion efficiencies (to 98%). Using O_2/RP–1/Al (5 wt% RP–1/Al) delivered 90 to 95% combustion efficiency, and the efficiency curve had no obvious strong peak. At a 55 wt% RP–1/Al loading the combustion efficiency was similar to the 5 wt% RP–1, and the peak occurred near 1.5 to 2.0 O/F.

During the testing with gelled RP–1 and the 5 wt% RP–1/Al, some residual propellant was found in the rocket chamber, coating the injector face and chamber walls. When this thin layer was wiped off, the metal surfaces exhibited minimal erosion—a marked contrast to the blackening of the O_2/RP–1 injector faces and injector-face erosion that occurred with the 55 wt% RP–1/Al. An improved cooling technique might be derived

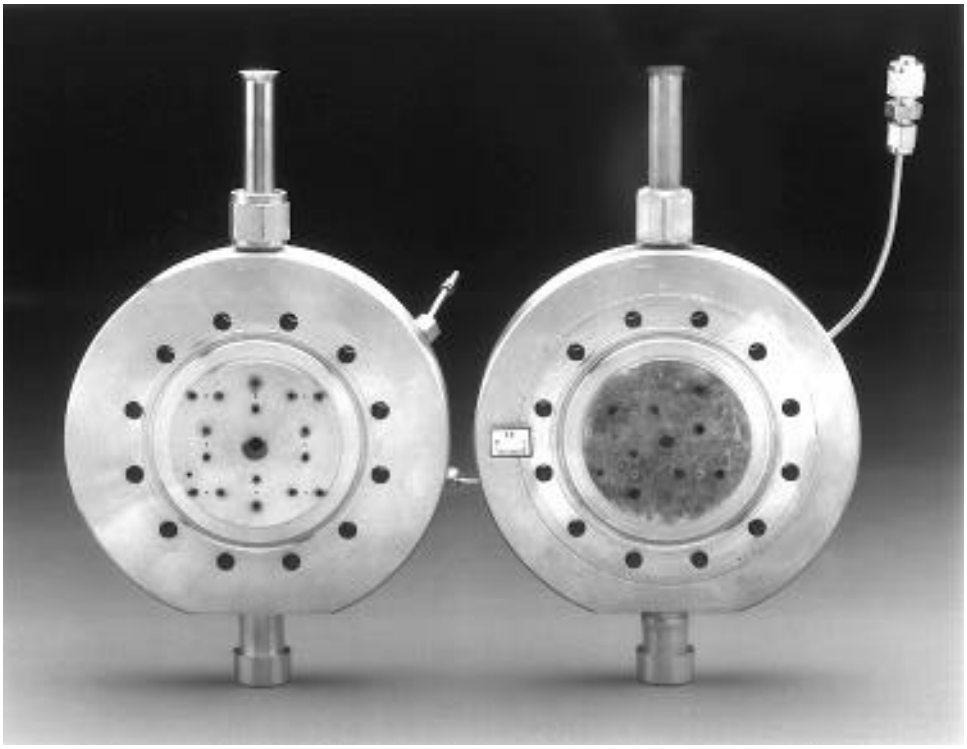

Erosion contrast for gelled propellant injectors.

from this effect. In the photograph the contrast of the shiny, almost unblemished 5 wt% RP–1/Al injector surface and the partially eroded 55 wt% RP–1/Al injector surface is clearly evident.

High-efficiency combustion of metallized gelled propellants was realized with even simple four- and eight-element triplet injectors. Combustion efficiencies above 90% were achieved, with the highest efficiency (95%) for the 55 wt% RP–1/Al. Although engine runs with that high metal loading experienced some agglomeration and erosion difficulties, the 0 and 5 wt% tests ran well, with a high combustion efficiency, and demonstrated a self-protective layer of gelled propellants and combustion products.

References

1. Arszman, J.; and Chew, W.: TACAWS Propulsion Development Program. JANNAF Propulsion Meeting, CPIA Publication 602, Vol. III, 1993.

2. Palaszewski, B.; and Rapp, D.: Design Issues for Propulsion Systems Using Metallized Propellants. AIAA 91–3484, Sept. 1991.

3. Mueller, D.; and Turns, S.: Some Aspects of Secondary Atomization of Aluminum/Hydrocarbon Slurry Propellants. J. Propulsion and Power, vol. 9, no. 3, May-June 1993.

4. Wong, W.; Starkovich, J.; Adams, S.; and Palaszewski, B.: Cryogenic Gellant and Fuel Formulation for Metallized Gelled Propellants: Hydrocarbons and Hydrogen With Aluminum. AIAA Paper 94–3175, June 1994.

5. Palaszewski, B.; and Powell, R.: Launch Vehicle Propulsion Using Metallized Propellants. AIAA Paper 91–2050, June 1991.

Lewis contact: Bryan A. Palaszewski, (216) 977–7493

Headquarters program office: OSAT

Rotor Coatings Tested for Cryogenic Brush Seal Applications

Engineers at NASA Lewis are testing brush seals in cryogenic fluids to determine their applicability to cryogenic turbopumps for rocket engine systems. Labyrinth seals in many aircraft gas turbine engines are being replaced by brush seals because brush seals are compliant, reliable, and cost competitive and have been shown to leak less and to enhance rotor stability. Hence, brush seals may be a good candidate in cryogenic turbopumps, where long-life, low-leakage, reliable seals are essential.

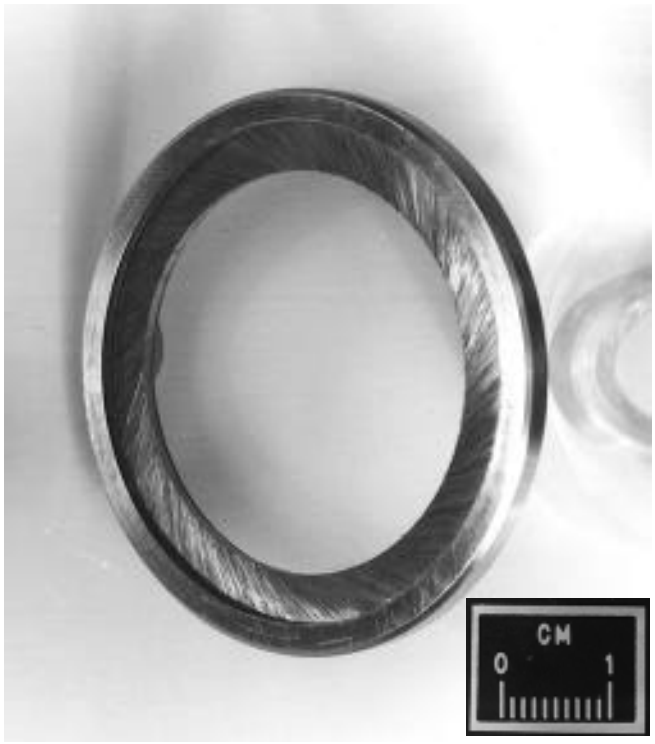

A typical brush seal.

A brush seal is simply a ring of wire bristles sandwiched between a front and back washer. The bristles usually have a 5- to 10-mil interference fit with the shaft and are installed at a 30° to 60° angle to the radius so that the bristles can bend as cantilever beams during shaft perturbations. The back washer is on the low-pressure side of the seal and has an inside diameter just slightly larger than the bristle bore diameter. It supports the bristles, preventing them from blowing downstream, and acts as a fixed-clearance seal should the bristles fail.

In a cryogenic turbopump brush seals may be used to seal either liquid hydrogen or liquid oxygen at locations near the pump or the bearings, or they may be used to seal hot gaseous hydrogen, warm gaseous oxygen, or helium at locations near the turbine or purge seals. In this environment large temperature gradients, oxygen compatibility, and hydrogen embrittlement are concerns. Also, the shaft speeds attained in cryogenic turbopumps for rocket engine systems are high, up to 200,000 rpm for a liquid hydrogen turbopump. Because brush seals are contact seals, their wear rates under these conditions are important.

To ensure that long life requirements will be met, several rotor coatings were tested against a brush seal in liquid hydrogen. The coatings tested were zirconium oxide, chromium carbide, and a Teflon-impregnated chromium. A bare Inconel 718 rotor was tested as the baseline material. The 2-in.-diameter bore brush seals had an initial interference with the rotor of 5 mils and were made with 2.8-mil-diameter, Haynes-25 bristles. Testing was done at 35,000 and 65,000 rpm to obtain surface velocities representative of those found in turbopumps for launch vehicles and orbital transfer vehicles, respectively. Pressure drops across the seal were as high as 175 psid. Leakage data were also taken. Although the data are still being analyzed, initial indications are that the bristle material transferred onto the bare Inconel 718 rotor, which did not happen in previous liquid nitrogen tests; that the zirconium oxide coating had the deepest wear groove; and that the chromium carbide and the Teflon-impregnated chromium wore somewhat better.

Further analysis is being done to quantify the wear rate and determine the wear mechanisms and the effects of coating techniques and coating density. The leakage data will be used to update and calibrate an analytical computer code developed at NASA Lewis that models brush seal performance.

Lewis contacts: Margaret P. Proctor, (216) 977–7526; James F. Walker, (216) 977–7465
Headquarters program office: OSAT

Electric Thruster Plume Impacts on Communications Signals Quantified

Electric propulsion has recently been accepted for use and is being considered for a wide range of applications from lightweight satellites to the next generation of geosynchronous communications satellites. Experience has shown that integration issues are a high priorty for users. To this end, NASA Lewis has established a large-scale propulsion test bed for assessing integration impacts. Recently, we successfully completed several major cooperative programs with both industrial and Department of Defense partners. New programs are in progress and requests for collaborative efforts to address integration issues have increased dramatically.

New NASA plume impacts test bed.

A specific area of increasing interest to users is the impact of electric thruster plumes on spacecraft communications. Until recently, the state of the art in this area was represented by a model developed at NASA Lewis. Intrusive diagnostics to quantify plume electrical characteristics were developed in-house (refs. 1 and 2), and an analytical model was developed under grant at the University of Texas (ref. 3). The UT code used experimental data to generate a plume model and then an analytic approach to determine both beam attenuation and squint for specific cases. Following the first demonstration of this code, General Electric's Astro-Space Division (now Martin Marietta) funded a study to evaluate arcjet plume impacts on communications for the specific case of the 7000 Series satellite. This approach was sufficient for low-power arcjets, which have very tenuous and well-behaved plumes. The simple arcjet model will not, however, be adequate for plumes associated with higher performance electric thrusters now under development for use by industry and in NASA programs.

To address this shortfall, NASA Lewis has developed a large communications impacts test bed (see photograph). In the arrangement shown, transmitting and receiving horns are positioned across the tank, and the thruster is on a movable stand and oriented so that the exhaust plume is in the path of the transmitted signal. Nanosecond gating electronics are used to mitigate effects from signals reflected from the tank walls. Attenuation and phase shift can be monitored with respect to thruster position and operating condition at frequencies to 18 GHz. Other experiments, using a movable receiving antenna, will allow the determination of beam squint. To date, the new test-bed capability has been successfully used to examine the impacts of a NASA 30-cm-diameter xenon ion engine plume on communications

signals. A cooperative program to use this new capability to characterize a commercial electric thruster system is being planned.

References

1. Zana, L.M.: Langmuir Probe Surveys of an Arcjet Exhaust. AIAA Paper 87–1950, July 1987. (Also NASA TM–89924.)

2. Sankovic, J.M.: Investigation of the Arcjet Plume Near Field Using Electrostatic Probes. NASA TM–103638, 1990.

3. Ling, H.; et al.: Near Field Interaction of Microwave Signals With a Bounded Plasma Plume. Final Report on NASA Grant NCC3–127, Jan. 1991.

Lewis contacts: Dr. Frank M. Curran, (216) 977–7424; and Dr. Afroz J.M. Zaman, (216) 433–3415
Headquarters program office: OSAT

Fiber-Optic-Based Methods Improve Gas Analysis and Concentration Monitoring

The ability to analyze the composition of a gas mixture and to monitor the constituent concentrations in real time has a broad range of applications. Using instant optical monitoring techniques to detect hazardous gas leaks will facilitate ground operations at space launch sites and reduce vehicle turnaround time. Gas-processing plants need to monitor processes in real time, and steel-processing plants need to monitor the composition of their endothermic gas. This monitoring now occurs with chemical sensors, which are often limited to single species, have a relatively slow response, and are sometimes quite inaccurate.

NASA Lewis has evaluated a Raman scattering system that uses fiber optics for species concentration determination. An optical probe head was designed to facilitate remote mounting. A single-mode fiber-optic delivers a 0.5-W green laser beam from an argon-ion laser to the probe, which focuses the beam into a gas sample. A photodiode inside the probe wall measures the laser beam intensity for reference purposes. The same probe collects the light scattered back from the molecules and couples this observed light into a second fiber-optic, which guides the light to the detection equipment, where the light intensity is measured. Calibration charts allow a direct readout of the species concentration.

Gas monitoring facility.

Initial measurements were performed on a gas mixture in an enclosed vessel at ambient temperature and containing 20% oxygen, 78% nitrogen, and 2% hydrogen. The pressure in the vessel was increased from 0 to 0.1 MPa while the scattered intensities of nitrogen, hydrogen, and oxygen molecules were monitored. A tradeoff existed between the speed and accuracy that could be obtained. In this example, a 30-sec time constant had been set, which caused a significant uncertainty. The lower limit of hydrogen detectability using the nonoptimal apparatus was 1 kPa. An improved, simpler design and upgraded components will greatly enhance the capability of this system. This approach to gas analysis opens exciting new possibilities in many areas of leak detection and process control.

Bibliography

de Groot, W.A.: The Use of Spontaneous Raman Scattering for Hydrogen Leak Detection. AIAA Paper 94–2983, 1994.

Lewis contact: Dr. Wim A. de Groot, (216) 977–7485
Headquarters program office: OSAT

High-Pressure, Compact Rockets Satisfy Small Satellite Requirements

Earth-storable-liquid-fueled apogee rockets for spacecraft applications developed during the past three decades are pressure fed with chamber pressures of typically 125 psia. Their propellant feed systems operate at a relatively low 260 psia compared with large rocket engines. This pressure is driven by the minimum gage for the tank metals. Recently developed lightweight, fiber-overwrapped tanks may have altered this system pressure optimization. In addition, new high-temperature, long-life rocket chamber materials, such as iridium-coated rhenium, can withstand the increased temperatures in high-pressure rocket chambers—without paying a performance penalty for fuel film cooling. These events have paved the way for development of a high-pressure, high-performance compact rocket engine for small, lightweight satellites.

NASA Lewis has established a research effort with two contractors, GENCORP Aerojet Propulsion Division and TRW Space and Technology Division, to develop high-pressure, Earth-storable-liquid-fueled rocket technology for lightweight satellites. Basic data on combustion efficiency and heat transfer were obtained in rocket test-bed hardware in preparation for flight rocket development. TRW tested a 50-lbf-class heat sink

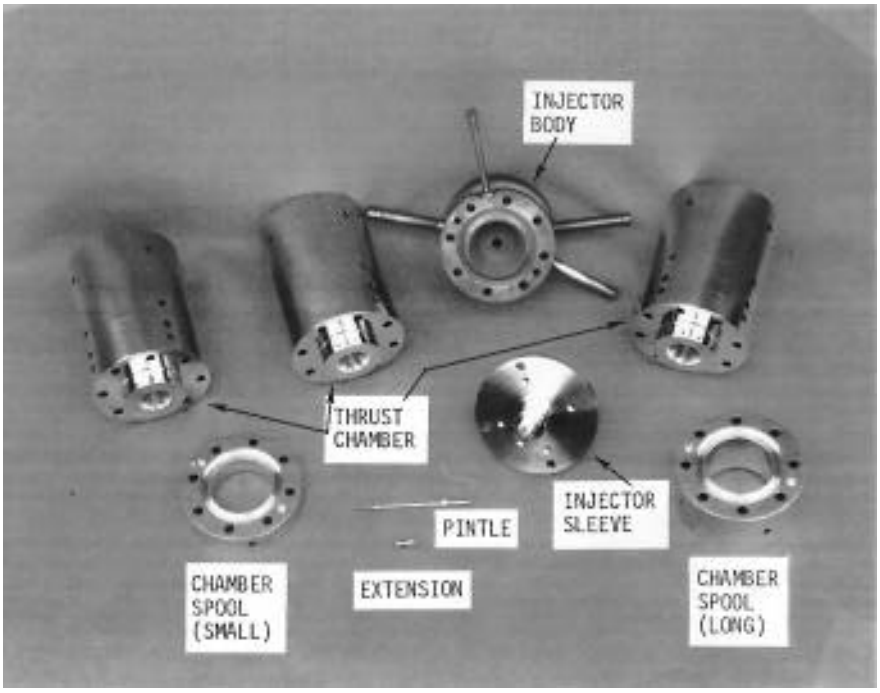

Small rocket test-bed hardware.

engine. The estimated performance was 338 sec at 500-psia chamber pressure and 150:1 area ratio using nitrogen tetroxide (NTO)–hydrazine propellants. Aerojet tested a 100-lbf-class chamber with a projected performance of 334 sec at 250-psia chamber pressure and a 300:1 area ratio also using nitrogen tetroxide–hydrazine propellants. High-pressure engines developed in this program are projected to fit into the tight volume and length constraints of small satellites. TRW estimates that as much as 80 lbm can be saved on the NASA Goddard Space Flight Center/TRW Total Ozone Mapping Spectrometer–Earth Probe mission by using this rocket technology.

Lewis contact: Dr. Steven J. Schneider, (216) 977–7484
Headquarters program office: OSAT

Engineering Model Ion Thrusters and Power Processors Developed

NASA Lewis and the Jet Propulsion Laboratory are developing xenon ion propulsion systems to be flight qualified and validated for planetary and Earth-orbital missions. Once validated, thruster/power processor modules operating at 2.5 kW or less will be used to build propulsion systems consistent with user's requirements. For example, 10- to 14-kW systems are envisioned for small-body planetary missions that also require thruster power throttling from 2.3 kW at about 3300-sec specific impulse to 0.55 kW. In-space operational lifetimes, at 2.3 kW, may be as high as 8000 hr for 15-year Earth-orbital missions with many spacecraft repositioning moves.

Ground and spaceflight validations of the ion propulsion technology will be conducted under the NASA Solar Electric Propulsion Technology Applications Readiness (NSTAR) Program. Thirty-centimeter-diameter xenon thrusters have been developed to a high level of maturity to satisfy near-term requirements for planetary and Earth-orbiting satellites. A functional engineering model thruster has undergone diagnostic vibration tests, performance tests using a thrust stand, and plume diagnostic tests. These data have been used to define the design of an engineering model thruster (EMT). The first EMT has been assembled and has completed a short-term design verification test. The EMT is now undergoing a 2000-hr wear test at 2.3 kW in a 0.3-mPa test chamber.

A breadboard power processor is being developed to operate from an 80- to 120-V power bus and provide 0.55 to 2.3 kW to the xenon thruster. A 50-kHz switching frequency was selected in a tradeoff aimed at reduced magnetics mass and high efficiency. The breadboard power processor design incorporates three power supplies for all

Breadboard supply for xenon ion thrusters.

thruster functions. Dual-use neutralizer and discharge power supplies each provide outputs for both a heater and an anode electrode. The beam/accelerator stage supplies voltages to the ion accelerator grids and also accommodates recovery from high-voltage faults or arcs. The two low-voltage power supplies employ a push-pull design, but the beam/accelerator stage utilizes a full-bridge topology. The breadboard power processor topology, a pathfinder, will be evaluated by NASA and an industrial contractor. A breadboard controller, using a microprocessor, completes the power processor assembly. It provides for startup, throttling, shutdown, and fault recovery and supplies subsystem data.

The low-voltage power supplies have been fabricated and are undergoing functional tests on resistive loads and ion thrusters. The high-voltage supply is being assembled. The breadboard power supplies will be separately integrated with an ion thruster before final tests with a full-up breadboard power processor. Projected specific mass of a flight-packaged power processor is about 5 kg/kW at an input power of 2.5 kW and an efficiency of 0.92.

The NSTAR ground-test program has developed, integrated, and tested three engineering model ion thrusters and two breadboard power processors. Thruster wear tests of 2000, 4000, and 12,000 hr will verify the thruster design, establish wear rates and symptoms of early and random failures, and demonstrate compatibility of the ion thruster and power processor with user requirements.

Bibliography

Hamley, J.A.; et al.: A 2.5-kW Power Processor for the NSTAR Ion Propulsion Experiment. AIAA Paper 94–3305, June 1994.

Patterson, M.J.; et al.: NASA 30-cm Ion Thruster Development Status. AIAA Paper 94–2849, June 1994.

Sovey, J.S.; et al.: Development Status of the NASA 30-cm Ion Thruster and Power Processor. AIAA Paper 94–3981, Aug. 1994.

Lewis contact: James S. Sovey, (216) 977–7454
Headquarters program office: OSAT

RL–10 Turbopump Flight Cooldown Characterized

The United States Air Force is sponsoring the Atlas Reliability Enhancement Program (AREP) to improve the reliability of the Martin Marietta-built Atlas launch vehicle. One program element looks at alternative methods of cooling the turbopumps used in the cryogenic-fueled RL–10 engines of Atlas' Centaur second stage. Presently, a complex helium system cools the turbopumps to cryogenic temperatures before lift-off. The simplest method proposed (since it requires only a new method of operating the existing hardware) is "percolation." The valve in front of the turbopump is opened to allow liquid to flow into the turbopump, but the engine shutoff valve is left closed. Key issues of the percolation method are the steady-state condition of the turbopump, time to reach that steady state, and whether the vapor can percolate up the supply lines into the supply tank without interrupting the cooling process.

To gain an understanding of the percolation process, NASA Lewis (with the support of the AREP team) has conducted a series of percolation

RL–10 turbopump and supply tank before installation of quartz viewing tube.

cooldowns with an instrumented turbopump at the Lewis Cryogenic Components Laboratory. Tests included cooling the oxidizer side of an instrumented turbopump by percolating with liquid nitrogen; cooling the fuel side of an instrumented turbopump by percolating with liquid hydrogen; studying the effects of the initial turbopump temperature and the supply pressure; and accelerating the cooling process by allowing some of the flow to continue through the turbopump and out a small valve (trickle-flow chilldown).

The cryogen is supplied from a test tank 11 in. in diameter by 8 ft high to simulate the Centaur tanks. A mockup of the Centaur oxygen feedline exits approximately 3 ft up the side of the test tank. A section of quartz glass tube was included in the line mockup so that flow within it could be observed and video taped. Temperature sensors were installed at more than 70 locations, both internal and external to the turbopump. The turbopump was mounted in an enclosure purged with helium to prevent frost formation.

Tests with liquid nitrogen resulted in a cooling time of 3 to 6 min (based on time to reach steady-state temperature). Cooling time decreased with increasing supply pressure and with the use of trickle flow. Observation of the flow through the quartz showed a stratified flow throughout the test without any backflow of liquid. The test with hydrogen was inconclusive because the hydrogen depleted before steady state was achieved. Percolation looks feasible, at least for cooling the liquid oxygen side, but further testing is planned to refine the cooling procedure.

Lewis contact: David J. Chato, (216) 977–7488
Headquarters program office: OSAT

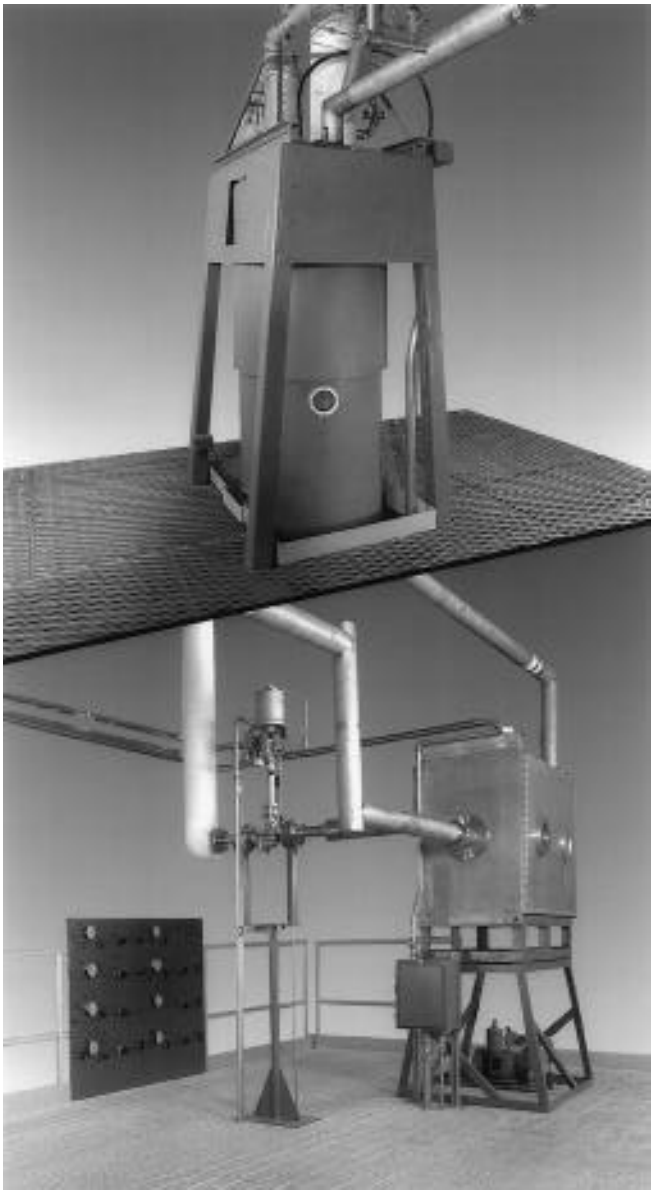

Small-scale hydrogen test system.

Small-Scale Hydrogen Test System Enables "Smaller, Faster, Cheaper"

NASA Lewis has constructed a new and unique test bed for conducting research with cryogenic fluids, such as liquid hydrogen densified into slush hydrogen. The small-scale hydrogen test system has been designed with the current NASA philosophy in mind: conducting research in a smaller, faster, and cheaper manner without compromising the quality of the data. The unique size of the test system allows high-quality test data on engineering systems to be obtained at low cost through quick and easy hardware installation and operating procedures involving minimal manpower, by a highly skilled and experienced team of engineers and technicians using advanced cryogenic instrumentation. The test system was built in-house wih the support of the National AeroSpace Plane Joint Project Office at Wright-Patterson Air Force Base.

The test system is located at NASA Lewis' Plum Brook Station K-site Facility in Sandusky, Ohio. The system's two parts (see photograph) are the 200-gallon, vacuum-jacketed test dewar (top) and

the fluid transfer system (bottom), connected to the test dewar with 4-in. vacuum-jacketed piping. The test dewar is unique in that the test fluid can be viewed through several ports on its lid and sides. The fluid transfer system consists of the vacuum-jacketed transfer lines and an instrumentation box, an evacuated aluminum box with a 2-in.-diameter, 1-ft-long clear test section for flow visualization. Advanced instrumentation to measure flow rates or fluid density can be installed in place of, or in series with, the clear test section.

Other test system capabilities include a 778-ft^3/min vacuum pump, a vent gas measurement system, a test dewar pressure control system, and a pressurant gas supply system. Fluids available at the facility include liquid hydrogen and nitrogen and small quantities of liquid helium and gaseous helium, hydrogen, and nitrogen. The data acquisition system can monitor 512 channels of instrumentation.

Instrumentation available in the test system includes a continuous liquid-level measurement using a capacitance liquid-level probe, a capacitance densimeter, a silicone diode and type E, T, and J thermocouple temperature sensors, various types of pressure transducer, orifice and thermoconductivity types of flowmeter for measuring gas flow, and several sizes of venturi for measuring liquid flow.

The test system has been operational since April 1994, when the slush hydrogen production optimization (SHPO) experiments began. (Slush hydrogen is composed of liquid and solid hydrogen and is 16% denser than liquid hydrogen.) A new slush hydrogen production technique reduced the previous slush production time by 50%, potentially lowering operating and capital costs of a full-scale slush hydrogen production plant. A new test program, sponsored by Martin Marietta of Denver, involving the chilldown of an RL–10 turbopump assembly is slated to begin in September 1994.

These two test programs have direct impacts on the NASA strategic plan. The SHPO program supports several studies showing that propellant densification (i.e., slush hydrogen) can reduce the weight of single-stage-to-orbit vehicles by 30 to 50%. NASA is seriously considering the use of propellant densification in the design of the next generation of reusable launch vehicles. Also, the industry-sponsored RL–10 turbopump chilldown tests are a perfect example of government/industry partnership.

Lewis contact: Nancy B. McNelis, (216) 977–7474
Headquarters program office: OSAT

Cryogenic Compression Mass Gage Passes Liquid Hydrogen Test

The ability to accurately measure quantities of cryogenic fluids in a low-gravity environment is critical for future space exploration missions. In low gravity the position of liquid in a container may be markedly different than it is on Earth. Instead of settling in the bottom of the container, the liquid may be located randomly throughout the container and be interspersed with a mixture of gas bubbles. Consequently, the familiar gaging methods used on Earth are not generally applicable in space. A gaging system that will work in low gravity is needed. The compression mass gage (CMG) testing effort led by NASA Lewis is addressing this technology problem.

The CMG concept is based on the principle that the pressure of a gas changes when its volume changes. In operation the tank volume is changed slightly by an oscillating bellows, and the corresponding change in tank pressure is measured.

Preliminary testing in a normal-gravity environment using a cryogenic simulant has concluded. Results from these tests have led to the development of a cryogenic compression mass gage. This gage was built by Southwest Research Institute under terms of a Space Act Agreement with NASA Lewis. It was tested in a liquid hydrogen dewar by Lewis in their Cryogenic Components Laboratory Cell 7. These tests verified the ability to operate the CMG in an actual cryogenic vessel while obtaining accurate results. Further enhancements to the CMG are currently being evaluated, as well as improvements to the algorithm used to calculate mass. Testing to date has met several critical milestones in proving out the design for use in future space systems.

Lewis contact: John M. Jurns, (216) 977–7416
Headquarters program office: OSAT

Cryogenic Two-Phase Nitrogen Flow Studied

An experimental apparatus has been built at the National Institute of Standards and Technology in Boulder, Colorado, to study two-phase flow of nitrogen under cryogenic conditions. Heat transfer and flow pattern data have been measured at heat and mass flux ranges 10 (or more) times lower than previously available. The data will be used to design heat exchangers for vaporizing cryogenic propellants in a low-gravity environment. These heat exchangers are a key component of thermodynamic vent systems used to supply gaseous propellants to electric orbital transfer vehicles. The same technology will later be used to control cryogenic storage tank pressure during long-duration space exploration missions.

NIST's unique apparatus can obtain flow pattern and heat transfer data at mass fluxes from 0.05 to 5 kg/m^2-sec and heat fluxes from 3 to 300 W/m^2. The apparatus has a horizontal flow orientation and is used for ground-based experimentation. It has view ports for visual observation of the two-phase flow.

Successfully determining two-phase flow patterns is the first step in correctly modeling the heat transfer to the fluid. A joint research effort with NASA Lewis has obtained some initial experimental results. The work is ongoing. Visual observations and videotapes have been made of the two-phase flow patterns. Preliminary measurements of heat transfer phenomena have also been obtained. These measurements include convective heat transfer coefficients, wall superheat at inception of boiling, and transient wall temperature histories during initial chilldown. This work is precursory to follow-on experiments in low gravity and will guide the development of these experiments.

Lewis contact: Neil T. Van Dresar, (303) 497–7553
Headquarters program office: OSAT

Power Technology

Tiny Sensors Will Measure Mars Dust

As scientists watched the Viking Probe return the first photographs from the surface of Mars, they were astonished to see, instead of the expected dark blue sky, that the sky was a light, almost pink color. The color is due to the scattering of light from tiny dust particles raised into the atmosphere by dust storms. Over time, dust in the sky of Mars settles out of the atmosphere. Very little is known about this settling process or whether the settled dust will cover the surfaces of solar arrays for power systems on Mars probes. Estimates of the optical obscuration of a solar array by settled dust vary by as much as a factor of 40. For design of future missions, which may require long surface operation times using solar power, we need better information on the rate at which dust settles from the Mars atmosphere. Accurate measurements of dust settling rates and the properties of atmospheric dust are also of considerable scientific interest. Dust properties affect the atmospheric solar absorption and thus the climate of Mars, as well as serving as nucleation sites for water and carbon dioxide frost.

Therefore, NASA Lewis has built two sensors, to fly on the Mars Pathfinder Rover mission, that will measure the accumulation of settled dust. Together, the Materials Adherence Experiment (MAE) instruments have a mass of less than 60 g and require an area of less than 4 cm^2, slightly larger than a commemorative postage stamp. The coverglass transmission sensor measures the change in transmission of a transparent solar cell coverglass as dust settles on the surface. This sensor uses an innovative, lightweight, shape-memory alloy actuator design to remove the glass cover from the sensor.

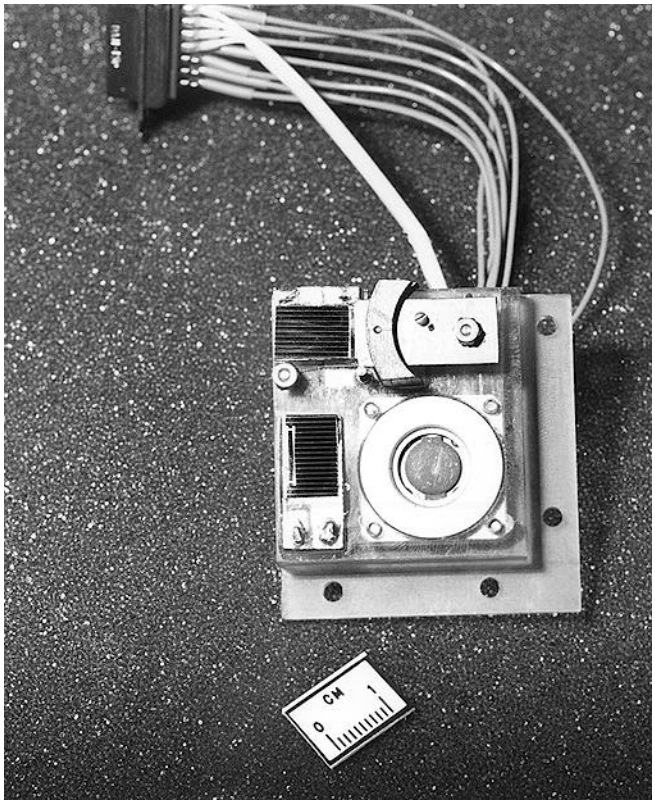

Mars dust sensor, barely larger than a postage stamp, containing a quartz crystal monitor and two small solar cells.

The second sensor in the experiment, a quartz crystal monitor, will measure accumulated dust loading. A quartz crystal monitor (QCM) is a thin wafer of quartz set to vibrate at a specific frequency. This resonant frequency is extremely sensitive to the mass deposited on the wafer. QCM's are used, for example, to measure angstrom-thick layers of film deposited by vacuum deposition. This experiment measures the mass of dust deposited as a function of time.

Both experiments will fly to Mars on the upcoming Pathfinder mission, scheduled for launch in 1996. To meet the tight schedule of this project, the two sensors have been completely developed, from initial proposal to tested flight hardware, in less than a year. The two tiny sensors will yield crucial information on the performance of solar panels in the Mars environment and will give valuable scientific information for understanding the weather and climate of Mars.

Lewis contacts: Geoffrey A. Landis, (216) 433–2238; PhilipP. Jenkins, (216) 433–2233; Lawrence G. Oberle, (216) 433–3647

Photovoltaic Array Experiment Launched on Pegasus

On August 3, 1994, the Photovoltaic Array Space Power Plus Diagnostics (PASP Plus) flight experiment was successfully launched into space aboard a Pegasus rocket. PASP Plus, the major experiment on the Advanced Photovoltaic & Electronic Experiments (APEX) satellite, is designed to test a variety of new and existing photovoltaic cell and array technologies within the space environment.

The PASP Plus experiment consists of 12 different experimental photovoltaic modules, along with numerous diagnostic instruments to measure the space environment and interactions between the experimental modules and that environment. The major goals of PASP Plus are

- To measure the performance of new photovoltaic cell technologies in space
- To determine long-term performance within the space radiation environment
- To measure the interactions between the experimental modules and the space plasma when the modules are biased at high positive or negative voltages.

APEX's highly elliptical orbit (1377×196 nautical miles, 70° inclination) provides exposure to space radiation as well as wide variations in the space plasma density for high-voltage bias testing. Understanding array interactions with the space plasma is critical to designing future power systems capable of providing higher bus voltages.

PASP Plus is a joint Air Force/NASA Lewis experiment. The Air Force's Phillips Laboratory at Hanscom Air Force Base has primary responsibility for managing the project. What started three years ago as an Air Force request for assistance in testing the individual experimental modules has gradually evolved into a major role for NASA Lewis. Our personnel have primary responsibility for the individual photovoltaic module experiments. Integration and modification of all the experimental modules was done at Lewis by NASA technicians. In addition to involvement in the experiment definition and planning, Lewis personnel provided key support during preflight testing, launch vehicle integration, and real-time operations. Lewis will continue to actively support PASP Plus throughout its planned three-year mission life with analysis of long-term module

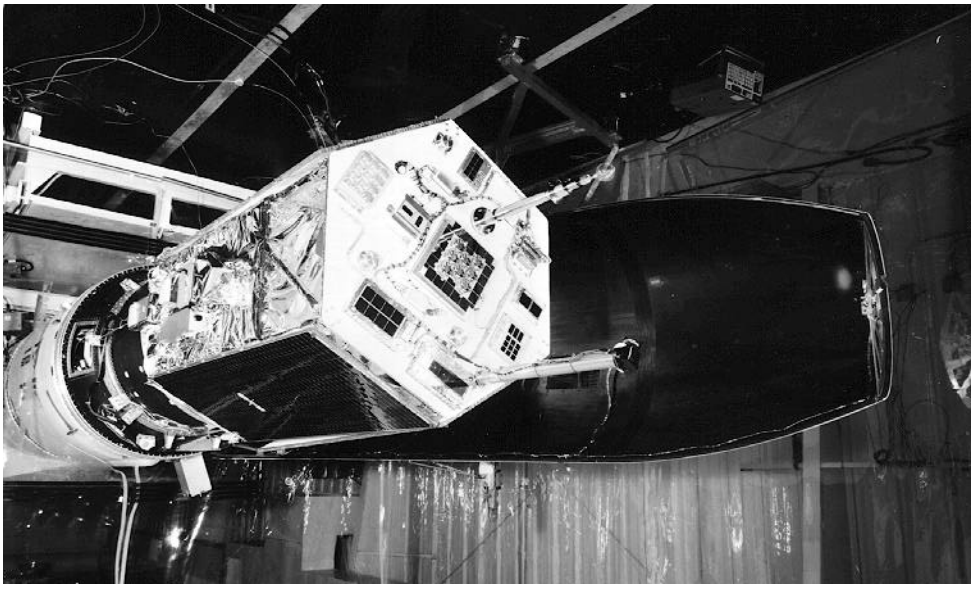

PASP Plus flight experiment on the APEX satellite just before launch on a Pegasus rocket. Courtesy of Orbital Sciences Corp.

performance and interpretation of environmental effects and interactions data.

In addition to Lewis' key role in management and operation of the overall PASP Plus experiment, it has also provided two of the photovoltaic experimental modules. The mini-dome Fresnel lens concentrator module is the first spaceflight test of this unique refractive concentrator technology, originally developed at Lewis through the Small Business Innovation Research Program. A four-cell module of the space station array is also being flown. Data from these individual experiments will provide valuable information for both current and future space missions.

Early results from the experiments have been very promising. Successful operation of the refractive concentrator technology and a variety of multijunction photovoltaic cell technologies has been demonstrated. Degradation due to space radiation has been observed in some modules. Plasma interactions in the form of leakage currents and arc rates are being obtained for a wide variety of orbital conditions. Continued data from PASP Plus will provide NASA, government, and industry organizations with invaluable information that will affect the design of future space power systems.

Lewis contacts: Henry B. Curtis, (216) 433–2231; MichaelF. Piszczor, (216) 433–2237
Headquarters program office: OSAT

Linear Photovoltaic Concentrator Prototype Panel Demonstrated

For two years NASA Lewis has been working with Entech, Inc., under the Small Business Innovation Research Program to develop a line-focus refractive concentrator for use in a photovoltaic power system designed for space applications. Earlier work had emphasized lens and cell development, but a key to demonstrating the viability of this concept was to integrate the individual components into a functional panel. In early 1994 Entech collaborated with Composite Optics, Inc., another small business with substantial experience in fabricating composite structures and using them in space. Together they fabricated a small prototype panel structure that fully integrated the concentrator lens and photovoltaic cell receiver assemblies into a stiff, lightweight structure.

The prototype panel was made from a variety of carbon composite materials. High-thermal-conductivity materials were used in specific areas where heat dissipation was critical. In a significant change from previous panel concepts, structural stiffness for the panel was provided by using a thin honeycomb panel on the back side of the cells. Earlier panel concepts maintained structural rigidity through a 4-cm-thick structure (which corresponded to the focal length of the concentrator lens). By moving the stabilizing structure to the back of the panel, the "unused"

Prototype module of linear refractive concentrator focusing sunlight.

focal length required for proper operation can now be collapsed for stowage during launch. This feature significantly decreases the stowage volume of the concentrator, a limiting factor under earlier versions, and increases radiation shielding to the back side of the cell.

The line-focus refractive concentrator design for space is directly comparable to Entech's current line of terrestrial photovoltaic concentrator systems and benefits from the operational and manufacturing knowledge gained by years of experience in this field. The concentrator concept is based on the same general principles as the point-focus minidome Fresnel lens concentrator and offers many of the same advantages. In addition to the generic benefits offered by photovoltaic concentrator systems for space (e.g., high array efficiency, inherent protection from space radiation effects, and minimized interactions with the space plasma), the linear concept offers two important advantages:

- Relaxation of precise array tracking requirements to only a single axis
- Low-cost mass production of the concentrator lens material

The potential cost and performance advantages of the linear refractive concentrator make it an attractive option for a variety of space missions. A number of commercial and military missions are specifically interested in this concept because of its inherent ability to operate in high-radiation environments. Therefore, a cooperative program is currently being established between NASA, industry, and other government agencies to push for an early spaceflight demonstration of this technology.

Lewis contact: Michael F. Piszczor, (216) 433–2237
Headquarters program office: OSAT

Aluminum/Oxygen Semicell Developed for Use in Unmanned Submarine

Under an contract funded by the Advanced Research Projects Agency that began in June 1991, Loral Defense Systems–Akron, with technical assistance from NASA Lewis personnel, has developed an innovative, high-energy, aluminum/oxygen semicell stack system. It will replace the 300-kW-hr silver/zinc battery system now being used in an unmanned underwater vehicle (UUV). The aluminum dioxide (Al/O_2) semicell technology is supplied by Eltech Research Corp. of Fairport Harbor, Ohio; the UUV is supplied by Draper Laboratories of Cambridge, Massachusetts.

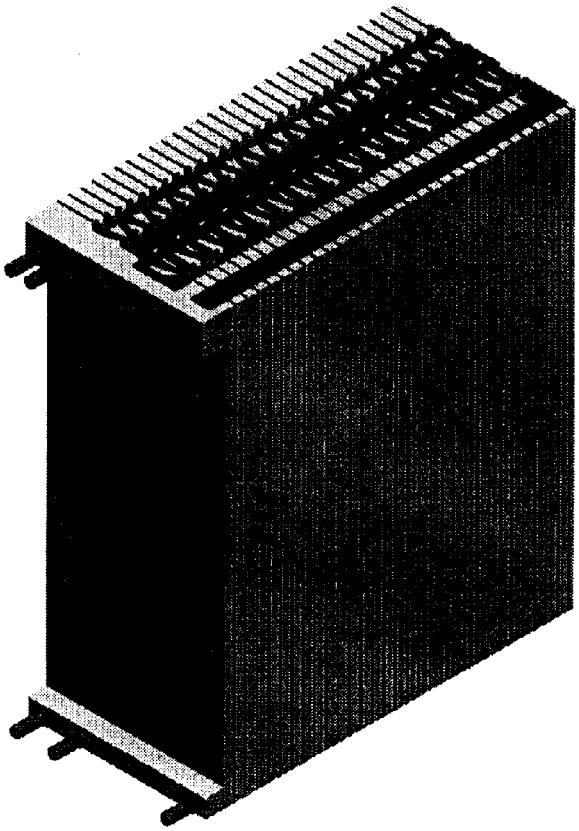

Cell stack configuration.

Considerable effort went into developing an aluminum alloy that has an extremely low corrosion rate in 4-molar potassium hydroxide (KOH), the electrolyte of choice. Success in this effort and in modifying Eltech's existing air cathode for use in 100% oxygen were major advances. Stack testing as many as nine cells has successfully progressed to where it is felt that the UUV requirements for 15-kW maximum power over 500hr and an available energy of at least 1MW-hr can be attained.

The system consists of 4-in. by 32-in. cells packed three to a single plate. Thirty such plates, stacked together with suitable manifold connections for oxygen, coolant (water), and electrolyte (4MKOH), will produce 7.5 kW. Two such stacks, which can operate independently of each other, with needed accessory units are designed to fit smoothly into the 44-in. UUV, replacing the silver/zinc batteries. In operation, Al reacts electrochemically with O_2 to form a solid aluminum hydroxide called hydrargillite. The electrolyte is pumped through each cell, and the hydrargillite is carried away to the electrolyte tanks where it is removed by a filter. A hydrogen removal system was developed that safely combines the small amount of hydrogen produced by the corrosion of Al with KOH. The cells and stack are cooled by water flowing in contact with each Al anode.

Loral is now procuring parts, building test facilities, and fabricating the necessary parts to test several 90-cell stacks separately as 7.5-kW units and in pairs to form the full 15-kW unit. The test program will cover all requirements for the UUV. Oxygen will be supplied by using sodium chlorate candles.

After testing, the powerplant development unit will be upgraded to fit into the 44-in. UUV supplied by Draper Laboratories for the land-based acceptance test. Sea trials, using some typical mission, are planned to complete the present program in 1996.

Lewis contact: Robert B. King, (216) 433–6122
Funding source: Advanced Research Projects Agency

Nickel/Hydrogen Battery Cells Selected for *International Space Station Alpha*

NASA Headquarters and its contractors are responsible for constructing the electrical power system for the *International Space Station Alpha* (ISSA), which will circle the Earth every 90 min in a low Earth orbit. Approximately 55 min of this orbit will be in sunlight and 35 min will be in the Earth's shadow (eclipse). The electrical power system must not only provide power during the sunlight portion by means of solar arrays, but also store energy for use during the eclipse. Nickel/hydrogen (Ni/H_2) battery cells were chosen as the energy storage system for ISSA. However, to expand the limited Ni/H_2 data base on life and performance characteristics under low-Earth-orbit (LEO) conditions, NASA Lewis began two test programs: one in-house and one at the Naval Surface Warfare Center in Crane, Indiana.

For the in-house test program Lewis built a Ni/H_2 battery cell test facility with a data acquisition system to screen a large number of cell designs. The cells were purchased from three vendors. The resulting 39-cell test matrix consists of 13 different cell designs. All cells are now undergoing LEO life testing at a 35-percent depth of discharge (DOD) at either –5 or 10 °C. As of September1994 ,

Lewis in-house battery cell test facility.

17 cells have completed over 5 years of life testing (29,200 cycles), 20 cells have completed over 4years, but two cells failed at 2.9 years and 3.3 years, respectively. The number of completed life cycles ranges from 27,564 to 32,113.

To verify the ISSA requirement of 5-year life at 35-percent DOD, a statistically significant number of Ni/H_2 battery cells are on test at the Naval Surface Warfare Center. The test matrix consists of Ni/H_2 battery cells from three vendors. All life testing is performed in either 10-, 8-, or 5-cell series-connected test packs at 35- or 60-percent DOD and at 10 or 5 °C.

In the life tests 100 Yardney Technical Products cells have accumulated between 12,325 and 24,065 cycles, and 108 Eagle-Picher Industries cells have accumulated between 13,579 and 18,644 cycles. Forty-eight cells are undergoing a special charge control study. Some of the cells are being charged by using the ISSA baseline charge profile, which incorporates a constant current charge followed by a taper charge to 100-percent state of charge. The other cells are being charged at a constant current terminating at 90- or 94-percent state of charge. The results of these tests were instrumental in the selection of a "standard" cell design from Eagle-Picher as a potential supplier for ISSA.

Another potential battery cell supplier for ISSA is Gates Aerospace Batteries. One hundred Gates cells have accumulated 9559 to 13,986 cycles. Thirty Gates cells are being used to assess the effect of potassium hydroxide electrolyte concentration with various charge management techniques.

The results to date have provided confidence in achieving a 5-year LEO life for Ni/H_2 battery cells at 35-percent DOD, which is the design point for the *International Space Station Alpha*.

Lewis contacts: Randall F. Gahn, (216) 433–6158; ThomasB. Miller, (216) 433–6300; John J. Smithrick, (216) 433–5255
Headquarters program office: OSF

Advanced Power Control Topology Developed for Spacecraft

In current satellites the battery charge control must be custom designed for each individual

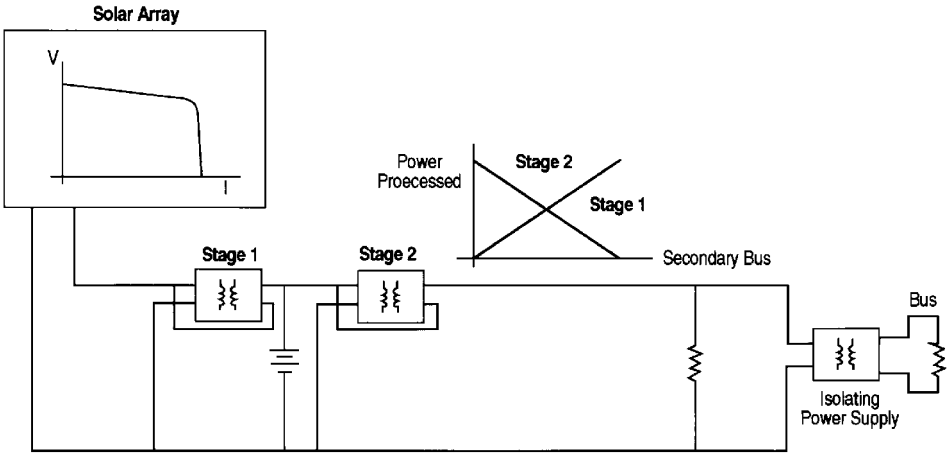

Advanced power control topology for spacecraft.

spacecraft. Economic competition in the small satellite market requires a battery charge control that is lightweight, efficient, inexpensive, and modular enough to be reused in several applications. In work performed on the *International Space Station Alpha* and on small satellites, NASA Lewis has developed a battery charging/power bus regulation topology that addresses these needs.

As shown in the figure, charging the spacecraft battery with a solar array is accomplished by using a standard transformer isolated buck converter. The converter is connected with a bypass loop in which the high input lead is connected to the ground of the output. This scheme has the effect of biasing the converter's return output to the solar array's high output. Because of this biasing, the converter only processes the fraction of power necessary to charge the battery above the voltage of the solar array. Likewise, the same converter hookup can be used to regulate the battery output to the spacecraft power bus with similar fractional power processing.

The advantages of this scheme are the following:

- Because only a fraction of the power to run the system is processed through a converter, the single-stage conversion efficiency is about 97%.
- The system is highly fault tolerant because in a converter failure the battery will continue to charge up to the output of the solar array.
- High-efficiency converters are not necessary to make the system highly efficient.
- The converters are easily paralleled, allowing higher power systems to be built up using a common building block. This common building block can then be reused in a variety of configurations to meet the needs of many applications.

Lewis contact: James F. Soeder, (216) 433–5328
Headquarters program office: OSAT

Electrical Wire Insulation Protected in Atomic Oxygen

Atomic oxygen erosion on spacecraft in low Earth orbit is an increasingly important issue because more spacecraft will be flying in these orbits.

The atomic oxygen durability of three types of electrical wire insulation (carbon based, fluoropolymer, and polysiloxane elastomer) was evaluated. These insulation materials were exposed to thermal-energy atomic oxygen, obtained by radiofrequency excitation of air at 11 to 20 Pa. All the carbon-based materials eroded at about the same rate as polyimide Kapton and therefore are not atomic oxygen durable. The erosion rates of fluoropolymers varied widely, and they must be evaluated on a case-by-case basis. For, example, test data suggest the formation of atomic fluorine during reactions of atomic oxygen with amorphous fluorocarbon. Dimethyl polysiloxanes (silicone) did not lose mass during atomic oxygen exposure but developed silica surfaces, which were under tension and

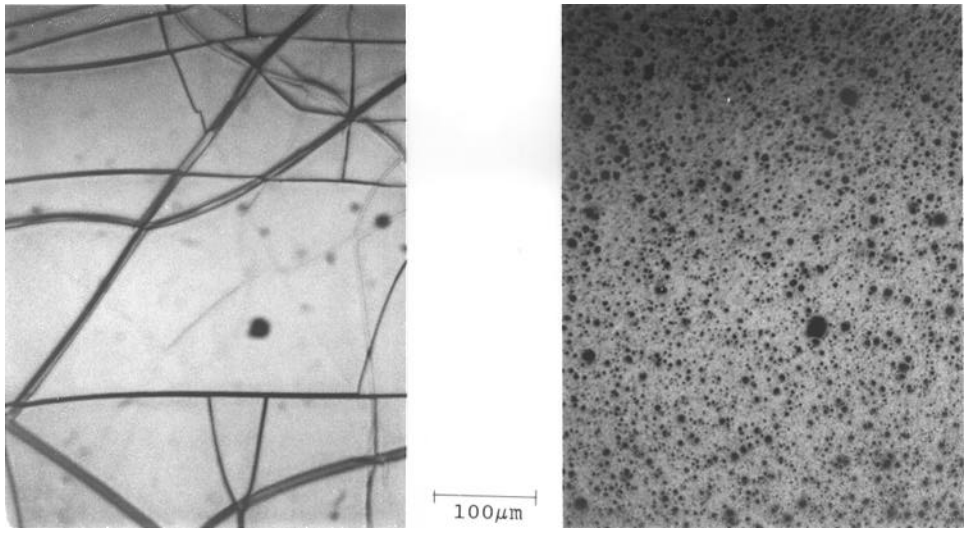

Silicone exposed to atomic oxygen. Smooth surface cracks (left), but textured surface does not crack (right).

frequently cracked from loss of methyl groups. However, if the silicone sample surfaces were properly pretreated to provide a certain roughness, atomic oxygen exposure resulted in a sturdy, noncracked, atomic-oxygen-durable silicon dioxide layer.

Crack-induced contamination by silicone can thus be reduced or completely stopped. With proper pretreatment silicone can be either a wire insulation material or a coating on wire insulation materials to provide atomic oxygen durability.

Lewis contact: Dr. Ching-cheh Hung, (216) 433–2302
Headquarters program office: OSAT

FASTMast Flexible Batten Protected Against Atomic Oxygen

A large, deployable truss structure called the folding articulated square truss mast (FASTMast) is used to support and articulate each solar array on space station. FASTMast provides the tensile load on the solar array blanket when deployed and collapses into the mast canister upon array stowage into the blanket box. The flexible batten (fiberglass-epoxy composite) is a structural component that stiffens the FASTMast when deployed and stores mechanical energy when compressed for stowage. Flexible battens, located around the periphery of the mast, are axially loaded at each end and function in an elastically buckled mode at all times. In low Earth orbit (LEO) the epoxy is readily oxidized by the ambient atomic oxygen (AO) environment. Therefore, a CV1144 silicone layer was applied to the composite material to provide environmental protection.

NASA Lewis is evaluating the long-term durability of both silicone-protected and unprotected flexible battens to the AO space environment. Development hardware and composite materials, provided by ACE-Able Engineering Co., were evaluated in ground testing facilities for AO durability and dynamic retraction-deployment cyclic loading representative of expected full-life in-space application. Static deployment loads were used for AO durability testing, and dynamic loads for retraction-deployment cycling.

The flexible battens were exposed to a maximum 15-year anti-solar-facing AO fluence level of 5.4×10^{22} atoms/cm^2 while loaded to a nominal strain level of 0.29%. The total vacuum ultraviolet (VUV) radiation exposure during AO testing, between the wavelengths of 125 to 180 nm, was more than 67,000 VUV equivalent Sun hours. The intensity of VUV radiation within this wavelength range was approximately 150 VUV equivalent Suns. The flexible battens underwent a total of 35 retraction-deployment cycles to a nominal strain level of 1.9%, conducted between AO exposure tests.

Results of the testing indicate that the CV1144 silicone protective coating was oxidized by AO

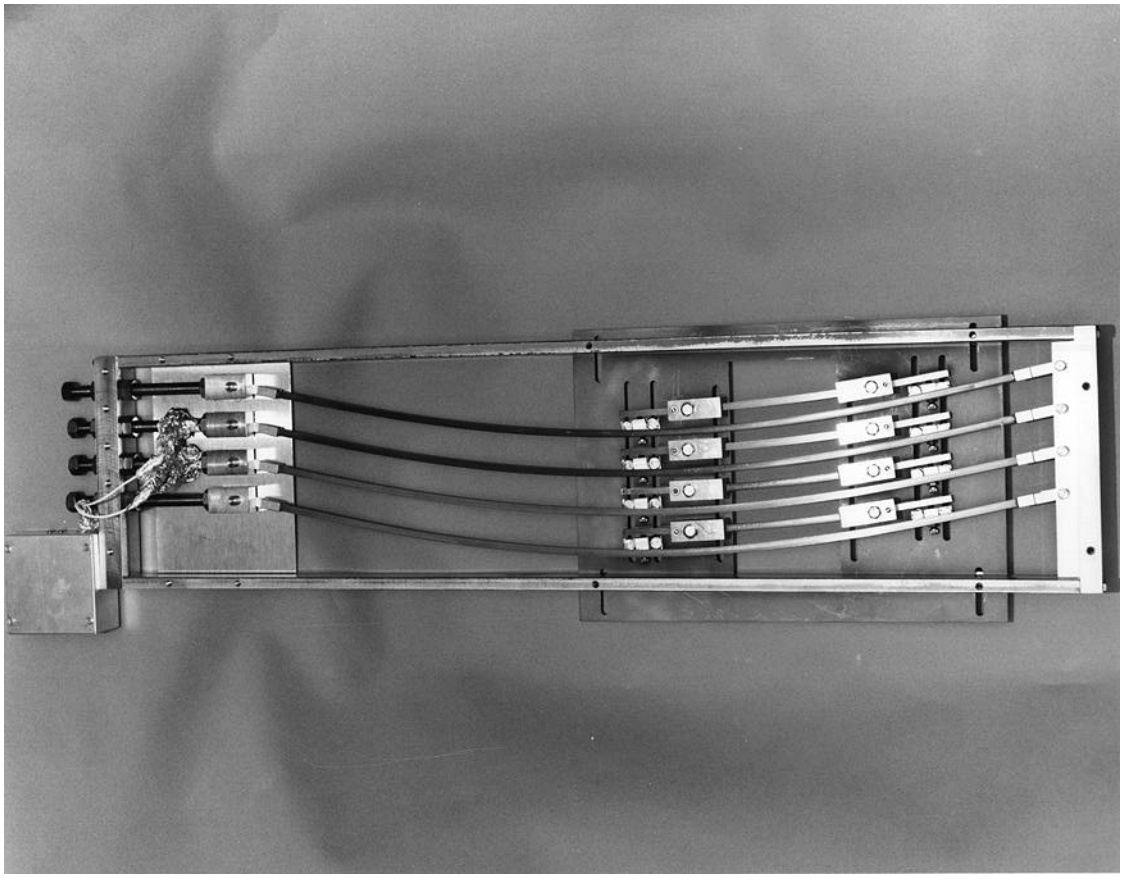

FASTMast fiberglass-epoxy flexible batten samples after atomic oxygen exposure.

reactions to form a brittle glassy (silicon dioxide) skin that formed cracking patterns on all sides of the coated samples. The cracking was observed in both mechanically stressed and nonstressed samples. The oxidized silicone randomly spalled in small localized areas on the flexible battens that underwent retraction-deployment cycling. The CV1144-silicone-coated samples had 19% less per-unit-area mass loss than the uncoated samples. The outer epoxy layer of the uncoated batten samples was completely removed, exposing fiberglass that fractured upon retraction-deployment cycling. The fractured fiberglass could be a source of particulate contamination if unprotected flexible battens were used.

The accompanying photograph shows flexible battens and short-segment batten material after testing. The unprotected flexible battens are light. Some darkening of the silicone, attributed to vacuum ultraviolet radiation, occurred. The CV1144 silicone coating adequately protected against AO degradation of the composite material and contained the fibers, thus maintaining the structural integrity of the flexible batten. Both silicone-coated and uncoated flexible battens maintained load-carrying capabilities for an equivalent 15-year lifetime on space station.

The testing program was completed with the support of Sverdrup Technology and Cleveland State University personnel.

Lewis contacts: Curtis R. Stidham, (216) 433–2299; Sharon K. Rutledge, (216) 433–2219
Headquarters program office: OISSA

Durable, High-Emittance Heat Receiver Surface Developed

NASA Lewis is managing the buildup and testing of a 2-kW Solar Dynamic Ground Test Demonstration (SD GTD) system. The SD GTD will demonstrate the production of solar dynamic power in Lewis' large thermal/vacuum space simulation facility (ref. 1). Haynes 188, a cobalt-based superalloy, will be used to make thermal energy storage containment canisters for the GTD

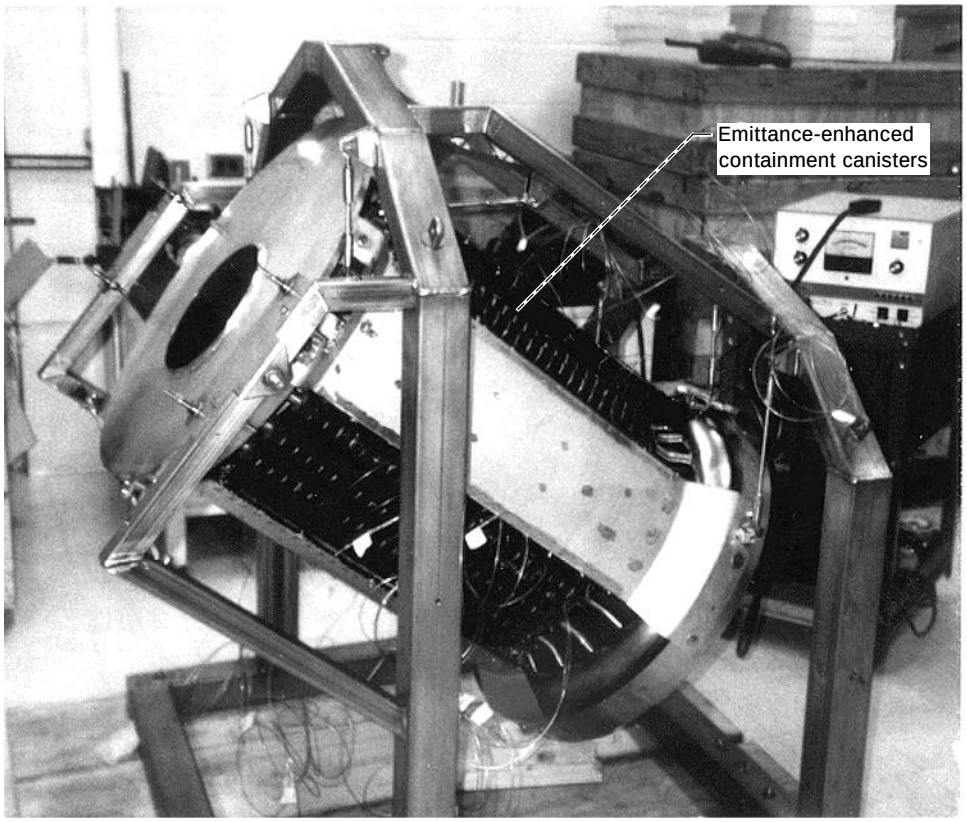

Partially assembled SD GTD heat receiver revealing some emittance-enhanced containment canisters.

receiver interior. Simulated solar energy will transfer through the containment canisters to the system working fluid. Haynes 188 containment canisters with high thermal emittance ε are desired to radiate heat away from local hot spots inside the receiver, improving heat distribution and extending canister service life. The canister surfaces also must be durable in an elevated-temperature, high-vacuum (830 °C, $<10^{-7}$torr) environment for an extended time.

Working with Allied Signal Aerospace, the GTD heat receiver contractor, NASA Lewis developed an extensive emittance enhancement and durability test program to develop a durable, high-emittance surface for solar dynamic receiver applications. Thirty-five Haynes 188 samples were exposed to 14 different surface modification techniques for emittance and vacuum heat treatment (VHT) durability enhancement—arc-texturing, grit blasting followed by air oxidation, physical texturing, and various emittance and/or durability enhancement coatings. Optical properties were obtained for the modified surfaces. Emittance-enhanced samples were vacuum heat treated for as long as 2692 hr at 827 °C and $\leq 10^{-6}$ torr with integral thermal cycling. Optical properties were taken intermittently during exposure and after final VHT exposure. The various surface modification techniques increased the emittance of pristine Haynes 188 (0.11) to 0.28 to 0.86 (ref. 2). Seven of the techniques provided surfaces that meet the SD GTD receiver VHT durability requirement ($\varepsilon \geq 0.70$ after 1000 hr). Two displayed excellent VHT durability (ref. 2): an alumina-based coating ($\varepsilon = 0.85$ after 2695 VHT hr) and a zirconia-based coating ($\varepsilon = 0.86$ after 2024.3 VHT hr). The alumina-based coating was chosen for the SD GTD receiver.

The SD GTD receiver canisters have been treated with the alumina-based emittance enhancement coating, and the receiver is ready for SD GTD testing. Initial testing is scheduled for late 1994 or early 1995. The alumina-based coating is also being used on the GTD parasitic load radiator. Technology from this program will help to ensure successful demonstration of solar dynamic power for space applications and has potential for

application in other systems requiring high-emittance surfaces.

References

1. Shaltens, R.K.; and Boyle, R.V.: Overview of the Solar Dynamic Ground Test Demonstration Program. Proceedings of the 28th Intersociety Energy Conversion Engineering Conference, Vol. 2, 1993, pp. 2.831–2.836.

2. de Groh, K.K.; Roig, D.M.; Burke, C.A.; and Shah, D.R.: Performance and Durability of High Emittance Heat Receiver Surfaces for Solar Dynamic Power Systems. Solar Engineering, Proceedings of the 1994 ASME/JSME/JSES International Solar Energy Conference, 1994, pp. 251–264.

Lewis contact: Kim de Groh, (216) 433–2297
Headquarters program office: OSAT

Retrieved Hubble Space Telescope Materials Analyzed

Solar power systems in low Earth orbit (LEO) will encounter a variety of harsh environmental conditions including atomic oxygen, ultraviolet radiation, thermal cycling, micrometeoroid and debris impact, and self-contamination—each of which can adversely affect performance. Combined effects can be even more detrimental. It is therefore crucial to understand how the space environment affects materials when designing LEO solar power systems. Materials retrieved from the recently serviced Hubble Space Telescope (HST), after 3.6 years in LEO, provide a unique and valuable source of information on long-term, in-space exposure.

The HST servicing mission brought one of the solar arrays and a few other materials back to Earth. Some of these materials are being evaluated for environmental durability by the NASA Goddard Space Flight Center with the help of NASA Lewis. The materials being jointly evaluated include aluminized-Teflon multilayer insulation (MLI) from the magnetic sensing system's electronics boxes, aluminized-Teflon MLI from the solar array's drive arm, and small pieces of the solar array and Kapton solar array cushion material. The MLI from both the drive arm and the two electronics boxes received a range of ultraviolet exposures because of their different orientations with respect to the telescope. For example (ref. 1), the electonics box MLI surfaces

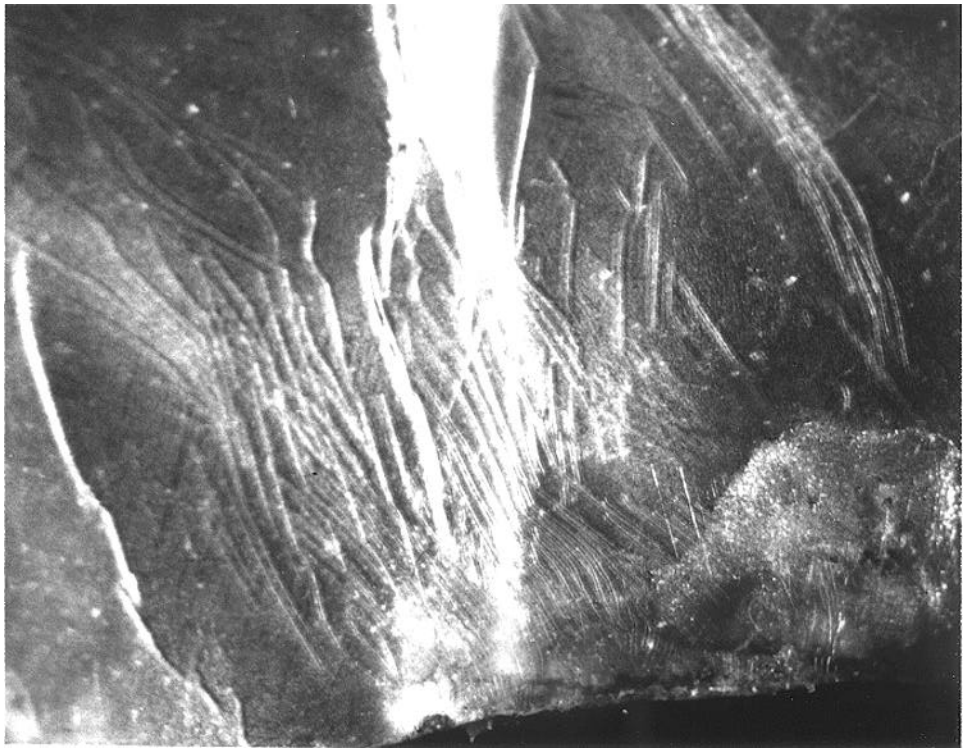

Embrittled Teflon from multilayer insulation on Hubble Space Telescope magnetic sensing system after 3.6 years in low Earth orbit.

had ultraviolet exposures varying from ≃4480 equivalent Sun hours (ESH) (≃0.5 year of direct solar exposure) to ≃16,670 ESH (≃1.9 years of direct solar exposure). The varying degrees of ultraviolet exposure these materials experienced provide a unique opportunity to study LEO solar effects on space materials—particularly to evaluate the rate of ultraviolet degradation.

Visual examination of the returned HST materials revealed signs of material degradation, particularly on solar-facing surfaces. These environmentally induced effects include discoloration, haziness, micrometeoroid or debris impact areas, contamination, and embrittlement of the exterior Teflon. The extent of Teflon embrittlement was unexpectedly high because recent ground testing indicated that Teflon would become only slightly embrittled during a simulated 5-year exposure on HST. Returned HST MLI surfaces that received high ultraviolet exposures have cracks in the Teflon (see photograph on page 101) which extend all the way through in many cases. Teflon embrittlement was not observed on any low-ultraviolet-exposure sides. These analyses show the need for high-fluence, in-space exposures to accurately calibrate ground testing.

The returned materials are being further analyzed at Goddard and Lewis. The results will be compared with changes in materials retrieved during future HST servicing missions. Of particular concern is the potential failure of the Teflon thermal shields placed on the HST bi-stem booms during the first servicing mission to reduce thermally induced jitter. When the solar arrays are rolled up during the next servicing mission, the resulting compression (and expansion upon deployment) of the thermal shields may cause them to tear if severely embrittled—decreasing the shielding capability and possibly producing particle contamination. The analysis of the returned materials will also be used for making ground-to-space correlations to improve the reliability of long-term durability predictions based on ground tests—benefitting the materials selection and durability of other spacecraft.

Reference

1. Hitch, T.L.: MSS Flux Analysis. Jackson and Tull Technical Note JT94–TN008, May 27, 1994.

Lewis contact: Kim de Groh, (216) 433–2297
Headquarters program office: OSS

Paintings Restored Using LEO Environment Simulator

Current techniques for removing varnish and other organic protective coatings from paintings involve contact with the surface. This contact can remove pigment or alter the shape and location of paint on the canvas surface. In addition, smoke-damaged paintings with soot deposits are difficult to restore without further damaging the painting surface. A thermal energy atomic oxygen plasma, developed to simulate the space environment in low Earth orbit, easily removes these organic materials through chemical reaction.

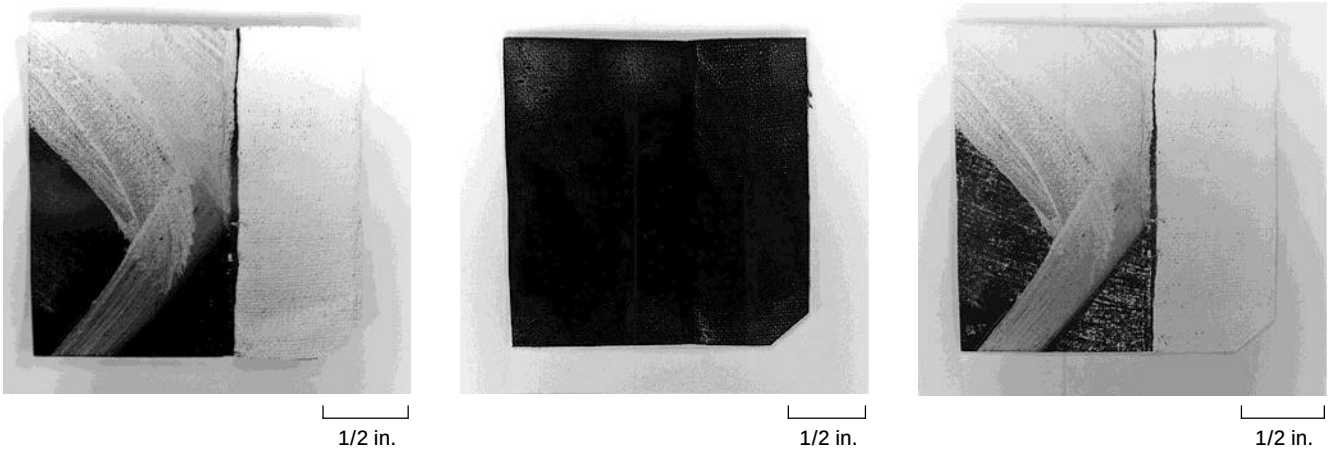

Original painting sample on canvas (left), sample after exposure to smoke (center), smoke-exposed sample after atomic oxygen cleaning (right).

Because atomic oxygen will not react with oxides that are already in their highest oxidation states, some paint pigments will not be affected by the reaction. For paintings containing organic pigments the exposure can be carefully timed so that the removal stops just short of the pigment. Atomic oxygen easily removes varnish from painting surfaces. Paints such as Alizarin Crimson, Prussian Blue, Sap Green, Chromium Oxide Green, Cadmium Yellow Deep, and Ultramarine Blue Synthetic have not shown any great changes in coloration during varnish removal. These colors are considered by conservators to be difficult to maintain during the restoration process. Reapplication of the varnish leaves a surface nearly indistinguishable from the original with reflectance spectroscopy. The process produces a slight microscopic texturing but does not remove or disturb the paint pigment on the surface.

Preliminary tests indicate that this technique can effectively remove smoke and soot from paintings damaged during building fires. NASA Lewis is working with several museums and the Cleveland Fire Department to further quantify and verify the performance of this technique.

Noncontact atomic oxygen cleaning may be a viable alternative to wet chemical cleaning techniques. It is especially attractive in cases where the organic protective surface cannot be acceptably or safely removed by conventional methods.

Lewis contact: Sharon K. Rutledge, (216) 433–2219
Headquarters program office: OTU

Environmental Testing Performed on Satellite Materials

Atomic oxygen is the predominant species in low Earth orbit at altitudes between 180 and 650 km. It is highly chemically reactive and will attack most polymers and some metals used on spacecraft and orbiting satellites. The reaction of atomic oxygen with these materials can form volatile products or nonadherent surface oxides, possibly leading to reduced mechanical and structural properties or undesirable optical and thermal properties. These concerns needed to be addressed for the materials making up the Tropical Rainfall Measurement Mission (TRMM) satellite. TRMM will carry a variety of instruments for studying rainfall and cloud formations in the tropics to gain a better understanding of global weather patterns.

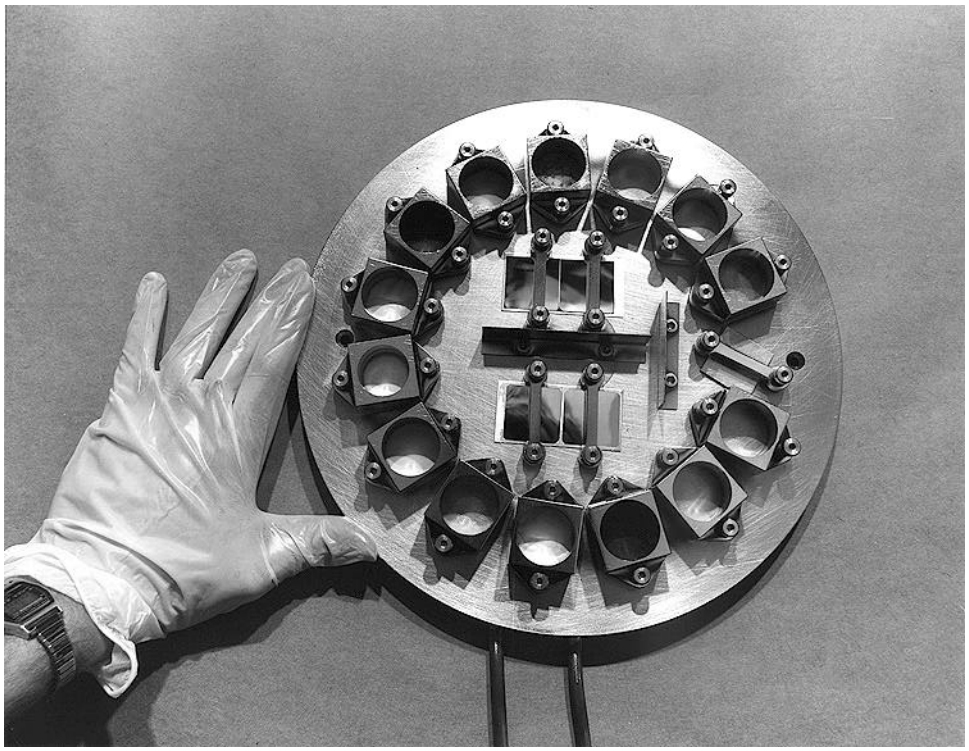

Material coupons to be evaluated for durability to an atomic oxygen environment.

NASA Lewis is using an atomic-oxygen-directed-beam facility, which simulates the space environment on the ground, to perform accelerated environmental testing on TRMM. Feedback is given to NASA Goddard Space Flight Center so that they can make an informed selection of the materials for various satellite components. Test results to date indicate that the thermal blanket material and optical surfaces are durable to the environment but that some silicone-containing materials may be of concern due to cross contamination. Further testing is planned to qualify the thermal blanket material lots that will go into making the thermal blankets for the satellite.

Use of accelerated exposure facilities of this type can greatly aid in more confident selection of materials for spacecraft and satellites.

Lewis contact: Sharon K. Rutledge, (216) 433–2219
Headquarters program office: OTU

Solar Array Connector Tested for Arcing

NASA Lewis has completed mating and demating tests on the space station solar array connector under simulated space conditions. The Solar Array Connector Arcing Test Program assessed the potential risks associated with mating and demating connectors to deadface power, upstream of the beta gimbal, before jettisoning a solar array assembly. Three options have been identified to accomplish this task:

- Demating the solar-array-blanket-box-to-mast-canister connector
- Removing the sequential shunt unit
- Inserting a shorting plug at the mast canister's test port

Test conditions simulated possible on-orbit conditions—low-pressure (neutral) vacuum and oxygen plasma environments—present during expected extravehicular activities.

Test results indicate that, when the array is deployed, the connectors at the blanket box/mast canister interface should be demated or mated in eclipse. If the connectors cannot be separated during eclipse, the array should be feathered before demating. The connectors should not be separated in insolation while the array is solar tracking, because sufficient energy was dissipated in the arcs during tests to cause minor damage on the pins and sockets. However, the connectors remained functionally operational. Demating the connectors proved to be a harsher procedure than mating. Tests at array open-circuit voltages to 320 V indicated no arc breakdown between completely separated connectors.

Charred 56-pin male D-connector after testing.

Results from tests concerning an alternative to deadfacing power indicate that a shorting plug at the mast canister test port can be safely demated or mated by using a high-resistance (100 kΩ) shunt. The sequential shunt unit's input can be either short or open circuited when the shorting plug is inserted. No damage was observed on the connectors used to simulate the test port/shorting plug when this high resistance was used. Installing a variable-impedance shunt, adjusted high for shunt installation across the solar array, and then decreasing the impedance to short the array will isolate the solar array. This procedure also minimizes the amount of energy dissipated in the arc while mating or demating the shorting plug in the test port. Adding a shorting plug, not currently baselined in the space station program, would short circuit the array and allow the sequential shunt unit to be safely maintained without retracting the array. Finally, adding a shorting plug at the test port will allow the secondary connector to be safely demated for array jettison, even during insolation.

All arcing detected during these connector mating and demating tests occurred between a pin and its socket. There was no pin-to-pin or socket-to-socket arcing. Results indicate that all arcing was contained well within the confines of connector shell overlap and that the pins and sockets were within calculated error of actually making contact when the arcing was detected.

The test program was designed and completed by NYMA Inc. support service contractors.

Lewis contact: Dawn L. Emerson, (216) 433–8901
Headquarters program office: OISSA

Thermal Cycling of Solar Dynamic Power System Reflectors Evaluated

Solar dynamic power systems collect solar energy by using specially contoured mirror segments that focus the Sun's energy into the aperture of a heat receiver. Solar dynamic power systems proposed for use in space will utilize triangular mirror facets having a spherical radius of curvature. Maintaining the reflectivity and contour of these facets is important for the efficient operation of the solar dynamic power system. In preparation for the Solar Dynamic Ground Test

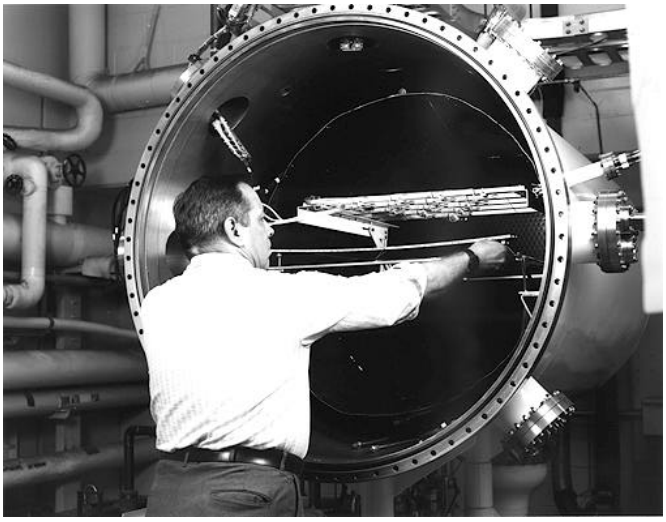

Solar dynamic mirror being installed into thermal vacuum chamber.

Demonstration to be conducted at NASA Lewis, a contractor-supplied facet was tested in a Lewis thermal vacuum facility. Total reflectivity, specular reflectivity, and radius of curvature were evaluated after repeated thermal cycling. Solar Kinetics, Inc., the subcontractor who makes the facets, provided one for thermal cycling. The facet has a 200-in. radius of curvature and is made from an aluminum honeycomb structure bonded between two aluminum facesheets. The reflective side of the facet has a proprietary leveling coating, a reflective aluminum coating, and a protective silicon dioxide coating.

Facet performance was evaluated before and after thermal cycling by several methods. Total reflectivity and specular reflectivity were measured at several random locations across the facet with calibrated reflectometers. Radius of curvature was measured with a coordinate-measuring machine, and slope error was evaluated from the coordinate-measuring machine data. No attempt was made to evaluate thermal distortions during testing. Thermocouples placed at different locations on the facet provided temperature data needed to evaluate thermal gradients in the structure. The facet was heated with an array of fifteen 100-W quartz halogen lamps that provided an intensity of 0.6 Sun. The facet was cooled through radiant heat transfer.

No change was observed in the performance of the facet after three thermal cycles. Its effective emittance was calculated from the thermocouple data. No delamination of the honeycomb structure

was observed. Hence, the thermal vacuum exposure of the production hardware has provided additional confidence in the overall system design.

Lewis contact: Dr. Donald A. Jaworske, (216) 433–2312
Headquarters program office: OSAT

New EMI Shielding Material Flight Tested

Weight savings as high as 80% could be achieved by simply switching from aluminum electromagnetic interference (EMI) shielding covers to covers made from intercalated graphite fiber composites. Because EMI covers typically make up about one-fifth of the power system mass, this switch would result in a power system more than 15% lighter. Intercalated graphite fibers are made by diffusing guest atoms or molecules, such as bromine, between the graphene planes. The resulting bromine-intercalated fibers have mechanical and thermal properties nearly identical to pristine graphite fibers, but their resistivity is lower by a factor of 5, giving them better electrical conductivity than stainless steel and making these composites suitable for EMI shielding.

Although there are intercalation compounds with lower resistivity, bromine is the intercalate of choice because it is stable. Unlike most intercalation compounds, bromine is not affected by water vapor so that its stability under ambient and high-humidity conditions is absolute. In addition, bromine's intercalation compounds are stable in high vacuum and at air temperatures of 200 °C, above the curing temperature of most resins. Although the stability of this material has undergone extensive ground testing, it was only recently flight tested in low Earth orbit, aboard the space shuttle. Six samples were characterized, exposed to the low Earth orbital environment for 40 hr, and then characterized again. The samples included a pristine P–100/epoxy composite, a bromine-intercalated P–100/epoxy composite, a bromine-intercalated P–100/epoxy composite coated with silicon dioxide, and three bromine-intercalated fiber/epoxy composites that were half-coated with silicon dioxide and half not. These last three samples were made with three grades of fiber, P–55, P–75, and P–100 and had copper screens placed over them to trap any bromine that might escape.

The spaceflight results were encouraging. The material reacted no differently than pristine graphite/epoxy composites and could be effectively protected from atomic oxygen attack by using 1000-Å-thick silicon dioxide coatings. There were no changes in the electrical conductivity of the test samples, so the shielding characteristics would not be degraded. In addition to shielding from EMI, these covers must also help to dissipate heat. The reflective ultraviolet-visible spectrum of the protected sample was unaffected by the spaceflight. The emittance of unprotected samples actually increased owing to the development of surface texture. The rate of erosion of the intercalated composites was indistinguishable from that of the pristine composites. These rates were similar to the erosion rates measured for other graphite/epoxy composites. Of particular concern was whether the bromine would leak out of the eroding composites and attack nearby electronics. Copper screens placed over three of the flight samples showed no detectable bromine attack, allaying those fears.

This flight test validated the ground test results, paving the way for utilization of these materials in future spacecraft.

Lewis contact: Dr. James R. Gaier, (216) 982–5075
Headquarters program office: OSAT

Solar Simulator Selected for Solar Dynamic Power System Testing

In 1995 NASA Lewis will conduct the 2-kW Solar Dynamic Ground Test Demonstration (SD GTD) experiment. This test must be conducted in a simulated space environment and will require an artificial Sun. Therefore, Lewis hired the Arnold Engineering Development Center (AEDC) to perform a solar simulator study. In addition, under a grant Cleveland State University's Advanced Manufacturing Center (CSU–AMC) conducted an experimental investigation of an advanced lamp system. NASA Lewis also conducted in-house efforts to support the project and directed the efforts of AEDC and CSU–AMC.

AEDC reviewed the following four existing solar simulator facilities: NASA Johnson Space Center's Chamber A, AEDC's Mark 1 Chamber,

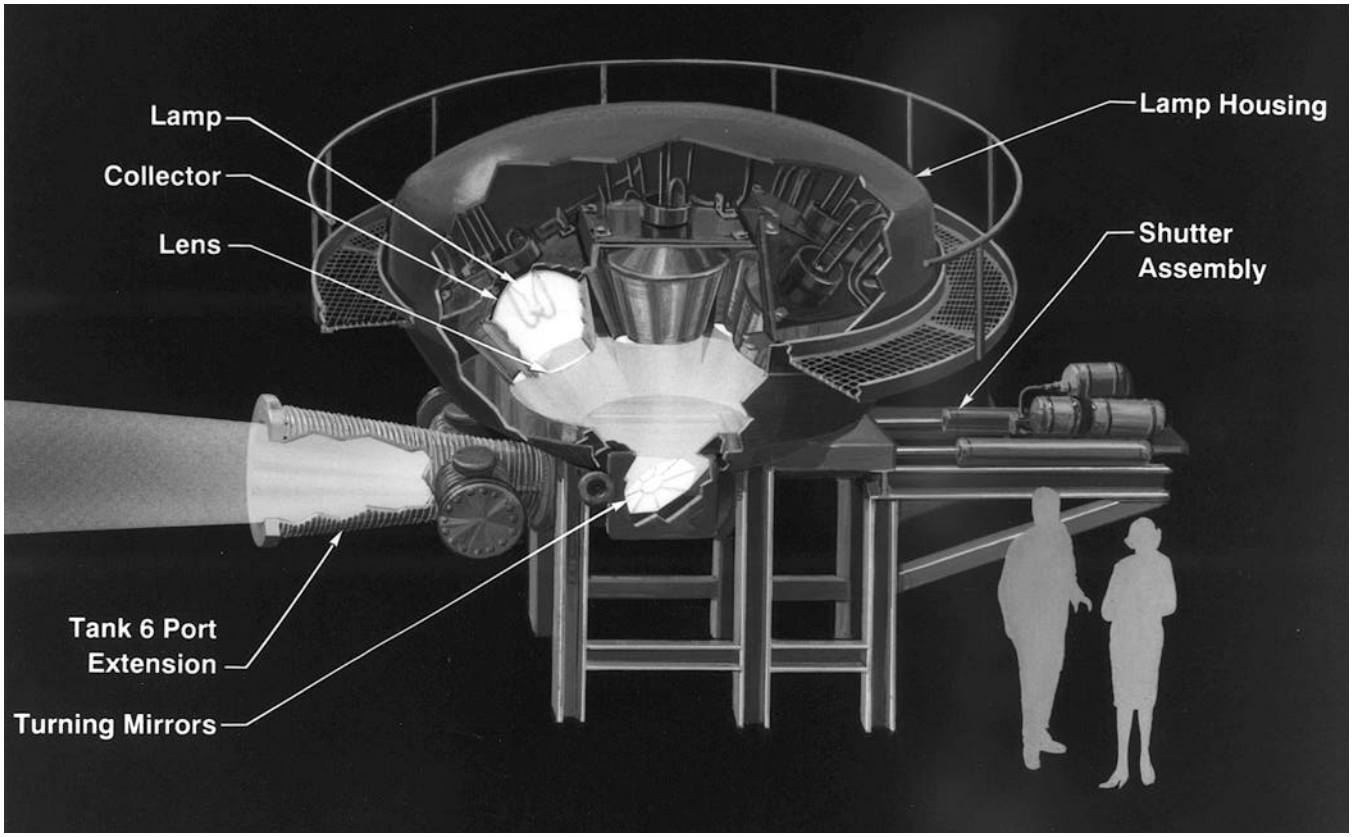

Advanced solar simulator.

NASA Jet Propulsion Laboratory's chamber, and AEDC's 12-V Chamber.

To satisfy system requirements for the SD GTD experiment, the solar simulator must provide a uniform light flux to the solar dynamic concentrator, provide the light within a subtense angle of 1°, and provide an intensity of 1 solar constant (1.37 kW/m^2) at airmass zero. Most solar simulators are designed for supplying heat loads to spacecraft, where a cone angle as large as 3° is acceptable.

CSU–AMC built and tested a scale model of an advanced solar simulator lamp module. They compared the observed magnitude and distribution of radiant power to that predicted by theory and verified the capability of the advanced module to provide the power, uniformity, and subtense angle necessary for the solar dynamic demonstration. They also verified that the parameters of the new design model could scale up to a full-size solar simulator.

As a result of AEDC's study and CSU–AMC's efforts, it was determined that available solar simulator facilities could not satisfy test requirements for the SD GTD and that attempts to duplicate existing facilities at Lewis would result in unacceptable costs and schedule impacts to the program.

The advanced solar simulator selected for solar dynamic system testing represents substantial cost savings—from $5 million for most existing simulators to between $2 million and $3million for the advanced system at Lewis. It will also use about one-half the power, lowering operating costs. This advanced solar simulator concept will advance the state of the art in precision optics and minimize costs associated with the 2-kW SDGTD. In addition to monetary savings, NASA Lewis will have a test facility with the potential for growth that could serve as a test bed for future static and dynamic power systems applications.

The efficiency of the advanced lamp module will

result in a simulator that costs less, requires less facility space, and is more efficient than existing simulators.

Bibliography

Jefferies, K.S.: Solar Simulator for Solar Dynamic Space Power System Testing. Proceedings of ASME International Society of Mechanical Engineers Conference, 1994.

Phipps, W.C.; and Holt, C.K.: Tank 6 Test Facility Solar Simulator Project Plan. Arnold Engineering Development Center, United States Air Force Materiel Command, Aug. 1992.

Pintz, A.; Bierling, R.; and Castle, C.: Uniform Magnification Lamp Module Evaluation. Cleveland State University Advanced Manufacturing Center, AMC–1002, NCC 3–143, Oct. 1992.

Tolbert, C.M.: Selection of Solar Simulator for Solar Dynamic Ground Test. Proceedings of 29th Intersociety Energy Conversion Engineering Conference, 1994.

Lewis contacts: Carol M. Tolbert, (216) 433–6167; RichardK. Shaltens, (216) 433–6138
Headquarters program office: OSAT

2-kW Solar Dynamic Ground Test Demonstration Program Updated

The 2-kW Solar Dynamic Ground Test Demonstration (SD GTD) Program will demonstrate a solar dynamic power system of sufficient scale and fidelity to ensure confidence in the availability of solar dynamic technology for providing continuous electric power in near-Earth orbit. Studies have shown that solar dynamic power with thermal energy storage can save significant life-cycle costs and launch mass relative to conventional photovoltaic power systems with battery storage. Applications include potential space station growth, communications and Earth-observing satellites, and electric propulsion.

The SD GTD program will demonstrate a complete solar dynamic system in a thermal-vacuum environment (i.e., the large space environmental facility, known as Tank 6, at NASA Lewis). An aerospace industry/government team is working together to design, fabricate, assemble, and test the system.

Solar dynamic component technologies have been developed by NASA programs during the past 30 years and are available for near-Earth-orbit

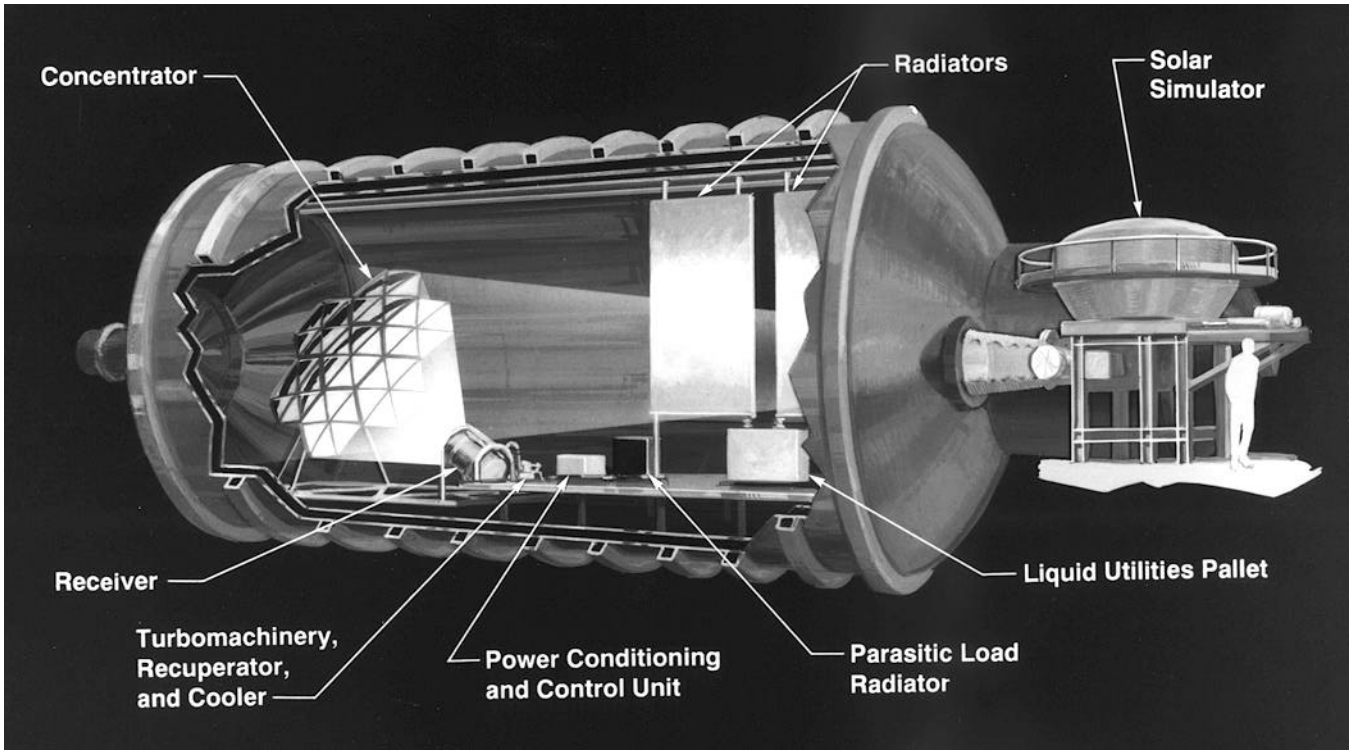

Solar dynamic system in Tank 6.

applications. However, several technical challenges identified during the Space Station *Freedom* Program can be resolved in this ground-based test. These key issues are flux tailoring (integrating the concentrator and receiver), control methodology (investigating methods of varying turboalternator/compressor speed and system management, transient mode performance (evaluating startup and shutdown transients), concentrator facet fabrication and manufacturing techniques, and thermal energy storage canister fabrication and manufacturing techniques.

The Tank 6 facility includes a solar simulator to supply the equivalent of 1 Sun, a liquid-nitrogen-cooled wall operating at 78 K to simulate the heat sink (140 K) provided by the space environment, and an electric load simulator that can dissipate 4kW of electrical power. A shutter is used to simulate various orbits.

The modular design of the solar dynamic system offers the potential for NASA to evaluate advanced subsystems and components at a later date. Flight-typical components are being used wherever possible to demonstrate the availability of these technologies. The major system components are solar simulator, concentrator, receiver, power conditioning and control unit, and turboalternator compressor. The advanced solar simulator gives a 50% improvement in system efficiency, significantly reducing its size and initial cost as well as future operating and maintenance costs. NASA Lewis personnel completed fabrication, assembly, installation, and checkout of the solar simulator integrated with Tank 6 in September 1994. The concentrator is 4.75 m wide by 4.55 m tall and is supported on a tripod. It will reflect and focus the simulated sunlight into the receiver. The receiver both transfers solar energy to the cycle working fluid and stores it for system operation during eclipse. The power conditioning and control unit includes the closed Brayton cycle conversion unit, which consists of the turboalternator compressor (which will produce a maximum of 2.2 kW of electric power), gas coolers, recuperator, ducting, and support structure.

The NASA/industry team is working together to show that we can do it "cheaper, faster, better" by successfully demonstrating dynamic power for space. We will begin testing the solar dynamic system in early 1995. The SD GTD program is ahead of schedule and within budget for completion in 1995.

Bibliography

Shaltens, R. K.; and Boyle, R.V.: Update of the 2 kW Solar Dynamic Ground Test Demonstration Program. NASA TM–106730, 1994.

Lewis contacts: Richard K. Shaltens, (216) 433–6138; Carol M. Tolbert, (216) 433–6167
Headquarters program office: OSAT

Space Electronics

Spacebridge to Moscow Marks Joint U.S./ Russian Venture in Telemedicine

The Telemedicine Spacebridge Demonstration Project began with a brief demonstration of a two-way video link between the International Telemedicine Conference in Bethesda, Maryland, and a television studio in Moscow, Russia, on December 10–11, 1991. This link through NASA Lewis in Cleveland, Ohio, demonstrated the feasibility of such a link for telemedicine applications. This demonstration spawned a project known as the Spacebridge to Moscow, a nine-month operational telemedicine demonstration linking the Central Hospital in Moscow, Russia, with four medical institutions in the United States: the Uniformed Services University of Health Sciences in Bethesda; Fairfax Hospital in Fairfax, Virginia; the University of Texas Medical Center in Houston; and the Latter Day Saints Hospital in Salt Lake City, Utah. The purposes of the Spacebridge included medical consultation, education, and exchange of information that could lead to standardized medical care in space for astronauts and cosmonauts as well as here on Earth.

Using a two-satellite system in a "double hop" configuration with NASA Lewis acting as the gateway facility, the Spacebridge began operation

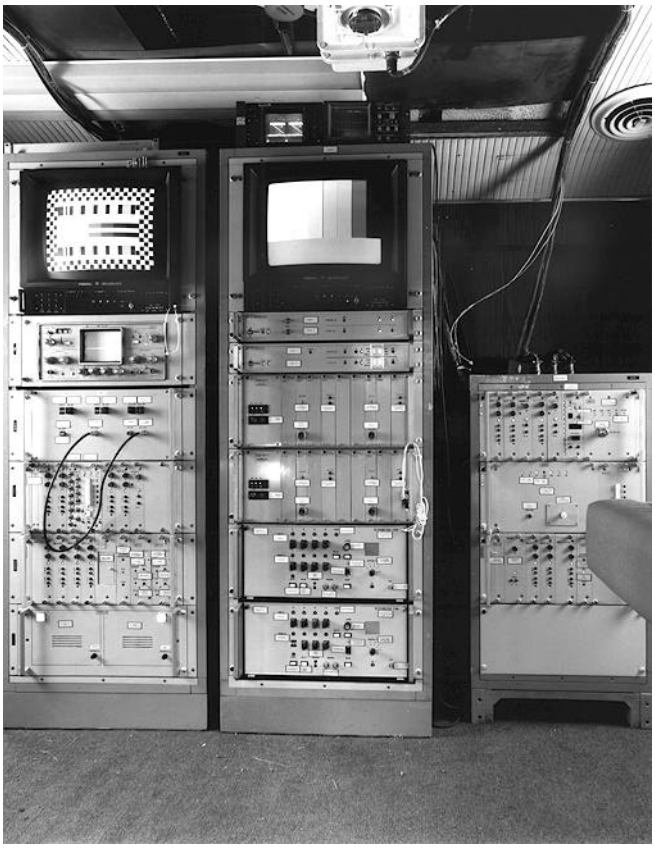

Russian SDRN ground terminal equipment installed in former CTS Bluebird bus.

in September 1993 and completed the last session in June 1994. The Spacebridge used the Russian western Space Data Relay Network (SDRN) satellite positioned in geostationary orbit at 16° west longitude over the Atlantic Ocean for the Moscow-to-Cleveland portion of the link and the domestic commercial communications satellite GTE GStar II for the U.S. portion of the link. The gateway facility in Cleveland comprised two Earth terminals—a domestic Ku-band, 5-m station capable of transmitting and receiving broadcast-quality video, and a special SDRN Earth terminal supplied by the Russians for this project. The four U.S. medical centers took turns hosting different sessions as the U.S. uplink site. The remaining U.S. medical centers participated through terrestrial telephone lines in a teleconference setup while viewing the video transmissions originating in both the United States and Russia.

Two notable highlights of the 16-session demonstration project were the inaugural session originating from the U.S. Senate Hart Building in Washington, D.C., and the emergency trauma sessions held in October 1993. The inaugural session occurred on November 5, 1993, and included a demonstration of teleradiology and telepathology using the Loral-Siemens medical diagnostic imaging support system and an excellent demonstration of the benefits of rural medical consultation from a doctor present at the inaugural site to a small town in West Virginia. A special T1 line between Elkins, West Virginia, and the Senate Hart Building was set up for this purpose.

Another major achievement of the Spacebridge to Moscow was in disaster assistance. The early autumn of 1993 was a tumultuous and chaotic time in the former Soviet Union. During this unrest the storming of the Russian Parliament regrettably resulted in numerous casualties and trauma cases. The Spacebridge link was used on two separate, unscheduled occasions to hold special sessions where many of these trauma cases were addressed.

Bibliography

Zuzek, J.E.; Cauley, M.A.; and Hollansworth, J.E.: The Telemedicine Spacebridge Project—A Joint U.S./Russian Venture in Long Distance Medicine Via Satellite. AIAA Paper 94–1119, Mar. 1994. (Also NASA TM–106523.)

Lewis contact: John E. Zuzek, (216) 433–3469;
Michael A. Cauley, (216) 433–3483
Headquarters program office: OLMSA

Digital Audio Radio Broadcast Systems Tested

Radio history is being made at NASA Lewis with the laboratory testing of a new concept called digital audio radio broadcasting (DARB). This satellite and terrestrial technology will open up new audio broadcasting opportunities both domestically and worldwide. It will improve the quality of amplitude-modulated/frequency-modulated (AM/FM) radio and introduce true over-the-air delivery of compact disc (CD) quality sound.

NASA Lewis is hosting the laboratory testing of seven proposed systems. There is no comparable program in the world to so thoroughly test all known systems. The tests are being conducted by the Electronic Industries Association's Consumer Electronics Group (CEG). Proponents delivered

Testing digital audio radio broadcast systems.

their test systems to Lewis in January 1994. Laboratory tests are scheduled to be completed in late December 1994. Then the systems will be field tested in the San Francisco, California, area.

The laboratory tests have been designed to comprehensively evaluate the technical performance of each system under a variety of impairment conditions. The impairments include noise, simulated mobile multipath, simulated airplane flutter, and cochannel, first-adjacent-channel, and second-adjacent-channel interference. For in-band systems the tests also measure analog-to-digital and digital-to-analog interference.

To test system performance, critical audio segments have been recorded that stress the audio coding used in the systems. These critical segments are played through each system under each impairment condition. Each system's audio output is recorded for various carrier-to-noise ratios at and around the point of failure and the threshold of audibility observed in the laboratory. Each audio sample is subjectively evaluated at the Communications Research Center (CRC) in Ottawa, Ontario, Canada, by an expert listener panel that rates the audio quality in a double-blind setting.

Although ideally suited for precise determination of noise and interference thresholds, laboratory tests cannot adequately measure performance in actual broadcast transmission through a nonlinear, dispersive radio channel. Thus, the CEG test and evaluation program will include extensive field tests planned for February 1995.

With the successful completion of these two tests the United States will be able to establish realistic standards for domestic digital audio radio broadcasting and be a key player in establishing it internationally.

Lewis contact: James E. Hollansworth, (216) 433–3458
Headquarters program office: OSAT

New-Technology Satellites Would Provide T1 and Higher Rate Service

The U.S. communications infrastructure is rapidly advancing. Fiber technology, deregulation, and competition have led to price decreases for traditional services, such as private-line digital T1 (1.5 megabits per second (Mbps)). The signal quality and bandwidth of fiber have also enabled

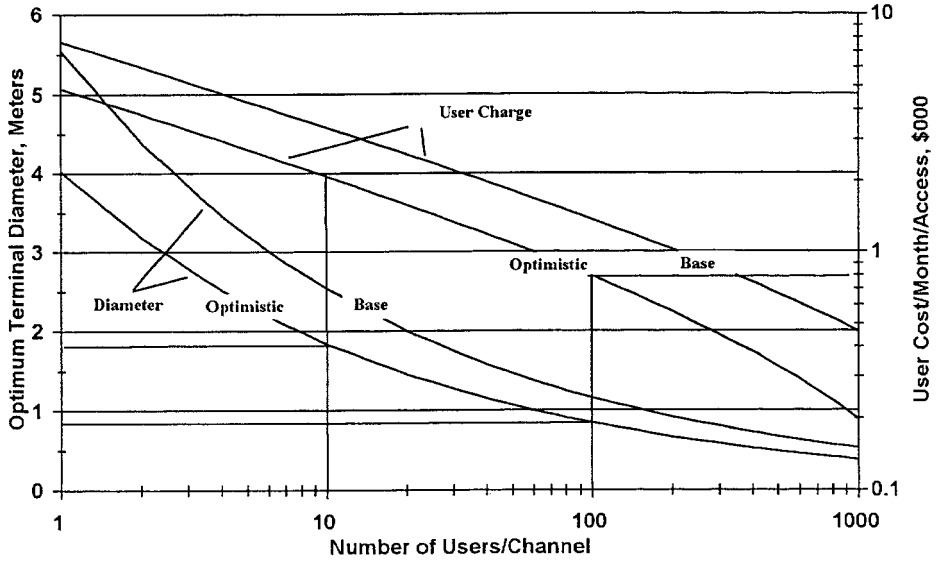

Optimum terminal diameter and user costs as a function of number of users per channel.

new network services, such as frame relay, switched multimegabit data, and asynchronous transport mode. Data rates to 100 Mbps are available nationally. A national information infrastructure, and even a global information infrastructure, may be the end product of these developments and would offer the ultimate in communications services, with bandwidth, flexibility, and affordability available to all. NASA has recently completed an effort to evaluate potential roles for new-technology satellites in this new era.

New-technology satellites appear to be very competitive for shared or switched services. In optimum (minimum service cost) systems very-small-aperture terminals (VSAT's) are used to access a major hub with very bursty data. The major differences are that the satellite plays the role of the hub (performing all message detection and routing) and that maximum user data rates are three to seven times greater than with conventional VSAT's. Because these systems favor bursty traffic, voice and real-time video are excluded as appropriate markets. However, these systems are suitable for multimedia communications, where video clips and sound bites are intermittent. Consequently, the prime application is viewed as multimedia communications within "VSAT-like" networks and is expected to be prevalent with the common use of Microsoft Windows and OS/2 operating systems. Because conventional VSAT technology cannot efficiently process such communications, the new-technology satellites are suggested as an alternative.

Within the accuracy of the study cost modeling, optimization techniques show that for private-line T1 and higher rate services large Earth terminals (4 to 5 m) are required to minimize user cost. The corresponding satellite technology includes multibeam antennas, onboard processing, and advanced bandwidth-efficient modulation techniques. Optimum satellite capacity exceeds 10gigabits per second (Gbps) per spacecraft. Thus, the multibeam antenna serves a dual role of high spectrum reuse as well as closing a link on the wideband services.

On the contrary, for shared services the optimization process indicates that the Earth terminals should be small (0.5 to 2 m) for T1 service. The corresponding satellite technology includes very large (5 to 7 m at Ka band) multibeam antennas for closing the link with the very small terminals. Spectrum reuse is an obvious additional advantage, but these satellites will probably be power limited so that any achieved spectrum reuse would be incidental. As an alternative to the large spacecraft antennas, it is suggested that the optimization process be

altered so as to constrain the minimum Earth terminal size. The resultant user costs triple, but the corresponding spacecraft would be far less risky.

Lewis contact: Grady H. Stevens, (216) 433–3463
Headquarters program office: OSAT

Advanced Traveling-Wave-Tube Circuit Simulated and Designed

A NASA Lewis program has significantly improved the ability to simulate and design traveling-wave-tube (TWT) circuits with computer models. With the implementation of the new three-dimensional, electromagnetic circuit analysis computer model MAFIA (an acronym for Solution of Maxwell's Equations by the Finite Integration Algorithm), TWT designers can accurately obtain radiofrequency (RF) phase shift, beam-RF interaction impedance, and power attenuation characteristics. These characteristics are used as input data for a Lewis-developed, coupled-cavity TWT model that simulates the interaction of an electron beam with a circuit. Together these two models accurately simulate the RF power performance of conventional and advanced TWT circuit designs.

The models are being used to design a new type of ring-plane TWT circuit. The copper circuit consists of a series of beam-circling rings supported by slotted planes. Two vanes stretch the length of the circuit to improve the frequency bandwidth. Simulations show that the new circuit has considerably higher RF power and greater power efficiency than a conventional coupled-cavity TWT circuit without a significant sacrifice in frequency bandwidth.

Bibliography

Connolly, D.; and O'Malley, T.: Computer Program for Analysis of Coupled-Cavity Traveling-Wave Tubes. NASA TN D–8492, 1977.

Kory, C.; and Wilson, J.: Three-Dimensional Simulation of Traveling-Wave Tube Cold-Test Characteristics Using MAFIA. NASA TP in publication, 1995.

Wilson, J.: Revised NASA Axially Symmetric Ring Model for Coupled-Cavity Traveling-Wave Tubes. NASA TP–2675, 1987.

Lewis contact: Dr. Jeffrey D. Wilson, (216) 433–3513
Headquarters program office: OSAT

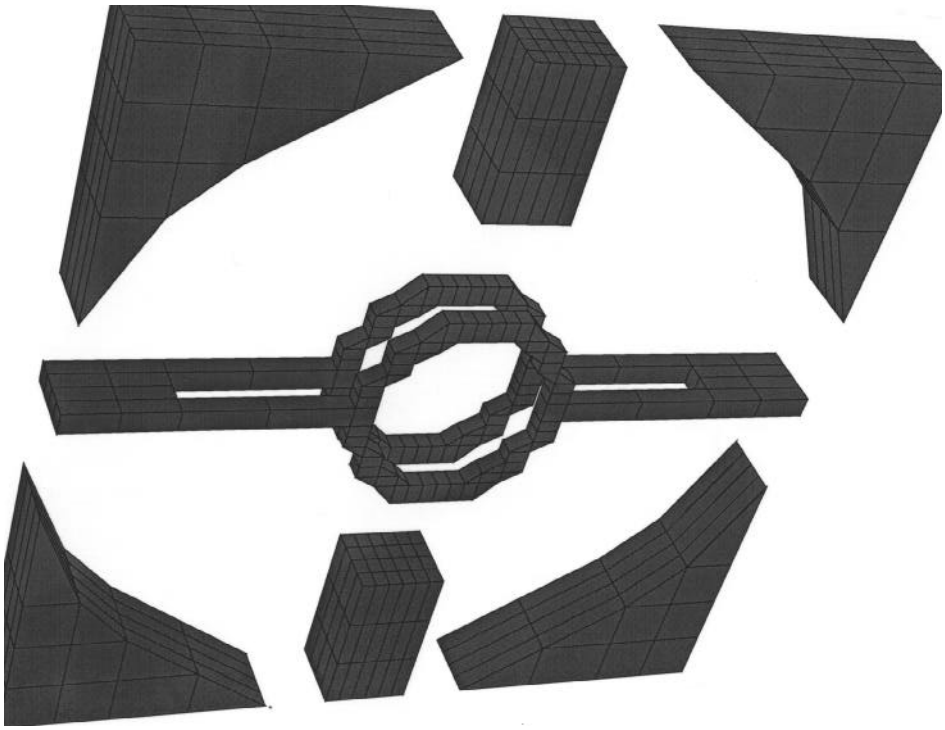

Three-dimensional grid for ring-plane, traveling-wave tube.

Cassini Mission Ka-Band TWTA Developed

A high-efficiency, 10-W, 32-GHz traveling-wave-tube amplifier (TWTA) has been developed and is being space qualified for delivery to the Jet Propulsion Laboratory (JPL). There it will be incorporated into the Ka-band transmitter package for the Cassini mission, planned for launch to Saturn in 1997. A TWTA includes a traveling-wave tube (TWT) and its power supply, an electronic power conditioner. The project, which began at NASA Lewis as a research demonstration of the efficiency enhancement of low-power TWTA's at 32 GHz, became a collaboration between NASA Lewis, Hughes Electron Dynamics Division, and JPL. The goal was to expand the original research demonstration to include delivery of an engineering qualification model TWTA and the flight model TWT's for the Cassini mission. To meet the requirements, the TWTA must produce a minimum of 10 W of radiofrequency output power while the input power to the electronic power conditioner is limited to approximately 30 W. Achieving that unprecedented performance level will enable operation of the Ka-band experiment package on Cassini, which includes a gravity wave experiment.

Designated the Hughes 955H, the TWT has demonstrated an overall saturated efficiency of over 40%. This goal has been reached by including a unique NASA Lewis-supplied dynamic velocity taper (DVT) helix and advanced multistage depressed collector (MDC) designs, along with MDC electrode surface treatment to suppress secondary electron emission, and innovations in mechanical and thermal design and fabrication introduced by Hughes. Specifically, the DVT in the TWT's output section is characterized by a continuous nonlinear reduction in helix pitch from a synchronous value near the output end of the circuit. This results in better synchronization between the circuit wave and the electron bunches in the electron beam than can be realized with a constant-pitch helix. The MDC design procedure defines optimum electrode surface configurations by predicting electron trajectories, taking into account secondarily emitted electrons. Further, the oxygen-free, high-conductivity copper MDC electrode surfaces were treated at NASA Lewis with an ion-bombardment process to produce a robust, highly textured surface with secondary electron emission characteristics sharply lower than those of untreated copper.

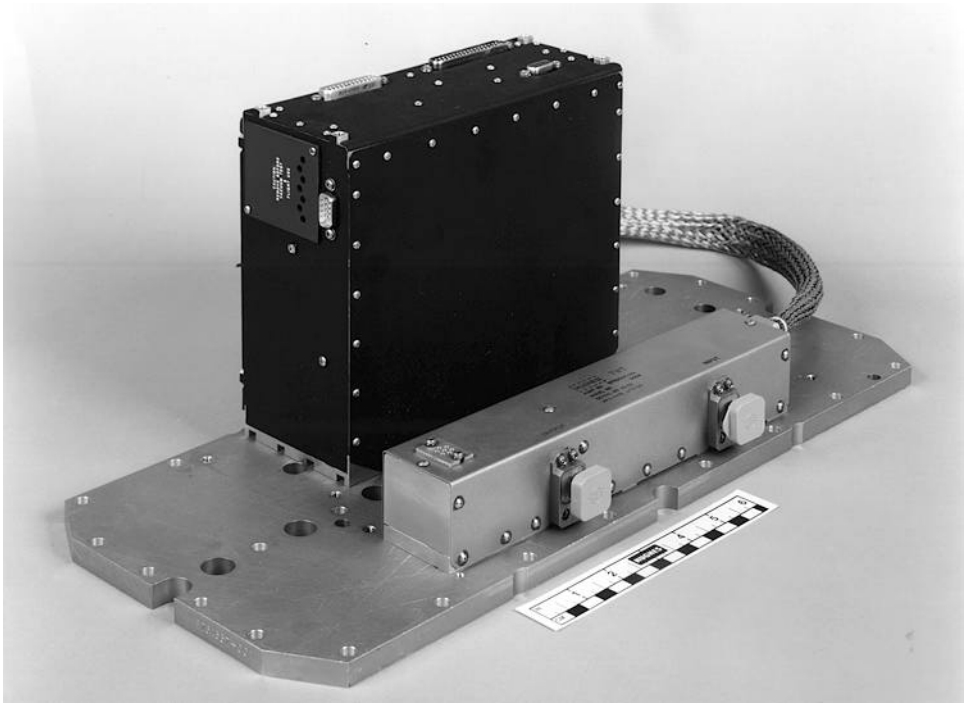

Packaged engineering qualification model Ka-band TWTA for the Cassini mission. The TWT is shown in the foreground. (Courtesy of Hughes Industrial Electronics Co.)

Two flight model TWT's have been fabricated that meet or exceed the Cassini mission requirements, along with engineering models of the TWT and electronic power conditioner. Space qualification testing, including thermal-vacuum, vibration, and pyroshock, is in progress. The mass of the flight-packaged TWT is 750 g and the mass of the EPC is 2.67 kg, for a total TWTA weight of just over 3.4kg. NASA Lewis has managed the contract with Hughes for model development. JPL has specified system requirements.

This TWTA development represents a significant advance in achieving high efficiency for low-power amplifiers at this frequency level. It also demonstrates the value of vacuum electron devices in low-power microwave applications—frequently conceded to solid-state devices in system planning. The production of flight hardware as part of a research effort has reduced overall cost and shortened delivery schedules.

Lewis contact: Arthur N. Curren, (216) 433–3519 (or fax (216) 433–8705)
Headquarters program office: OSAT

Electrical Properties of Heterostructures for Advanced High-Speed Electronics Determined

The semiconductor transistor is the building block of most modern electronic circuits. The two most important electrical parameters of the semiconducting material used to build these transistors are the concentration and mobility of the charge carriers. Both parameters can be measured by a technique based on the Hall effect. In this technique a fixed magnetic field is applied to the semiconducting material, and both the longitudinal and transverse resistances are measured. These two experimental numbers yield the concentration and mobility of the carriers. The quality of the semiconducting material has to be measured before device processing starts, to assure the proper operation of the final circuit.

In the past decade new types of devices have been developed for high-speed electronics, for both digital and analog applications. These devices are based mainly on III–V compound semiconductor heterostructures, but new materials such as silicon-germanium/silicon are now being introduced. The most common device, a modulation doped field-effect transistor (MODFET), includes an active channel layer and several auxiliary layers (i.e., for contacts, barrier, buffer, etc). Carrier mobility is higher in the active channel layer than in any of the other layers. Although predicting proper device operation requires knowing the concentration and mobility of the carriers in the active channel only, the normal Hall effect technique can give only an average of these parameters in all the layers—which can be very different from the active channel values. Therefore, the Hall effect technique cannot be used as a good, quantitative predictor of material quality.

In the work done at NASA Lewis the room-temperature Hall effect technique and analysis were completely revised, without requiring hardware modifications, to obtain the desired active channel parameters. In the new technique the Hall effect measurements are repeated at many values of the magnetic field. The experimental results are the longitudinal and transverse resistances as functions of the magnetic field. As we are interested only in the active channel parameters, we analyze the data in terms of only two layers: the active channel and an average of all other layers, for a total of four parameters. A least-squares fit of all experimental points is used to obtain the value of these four parameters. Special care is needed in this least-squares fit, as the absolute value of the experimental results includes both very large and very small numbers. The results are checked for accuracy by using a much more complex technique that can directly measure the carrier concentration (but not the mobility) in the active channel, called the Shubnikov–de Haas technique. Our results for the carrier concentrations estimated by the two methods agree to better than 15%. Representative results obtained by the new technique for two samples are given in table I. In the table n and μ represent carrier concentration and mobility in units of 10^{12} per square centimeter and square centimeters per volt-second, respectively; the index 1 represents the active channel; the index 2 is associated with the average combined parallel layers; and the index H represents the regular Hall effect results. It is obvious that the Hall effect data are not useful for the active channel description.

TABLE I.—CARRIER CONCENTRATIONS AND MOBILITIES IN MODFET'S

Sample	n_1	n_2	n_H	μ_1	μ_2	μ_H
A	1.09	3.22	2.80	7570	1850	5080
B	.557	4.13	2.92	8080	1810	4060

Lewis contact: Dr. Samuel A. Alterovitz, (216) 433–3517
Headquarters program office: OSAT

Graphical Display Designed for Communications Satellite Test Bed

The Configuration Data Display (CDD) is an interactive, graphical display designed to enable the test engineer to view data in near "real time" as a test is being conducted. The CDD displays data collected from the Advanced Satellite Communications Laboratory test bed. This sophisticated communications satellite simulation test bed produces data on source-to-destination connectivity and bit-error-rate measurements.

The CDD utilizes modern client-server technology and runs in the popular DOS/Windows environment. Windows Dynamic Data Exchange is used to transfer data between the client and server modules. This graphical display was developed by using an off-the-shelf graphical user interface development package and object-oriented programming techniques.

The CDD consists of a main display window containing buttons representing the test bed components. The test bed is designed to accommodate three Earth terminals, each of which includes three data sources and three data destinations. Clicking on a button in the main display window calls up a secondary window that displays more detailed information about specific components. This information includes data type, data rate, data destination, bit error rates, block diagrams, status, signal power levels, and the signal-to-noise ratio.

The CDD provides the engineer with an easy-to-use, real-time, graphical display of data collected from tests varying from component characterization to networking experiments.

Lewis contact: Elaine S. Daugherty, (216) 433–3456
Headquarters program office: OSAT

Real-Time Compression of Digital Video Achieved

A digital video compression algorithm was developed to process eight-bit samples of composite color National Television Systems Committee (NTSC) video signals taken at four times the color subcarrier frequency. After compression the amount of digital data required for video transmission is reduced by over 75% without noticeable degradation in picture quality.

The algorithm is based on differential pulse-code modulation (DPCM), a predictive compression technique where the anticipated value (prediction) of an incoming pixel is subtracted from the actual value. This difference is then assigned to a level from a limited set of quantization groups. For this implementation all predictions of an incoming pixel are done on an intrafield basis to eliminate motion degradation and minimize the complexity of the processing circuits.

To improve on DPCM, the compression algorithm additionally uses a nonuniform quantizer, a nonadaptive predictor, and a multilevel Huffman coder. The nonuniform quantizer improves resolution of the reconstructed video, the nonadaptive predictor increases edge preservation, and the multilevel Huffman coder provides additional data rate reduction.

Several issues must be resolved to transmit Huffman-coded digital video over a constant-rate serial channel. Two such issues are rate conversion (from variable to a fixed rate) and recovery from communication errors. An intelligent data rate buffer was implemented to perform the rate conversion while also efficiently storing the compressed data and guarding against memory underflow and overflow. An error concealment circuit was implemented to allow the decoder to mask and gracefully recover from bit errors.

A real-time system has been developed to implement the enhanced DPCM video compression algorithm. The hardware reduces the digital video information from 114 Mbps to 26Mbps ($\simeq$1.8 bits per pixel). Quality of the reconstructed video is excellent with no motion degradation.

Lewis contact: Thomas P. Bizon, (216) 433–8121
Headquarters program office: OSAT

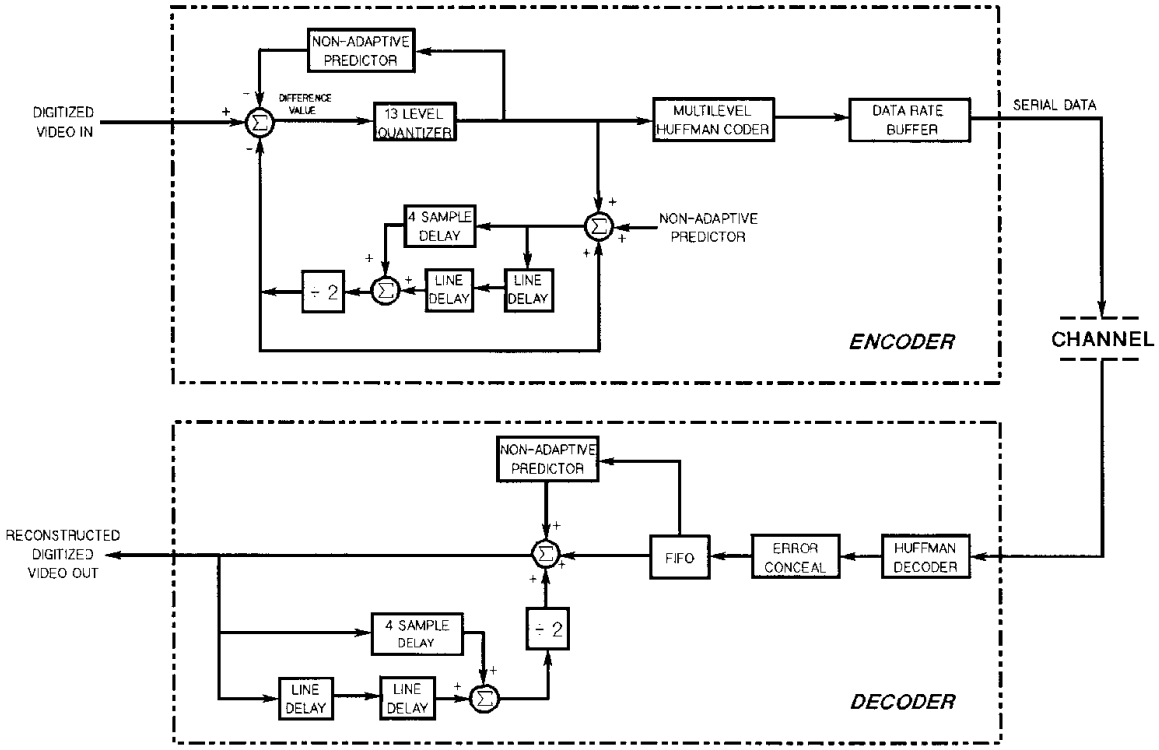

Enhanced DPCM video compression algorithm.

Shared-Memory-per-Beam Architecture and Simulation Completed

NASA Lewis has been developing a multichannel-communications, signal-processing satellite (MCSPS) architecture as part of a flexible, low-cost, meshed very-small-aperture network (ref. 1). The information switching processor (ISP), the heart of the system, has been developed and simulated in-house by using very high-speed, integrated-circuit hardware description language (VHDL).

This ISP design is based on a shared-memory-per-beam approach (ref. 2). The architecture has three major subsystems: the input module, the control module, and the shared-memory module. In addition, a test bench has been added to simplify packet generation.

The input module enables the correct destination dwell first-in–first-out memory (FIFO), depending on point-to-point or multicast (point to multipoint) connection. Although true multicast is allowed at a beam level, the switch performs only broadcast (all dwells) at a dwell level (ref. 1).

The control module synchronizes the system by generating subpacket, subframe, and frame clocks for both the uplink and downlink. It also monitors and controls the dwell FIFO's, the address control memories, the address-pool FIFO, and the shared random-access memory.

The shared-memory module stores the uplink data and transmits them back to the ground. It also performs temporal switching by writing sequentially and reading randomly the address control memories. A multicast signal is created to prevent multicast packets' addresses from being written back prematurely into the address-pool FIFO.

The ISP test bench consists of a subpacket generator module. This module creates subpackets that are easily traced, by filling their fields with numbers representing the frame, subframe, subpacket, source, and destination. In this way we can easily verify proper operation of the architecture. When an error is detected in the received data, these self-identifiable subpackets can lead us to the potential problem. In total, 69 downlink subpackets of the available 80 are used in this example, with dwell usage ranging from 60 to 100%.

During the process of simulating the architecture, we made several modifications to the original

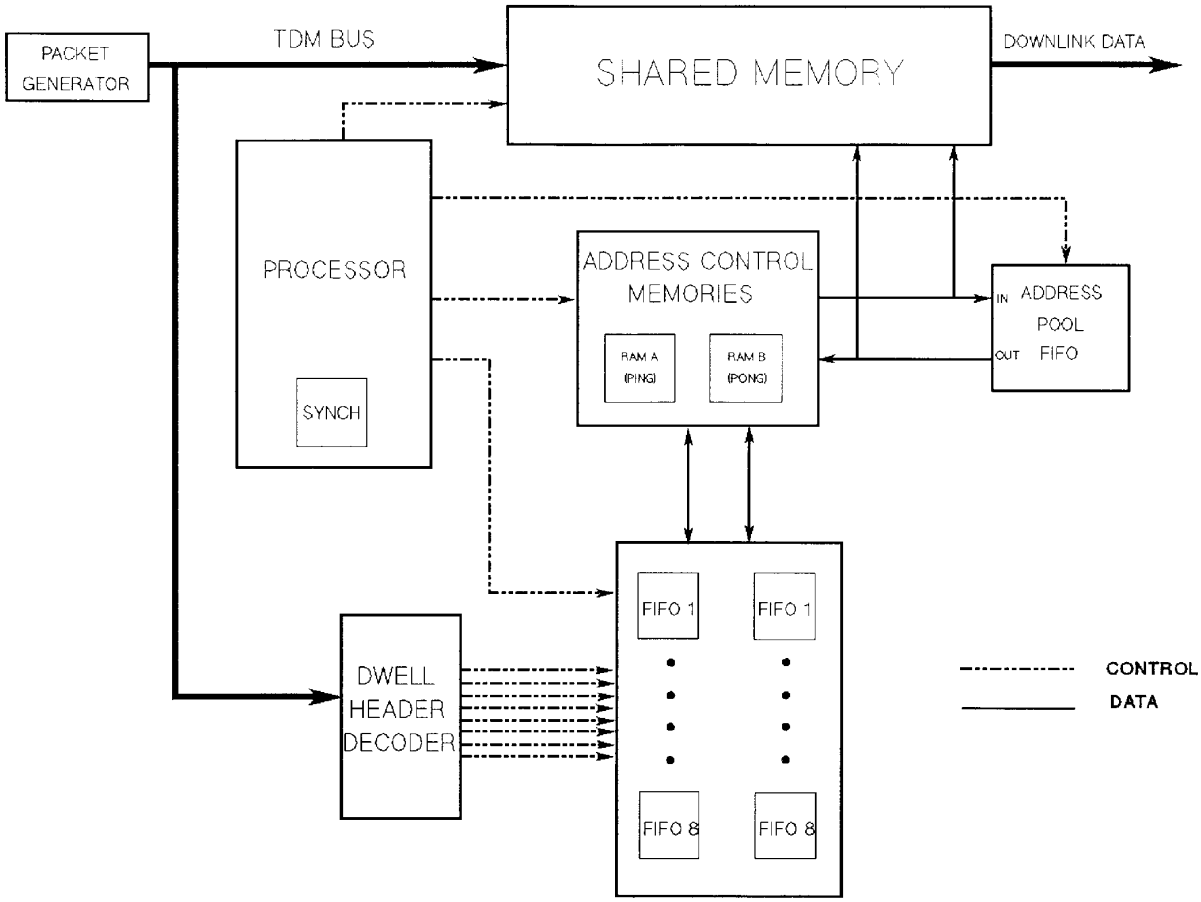

Shared-memory-per-beam architecture.

concept. The bus width was reconfigured to be 32bits to comply with existing digital electronic speeds and memory access times. For simulation purposes only, the uplink frame was reduced to 256 subpackets of data per subframe (instead of 8192) as it seemed impractical to simulate and verify so many subpackets. This resulted in the proportional scaling back of the downlink frame to 80 subpackets per subframe. This scaled-back system configuration greatly reduced the amount of central processing unit time needed to simulate and debug the architecture.

The shared-memory-per-beam architecture has been simulated successfully by using VHDL. This approach allows the designer to test for multiple configurations and eases the debugging process by increasing the system's flexibility. This successful simulation greatly diminishes the probability of errors when testing and debugging hardware. If errors occur, the code is easily modified and all the programmable logic reprogrammed. This flexibility results in a faster and more efficient implementation of the design.

References

1. Ivancic, W.D.; Shalkhauser, M.J.; and Quintana, J.A.: A Network Architecture for a Geostationary Communications Satellite. IEEE Communications Magazine, July 1994.

2. Shalkhauser, M.J.; Quintana, J.A.; and Soni, N.J.: Fault Tolerant Onboard Packet Switch Architecture for Communications Satellites: Shared Memory Per Beam Approach. AIAA Paper 94–1101, Feb. 1994. (Also NASA TM–106397.)

Lewis contact: Jorge A. Quintana, (216) 433–6519
Headquarters program office: OSAT

Aerospace Technology Facilities

NASA's Largest Cryoshroud Installed in World's Largest Vacuum Chamber

An 80-ft-long by 40-ft-wide by 23-ft-high cryoshroud was installed inside the Space Power Facility (SPF) to support space station thermal vacuum testing. The Space Station Program required a facility where the thermal conditions of space could be duplicated for three ground tests:

- Deployment of the photovoltaic module radiator
- Deployment of the thermal control system radiator
- Mission simulation test of the photovoltaic module

The cryoshroud simulates the radiative coldness of space by surrounding a test article (75ft ×

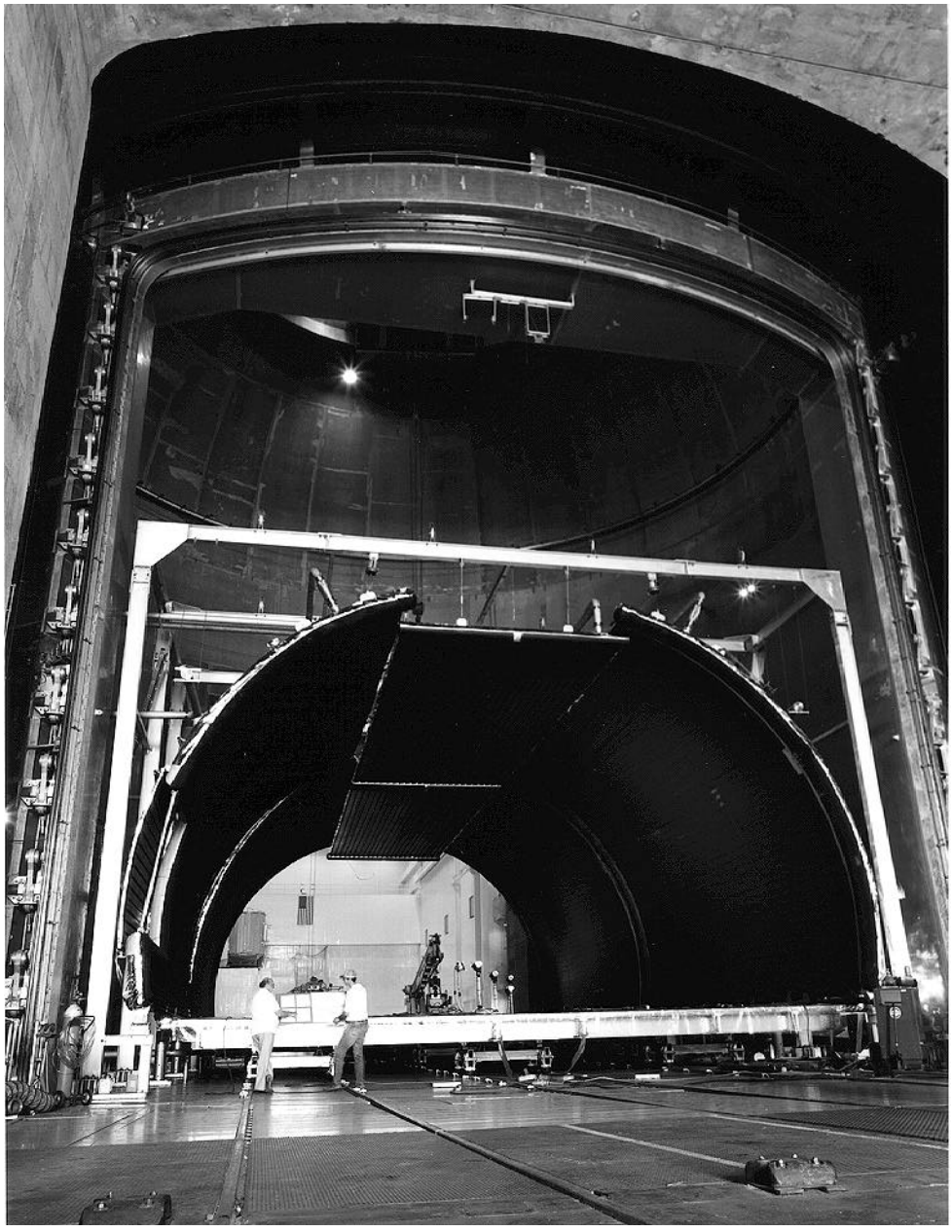

Cryoshroud for thermal vacuum testing at SPF.

15ft) with black-painted cold panels chilled by flowing –250 °F gaseous nitrogen through tubes attached to them.

The Space Power Facility at Plum Brook Station near Sandusky, Ohio, contains the largest vacuum chamber in the world—a 100-ft diameter by 75-ft-high cylinder topped by a 50-ft hemispherical dome (125-ft centerline height). SPF simulates a space environment over a wide range of thermal and vacuum conditions to test advanced propulsion and space power systems. SPF was chosen for these space station tests because of its unique size. No other vacuum chamber has the 75-ft-long by 35-ft-wide floor area required for the space station tests.

The cryoshroud was successfully operated during a series of checkout tests in August 1994. Its primary requirement was to produce a uniform cold soak temperature below –200 °F to approximate the cold sink temperatures of low Earth orbit. During the test 97% of all the thermocouples produced readouts below –230 °F and all the thermocouples read below –220 °F, exceeding the requirements.

The unique qualities of the cryoshroud include

- Its physical size of 80 ft long by 40 ft wide by 23 ft high. No cryoshroud is as long and still has the same width.
- A cold floor that can move on rail tracks in and out of the chamber—allowing test article and support hardware buildup outside the chamber, where large cranes are available
- The ability to provide a uniform soak temperature ranging from –230 to 85 °F
- The ability to be removed or reinstalled, depending on the thermal requirements of individual test programs. Setup time is estimated to be 4 weeks, and removal and storage takes 2 weeks.
- Ten individually controlled zones where coolant flow rate can be adjusted to produce a more uniform cold soak condition

The cryoshroud was provided by Process Systems International, Inc., of Westborough, Massachusetts.

Lewis contact: Henry J. Speier, (216) 977–7420
Headquarters program office: OSF

Space Flight Systems

Space Experiments

Soot Volume Fraction Determined by Laser-Induced Incandescence

Soot emission from flames and fires is a primary source of unwanted pollution. But it is also a product from some manufacturing industries and is necessary to enhance performance efficiency in furnaces. A fundamental understanding of the processes leading to soot particle formation, growth, and oxidation is needed to develop methods for predicting and controlling these combustion processes. Laser-induced incandescence (LII), a new, two-dimensional imaging diagnostic for the measurement of soot volume fraction, provides unparalleled temporal and spatial resolution and insight into soot formation and oxidation processes.

Laser-induced incandescence uses pulsed laser excitation to heat soot to far greater temperatures than the flame and exploits the resultant emission. The laser light is directed through the flame in a line or sheet. The LII signal is then collected and sent to a monochromator or camera for detection and analysis. LII achieves high temporal resolution by obtaining a signal induced by a single laser pulse. The temperature of a soot particle rapidly rises to its vaporization temperature, roughly 4000 K, for high laser intensities. The particle thermal emission at these elevated temperatures increases and shifts to the blue, in contrast to the non-laser-heated soot and flame gases.

The LII signal is linearly proportional to, and may be interpreted as a relative measure of, soot volume fraction. The technique can be absolutely calibrated by in-situ comparison of the LII signal to a system with a known soot volume fraction. Point measurements are easily made by using a photomultiplier tube. One- and two-dimensional imaging measurements can be made with a gated, intensified array camera.

Knowledge of the soot volume fraction and its spatial distribution is central to understanding several types of combustion phenomena. Formation of a soot shell around isolated burning droplets controls the radiative heat transfer from the flame back to the droplet and controls the burning rate. The small spatial scale and transient nature of droplet combustion impede measurement of soot volume fraction by traditional techniques. Although gas-jet diffusion flames may be steady state, LII measures soot volume fraction independently of contributions from scattering by soot aggregates and absorption by polycyclic aromatic hydrocarbons. LII can measure soot in turbulent combustion, as measurements can be collected with a single laser pulse. LII possesses geometric versatility not available in traditional line-of-sight techniques.

Since its initiation in 1994 we have characterized the spectral and temporal nature of the LII signal and excitation wavelength dependencies and demonstrated linearity between the LII signal and soot volume fraction. The next effort is to complete the technique verification by examining photochemical interferences and the effects of soot aggregate composition and size on the LII signal and by establishing the technique on a quantitative basis. Future work includes laboratory and reduced-gravity demonstrations.

Lewis contact: Karen J. Weiland, (216) 433–3623
Headquarters program office: OLMSA

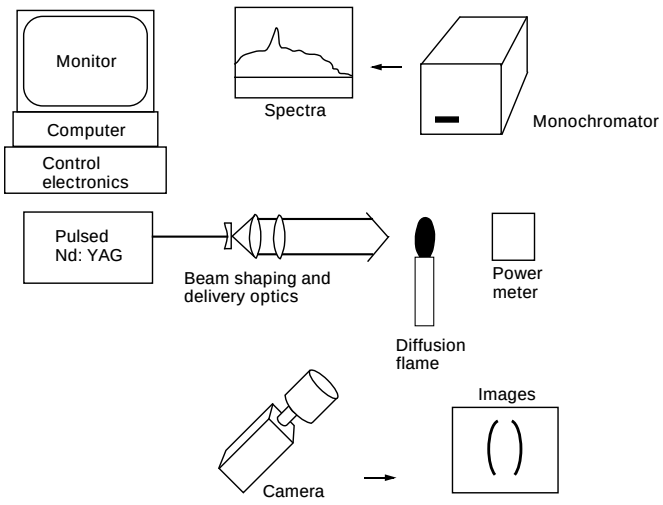

Experimental schematic of laser-induced incandescence for point and imaging configurations.

Excitable Dynamics Studied in High-Lewis-Number Premixed Gas Combustion

Scientists at NASA Lewis are investigating a combustion experiment that may help prove the long-standing diffusive-thermal theory which suggests flames will develop instabilities under certain conditions. We are using a special high-speed intensified camera that captures 1000 pictures per second to see this effect. This experiment studies a new gas-phase chemical system, the combustion of premixed gaseous reactants. It will help us understand how flames behave on Earth and in space (microgravity) and will improve our fundamental understanding of heat and mass transport in chemical reactions. It may also enlarge our understanding of solid fuel combustion for fire safety research.

Interestingly, the patterns formed by these flames are similar to those that occur in the formation of galaxies, the electrical patterns formed around the heart when it beats, the solitary pulses that travel along nerve fibers, and the patterns and spots on animals. It is thought that such a system may even give a hint to the origin of life. This similarity came as quite a surprise since, at first glance, these systems are remarkably different, yet after careful consideration we realized that they all involve some sort of diffusional process (thermal, molecular, and/or electrical) and a chemical reaction.

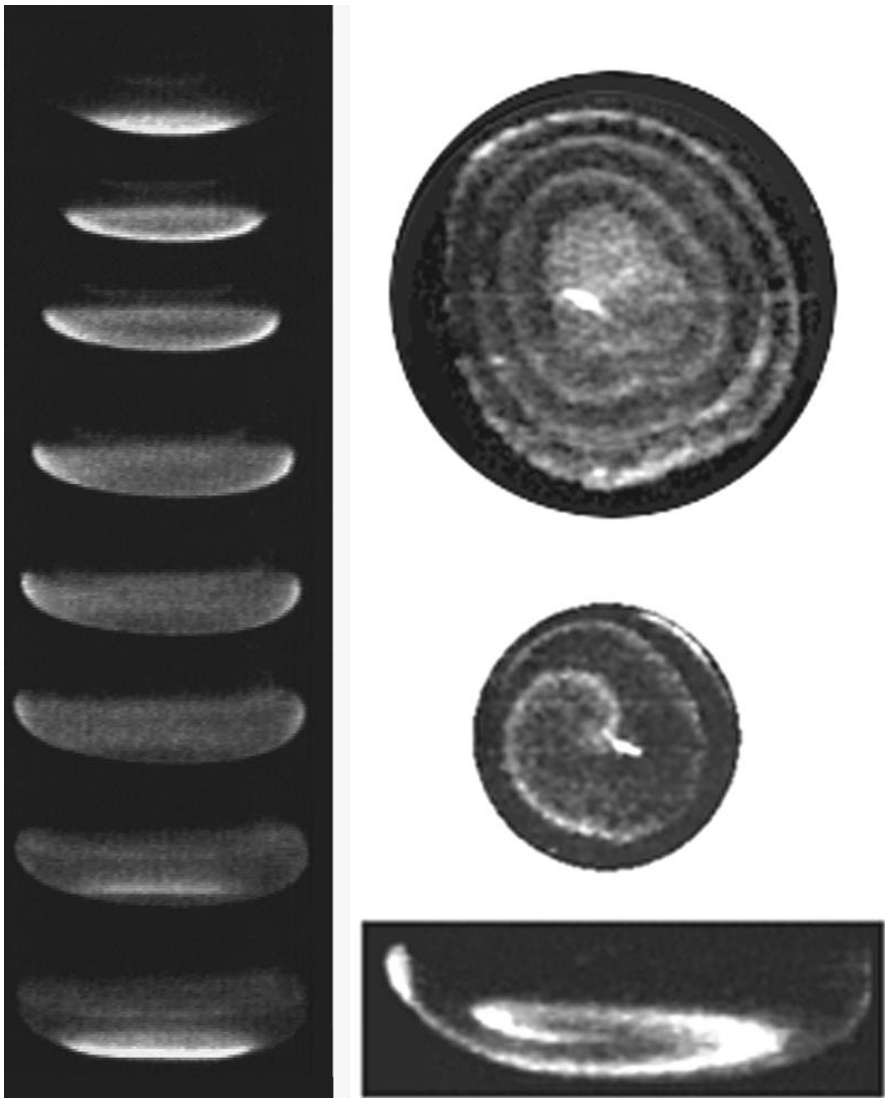

(Left) Axial view of propagating radial pulsation as flame propagates through tube. (Right top) Radial view of first four frames. Time between consecutive images, 1/500th sec. (Right bottom) Axial and radial views of rotating spiral wave.

This premixed gas system—a lean mixture of butane and oxygen diluted with helium—is characterized by a high Lewis (Le) number, where Le is a relative measure of the rate at which heat liberated by the flame preheats the reactants versus the rate at which the stoichiometrically deficient component in the mixture diffuses into the flame by its own molecular Brownian motion.

In this mixture the flame propagates in one of two possible intrinsically unstable modes: it pulsates or it pulsates and spins. The first mode, termed radial pulsation, consists of a single, centrally located pacemaker site (bright spot in the middle), which propagates radially outward as its luminosity monotonically decreases. When the flame approaches the tube wall, it extinguishes, another pacemaker site appears at (or near) the center of the tube, and the cycle repeats. In contrast, the spinning (traveling wave) instability assumes the form of a rotating spiral wave that winds its way through the tube as the flame consumes the reactants.

Researchers believe that these instabilities are caused by a sufficiently large imbalance between the rate at which the flame can heat (energize) the reactants and begin their chemical conversion to products versus the rate at which the stoichiometrically deficient component (governing the reaction rate) can diffuse into the flame. Presently, experimental studies are attempting to isolate the role of chemical kinetics from diffusive transport (i.e., Le-number effects). This is inherently fundamental to our understanding of transport phenomena in the presence of chemical reaction and the stability of premixed flames.

Lewis contact: Dr. Howard Ross, (216) 433–2562
Headquarters program office: OLMSA

Spacelab Facility Shows Migration and Interactions of Bubbles and Droplets

The bubble droplet particle unit (BDPU) was built by the European Space Agency's (ESA) Technology Center in Noordwijk, Netherlands. This Spacelab-based multiuser facility flew for the first time in July 1994 on International Microgravity Laboratory 2 (IML–2). Primarily designed to conduct fluid physics experiments in transparent fluids, it performed experiments having both European and U.S. principal investigators. The experiment of Dr. R.S. Subramanian of Clarkson University in Potsdam, New York, illustrates the facility's capabilities.

Dr. Subramanian's experiment, Thermocapillary Migrations and Interactions of Bubbles and Drops, studies the bubble's (or droplet's) velocities and shapes as it travels (or migrates) through another fluid medium having a linear temperature distribution. Local temperature gradients around the bubble impose a surface tension gradient on the bubble interface and produce motion in the film. This motion is typically from the bubble's hot side to its cold side, causing a jetting action that propels the bubble toward the relatively hotter areas of the surrounding fluid.

This type of science can only be done in low gravity, which can isolate the thermocapillary effects from the dominant effects of buoyancy and natural convection always present in normal gravity (1 g). The results have applications in ceramic and glass formation, as well as in metal and alloy solidification, on Earth. Better understanding of these thermocapillary effects can lead to superior bubble management techniques for crew life support processes required in the exploration of space.

This facility was designed and constructed under ESA Technology Center management by various Italian, German, and Belgian contractors (amongothers). NASA Lewis' function was to assist with the two U.S. BDPU experiments—of Dr. Subramanian (described above) and Dr. J.N. Koster of the University of Colorado, Boulder, in design and ground testing and during conduct of the flight experiment. The facility comprises various modules. The service and power modules provide computer and power control, respectively. But the backbone of the experiment is contained in the basic experiment module, an optics bench surrounding the specific test container. Only the test container is changed out between experiments.

The facility and test container hardware for this experiment performed very well. Overall, the total

number of bubble and droplet migrations for the Subramanian experiments performed in separate test containers exceeded his expectations, and the video data were also considered excellent.

Lewis contact: Myron E. Hill, (216) 433–5279
Headquarters program office: OLMSA

Combustion Module 1 Chamber Mockup Proves Multiuser Concept

The combustion module 1 (CM–1) is being developed to accommodate microgravity combustion experiments designed to help explain and predict the behavior of combustion processes. CM–1 is planned for flight in the Microgravity Science Laboratory 1 (MSL–1) Spacelab module and will accommodate two principal investigators' experiments. CM–1's modular, investigation-unique hardware will be installed and changed out by astronauts on-orbit. To prove the feasibility of this modular concept, a mockup of the combustion chamber and the investigation-unique inserts, called experiment mounting structures, was built.

Although both CM–1 principal investigators are studying combustion processes, their investigations are quite different. Professor Paul D. Ronney of the University of Southern California will examine structures of flame balls at low Lewis numbers (SOFBALL) in which a variety of fuel-lean gaseous mixtures fill the combustion chamber and are ignited. Professor Gerard M. Faeth of the University of Michigan will investigate laminar soot processes (LSP) by studying the key properties of burning gas jets of fuel, employing different fuels and nozzle sizes. CM–1 was challenged to meet the needs of these broadly different investigations and to plan ahead to the space station era, where the same concept will be employed for a multitude of investigations.

A chamber mockup and two experiment mounting structure mockups were fabricated in-house. The chamber mockup was constructed of clear Plexiglass to enable visualization. Other components, such as the power, fuel, and data connectors, were chosen to give realistic flight-like operation. Of critical importance for mission success and safety considerations, each make/break connection and seal has to be tight when reassembled.

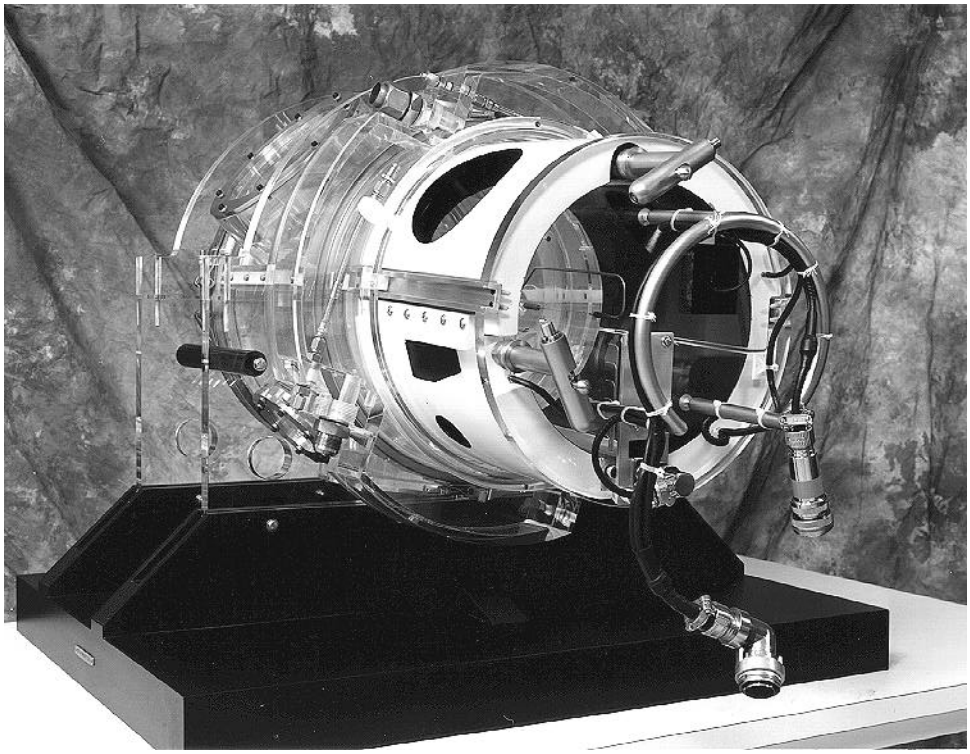

CM–1 chamber mockup with SOFBALL experiment mounting structures pulled out.

The completed mockups illustrated both nominal and off-nominal operations and design feasibility. The engineers who designed the hardware were able to check out the form, fit, and function of many components. Several changes were made to improve the design, which was then critiqued by personnel knowledgeable in crew operations, including NASA Marshall Space Flight Center Spacelab Integration, leading to more design refinement. Next, the operational feasibility and timing requirements were tested by subjects who spanned the full size range of astronauts (5% female, 95% male). The final checkout was performed by three crew members with flight experience, who offered relatively minor criticism and gave the concept a "thumbs up" for operability in space.

At this time the flight chamber and experiment mounting structure are being fabricated in-house, and the entire CM–1 experiment will be assembled, qualified, and functionally tested beginning in early 1995, supporting a launch date of April 1997.

The CM–1 chamber mockup has served its primary purpose, but it continues to be an asset to the CM–1 project for crew training and the demonstration of CM–1 for several audiences, including shuttle safety personnel and Lewis visitors.

Lewis contact: Ann P. Over, (216) 433–6535
Headquarters program office: OLMSA

Droplet Dispensing, Deployment, and Ignition System Developed

The Droplet Combustion Experiment (DCE) is designed to study the combustion of single, pure, hydrocarbon fuel droplets in microgravity over a wide range of mixtures and pressures in oxygen and helium atmospheres. This classical combustion problem, when successfully completed in space, will become a textbook example of how combustion theoretical modeling and experimentation are used to gain understanding of combustion chemistry. Droplet burning rates, flame-zone standoff diameters, and droplet extinction diameters will be measured and compared with predicted behavior. Droplet combustion is common in many power and heat generation systems here on Earth, such as household oil furnaces, steam generation plants, and even automobiles.

By studying this phenomenon we expect to also advance our basic understanding of combustion in space. Fuel spills in the form of liquid droplets can occur anywhere. Methods of detecting fires that result from liquid droplet combustion in space will need to be modified because of the absence of buoyancy.

The experiment was conceived by Prof. Forman A. Williams of the University of California at San Diego, with the help of his co-investigator, Prof. Frederick L. Dryer of Princeton University, and developed by NASA Lewis.

Before flight hardware could be developed for this experiment, it was essential to develop and test in microgravity a system for dispensing, deploying, and igniting single droplets. The science of this experiment requires precisely sized droplets (1 to 5 mm in diameter) free from all physical support, moving at very low (millimeters per second) velocities, and rapidly ignited. To be avoided are overdriving the flame with too hot an igniter or the ignition system causing the hot gas surrounding the heating source to push on and move the droplet.

The droplet is dispensed by using a precision fuel syringe precisely controlled by a stepper motor. The fuel, once it passes shutoff valves, flows to two opposed needles. These needles, each mounted on a servodisk motor, are precisely aligned to flow fuel to the gap between them. The correct amount of fuel is fed to the dispensing site, and then the gap between needles is adjusted so that the tips of the needles are on the surface of the droplet. The droplet is deployed when the two needles simultaneously retract at very high speed. In microgravity the droplet is then floating in the gas. Ignition takes place immediately after deployment when two prepositioned, opposed hot-wire igniters are quickly turned on, igniting the droplet. The hot-wire igniters, after being switched off, are quickly removed from the area near the droplet combustion site. The droplet combustion process can occur over the next 10 to 20 sec.

Testing in the Lewis 5-sec Zero-Gravity Facility has demonstrated the feasibility of this technique for a wide range of test conditions. The testing showed that the hardware, when the correct

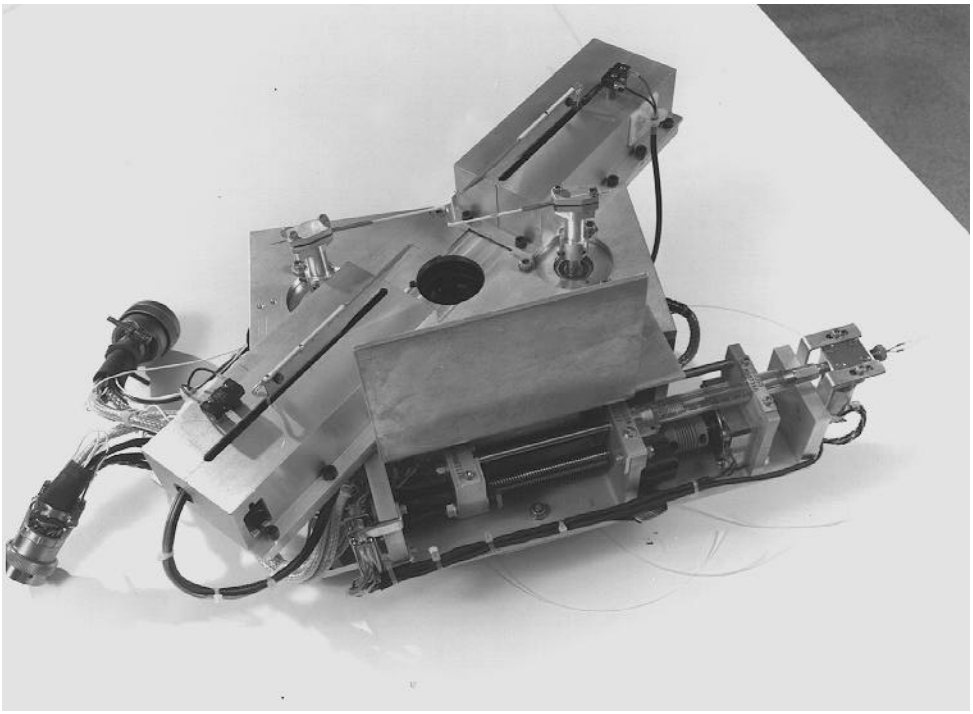

Droplet Combustion Experiment internal apparatus for drop tower testing.

operational timing was used, performed virtually 100% of the time. The feasibility demonstration in this facility has allowed flight hardware development to be started. Testing will continue to improve understanding of the correct operating parameters for each point in the spaceflight test matrix. DCE is expected to fly in April 1997.

Lewis contacts: John B. Haggard, Jr., (216) 433–2832; Beth A. Parent, (216) 433–5284
Headquarters program office: OLMSA

Surface-Tension-Driven Convection Experiment Rebuilt for Second Flight

Surface tension causes liquids to form spheres if in small areas, such as capillary tubes, or if free-falling without gravity. Surface tension can also create convection when a colder surface with higher tension pulls fluid from a warmer surface with lower tension. Bulk liquid then flows to the warmer surface. These thermocapillary flows were studied in the Surface-Tension-Driven Convection Experiment (STDCE), planned by the principal investigators from Case Western Reserve University (CWRU), Simon Ostrach and Yasuhiro Kamotani.

STDCE was designed and built at NASA Lewis for a Spacelab rack on the 14-day United States Microgravity Laboratory 1 (USML–1) mission launched in June 1992. A test cell, 10 cm in diameter and 5 cm deep, was filled with 10-cSt silicone oil centrally heated with a submerged cartridge or with laser radiation. Flows were measured by using a laser light sheet and a video camera to record light from particles in the oil. Oil surface temperatures were measured with an infrared scanning imager. Analysis of the 38 tests conducted (12.5 hr of data recorded) showed good agreement with the CWRU model, which predicted that, even though the critical Marangoni number was exceeded, oscillations would not occur because the test cell was too large and the oil too viscous.

STDCE was rebuilt at Lewis for a second experiment using 2-cSt silicone oil and smaller test cells (diameters of 1.2, 2.0, and 3.0 cm) in six test modules: three using laser heating (constant flux) and three using submerged heaters (constant temperature). New optics include the free-surface-deformation measurement system, a single-channel Ronchi method for determining surface slopes of 5 to 30 μm/mm; the three-dimensional flow visualization system; an infrared telescope for the infrared imager; and changes to the laser focus to produce smaller heating zones (0.5 to 6 mm).

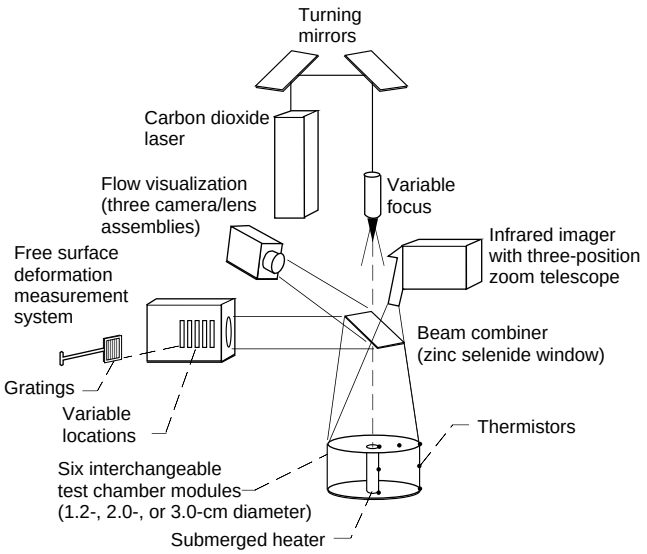

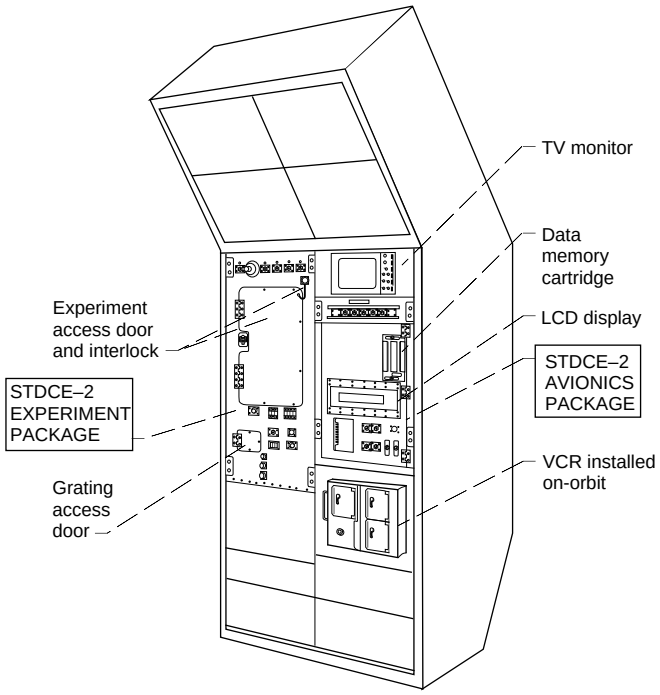

Optical system for STDCE–2 and STDCE–2 in Spacelab rack.

Other modifications will allow the crew to change out test modules and to optimize the measurements. Electrical and software systems were upgraded on the basis of lessons learned from USML–1 and to allow more crew interaction (73 hr of operation) and add a three-deck video cassette recorder. Three video pictures (infrared imager, flow visualization, and free-surface deformation) will be recorded and also downlinked to the payload operations control center at NASA Marshall Space Flight Center and to the user operations facility at Lewis. The STDCE–2 payload operations team was chosen to assist Ostrach and Kamotani in conducting the experiment during the 16-day USML–2 mission that will occur in autumn 1995. Three shifts will operate around the clock at Marshall, and one shift will operate at Lewis.

During fiscal 1994 the STDCE team completed the design and fabrication of flight hardware and entered the final stages of testing. Many serious challenges were met during the STDCE development, especially with optical systems alignment and the completion of the test modules. The STDCE rack simulator was used for astronaut crew training in July and then sent, along with a tabletop simulator of the optical systems, to Marshall and installed in their Spacelab mockup. Crew training on the flight hardware was completed at Lewis in September.

Bibliography

Kamotani, Y.; and Ostrach, S.: Design of a Thermocapillary Flow Experiment in Reduced Gravity. J. Thermophysics and Heat Transfer, vol. 1, no. 1, Jan. 1987, pp. 83–89.

Kamotani, Y.; Ostrach, S.; and Pline, A.D.: A Thermocapillary Convection Experiment in Microgravity. Heat Transfer in Microgravity, ASME HTD, vol. 269, 1993, pp. 22–30.

Kamotani, Y.; Ostrach, S.; and Pline, A.D.: Some Results From the Surface Tension Driven Convection Experiment Aboard USML–1 Spacelab. AIAA Paper 94–0238, 1994.

Kamotani, Y.; Ostrach, S.; and Pline, A.D.: Some Velocity Field Results From the Thermocapillary Flow Experiment Aboard USML–1 Spacelab. Presented at the 1994 COSPAR Meeting in Hamburg, Germany, July 11–21, 1994.

Pline, A.D.; and Butcher, R.L.: Spacelab Qualified Infrared Imager for Microgravity Science Applications. SPIE, vol. 1313, Thermosense XII, Apr. 1990, pp. 250–258.

Pline, A.D.; Jacobson, T.P.; Kamotani, Y.; and Ostrach, S.: Surface Tension Driven Convection Experiment. AIAA Paper 93–4312, 1993.

Lewis contacts: Thomas P. Jacobson, (216) 433–2872; Robert L. Zurawski, (216) 433–3932; Alexander D. Pline, (216) 433–6614; Nancy Rabel Hall, (216) 433–5643
Headquarters program office: OLMSA

Zeno Flies Successfully on STS–62

The Critical Fluid Light Scattering Experiment was dubbed "Zeno" by the principal investigator in honor of the Greek philosopher Zeno of Elea who first pondered the paradox of infinity. The Zeno experiment analyzed laser light scattered from a fluid (xenon) in low-gravity conditions to study physical properties very near critical temperature T_c. In the low gravity of space these measurements can be made 100 times closer to the critical point than is possible on Earth. Scientists are interested in what happens at the critical point because critical-point phenomena are common to many materials. Physically different systems act similarly near their critical points. Understanding how matter behaves at the critical point can provide insight into a variety of physics problems ranging from phase changes in fluids to changes in the composition and magnetic properties of solids.

Light-scattering spectroscopy and correlation analysis was used to study the density fluctuations in xenon at temperatures very near the liquid-vapor critical point of this ideal fluid. The density fluctuations observed near the critical point reflect the underlying heat modes of the fluid and decay by thermal diffusion. The ultimate impact of this careful test can be far reaching because the theories to be compared with these measurements provide "universal" descriptions of many critical-point phase transitions, such as ferromagnetization, superconductivity, superfluidity, and binary fluid miscibility limits.

The principal investigator, Prof. Robert W. Gammon of the Institute for Physical Science and Technology at the University of Maryland, led a team of 15 scientists and engineers during nearly 14 days of continuous operations to make unprecedented measurements of a critical fluid in the low gravity of the space shuttle during the March 1994 STS–62 mission of the space shuttle *Columbia*. The instrument, built by Ball Aerospace Corp. and the University of Maryland, operated with no failures or problems for the duration of the mission, a total of 326 hr on orbit.

During the mission both autonomous and commanded operations were conducted. Approximately 480 commands were sent to the instrument to accomplish:

- Five scans for T_c (one lasting $\simeq$65 hr)
- Light scattering measurements at 30 isothermal set points
- Over 500 dual correlograms providing the fluctuation decay time data

The remarkable behavior of the fluid very near the critical temperature provided data exceeding the team's expectations and will challenge the scientific community for many years to come. The most difficult part of the experiment, locating the critical temperature to the required precision, was finally accomplished to a precision of about $\pm$100 μK.

Preliminary analyses show that the measured decay rates exhibit the required precision within $\simeq$300 μK of the critical temperature. Additional high-quality measurements were made within a few microkelvins of the critical temperature, and the density fluctuation correlation data exhibit, as predicted, an ever slower rate of decay. Measurements below the critical temperature, in the two-phase region, were also made. All measurements closer than 10 mK from T_c reflect data unattainable on Earth at the required accuracy of 1%.

Lewis contact: Dr. Richard W. Lauver, (216) 433–2860
Headquarters program office: OLMSA

Isothermal Dendritic Growth Experiment Achieves Unqualified Success

The scientific objective of the Isothermal Dendritic Growth Experiment (IDGE) was to test fundamental assumptions about dendritic solidification of molten materials. Dendrites—from the ancient Greek word for tree—are tiny branching structures that form inside molten metal alloys when they solidify during manufacturing. The size, shape, and orientation of the dendrites have a major effect on the strength, ductility (ability to be molded or shaped), and usefulness of an alloy. Nearly all cast metal alloys used in everyday products, such as automobiles and airplanes, are composed of thousands to millions of tiny dendrites. Gravity, present on Earth, causes convection currents in molten alloys that disturb dendritic solidification and make its precise study impossible. In space, gravity is negated by the orbit of the space shuttle. Consequently, IDGE gathered the first

precise data on undisturbed dendritic solidification.

IDGE used an apparatus designed, built, tested, and operated by NASA Lewis personnel at less than half the normal cost. It flew aboard the space shuttle *Columbia* (STS–62) from March 4 to 17, 1994. This IDGE mission was the first of three planned as part of the United States Microgravity Payload (USMP) series. It was suggested by the principal investigator, Professor Martin E. Glicksman from Rensselaer Polytechnic Institute in Troy, New York.

The IDGE mission was an unqualified success. In fact, by one important measure, it was 370% successful. This extraordinary success was possible because IDGE was fully operable by remote control from Earth (scientists on the ground monitored progress and sent up commands to alter IDGE programming). During the flight, dendritic solidification behaved differently than the scientists had expected—experiments could be completed more quickly. Remote operation (and some heroics from the Lewis operations team in sending a near record 8000 discrete commands over nine days) permitted IDGE to take advantage of the situation and operate far outside its programmed limits. Fifty-eight dendrites were solidified at more than 20 different supercoolings, ranging from about 0.05 to 1.93 K (supercooling is the condition in which a dendrite solidifies at a temperature below its normal freezing point). The data consisted of more than 400 photographs and 800 television images of dendrites solidifying in space, along with associated supercooling, pressure, and acceleration data. Similar data, more than 1200 photographs, were taken on Earth before and after the flight. Photographs were possible because the test material was transparent succinonitrile, which mimics the behavior of iron when it solidifies.

Dendrite tip radii, tip solidification speed, and volumetric solidification rates have been determined from the space and Earth data. These rates were compared with predictions made by theorists over the last 50 years and used for metal production here on Earth. IDGE results indicate that the theories, although sound in some respects, are flawed. Consequently, corrected

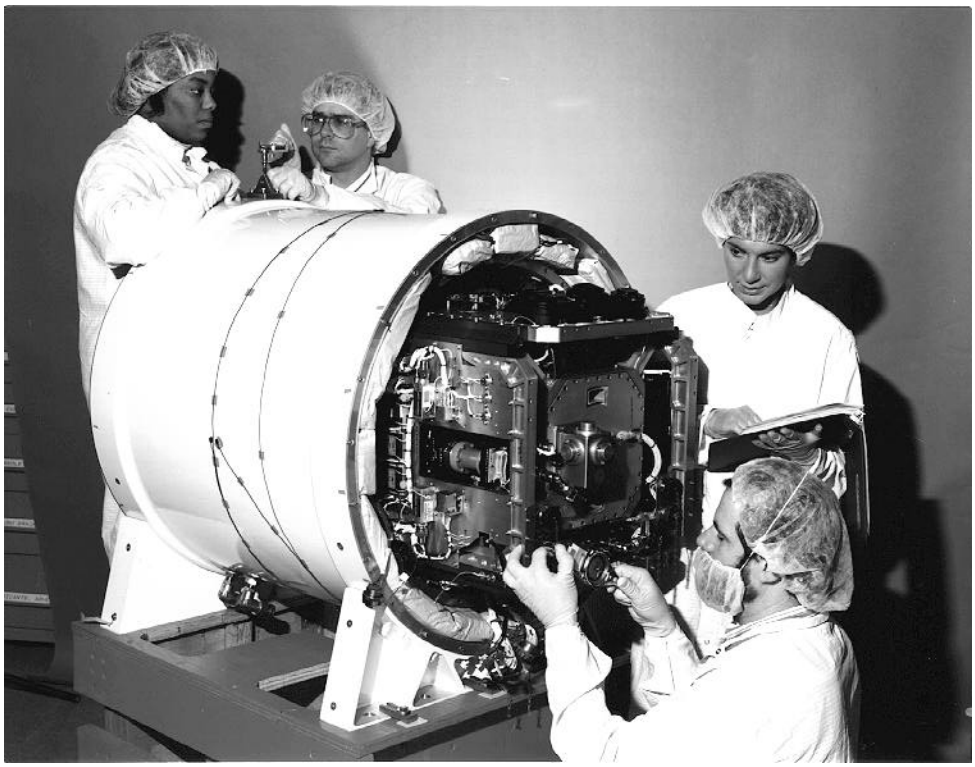

Members of the Lewis-based IDGE team assemble the flight unit. One of the IDGE 35-mm cameras and the Space Acceleration Measurement System (SAMS) sensor head are visible.

theories based on IDGE data should result in improved industrial metal production here on Earth.

The IDGE STS–62 data will provide a benchmark for testing theoretical developments for decades to come. Additional flights in 1996 and 1997 will provide data to test advanced solidification theories and the universality of their applicability.

Lewis contact: Edward A. Winsa, (216) 433–2861
Headquarters program office: OLMSA

Solid Surface Combustion Experiment Completes Seventh Flight

The purpose of the Solid Surface Combustion Experiment (SSCE) is to study the physical and chemical mechanisms of flame spread over solid fuels in the absence of gravity-driven buoyant or externally imposed airflows. Because the controlling mechanisms of flame spread are different in low gravity than in normal gravity, the SSCE results have a practical application in the evaluation of spacecraft fire hazards.

The SSCE was the first combustion experiment to fly on the space shuttle—and the first such experiment in the NASA spaceflight program since Skylab. It was conceived by Professor Robert A. Altenkirch, Dean of Engineering at Mississippi State University. NASA Lewis designed the SSCE and built the flight payload in-house, providing all engineering, testing, flight qualification, scientific, and flight operations support functions. The SSCE project was supported in some way by nearly every major element of the Lewis organizational structure.

In the first five flights (conducted in 1990–92) thin-fuel samples made of ashless filter paper were burned in a sealed chamber filled with mixtures of 50% or 35% oxygen in nitrogen at pressures of 1.0, 1.5, or 2.0 atm. In the other three flights thick-fuel samples of PMMA (polymethylmethacrylate) were burned in 50% or 70% oxygen in nitrogen at 1.0 or 2.0 atm. The second of the thick-fuel flights was conducted onboard the space shuttle *Discovery* as part of the STS–64 mission, completing the seventh successful flight of eight planned spaceflights. During this mission two fuel samples were burned in a quiescent mixture of 50% oxygen and 50% nitrogen. The flight hardware performed without incident and provided all the required science data.

In orbit the fuel samples are ignited by the astronauts using an incandescent wire. Two 16-mm motion picture cameras photograph the flame from perpendicular perspectives while the fuel and flame temperatures and the chamber pressure are recorded by a digital data acquisition and control system. The fuels, the atmospheric conditions, and the measurement systems were chosen to provide benchmark data for comparison with evolving theory.

The principal investigator, Professor Altenkirch, has developed a time-dependent numerical simulation of the flame-spreading process from first principles (of fluid mechanics, heat transfer, and reaction kinetics). The spread rates, flame shape, and thermodynamic data from the completed SSCE flights have been compared directly with the results of the computational model, confirming the prediction that radiation heat transfer mechanisms must be included to accurately predict the behavior observed in the flight experiments. Without the radiation mechanisms the effects of pressure observed in the flight experiments are not captured by the model. The flight temperature data are being used to develop an improved numerical model of gas-phase radiative heat loss from the flame, which has been identified as a rate-limiting mechanism in many low-gravity flames. As the fundamental understanding of the flame-spreading process is enhanced by the results of the SSCE, the engineering of fire safety in spacecraft and on Earth can be improved with better knowledge of safety margins and fire prevention techniques.

Bibliography

Altenkirch, R.A.; Bhattacharjee, S.; and Sacksteder, K.R.: Implications of Spread Rate and Temperature Measurements in Flame Spread Over Thin Fuel in a Quiescent, Microgravity Space-Based Environment. Combustion Sci. and Technol., vol. 91, 1993, pp. 225–242.

Bhattacharjee, S.; Altenkirch, R.A.; and Sacksteder, K.R.: Effect of Ambient Pressure on Flame Spread Over Thin Cellulosic Fuel in a Quiescent, Microgravity Environment. To be published in J. Heat Trans., 1995.

Ramachandra, P.A.; Altenkirch, R.A.; Tang, L.; Wolverton, M.K.; Bhattacharjee, S.; and Sacksteder, K.R.: Behavior of Flames Spreading Over Thin Solids in Microgravity. To be published in Combust. and Flame, 1995.

Vento, D.M.; Zavesky, R.; Sacksteder, K.R.; and Altenkirch, R.A.: Solid Surface Combustion Space Shuttle Experiment Hardware Description and Ground Based Test Results. AIAA Paper 89–0503, 1989. (Also NASA TM–101963.)

Lewis contacts: John M. Koudelka, (216) 433–2852; Kurt R. Sacksteder, (216) 433–2857
Headquarters program office: OLMSA

Pool Boiling Experiment Has Third Successful Shuttle Flight

The Pool Boiling Experiment (PBE) is designed to improve understanding of the fundamental mechanisms that constitute nucleate pool boiling. Nucleate pool boiling occurs when a stagnant pool of liquid is in contact with a surface that can supply heat to the liquid—as when a pot of water boils. If the liquid absorbs enough heat, a vapor bubble can be formed. Nucleate boiling has many Earth-bound applications, such as steam-generated powerplants and petroleum and other chemical plants. Also, by studying the test fluid R–113, some basic understanding of the boiling behavior of cryogenic fluids could be obtained without the large cost of an experiment using an actual cryogen.

The Pool Boiling Experiment was conceived by Dr. Herman Merte of the University of Michigan and developed by NASA Lewis. The experiment was conducted on three space shuttle missions. The prototype system, first flown on STS–47 in September 1992, acquired a considerable amount of scientific data at different heat flux levels. Some minor modifications were made in the timing sequences in the test matrix for the STS–57 flight (June 1993). The prototype system was reflown on STS–60 in February 1994 as essentially a repeat of the STS–47 mission. The following general observations and conclusions are based on the data from all three flights:

- Three phases in the boiling process in microgravity were observed: nucleation or onset of boiling; bubble growth and/or spreading; and quasi-steady heat transfer behavior.
- Instead of traditional film boiling, dryout occurred in the high-heat-flux cases (8 W/cm^2) and partial dryout and rewetting in the mid-heat-flux cases (4 W/cm^2).

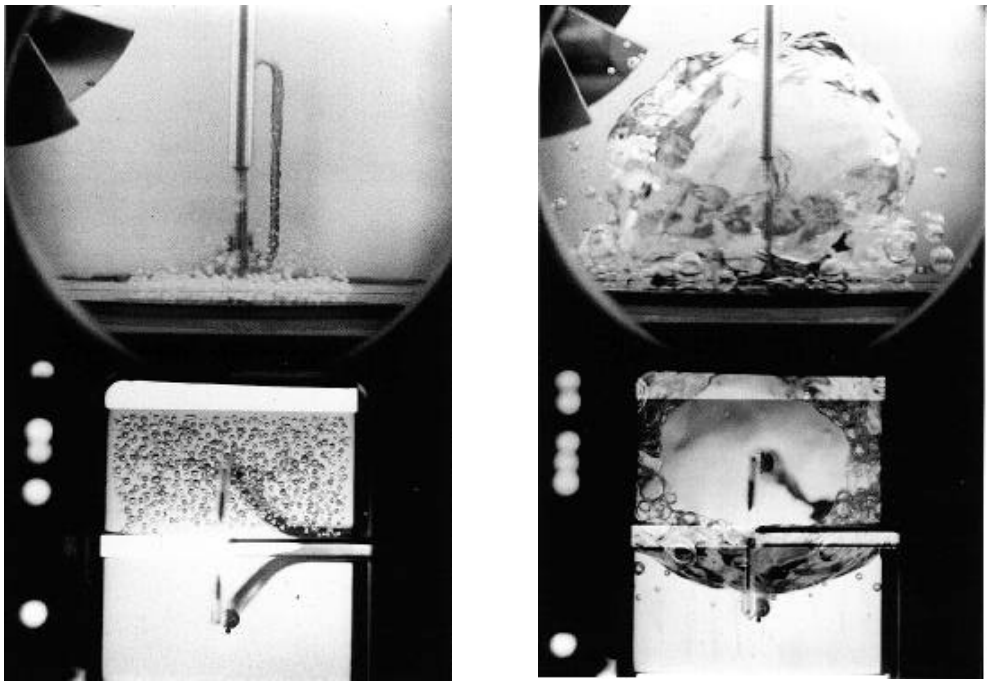

Side and bottom views of R–113 at 8 W/cm^2 boiling on Earth (left) and during STS–47 mission (right).

Also, two interesting, heretofore-unobserved phenomena have been disclosed:

- In microgravity the heater surface superheat at nucleation goes through a maximum as the imposed heat flux is reduced. Furthermore, increasing the bulk liquid subcooling reduces the heater superheat at nucleation in microgravity, all other conditions being held constant.
- An extremely dynamic and unusual initial vapor bubble growth has been observed under certain conditions in microgravity. Appearing to be associated with an instability problem, it produces an unusual interfacial behavior.

These were the first nucleate boiling experiments performed for long periods in microgravity, and the matrix test conditions were selected in part to cover a reasonably broad range of parameters. Two additional flights have been approved to study the phenomena of dryout and rewetting during pool boiling in a microgravity environment. The existing hardware units will be modified and delivered to Kennedy Space Center in 1995.

Lewis contact: Angel M. Otero, (216) 433–3878
Headquarters program office: OLMSA

Bismuth-Tin Crystal Growth Monitored Using MEPHISTO Furnace

Chemical and physical imperfections affect the quality of semiconductor crystals, and hence, to a major extent, their usefulness in electronic devices. Because these complications may be significantly reduced in low gravity, experimental data are needed to explain the crystal-growth process in that environment. The outcome will be techniques for growing higher quality crystals on Earth.

In this experiment molten bismuth-tin material within a furnace is cooled at one end and begins to solidify as the temperature of the liquid falls below the freezing point. It is important to know the position of the boundary between the solid and liquid material as well as how fast it moves during crystal growth. Hence, the data being sought are the rate at which the crystal grows, the mechanism by which it grows, and the structure and chemical composition of the crystal produced.

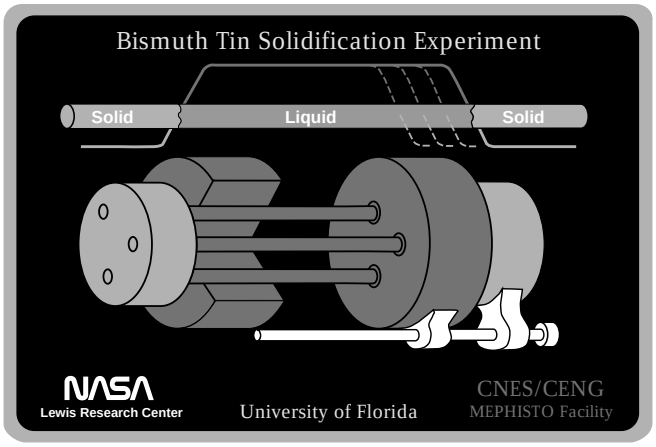

The In-Situ Monitoring of Bismuth-Tin Crystal Growth Experiment is a collaborative United States and French investigation of crystal growth fundamentals. The United States experimenters are studying bismuth doped with tin, and the French are studying tin doped with bismuth. The results of these two sets of experiments will be of fundamental importance to the semiconductor industry, which supplies the solid-state components, such as integrated circuits, for the manufacture of electronic equipment.

This experiment was conceived, designed, and developed by Professor Reza Abbaschian of the University of Florida and managed by NASA Lewis. It was conducted in the MEPHISTO furnace facility, a French-designed and -built materials processing furnace, on United States Microgravity Payload 2 (USMP–2).

The experiment flew aboard *Columbia* (STS–62) in March 1994. The MEPHISTO furnace carried three bismuth-tin samples, each approximately 1 m long and 6 mm in diameter. The middle portion of each sample was melted by the two heating elements in MEPHISTO, thus creating two solid-liquid interfaces. One of the heaters was kept stationary while the other was moved back and forth at specified rates to melt or solidify at that side of each sample. More than 55 melting and solidification cycles with different thermal and velocity conditions were performed during the mission, and more than 45 “interface temperature histories” were obtained during these cycles.

Other data obtained were the continuous monitoring of the sample resistance, the heater translation histories, and the thermal measurements.

Lewis contact: Richard L. DeWitt, (216) 433–2601
Headquarters program office: OLMSA

Gravitational Role Studied in Liquid-Phase Sintering

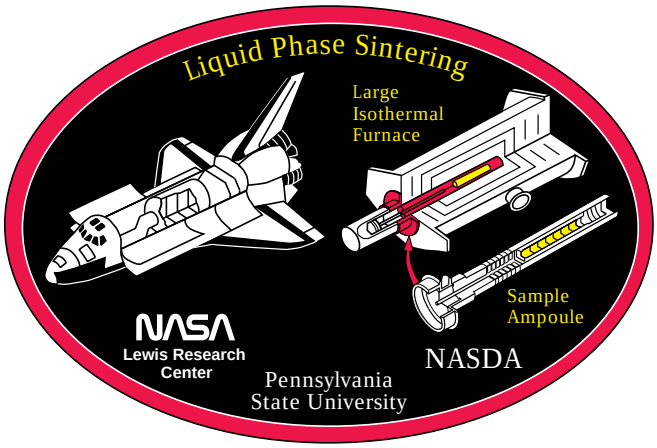

"Sintering" means welding or fusing metal or ceramic powders by heating them without melting. Frequently, it is aided by applying pressure in a special high-temperature press to squeeze the particles together. The Liquid-Phase Sintering Experiment explores a different mechanism, by adding a portion of a powder that melts at a lower temperature and surrounds the powders that remain solid. This liquid then lets particles and materials move more easily, allowing the powders to more rapidly form a solid compact. However, problems, such as separation of the solid and liquid due to gravity (manifested by settling of the solid particles), still remain. Access to the low-gravity environment of Earth orbit provides a unique opportunity to study liquid-phase sintering without separation, settling, or other gravity-induced complications. Better understanding of the process will help introduce new industrial applications of liquid-phase sintering, such as automotive components—resulting in new and improved products.

In this investigation mixed powders of tungsten, nickel, and iron were initially cold compacted under pressure in the shape desired for the final product. The compacts were then heated to just below the nickel-iron alloy melting temperature to provide handling strength, a process called presintering. In the experiment they were heated above 1465 °C to form a liquid-solid mixture. The tungsten, with its very high melting point (3370 °C), remained a solid while the nickel and iron, with much lower melting points, became liquid. The liquid permitted more rapid transport of material for faster sintering than would be possible if all the material were solid. After sintering, the microstructure of the samples (i.e., the structure when viewed under very high magnification), consisted of connected tungsten grains surrounded by the solidified liquid.

This experiment was conceived, designed, and developed by Professor Randall M. German of Pennsylvania State University. It flew as part of International Microgravity Laboratory 2 (IML–2) in July 1994 aboard the space shuttle *Columbia*. The experiment was conducted in an apparatus called the large isothermal furnace (LIF), which can operate at the high temperatures required. The LIF was developed by Ishikawajima-Harima Heavy Industries Co., Ltd., for the National Space Development Agency of Japan. This project was managed by NASA Lewis.

The LIF test specimens consisted of three different cartridges, each containing seven samples 10 mm in diameter by 10 mm high. One cartridge was tested at each of the three critical sintering periods identified in earlier ground-based experiments: 1, 15, and 120 min. In 1 min liquid penetrates along existing solid-solid boundaries; 15 min is needed for full densification; 120 min is needed to observe grain rotation and coalescence events.

In summary, a nominal temperature of 1506 °C (±4 deg C) was achieved for each test time. Free drift of *Columbia* during the appropriate times was confirmed. All functional objectives were achieved. The samples will be analyzed at the laboratories of Pennsylvania State University.

Lewis contact: Richard L. DeWitt, (216) 433–2601
Headquarters program office: OLMSA

Solar Array Module Plasma Interactions Clarified

Satellites and spacecraft have evolved in size, weight, and sophistication to the point that they now require high operating voltages. This demand creates a new challenge for spacecraft designers—contending with the interaction of space plasma with materials and systems. The objective of the Solar Array Module Plasma Interactions Experiment (SAMPIE) was to determine the environmental effects of the low-Earth-orbit (LEO) space plasma environment on modern solar cells and space power system materials. The results will play a key role in the design and construction of high-voltage space power systems. SAMPIE was developed at NASA Lewis.

The experiment plate included solar cell samples of standard silicon cells, *International Space Station Alpha* (ISSA) cells, Advanced Photovoltaic Solar Array (APSA) cells, and solar cells modified to suppress arcing effects. Various other samples of power system materials were also tested to investigate snapover effects, pinhole effects in insulators, and metal-to-metal variations in arcing effects.

During the 16-day mission of the space shuttle *Columbia* in March 1994, SAMPIE operated for more than 70 hr in space. The primary set of required measurements were taken with the *Columbia* payload bay oriented in the "ram" direction (coincident with the velocity vector). In this orientation all planned current collection data at direct-current voltages to 300 V were collected, all low-voltage arcing data (at voltages down to –300 V dc) were collected, and 90% of the high-voltage data (at voltages down to –600 V dc) were collected.

In the other required attitude orientation, known as the "wake" direction (with the payload bay oriented 180° away from the velocity vector), the planned low-voltage (to 300 V dc) current collection measurements were not taken owing to on-orbit problems with the high-voltage bias line of one power supply. The other high-voltage power supply was used to collect high-voltage arcing data in the wake. This step was not in the original plan because it had been assumed that there would be no arcing in the wake owing to the low plasma density. In fact, arcing was seen on several samples in the wake, providing unexpected information to the SAMPIE team. During both orbiter attitudes the plasma diagnostic instruments collected high-fidelity data on plasma temperature, plasma turbulence, and orbiter vehicle potential. These data will be used to "normalize" the arcing and current collection

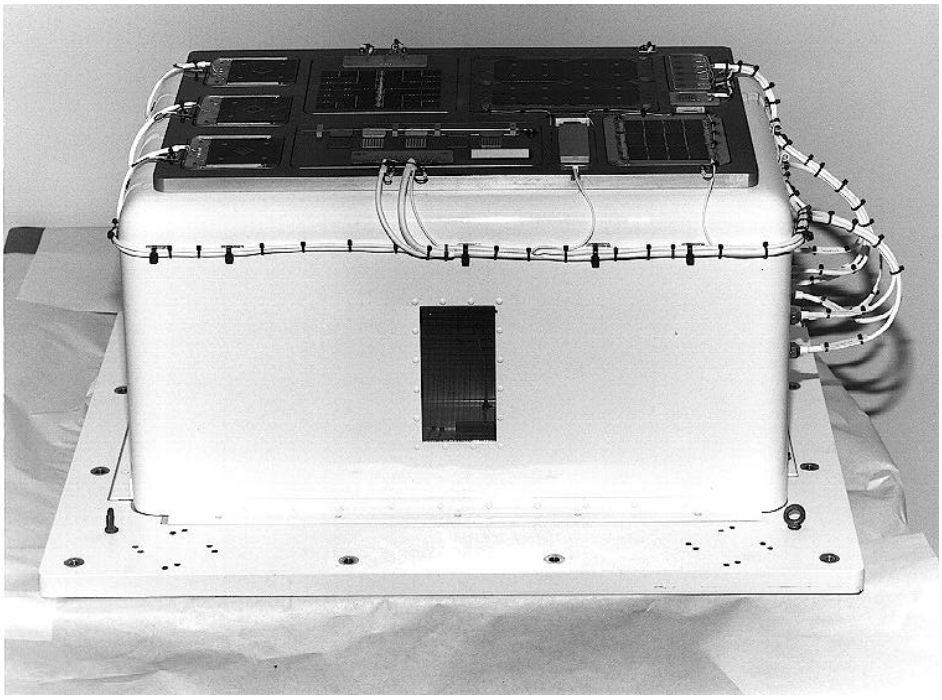

Exterior view of SAMPIE electronics enclosure and experiment plate.

data, removing variations due only to plasma variations.

The flight data are now being analyzed by the SAMPIE principal investigator, Dr. Dale Ferguson. He has already used the flight data to validate the design of the ISSA plasma contactor program. The flight data will also be used to help validate computer modeling codes developed at Lewis in support of space power system design. The SAMPIE flight hardware is presently awaiting another flight opportunity.

Lewis contacts: Lawrence W. Wald, (216) 433–5219; Dr. Dale C. Ferguson, (216) 433–2298; Dr. G. Barry Hillard, (216) 433–2220
Headquarters program office: OSAT

First Thermal Energy Storage Test Conducted

The first Thermal Energy Storage (TES) Experiment was successfully flown on STS–62 in March 1994. Such data have never before been obtained and have direct application to using on-orbit solar dynamic power systems. These systems will store solar energy in a thermal energy salt, such as lithium fluoride, when the salt is melted by the Sun. The energy is then extracted during the non-Sun, or shade, portion of the orbit, enabling the solar dynamic power system to provide constant electrical power during the entire orbit. Four TES experiments are planned to provide an understanding of the long-duration microgravity behavior of thermal energy storage fluoride salts that undergo repeated melting and freezing. Two types of results were obtained from the TES–1 flight experiment: images of the lithium fluoride in its final frozen state and canister temperatures throughout the four heating/cooling cycles.

Upon return from flight STS–62 the annular test section was examined nondestructively. By a technique called tomography, computer-assisted radiographic images were developed of the phase-change material inside the annular volume. Cross sections of the lithium fluoride were examined axially and at 10 equidistant points perpendicular to the axis.

The predominance of the frozen fluoride at the radiator end of the canister indicated the sensitivity of the surface tension at the liquid/vapor interface to temperature. The void (bubble) was designed to be at 0° orientation during the melt phase (by the higher flux heater strip) but was allowed to seek its own position when the heat input was shut off and heat was allowed to pass to the radiator. The temperature gradient drove the bubble to the hotter end of the annulus, where it remained while the fluoride was gradually being frozen.

A temperature history was obtained from more than 40 thermocouples on and about the test canister. These readings are being analyzed in conjunction with the analytical program, which is being developed to predict the two-phase behavior of materials under microgravity.

Comparing the temperature history of any sets of thermocouples indicated that the results were repeatable well within the four melt/freeze cycles conducted. The temperature history of the first cycle differed noticeably from the subsequent cycles because of the phase-change material's location. When installed, the lithium fluoride was frozen with the canister axis horizontal, with the void at 0° orientation. The void under microgravity was at a very different location. The first temperature cycle reflects the transition.

Although most temperatures continually increased during the heating phase of the cycle, some decreased for a short period before increasing again. Earlier ground experiments showed the same phenomenon, the changes in inflection of temperature occurring at the 90° and 270° points. Because the melt line would pass these points during heating, and recognizing the large change in density as lithium fluoride changes phase, it is reasonable to expect that abrupt temperature changes may occur.
The TES–1 flight results have produced reliable data and information on materials melting and freezing under microgravity. Development of the computer analysis is under way and will enable predictions of such behavior. NASA Lewis provided the funding, project management, and scientific oversight for the design and development of the flight experiment, as well as safety, quality assurance, specialized hardware development, and unique skills required for experiment assembly. Work was accomplished by an in-house dedicated project team of engineers and technicians from NASA and NYMA.

Bibliography

Namkoong, D.: Thermal Energy Storage Flight Experiment in Microgravity. NASA TM–108721, 1992.

Szaniszlo, A.J.: Thermal Energy Storage Flight Project. Presented at 1992 Space Power Workshop, El Segundo, CA, April 7–10, 1992.

Lewis contacts: Carol M. Tolbert, (216) 433–6167; James R. Faddoul, (216) 433–6322
Headquarters program office: OSAT

Integrated Microgravity Measurement and Analysis Effort Supports Microgravity Science

Scientists need to know the gravity levels on manned spacecraft while their experiments are being performed. If unexpected results occur, the scientists can determine if these results were caused by a disturbance or are a result of the experiment. Such data can also help scientists plan the location of an experiment sensitive to certain types of disturbances.

NASA Lewis has combined the activities for several different projects into a single project to serve the microgravity environment needs of the scientists participating in the NASA microgravity science program. The Space Acceleration Measurement System (SAMS) Project, the SAMS–II Project, the Orbital Acceleration Research Experiment (OARE), and the Acceleration Characterization and Analysis Project (ACAP) were combined into the Microgravity Measurement and Analysis Project (MMAP) in April 1993.

SAMS measures the microgravity environment on the orbiter to support science experiments mounted in the middeck, the cargo bay, and the Spacelab and Spacehab modules. The eighth SAMS flight supported the Spacehab-01 payload on STS–60 in February 1994. The ninth flight supported four experiments of United States Microgravity Payload 2 (USMP–2) on STS–62 in February 1994. This mission provided near-real-time acceleration data to the scientists in the payload operations center. The tenth flight supported multiple science experiments in the Spacelab module of the International Microgravity Laboratory 2 (IML–2) payload on STS–65 in July 1994.

SAMS also delivered one flight unit to Moscow early in the year for launch to the Russian space station, *Mir*. In August 1994 the SAMS unit, along with the other American and Russian equipment, was successfully launched and docked with *Mir*. Operations are planned to begin during October 1994 and will extend for several years.

The OARE instrument was originally prepared for aerodynamic investigations of the orbiter at orbital altitudes. When that program finished, the OARE device, a sensitive accelerometer, was acquired by the microgravity science program to support microgravity characterization for science experiments. The OARE instrument flew on STS–62 and STS–65 in support of the USMP–2 and IML–2 payloads on those missions. An OARE data downlink from the orbiter to the payload operations center was developed to relay low-frequency acceleration data to the scientists in a timely fashion.

SAMS–II has continued developing an advanced SAMS-type system for the *International Space Station Alpha* (ISSA). The SAMS–II flight unit and its associated data and control equipment will take advantage of the unique ISSA operating environment to provide more dynamic and useful information to scientists conducting experiments on ISSA.

The Principal Investigators Microgravity Services Project was formed to acquire the functions of ACAP to provide microgravity information to the microgravity science investigators.

Mission summary reports were prepared for SAMS and OARE operations on STS–57, STS–60, and STS–62. These reports summarize mission activities and map the microgravity environment for the mission. Consultation was also provided on ISSA microgravity requirements and vibration isolation technology.

Lewis contact: Pete A. Vrotsos, (216) 433–3560
Headquarters program office: OLMSA

Stereoscopic Imaging Velocimetry Being Developed

The Stereoscopic Imaging Velocimetry Project aims to provide a diagnostic tool that will produce three-dimensional fluid flow information using two-dimensional image data. In the field of microgravity fluid sciences the ability to accurately quantify the three-dimensional fluid flow velocity in fluid physics experiments would significantly increase both the quantity and quality of the information available. Current experiments that would benefit from this measurement capability are surface-tension-driven convection studies, examination of heat transfer by boiling, and crystal growth or solidification investigations.

The goal of this project is to provide a means to measure three-dimensional fluid velocities quantitatively and qualitatively in space at many points. The method would apply to any system with an optically transparent fluid that can be seeded with tracer particles. Except for the tracer particles this measurement technique is nonintrusive. Velocity accuracies should be 1% to 5% of full field for flows in the 1-mm/sec range over a field of view of 3 to 4 cm.

Although stereoscopic imaging velocimetry can now be performed in a few research laboratories using two-camera systems, the technology is neither commercially available nor mature enough to be used in microgravity flight experiments. This Advanced Technology Development Project is drawing on the work of earlier researchers to produce a system more standardized in nature, more precise in performance, and easier to use. The velocimeter will be fully automatic and usable on any flow pattern within its specified speed regime, and it will track at least 500 tracer particles. The tracer particles will be chosen on the basis of neutral buoyancy, chemical compatibility, and optical reflectance.

Image data are recorded by two independent digital charge-coupled device cameras. These two cameras, oriented at 90° with respect to each other, provide a stereo pair of two-dimensional images. These images are stored on an optical disk in real time (30 frames/sec), and four types of off-line data processing are performed using the stored images.

- The first process applies camera calibration information to the images, correcting for distortions introduced by lens nonlinearities while providing a two- to three-dimensional mapping technique.
- The second process determines the centroid of each particle by using a neural network algorithm that compensates for overlapping particles.
- The third and fourth processes involve tracking particle motions through time and identifying image pairs for stereoscopic matching.

Stereoscopic imaging velocimetry may benefit many fluid experiments now being contemplated—such diverse experiments as the study of multiphase flow, bubble nucleation and migration, pool combustion, and crystal growth. Such a system will be useful to the microgravity science community as knowledge of heat-transfer, surface-tension, and concentration-gradient-driven anomalies and residual effects from g-jitter are enhanced through investigations of fluid behavior in reduced-gravity environments. A fully operational breadboard system should be complete by mid-1995.

Lewis contacts: Mark D. Bethea, (216) 433–8161;
Thomas K. Glasgow, (216) 433–5013
Headquarters program office: OLMSA

Thermal Equilibration Studied in One-Component Critical Fluid

The “critical point” of a pure fluid is the thermodynamic state with uniquely defined temperature and pressure at which the liquid and gas phases of a pure substance become indistinguishable. Moreover, at the critical point the fluid is highly compressible. The diverging compressibility under normal gravity causes the fluid to collapse under its own weight and results in only a very thin critical zone usable to study the critical-point phenomenon. To perform critical-point phenomenon research, a microgravity environment is needed because it reduces the weight of the fluid and widens the critical zone, allowing closer approach to the critical point. Critical-point phenomenon research

can be applied to a wide range of fluids, including "supercritical fluids," which are simultaneously dense and compressible. Supercritical fluids are increasingly being used in a number of technological applications, such as caffeine extraction from coffee. However, the real motivation of this science is fundamental research. Scientists hope that the current research in nonequilibrium dynamics can enable future economic opportunities and activities as yet unforeseen.

In general, a fluid can receive or release energy or transfer energy from one part of the fluid to another in two ways: heat diffusion and imposed work (e.g., pressure-volume work). Very close to the critical point these two energy transfer mechanisms become quite different—with very different time scales. Studying quantitatively the competition and the interaction of these mechanisms is the goal of this experiment, which consists of two parts, each with its own separate thermostat. One part, called Thermal Equilibration Bis (TEQB), studies heat diffusion. The other part, called Thermal Adiabatic Fast Equilibration (AFEQ), studies how pressure-volume work transports energy. Each thermostat has one interferometer and one visualization cell. Each cell will contain a layer 1 or 2 mm thick of the fluid sulfur hexafluoride (SF_6) confined between parallel transparent windows and at the proper critical density.

The response of the fluid in the TEQB cells was monitored by video camera, light attenuation, and interferometry. Because fluid opalescence (light attenuation) becomes more intense near the critical point, it is a sensitive measure of temperature changes. Interferometry gives information on the local fluid density changes in various parts of the cells. An analysis of the time evolution of the interferograms determines the rate of relaxation of the fluid toward equilibrium, as a function of how far it is away from the critical temperature.

In AFEQ the temperature of the fluid is changed in the normal way by changing the temperature of the confining cell. More attention was directed to the rapid changes in the fluid that are induced internally, by heat from a current pulse through a resistance wire inside the cell. The wire was also used as a high-voltage electrode. When the wire was charged to a static potential of 500 V, the resulting pull of the SF_6 molecules into the electric field surrounding the wire causes a local and global density change that can be observed interferometrically. Hence, there are two ways to induce nonequilibrium, one with heat and one without.

AFEQ and TEQB flew on International Microgravity Laboratory 2 (IML–2) in July 1994. They are sequel experiments to TEQ, which flew in January 1992 on IML–1. The principal

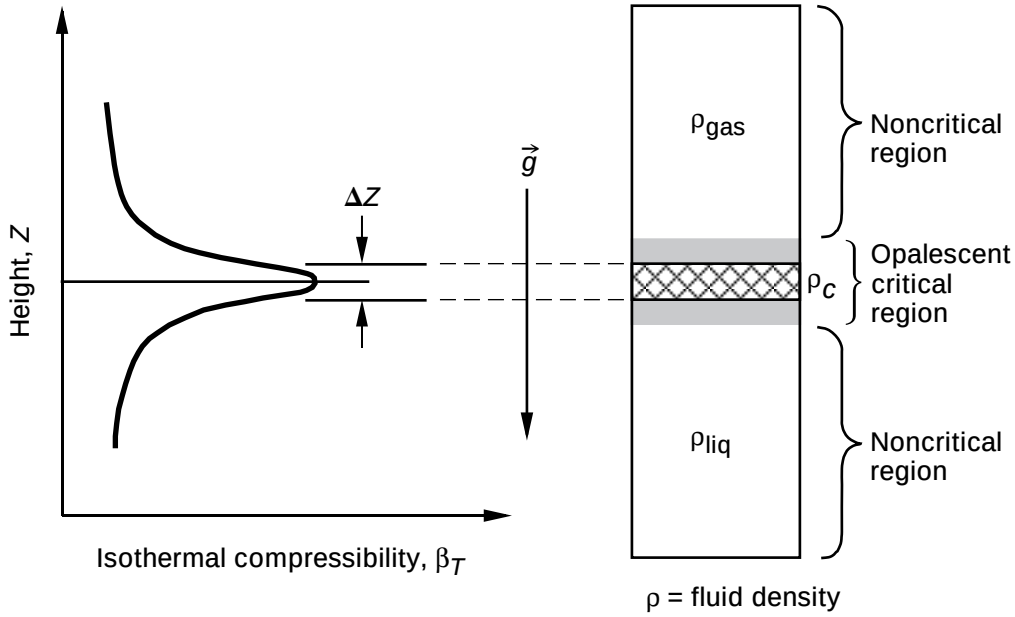

Fluid compressibility with height near critical point. (The smaller g the larger ΔZ and the easier to measure critical fluid properties.)

investigator for the AFEQ and TEQB experiments was Professor Richard Ferrell from the University of Maryland. The AFEQ–TEQ team, based at NASA Lewis, designed and built the test cells.

The AFEQ–TEQB experiment team is now developing the necessary software to store and access the digital images acquired during the experiment and converting the high-rate-multiplexer videotapes from the European video standard (PAL) to the National Television System Committee (NTSC) configuration. Moreover, the team, the principal investigator, and the co-investigators are analyzing the data from AFEQ and TEQB events performed by the critical-point facility on IML–2. For instance, analyses of the fringe-shift data induced by a heat pulse and electric field in the AFEQ cell and of the relaxation time constant of SF_6 fluid in the TEQB cell are under way.

Bibliography

Behringer, R.P.; Onuki, A.; and Meyer, H.: Thermal Equilibration of Fluids Near the Liquid-Vapor Critical Point: He_3 and He_3-He_4 Mixtures. J. Low Temp. Phys., vol. 81, no. 1, 1990, pp. 71–102.

Boukari, H.; Shaumeyer, J.N.; Briggs, M.E.; and Gammon, R.W.: Critical Speeding up in Pure Fluids. Phys. Rev. Lett., vol. 65, no. 2654, 1990, pp. 2260–2263.

Ferrell, R.A.; and Hao, H.: Adiabatic Temperature Changes in a One-Component Fluid Near the Liquid-Vapor Critical Point. Physica A, vol. 197, 1993, pp. 23–46.

Moldover, M.R.; Sengers, J.V.; Gammon, R.W.; and Hocken, R.J.: Gravity Effects in Fluids Near the Gas-Liquid Critical Point. Rev. Mod. Phys., vol. 51, no. 1, Jan. 1979, pp. 79–99.

Onuki, A.; and Ferrell, R.A.: Adiabatic Heating Near the Gas-Liquid Critical Point. Phys. A, vol. 164, 1990, pp. 245–264.

Onuki, A.; Ferrell, R.A.; and Hong, H.: Fast Adiabatic Equilibration in a Single-Component Fluid Near the Liquid-Vapor Critical Point. Phys. Rev. A, vol. 41, no. 4, 1990, pp. 2256–2259.

Zappoli, B.; Dailly, D.; Garrabos, Y.; LeNeindre, B.; Guenoun, P.; and Beysens, D.: Anomalous Heat-Transport by the Piston Effect in Supercritical Fluids Under Zero Gravity. Phys. Rev. A, vol. 41, no. 4, 1990, pp. 2264–2267.

Lewis contacts: Dr. R. Allen Wilkinson, (216) 433–2075; Henry K. Nahra, (216) 433–5385
Headquarters program office: OLMSA

Advanced Space Analysis

Solar Electric Propulsion Proposed for Diana Mission

NASA Lewis not only works to develop space technologies that contribute to U.S. leadership, but also works with industry and end-user organizations to infuse technologies into civilian space system development efforts. During 1994 Lewis has placed special emphasis on xenon ion solar electric propulsion, with the goal of developing partnerships with industry and user communities to apply this technology whose time has come.

The NASA Solar Electric Propulsion Technology Application Readiness (NSTAR) Program began ground testing during 1994 to validate 30-cm xenon ion propulsion for flight readiness. In parallel, the Advanced Space Analysis Office led an intracenter team to identify opportunities for the first application of this technology. We identified the NASA Office of Space Science's Discovery Program, which issued an announcement of opportunity for planetary missions in summer 1994, as an excellent chance to propose a NASA first application of xenon ion solar electric propulsion to pave the way for infusion of this technology.

In advance of the announcement of opportunity, we contacted members of the planetary science community to identify promising missions for

solar electric propulsion application. We also performed analyses to identify the feasibility of mission applications and to develop a top-level mission concept. During spring 1994 we identified an exciting mission to the Moon and on to Comet Wilson-Harrington. This mission takes unique advantage of the benefits of solar electric propulsion by reaching two inner solar system targets on one mission—an impossible feat with chemical propulsion within the constraints of the Discovery Program.

The lunar/cometary mission, named Diana for the Greek goddess of the Moon and the hunt, was proposed to the Discovery evaluation process in October 1994. Although the winners will not be known until early 1995, the Diana mission concept has nonetheless demonstrated the feasibility and benefits of 30-cm xenon ion solar electric propulsion for practical application to low-cost, constrained-schedule programs such as Discovery.

Lewis contact: Mark Hickman, (216) 977–7105
Headquarters program offices: OSS and OSAT

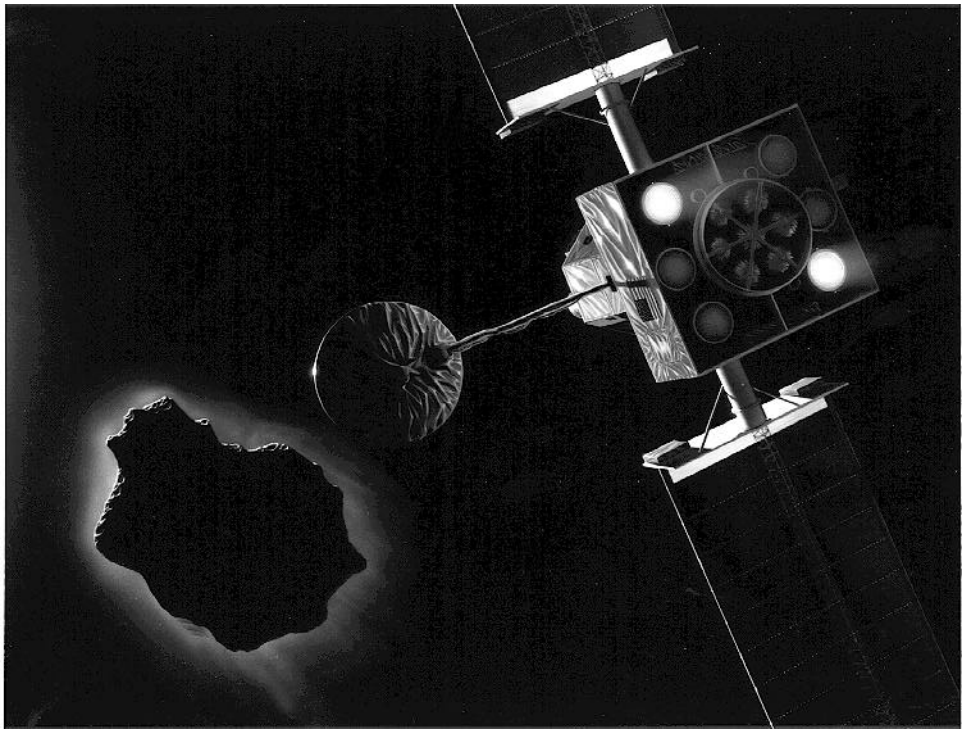

Artist's illustration of Diana solar electric propulsion spacecraft concept developed as a Discovery mission to the Moon and Comet Wilson-Harrington.

Engineering and Computational Support

Structural Systems

Acoustic Fill Effects Test Program Completed

Understanding acoustic fill effects for specifying an acoustic environment is critical for payload hardware design and testing. Fill effects is the term used to describe the changes in the interior sound levels of an expendable launch vehicle's (ELV's) payload fairing or the space shuttle's cargo bay caused by the presence of the payload. Often, the acoustic environment defined for the shuttle or an ELV represents the unfilled environment (i.e., the environment expected for an empty cargo bay or payload fairing). It then becomes necessary to account for the presence of the payload fill and its effects on the interior acoustic environment.

Before this test program the fill effects on the acoustic environment were determined from one of three fill factor curves available within the aerospace community. To reduce disputes between multiple organizations involved with a NASA program while maintaining the proper acoustic environments, NASA had to develop a fill effects standard.

NASA Lewis, in conjunction with General Dynamics Space Systems Division (GDSSD), has completed a test program to investigate the acoustic fill effects for an unblanketed payload fairing. This testing was performed in March 1994 at GDSSD's acoustic test facility. Excellent test data were obtained and used to quantify the effects of payload shape, size, and volume on the acoustic levels for four spacecraft payloads.

The test data were also used to benchmark a statistical energy analysis methodology that can predict the fill effects for any size payload. This methodology has been incorporated into the 1994 NASA standard Payload Vibroacoustic Test Criteria.

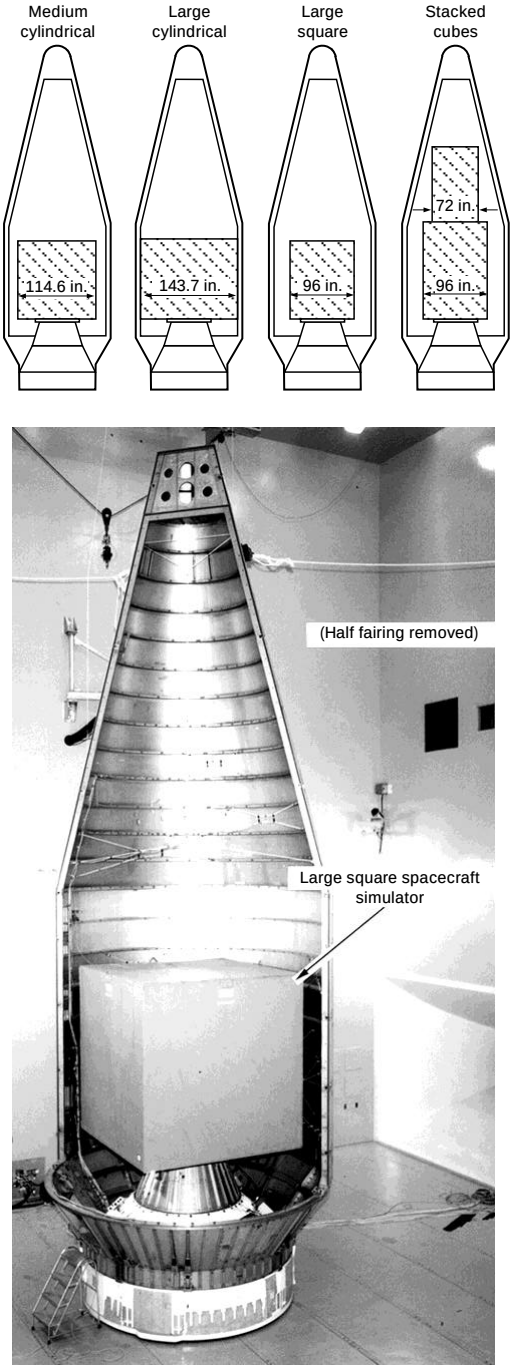

Spacecraft payload acoustic test configurations and test setup for large square spacecraft simulator.

Bibliography

Forssen, B.: Test Plan for Measuring Acoustic and Structural Responses of Generic Spacecraft/Nose Fairing Configurations. General Dynamics Space Systems Division, 1994.

Hughes, W.O.; McNelis, M.E.; and Manning, J.E.: NASA LeRC's Acoustic Fill Effects Test Program and Results. NASA TM–106688, 1994.

Lewis contacts: William O. Hughes, (216) 433–2597; Mark E. McNelis, (216) 433–8395
Headquarters program office: OSAT

Computational Support

Personal-Computer-Based Data Acquisition System Developed

NASA Lewis has about 60 medium- to large-scale facilities for testing space and aeronautical structures, systems, and components—from full-scale jet engines to chemical rockets, multistage compressors, single-cell batteries, and simple stationary airfoils. The Scientific Data Systems group at Lewis has supported these test facilities with a scaleable set of minicomputer-based data systems for many years, using an evolved suite of on-line data-processing services. Also supporting these test facilities are numerous test stands and laboratories with less-demanding data acquisition requirements, and typically less funding for data acquisition systems. Over the past year we have developed a prototype, low-cost, personal-computer-based data acquisition system for use in small-scale test facilities.

For example, the NASA Solar Electric Propulsion Technology Application Readiness (NSTAR) Program's ion thruster is a state-of-the-art design thruster for satellite stationkeeping applications. It uses the ionization of a rare gas, such as xenon, to produce a very efficient low-thrust beam. An experiment was undertaken to demonstrate 2000 hr of continuous operation of the NSTAR thruster in a space vacuum tank at Lewis. The data acquisition requirements were to acquire, monitor, and record thruster voltages, currents, and gas flows and to provide open-loop control of a pair of thruster preheaters. The data acquisition hardware selected for this task consisted of a 16-channel analog-to-digital converter, a 16-channel analog multiplexer with channel-selectable signal conditioning, and two 4-channel digital-to-analog converters. All these components adhere to the IEEE 488 communications standards. This hardware was interfaced to a 486 DX2 personal computer through a general-purpose interface bus card. The software package LabVIEW for Windows, from National Instruments, was chosen as the programming language. LabVIEW, a graphical programming language, provides a graphical user interface with a data flow programming methodology.

Using LabVIEW, the following suite of services were programmed on the personal computer (PC):

- Data acquisition, engineering unit conversion, limit checking, abort triggering
- Mathematical model execution to calculate thruster performance parameters
- Update of alphanumeric and graphical windows
- Continuous data scanning, timer-based cyclical data recording, limit-violation logging, and circular history file recording
- Real-time backup of data and log records to floppy disk
- Sequenced heater control

For the NSTAR thruster life test the PC is performing these services at a steady 6-sec update rate. Data for the permanent record of the life test are being recorded once per hour. The history file contains a data record for every 2 min over the last hour and is frozen when an abort occurs. The PC can shut down the thruster in response to either low vacuum tank pressure or degraded performance of any of several thruster measurements. To date, the NSTAR ion thruster has logged over 1200 hr of operation. The total cost for the PC-based data acquisition system was less than $10,000, including the cost of the PC.

Lewis contact: Vincent J. Scullin, (216) 433–5156
Headquarters program office: OSAT

Asynchronous-Transfer-Mode Application Program Interface Developed To Support Parallel Virtual Machine

Two projects that use Fore Systems asynchronous-transfer-mode (ATM) interfaces required us to examine and possibly modify or develop the adapter and the application program interface (API) code. Both projects use ATM as a high-speed data communications medium in a distributed processing environment, such as the parallel virtual machine. In particular, we are examining the usefulness of ATM to support cluster-based computing and also as a fabric to provide high-performance communications between supercomputers and high-end workstation clusters. We need to determine if ATM will provide sufficient performance for the level of integration and interoperability required.

Both projects require not just high throughput but also low latency. Low latency is needed in a connectionless style of communications (as in personal or switched virtual circuits with rapid bandwidth reallocation capability) when the connectivity patterns are not known a priori, as well as in a more connection-oriented style. For example, in a parallel application written to execute on an Intel, the connectivity patterns are well known, and we could map a virtual topology to the ATM network so that the program could run without modification. Low-latency support is required in the context of a local environment. Geographically distributed computing will always have a high latency owing to the propagation delay, but we can often overlap this through problem partition.

Because we are using ATM for its high speed, we need to reduce the overhead that diminishes its performance. Much of the difficulty in terms of latency results from context switches and invoking the operating system through system calls. It is our understanding that the API was developed with the primary goal of increasing the maximum throughput. We intend to examine the API to see if the latency can be reduced, perhaps with a slight tradeoff in throughput, while also retaining the multiuser nature of the design.

We also want to examine a possible high-performance, single-user mode, which might be useful to a cluster, such as the Lewis Advanced Computing Environment (LACE), where general communication would be supported through the usual network (Ethernet, Fiber-Distributed Data Interconnect (FDDI), and Fiber Channel) and interprocessor communication would be supported over the ATM network. This configuration would significantly reduce API overhead but would constrain use of the interface to a single user. This secondary objective will be useful in specialized situations, such as with the LACE cluster, but will not be of general interest due to the strong constraint.

The first project using Fore System's ATM is an initial study of porting a version of a message-passing library, such as the parallel virtual machine or the message-passing interface, to communicate directly over ATM by way of the API. This capability will be needed because we expect that, once we have the API code and understand how it works, we will need to optimize use of the ATM API by the message-passing library to most effectively use this resource. Also, we will examine the possibility of having direct communication "hooks" in the adapter code. This particular application is usually characterized by initial broadcast traffic and then bursty and intermittent traffic.

The second project is a study of ATM as a communications medium between a supercomputer and high-end workstation clusters. The supercomputer generates numerical data, and the workstations are used for distributed computation, data fusion, and graphic visualization. Hardware inadequacies make it necessary to stripe the data over multiple network interfaces. To reduce the costs associated with this operation, we will examine the possibility of moving this striping function into the lower level code of the adapter or API.

Lewis contact: Jose M. Davis, (216) 433–5407
Headquarters program office: OA

Satellite and Terrestrial Network Applied to Engine Inlet Simulation

One of the ways NASA Lewis supports the High-Performance Computing and Communications (HPCC) Program is by developing new technology that will help U.S. industry maintain its world leadership and then transferring this technology in a timely manner. A technology that will help

make the U.S. aerospace industry more technologically and economically competitive is the Numerical Propulsion System Simulation (NPSS), a "numerical test cell" that will use high-speed computing and communications in place of conventional testing.

Because the current communications networks connecting Lewis to its industrial collaborators cannot provide the necessary bandwidth for remote flow visualization, the HPCC Office is proposing use of the Advanced Communications Technology Satellite (ACTS) to link Lewis with remote industry sites. This concept will be tested by using ACTS to link Boeing and Lewis as they conduct a remote turbine engine inlet simulation in support of the High-Speed Civil Transport Program.

The purpose of this study is to prototype a "numerical wind tunnel" using high-speed computing and communications in place of a conventional wind tunnel. A series of numerical experiments will be conducted to develop a mixed-compression inlet control system, but these studies should be prototypical of any remote numerical analysis that requires near "real time" results. The inlet simulator will be executed on the Lewis Cray YMP supercomputer but controlled by Boeing in Seattle, Washington. Flow visualization information will be transported by ACTS to the remote site for quasi-real-time display on high-performance, three-dimensional graphics workstations.

The experimental ACTS satellite network will allow aerospace manufacturers to remotely access NASA's distributed engine inlet simulation application. Synchronous Optical Network/asynchronous transfer mode (SONET/ATM) traffic studies will be performed on the experimental network to evaluate its performance in the NASA engine inlet simulation application. The network's performance for this application will be optimized experimentally and then compared with the performance of an all-terrestrial, long-haul SONET/ATM network for this application.

Bellcore's High-Speed Switching and Storage Technology Division will participate with NASA Lewis in systems engineering and traffic studies on the experimental high-speed SONET/ATM test bed. This test bed operating at both the 622- and 155-Mbps rates will interconnect a Cray YMP supercomputer at NASA Lewis to high-end workstations at Boeing.

This experimental network will be among the first integrated demonstrations of numerous advanced high-speed technologies in support of state-of-the-art aeronautical and network research.

Lewis contact: Isaac Lopez, (216) 433–5893
Headquarters program office: OA

Heterogeneous, Geographically Dispersed ATM-Based Distributed Computing Assessed

NASA Lewis has experimentally assessed the coupling of two emerging fields: asynchronous transfer mode (ATM) and cluster-based computing. Cluster-based computing has become an area of serious interest owing to the large numbers of commonly available high-end workstation processors. The goal is to harness the enormous number of idle computing cycles for use in a distributed application. The economic factors and the risk amortization, when compared with the purchase of a supercomputer system, make this approach extremely attractive.

However, cluster-based computing requires a network to support low-latency interprocessor communication. Although approaches such as Fiber-Distributed Data Interconnect (FDDI) have been developed for this environment, ATM is particularly attractive mainly for its low-cost, scaleable performance and its potential support of geographically distributed computing. Low cost is essential. One reason why ATM has attracted so much interest in this environment is its initial lower cost compared with FDDI interface cards when they were first introduced.

This work uses an ATM test bed to evaluate the performance implications of flow creation and warm-start behavior. It also identifies the latency and throughput characteristics achievable via the traditional protocol stack of transmission control protocol/Internet protocol (TCP/IP), with both ATM adaptation layer (AAL) 3/4 and AAL 5. The overhead of the message-passing library, such as parallel virtual machine (PVM), which uses the user datagram protocol (UDP), is examined. The NASA numerical aerodynamic simulation (NAS)

benchmark suite is used to study application-level performance implications of the processes communicating through PVM on the ATM test bed. The operating system interface to PVM is then modified to circumvent UDP/IP and allow direct communication between the adaptation layer and the message-passing library to assess the performance implications of eliminating the transport layer protocol overhead together with the additional buffer copies.

Lewis contact: Russell W. Claus, (216) 433–5869
Headquarters program office: OA

High-Performance Computing and Communications K–12 Project Supports Schools

NASA Lewis began the K–12 project to inspire students from kindergarten through high school to pursue careers in science and engineering. A particular focus is on underrepresented schools and minorities.

We have involved teachers early on and continually throughout the project, making training available to raise all participants to the same level of expertise and to standardize on computing platforms so that all participants could easily share advances within the project. The K–12 project focuses on three areas of development:

- Teacher and student training
- Curriculum supplemental material
- Computing and network infrastructure within the schools

We have trained 25 teachers from 14 schools, high school and elementary, and have given nine schools Apple MacIntoshes and network equipment for connecting to Internet. The two-week teacher training conducted each summer consists of instruction by Lewis personnel on topics including Mac Basics, Internet, visualization, computer languages, Unix, Interactive Physics, Maple, Animation Works, and Spyglass. One result is that Barberton High School will teach a new course entitled High Performance Computing at the 10th and 11th grade level. We have implemented customary and innovative network efforts within the K–12 project. Support for connections to Internet ranges from basic telephone line access to a successful implementation of radiofrequency technology at sustained T1 speeds (1.5 Mbps). Cleveland East Technical High School has partnered with Cleveland State University to acquire Internet access and to demonstrate the cost-effective use of this “wireless” communications path.

The K–12 project inspires students, teachers, and NASA personnel to develop and enhance school curricula into living entities that can grow and accommodate the technology already available outside the classroom. The program will continue to provide two weeks of teacher training annually, computers to selected schools, and basic Internet connections. In fiscal 1995 we propose working with the sight impaired and developing the Lewis Teacher Resource Center into a functioning instructional facility for year-round K–12 use.

Lewis contacts: Gregory J. Follen, (216) 433–5193; Gynelle C. Mackson, (216) 433–8258

Lewis Research Academy

Turbomachinery Flow Codes Made Available to Industry

A mathematical analysis has yielded a set of equations governing the conceptual flow model used to design turbomachinery blading. These equations govern the time-averaged flow state existing within a typical passage of a blade row embedded in a multistage machine. They have formed the basis of a series of computer codes, some of which have been written to operate on parallel computing platforms. This flow model is called the average-passage flow model. To date, these codes have been used to examine radial, mixed, and axial flow turbines and axial and centrifugal compressors. These simulations addressed subsonic, transonic, and supersonic machines.

The computer code that solved for the time-averaged flow state existing within a typical passage of a blade row and the code for the associated unsteady flow state have been made available to industry. In addition, gas turbine manufacturers have begun to incorporate the average-passage flow model into their design systems. Results obtained by industry researchers clearly show the unique prediction capability of both the time-averaged and unsteady flow solvers.

Lewis contact: Dr. John J. Adamczyk, (216) 433–5829
Headquarters program office: OA

New Technique Calculates Properties of Surface Alloys for Immiscible Metals

Recently, some exciting new experimental observations have been made with the scanning tunneling microscope regarding the formation of surface alloys from immiscible materials (ref. 1). Gold, which would not mix with nickel in the bulk, was incorporated into the top atomic surface layer of nickel. This result leads to the fascinating possibility of having a new class of materials that can alter the catalytic properties of surfaces as well as have special bonding properties at interfaces. An example would be electrical contacts on high-temperature silicon carbide electronic components.

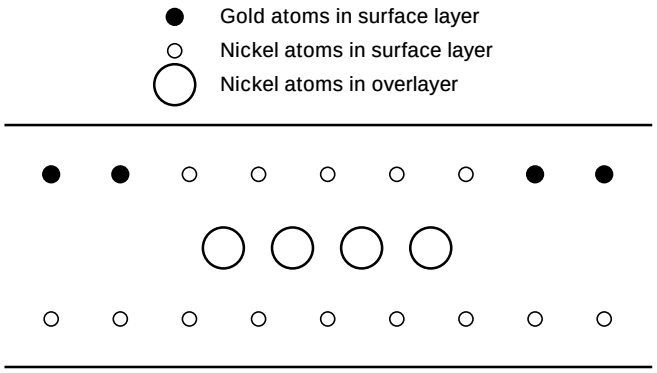

Lowest energy configuration for gold-nickel surface alloy for 0.067 monolayer coverage.

The experimental exploration of this class of materials requires specialized equipment and a great deal of effort. We have applied a new theoretical technique for calculating alloy properties: the Bozzolo, Ferrante, and Smith method (BFS) (ref. 2), invented at NASA Lewis to study these alloys. With a minor theoretical effort we were able to verify the experimental results—a surface alloy in the top atomic plane for coverages less than half a monolayer, no incorporation of the gold into the second layer, and phase separation for coverages greater than half a monolayer. We also examined a wide range of geometrical configurations that would be difficult to resolve experimentally. The illustration shows the preferred configuration from both the experiment and our predictions.

The efficiency of the BFS method will allow the examination of a multitude of possible materials, which, combined with ab-initio methods, will enable both the bonding and electronic properties of the materials to be determined. These efficient theoretical methods will aid in recommending the best candidate materials for various catalytic, structural bonding, and electronic applications.

References

1. Pleth Nielsen, L.; Besenbacher, F.; Stensgaard, I.; Laegsgaard, E.; Engdahl, C.; Stolze, P.; Jacobsen, K.W.; and Norskov, J.K.: Initial Growth of Au on Ni(100): Surface Alloying of Immiscible Metals. Phys. Rev. Letters, vol. 71, Aug. 1993, pp. 754–757.

2. Bozzolo, G.; Ibanez-Meier, R.; and Ferrante, J.: Growth of Au on Ni(100): A BFS Modeling of Surface Alloy Phases. NASA TM–106732, 1994.

Lewis contact: Dr. John Ferrante, (216) 433–6069
Headquarters program office: OA

Extended Mixing and Transition Control Theory Evaluated Numerically

Considerable progress in understanding nonlinear phenomena in both unbounded and wall-bounded shear flow transition has been made by using a combination of high-Reynolds-number asymptotic and numerical methods. But we are working to fully understand the nonlinear dynamics so that, ultimately, effective means of mixing and transition control can be developed and better understanding of the source terms in the aeroacoustic noise problem achieved.

Two important aspects of the analyses are

- That the disturbances must evolve from strictly linear, finite-growth-rate instability waves on weakly nonparallel mean flows so that the proper upstream conditions are applied in the nonlinear or wave-interaction streamwise region
- That the question of proper outflow boundary conditions—still a research issue for direct numerical simulations of convectively unstable shear flows—not arise, since the asymptotic formulations lead to parabolic problems

Composite expansion techniques are used to obtain solutions that account for both mean-flow evolution and nonlinear effects.

A previously derived theory for the amplitude evolution of a two-dimensional instability wave in an incompressible mixing layer—which agrees quantitatively with available experimental data for the first nonlinear saturation stage of a plane-jet shear layer, a circular-jet shear layer, and a mixing layer behind a splitter plate—has now been extended to include a wave-interaction stage with a three-dimensional subharmonic. The ultimate wave-interaction effects can give rise to either an explosive growth or an equilibrium solution, both of which are intimately associated with the nonlinear self-interaction of the three-dimensional component. The extended theory is being evaluated numerically.

Wall-bounded shear flow transition in technological devices often occurs in regions with adverse-pressure gradients, causing the onset of turbulence usually within a relatively short streamwise distance. The unsteady flow evolves through a number of stages. For sufficiently small initial disturbances the initial nonlinear stage is associated with a resonant-triad interaction between a fundamental two-dimensional mode and a pair of oblique subharmonic modes. Some of the details depend on the relative amplitudes of the components. When the initial subharmonic amplitude is larger than that of the fundamental, the wave interaction rapidly becomes fully coupled. In the opposite situation the fundamental initially undergoes nonlinear saturation due to self-interaction effects, and subharmonic evolution becomes controlled by the parametric-resonance effects. The subharmonic amplitude continues to increase during this nonlinear-fundamental stage, even when the fundamental amplitude saturates, eventually becoming large enough to influence the fundamental. Thus, the fully coupled stage of development also occurs in this situation—but now with viscous effects being unimportant. The amplitude solutions in the fully coupled stages always end in a finite distance singularity. The theoretical predictions are being compared with available experimental results.

Bibliography

Goldstein, M.E.; and Lee, S.S.: Fully Coupled Resonant-Triad Interaction in an Adverse-Pressure-Gradient Boundary Layer. J. Fluid Mech., vol. 245, 1992, pp. 523–551.

Wundrow, D.W.; Hultgren, L.S.; and Goldstein, M.E.: Interaction of Oblique Instability Waves With a Nonlinear Plane Wave. J. Fluid. Mech., vol. 264, 1994, pp. 343–372.

Lewis contact: Dr. Lennart S. Hultgren, (216) 433–6070
Headquarters program office: OA

Thermal Radiation Effects Analyzed in Semitransparent Materials

Ceramic materials and coatings must be used for some engine parts to withstand the high temperatures in advanced aircraft engines. Some ceramics are partially transparent to thermal radiation in some portions of the radiation spectrum. Infrared and visible radiation from hot surroundings, as in a combustion chamber, can penetrate the material and heat it internally—like heating food in a microwave oven. Because engines operate at high temperatures, emission of radiation within the semitransparent materials is also important. Internal temperatures depend on radiative effects combined with heat conduction and convective heating or cooling at the boundaries. In addition to steady conditions, transient heating effects must be considered, since radiant penetration can provide more rapid internal heating than conduction alone. Analytical and numerical methods are being developed to predict steady and transient internal temperatures in composites with properties typical of ceramics. The solutions provide thermal performance, and the temperature distributions can be used to examine thermal stresses.

The use of radiative analysis to predict temperature distributions and heat flows in partially transmitting materials is a continuing in-house effort. Composites of several layers are being analyzed where each layer can have a different refractive index. The differing refractive indices cause internal reflections at the internal interfaces and boundaries. The reflections tend to distribute energy within the layers by providing additional transmission paths in the portions of the spectrum that are not optically dense—affecting the temperature distributions within the layers.

The radiative transfer relations are rather complex integral equations, so it is useful to consider approximate techniques that might be incorporated more conveniently into computer design programs. One approximate technique is the two-flux method. It has the form of simultaneous differential equations and is relatively easy to solve for layers that are not optically dense. For dense layers a radiative diffusion method can be used that has the form of a single differential equation. In some recent work these methods were combined to obtain steady-state thermal behavior of a two-layer composite where one layer is optically dense. The approximate solutions were compared with numerical solutions of the radiative transfer equations.

The graph shows results for a somewhat-transparent coating (layer 1) on a substrate (layer2) that is more optically dense. Radiative penetration is reduced in the dense substrate, and heat conduction is more dominating. The coating has two spectral absorption bands. Both external boundaries are being cooled by convection. The three sets of curves are for various levels of radiation flux incident on the hot side. Temperature distributions by the two-flux and diffusion method are in excellent agreement with the numerical solutions. The total heat flow through the composite by combined radiation and conduction agrees within better than 1% with the numerical results.

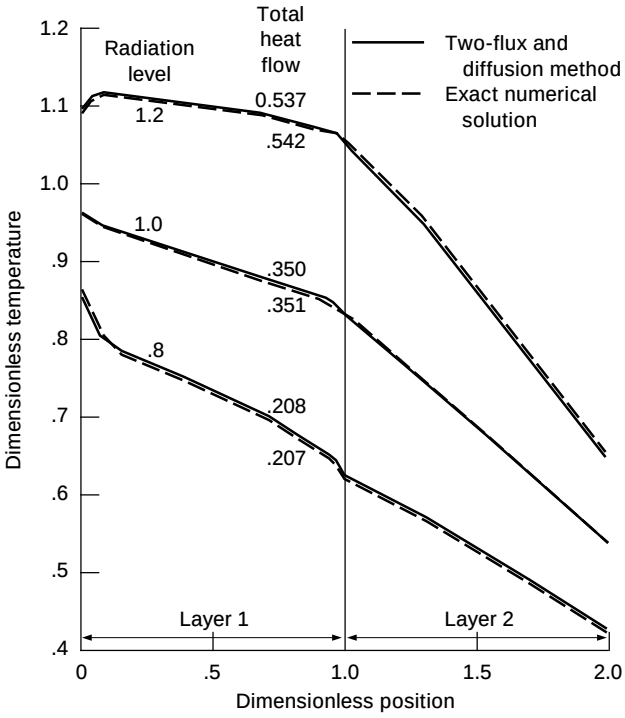

Temperatures and heat flows predicted by combined two-flux and diffusion method in two-layer composite with refractive indices of 1.5 and 3.

Bibliography

Siegel, R.; and Spuckler, C.M.: Approximate Solution Methods for Spectral Radiative Transfer in High Refractive Index Layers. Int. J. Heat Mass Trans., vol. 37, suppl. 1, Mar. 1994, pp. 403–413.

Siegel, R.: Refractive Index Effects on Transient Cooling of a Semitransparent Radiating Layer. To be published in J. Thermophys. Heat Trans., vol. 9, 1995.

Spuckler, C.M.; and Siegel, R.: Refractive Index and Scattering Effects on Radiation in a Semitransparent Laminated Layer. J.Thermophys. Heat Trans., vol. 8, no. 2, Apr.-June 1994, pp.193–201.

Spuckler, C.M.; and Siegel, R.: Two-Flux and Diffusion Methods for Radiative Transfer in Composite Layers. Presented at ASME Winter Annual Meeting, Chicago, IL, Nov. 6–11, 1994.

Lewis contact: Dr. Robert Siegel, (216) 433–5831
Headquarters program office: OA

Technology Transfer

Feature Extraction Improves Rocket Engine Operational Efficiency

Increased launch vehicle flight reliability and reduced operational costs are targeted by the aerospace industry. Continuous and comprehensive automated monitoring and analysis of launch system data are key elements in achieving these objectives. Automated analysis mimics the reasoning used by engineers during pre- and postflight checkout. Feature extraction, the identification of prominent events of a sensor trace, enables this automation by identifying both scheduled and unscheduled events in the launch vehicle data stream. Feature extraction algorithms and technology developed to aid space shuttle main engine testing and checkout were applied to Atlas-Centaur data and transferred to Martin Marietta. With minor modifications these algorithms successfully identified drifts, level shifts, peaks, and spikes in pneumatic and electrical data. Detecting these features on a variety of electrical and mechanical systems has demonstrated the flexibility of the algorithms.

To meet the requirements of a fast, thorough system that is operationally efficient and increases vehicle reliability, Martin Marietta has undertaken a development program using a rule-based expert system to automate data analysis tasks. Given the large amount of data that must be analyzed, it is not feasible to reason on each data sample. To function efficiently and to minimize demands on system engineers, automated analysis processes must be event driven. Specific system events can be identified by characteristic signatures of associated vehicle measurements. Once the events in the data stream have been identified, the expert system can be used to distinguish and resolve expected and unexpected events.

NASA Lewis has developed and demonstrated feature extraction algorithms for a post-test diagnostic system (PTDS). The PTDS is an off-line aid to engineers who are responsible for detecting and diagnosing space shuttle main engine (SSME) anomalies. Feature extraction algorithms are at the root of the PTDS. These algorithms provide events to the rule-based expert system in the PTDS. They identify deviations within the data stream during steady-state operation. The algorithms reduce sensor traces into peaks, level shifts, spikes, and drifts; detect excessive noise, exceedance violations, and erratic regions; and check for consistency among redundant channels.

The feature extraction algorithms, as developed for the SSME PTDS, are inherently independent of the system to which they are applied. A

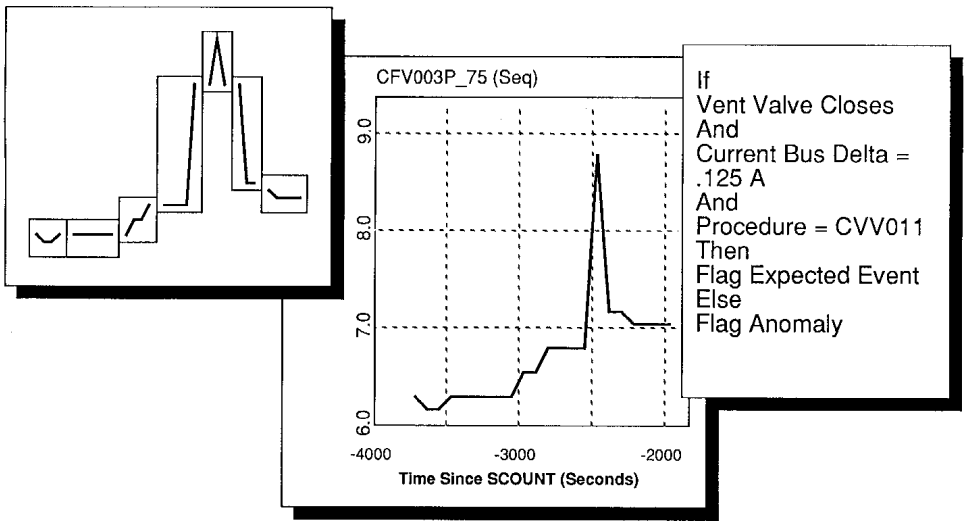

Feature extraction.

cooperative effort between Martin Marietta and Lewis was undertaken to demonstrate the flexibility of the algorithms and to transfer the feature extraction technology and code to Martin. The effort successfully applied four feature extraction algorithms (spikes, level shifts, drifts, and peaks) to 15 parameters from the Centaur pneumatic and electrical subsystems and was completed within four months.

The feature extraction algorithms are being validated and will be incorporated into a ground-based expert system to enable automated data monitoring and analysis in support of day-to-day test and checkout activities. This work, to be implemented at Cape Canaveral, will reduce diagnostic time by an order of magnitude and increase diagnostic accuracy. Activities are planned to complete transfer of the algorithms and to aid in applying them to Atlas-Centaur propulsion system parameters.

Bibliography

Erickson, T.J.; Zakrajsek, J.F.; Sue, J.J.; Jankovsky, A.L.; Fulton, C.E.; and Meyer, C.M.: Post-Test Diagnostic System Feature Extraction Applied to Martin Marietta Atlas-Centaur Data. AIAA Paper 94–3224, June 1994.

Zakrajsek, J.F.: The Development of a Post-Test Diagnostic System for Rocket Engines. AIAA Paper 91–2528, June 1991.

Zakrajsek, J.F.; Fulton, C.E.; and Meyer, C.M.: Feature Extraction for Post-Test Diagnostics. Advanced Earth-To-Orbit Propulsion Technology Conference 1994, May 1994.

Lewis contact: June F. Zakrajsek, (216) 977–7470
Headquarters program office: OSAT

Advanced Arcjet Technology Commercialized

First-generation arcjets are now operational on the AT&T Telstar 401 spacecraft and are baselined on three other geosynchronous satellite series. The arcjet system (thruster, power processor, and gas generator) uses electrical energy from the spacecraft batteries to increase the enthalpy of the propellant before it is exhausted at high velocities through a conical converging/diverging nozzle. Use of an arc discharge heating process is the unique feature of the device. Although the arc reaches temperatures of 17,000 °C, the engine design ensures that critical internal surfaces are protected by a cool gas boundary layer. Materials limits inherent to conventional thrusters are thus avoided, and the first-generation devices, with an average specific impulse level of 502 sec, have more than 1.5 times the fuel economy for north-south stationkeeping of state-of-the art chemical and

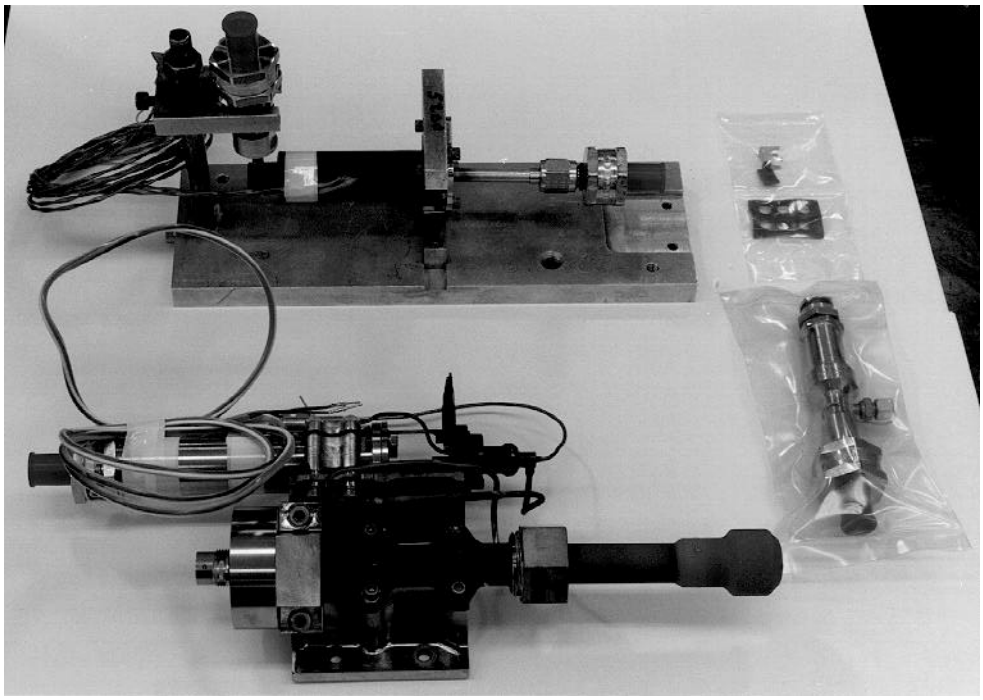

Advanced hydrazine arcjet system.

resistojet systems (ref. 1). Following acceptance of the technology on commercial satellites, an industry requirement for higher performance arcjets was identified, and a 600-sec arcjet was baselined on a new (next generation) satellite series. A NASA Lewis/industry effort to develop next-generation hydrazine arcjets has just been completed. The program has developed and demonstrated a 2-kW arcjet with a mission-average specific impulse of 607 sec and a 1000-hr/1000-cycle life.

The high-performance arcjet program was conducted through in-house efforts and a contract with Olin Aerospace Co. The successful completion of the program has resulted in the technology being added to Olin's product line. Early program efforts demonstrated that state-of-the-art materials used for the anode have unacceptable throat deformation at the higher temperatures encountered at higher performance levels. After an extensive search a high-strength, high-temperature material was identified. This tungsten-based alloy containing rhenium, hafnium, and carbon was first developed at NASA Lewis. Initial tests of an anode made from the material indicated that its performance would exceed program goals (ref. 2). A commercial source for the new alloy was established, and a flight-representative system was fabricated. After 1000 hr of operation at an average specific impulse level of 607 sec, the test was voluntarily terminated. Post-test examination showed minimal erosion.

The long-term program goal is to ensure U.S. competitiveness in low-thrust arcjets. The program is investigating strengthening the new tungsten alloy to increase thruster performance even further. Also, efforts have been redirected toward lower power level thrusters to provide propulsion options for smaller, power-limited spacecraft.

References

1. Curran, F.M.; and Byers, D.C.: New Developments and Research Findings: NASA Hydrazine Arcjets. AIAA Paper 94–2463, 1994.

2. Lichon P.G.; and Sankovic, J.M.: Development and Demonstration of a 600 Second Mission Average Arcjet. IEPC Paper 93–087, 1993.

Lewis contact: John M. Sankovic, (216) 977–7429

Headquarters program office: OSAT

Paint Sampling Automated for Art Restoration

A Lewis resource developed to advance space age materials has been used to better understand ancient works of art.

The Paintings Conservation Laboratory at the Cleveland Museum of Art has as its major role the preservation and restoration of the museum's renowned paintings collection, which ranges from the 13th century to the present day. An essential part of this task is preventive conservation. In some cases deteriorated original canvases have to be infused with adhesive and/or supported by new fabric. Old layers of dirt, discolored varnish, and former restorations are removed, followed by revarnishing and in-painting of losses, to dramatically improve the visual appearance of paintings.

The conservators at the Cleveland Museum of Art often undertake technical research to analyze an artist's technique. The resulting information is used both by conservators and art historians and can sometimes provide the vital clue in questions of authenticity. Important discoveries are added to the growing body of literature on artists' techniques. In paintings with complex layering, cross-sectional analysis is done before attempting a conservation treatment—for instance, when deciding whether a certain paint layer is original or a restoration.

Cross-sectional analysis of paint layers is one of the most valuable methods available to the painting conservator. A cross section displays a chronology of the artist's working methods, from the initial preparatory layers through the paint and varnish layers. The painter builds up the paint layers to develop subtle effects of tone, color, and surface texture, resulting in a complex three-dimensional structure. In addition to being viewed in normal light under a microscope, cross sections can be viewed by using ultraviolet light excitation in association with a variety of filters. Under these different lighting conditions, restoration layers can be distinguished visually from original layers.

The composition of medium-rich layers can often be determined by using biological staining tests, which can be important when deciding whether to remove surface coatings. Where further analysis is necessary to solve a particular cleaning problem or to understand the techniques of a certain

artist, cross sections can be analyzed with the scanning electron microscope. This method determines the element content in the various layers, which gives an indication of pigments present and is a guide to binding media.

Polishing a cross section is difficult because of small sample size and paint chemistries and solubilities. Samples are rarely flat enough for viewing magnifications, and final surfaces are marked by scratches and other flaws. Results of the analyses are rarely of a quality suitable for publication. At the museum cross sections have traditionally been prepared by a hand-operated process from start to finish. First, a chip of paint, no bigger than a pinhead, is removed from the painting with a scalpel. This fragment is mounted and the layers are exposed by sanding and polishing.

Cross-sectional paint samples from an oil painting on canvas by John Harrison Witt (1840–1901) were given to NASA Lewis for experimentation. These samples posed particular difficulties for preparation as one of the lower paint layers is water soluble. During initial attempts to mount specimens in epoxy resin and polyester, we observed contamination from the mounting media on the surface of the cross section. An alternative medium composed of a modified polyester resin eliminated the contamination. The paint specimens were then mounted in standard mounts for automated preparation. All preparation steps were performed using standard NASA polishing techniques. Optical microscopy, with both bright field and polarized light, was used to locate and measure the position of the paint specimen during grinding and polishing. The resulting cross section was perfectly flat, intact, and suitable for photography and further analysis. Automated repolishing of samples after biological staining is also possible.

This automated preparation method has been used successfully on cross-sectional samples from a wide range of paintings in the Cleveland Museum of Art's collection. These include Titian's *Adoration of the Magi* (ca. 1508), Abbott Handerson Thayer's *Self Portrait* (1920), and Martin Johnson Heade's *Point Judith, Rhode Island* (ca. 1867–68).

Lewis contact: William Waters, (216) 433–5564
Headquarters program office: OSAT

New Material Removes Toxic Metals From Waste Water

NASA Lewis is developing a new innovative ion exchange material (IEM), a polymer that removes toxic metals from water. This IEM, a spinoff from research on space battery separators, is a blend of readily available, inexpensive chemicals. It can be made as thin films, fine beads, coated magnetite beads, porous sheets, and fine fibers and as a coating on screens and fibers. Since 1991 the Technology Utilization Office in partnership with Lewis' Office of Environmental Programs has been working to bring this IEM technology from the laboratory to a mature state that will encourage industry to license and market it. (A patent is to be issued in late 1994.)

With the funding assistance of the Lewis Director's Discretionary Fund, the U.S. Environmental Protection Agency (EPA), and the U.S. Army Corps of Engineers, this IEM technology has been significantly advanced. The film form is near maturity. A production run of a 4000-ft-long strip of film was successfully achieved under contract by a small Cleveland-area company, Chemsultants International, Inc. The Southwest Research Institute (SWRI) in San Antonio, Texas, has been conducting research, under a grant, to develop the fine porous bead form of the IEM. Thus far SWRI has successfully produced IEM powder, magnetic particles encapsulated in IEM, and hollow IEM beads. Developing the process to make porous beads is their next project. The technology of fine fibers is still at the laboratory stage.

The uptake performance of the film form has been measured in laboratory tests, with the assistance of Baldwin-Wallace College in Berea, Ohio, and the University of South Florida, using water contaminated with a single toxic metal. Among the 20 metals tested were lead, copper, zinc, cadmium, and mercury. Lead in water was reduced in concentration from 150 parts per billion (ppb) to less than 2 ppb, well below the EPA action limit. Tests to measure the uptake performance of the beads are under way. Other tests have shown that the IEM is easy to use and inexpensive to make; strong, flexible, and not easily torn; and chemically stable in storage, in aqueous solutions, and in acidic or basic solutions. Although no toxicity tests have been performed, it is anticipated that this IEM is safe and nontoxic to handle.

The IEM has a number of important features. Unlike many commercial ion exchange resins, the Lewis IEM removes the metal cations even when calcium is present (i.e., in ordinary hard water). It also promises to be much less expensive than many resins on the market. Its chemical constituents are plentiful and modestly priced, and the manufacturing equipment for making it is quite common. Adsorbed metals can be easily reclaimed by either a destructive or a nondestructive process. In the former the spent IEM is ashed, thereby producing carbon dioxide, water vapor, and oxides of the adsorbed metals, which can be recycled. In the latter the heavy metals are removed from the IEM and reclaimed by acid stripping. The IEM is then reusable and the metal concentrate can be recycled.

Because the commercialization potential for the IEM appears to be very large, the Lewis Technology Utilization Office has been actively working with industry partners to test and evaluate it in industrial applications and to commercialize the technology. The IEM can be used in many industries—electroplating, electronics, and mining, which produces large amounts of waste water containing hazardous amounts of mercury, lead, cadmium, silver, copper, and zinc ions. The TU Office has written agreements with five companies to work with Lewis in joint demonstration tests and evaluations. All say they will use the IEM if its performance and cost effectiveness is acceptable. At least two companies wish to license the technology to make and market it for profit. One important demonstration test scheduled for late 1994 will determine the feasibility of removing the zinc dissolved in the rinse water of a zinc plating operation at the Aetna Plating Co. in Cleveland, Ohio. Cleveland State University and its affiliate the Advanced Manufacturing Center, under a cooperative agreement, are developing the test apparatus and conducting the test.

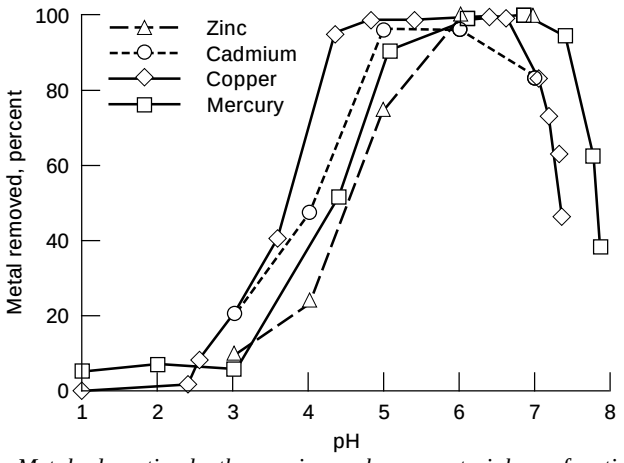

Metal adsorption by the new ion exchange material as a function of the solution pH.

The research done to develop the IEM has produced a number of papers that were delivered at conferences and published. Two were award-winning papers by student interns, one from Baldwin-Wallace College and one from the University of Akron.

Bibliography

Hill, C.M.; Street, K.W.; Philipp, W.H.; and Tanner, S.P.: Determination of Copper in Tap Water Using Solid Phase Spectrophotometry. Analytical Letters, vol. 27, no. 13, 1994, p. 2589. (Also NASA TM–106480.)

Hill, C.M.; Street, K.W.; Philipp, W.H.; and Tanner, S.P.: Spectrophotometric Method for Determining Metal Ion Concentrations in Water Systems Using Ion Exchange Membranes. 44th Pittsburgh Conference on Analytical Chemistry and Applied Spectroscopy, Atlanta, GA, Mar. 1993.

Street, K.W.; Philipp, W.H.; Hill, C.M.; and Tanner, S.P.: Luminescence Technique for Determining Metal Ion Concentrations After Preconcentrating on Ion Exchange Membranes. Abstract 52, Federation of Analytical Chemistry and Applied Spectroscopy Societies, 20th Annual Meeting, Detroit, MI, Oct. 1993.

Philipp, W.H.; Street, K.W.; and Savino, J.: A New Material for Removing Heavy Metals From Waste Water. Technology 2003, Anaheim, CA, Dec. 1993.

Street, K.W.; Philipp, W.H.; Tanner, S.P.; and Hill, C.M.: Preparation and Characterization of a New, Weak Acid Ion Exchange Film. Cleveland Section of American Chemical Society Meeting in Miniature, Cleveland, OH, Mar. 1994.

Talu, O.; Shah, D.B.; Street, K.W.; Philipp, W.H.; and Wan, W.: A New Ion-Exchange Medium for the Removal of Heavy Metal Ions From Aqueous Solution. Presented at American Chemical Society National Meeting, San Diego, CA, Mar. 1994.

Talu, O.; Shah, D.B.; Sun, S.; Street, K.W.; Philipp, W.H.; and Wan, W.: A New Ion-Exchange Media for Heavy Metal Removal From Solutions and Slurries. Presented at American Institute of Chemical Engineers National Meeting, San Diego, CA, Nov.1994.

Talu, O.; Shah, D.B.; Sun, S.; Street, K.W.; Philipp, W.H.; and Wan, W.: Continuous Heavy Metal Removal From Solutions and Slurries by Films of a New Ion-Exchange Medium. Presented at American Institute of Chemical Engineers National Meeting, San Diego, CA, Nov. 1994.

Lewis contact: Dr. Joseph M. Savino, (216) 433–5531

Consortium on Advanced Coatings and Surface Modifications Formed

The Great Lakes Industrial Technology Center (GLITeC) formed the Consortium on Advanced Coatings and Surface Modifications to help transfer advanced coating and surface modification technologies developed at NASA Lewis to its member companies. NASA Lewis' participation in the consortium will consist of private consultations by Lewis researchers with member companies and the preparation of samples for evaluation by member companies. All NASA work will be reimbursed through a reimbursable Space Act Agreement between NASA Lewis and GLITeC. GLITeC manages the consortium, collects member fees, and arranges with NASA Lewis the various activities for each industry member.

In addition to NASA's services each member receives a comprehensive report that describes selected surface-treatment and coating technologies and their potential applications. This report is prepared by researchers and consultants at the Battelle Memorial Institute in Columbus, Ohio. GLITeC is a division of Battelle.

The first companies joined the consortium in January 1994. (Of the basic membership fee of $10,000, $7500 is earmarked for reimbursable services performed by NASA Lewis.) Included in this group are companies involved in the manufacture of ion sources for industrial processes and companies investigating advanced coatings for potential processing equipment, consumer products, and medical applications.

Lewis contact: Stephen M. Riddlebaugh, (216) 433–5565
Headquarters program office: OSAT

Lewis Technologies Selected for Evaluation by Federal Laboratory Consortium

The Midwest Region of the Federal Laboratory Consortium (FLC) for Technology Transfer is conducting the Strategic Technology Evaluation Program (STEP) to evaluate the marketability of candidate technologies submitted by all Federal laboratories in the six-state region. The FLC STEP is patterned after the NASA STEP conducted at Lewis in 1993.

FLC member laboratories in the Midwest Region states (Ohio, Michigan, Indiana, Illinois, Wisconsin, and Minnesota) submitted candidate technologies to the Regional Advisory Panel of the FLC. Of the 10 technologies selected by the panel for market evaluation, two came from NASA Lewis: "Guanadine, a Unique Strong Organic Base," by Warren H. Philipp and Joseph M. Savino; and "Gas Chromatic Mass Spectrometer," by Chowen C. Wey.

The FLC contracted the Great Lakes Industrial Technology Center to conduct market surveys for each technology.

Lewis contact: Stephen M. Riddlebaugh, (216) 433–5565
Headquarters program office: OSAT

Author Index

REPORT DOCUMENTATION PAGE

Form Approved
OMB No. 0704-0188

1. AGENCY USE ONLY (*Leave blank*)	2. REPORT DATE	3. REPORT TYPE AND DATES COVERED
	January 1995	Technical Memorandum

4. TITLE AND SUBTITLE

Research & Technology 1994

5. FUNDING NUMBERS

None

6. AUTHOR(S)

7. PERFORMING ORGANIZATION NAME(S) AND ADDRESS(ES)

National Aeronautics and Space Administration
Lewis Research Center
Cleveland, Ohio 44135–3191

8. PERFORMING ORGANIZATION REPORT NUMBER

E–9207

9. SPONSORING/MONITORING AGENCY NAME(S) AND ADDRESS(ES)

National Aeronautics and Space Administration
Washington, D.C. 20546–0001

10. SPONSORING/MONITORING AGENCY REPORT NUMBER

NASA TM–106764

11. SUPPLEMENTARY NOTES

Responsible person, Walter S. Kim, organization code 9400, (216) 433–3742.

12a. DISTRIBUTION/AVAILABILITY STATEMENT

Unclassified - Unlimited
Subject Categories 01 and 31

12b. DISTRIBUTION CODE

13. ABSTRACT ***(Maximum 200 words)***

This report selectively summarizes the NASA Lewis Research Center's research and technology accomplishments for the fiscal year 1994. It comprises approximately 200 short articles submitted by the staff members of the technical directorates. The report is organized into six major sections: Aeronautics, Aerospace Technology, Space Flight Systems, Engineering and Computational Support, Lewis Research Academy, and Technology Transfer. A table of contents and an author index have been developed to assist the reader in finding articles of special interest. This report is not intended to be a comprehensive summary of all research and technology work done over the past fiscal year. Most of the work is reported in Lewis-published technical reports, journal articles, and presentations prepared by Lewis staff members and contractors. In addition, university grants have enabled faculty members and graduate students to engage in sponsored research that is reported at technical meetings or in journal articles. For each article in this report a Lewis contact person has been identified, and where possible, reference documents are listed so that additional information can be easily obtained. The diversity of topics attests to the breadth of research and technology being pursued and to the skill mix of the staff that makes it possible.

14. SUBJECT TERMS

Aeronautics; Aerospace engineering; Space flight; Space power; Materials; Structures; Electronics; Space experiments; Technology transfer

15. NUMBER OF PAGES

170

16. PRICE CODE

A08

17. SECURITY CLASSIFICATION OF REPORT	18. SECURITY CLASSIFICATION OF THIS PAGE	19. SECURITY CLASSIFICATION OF ABSTRACT	20. LIMITATION OF ABSTRACT
Unclassified	Unclassified	Unclassified	